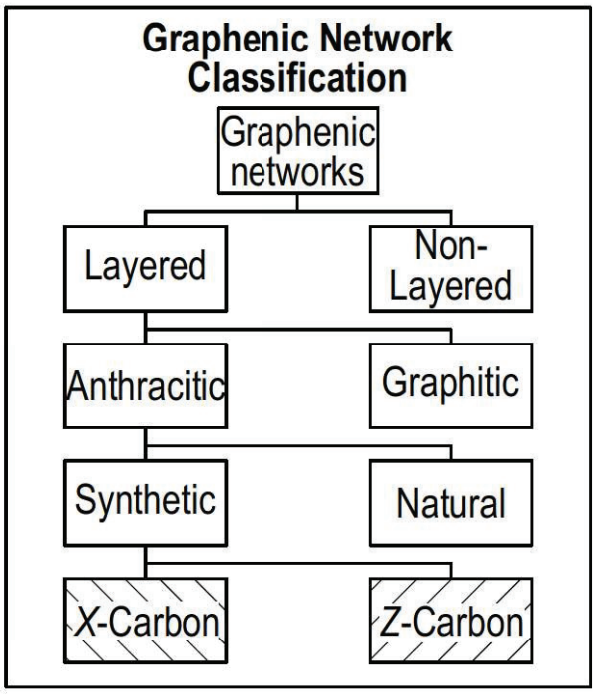
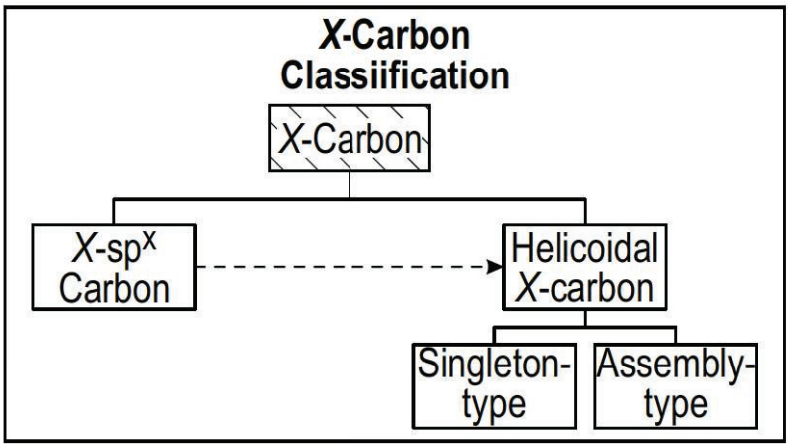

Graphenic Network Classification
Graphenic networks
Layered
Non-Layered
Anthracitic
Graphitic
Synthetic
Natural
X-Carbon
Z-Carbon


X-Carbon Classiification
X-Carbon
X-sp^x Carbon
Helicoidal X-carbon
Singleton-type
Assembly-type

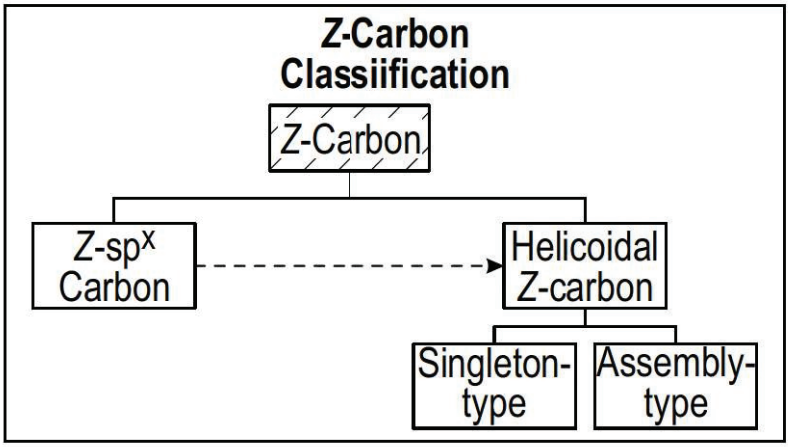
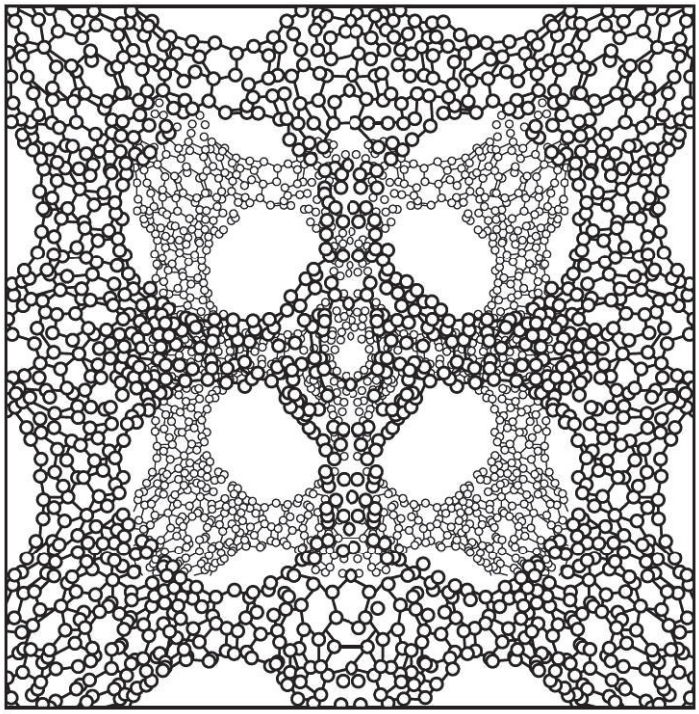

Z-Carbon Classiification
Z-Carbon
Z-sp^x Carbon
Helicoidal Z-carbon
Singleton-type
Assembly-type

FIG. 1



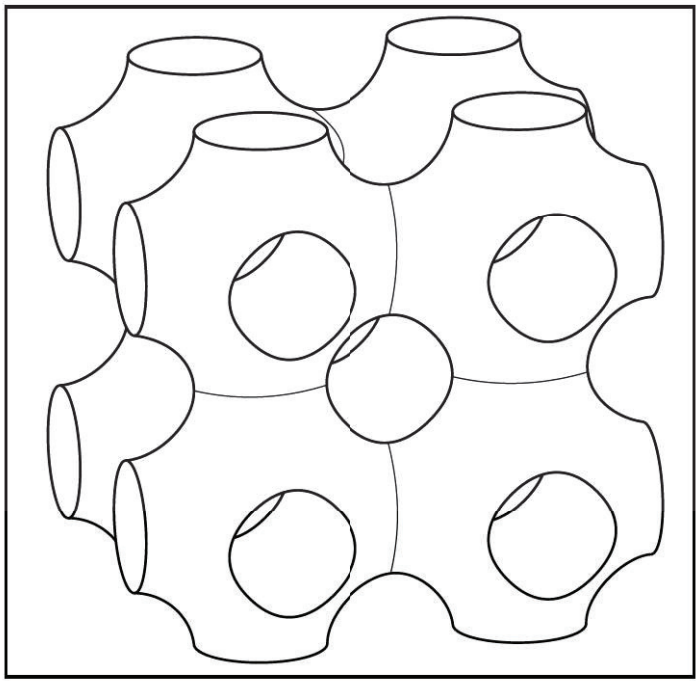


FIG. 2

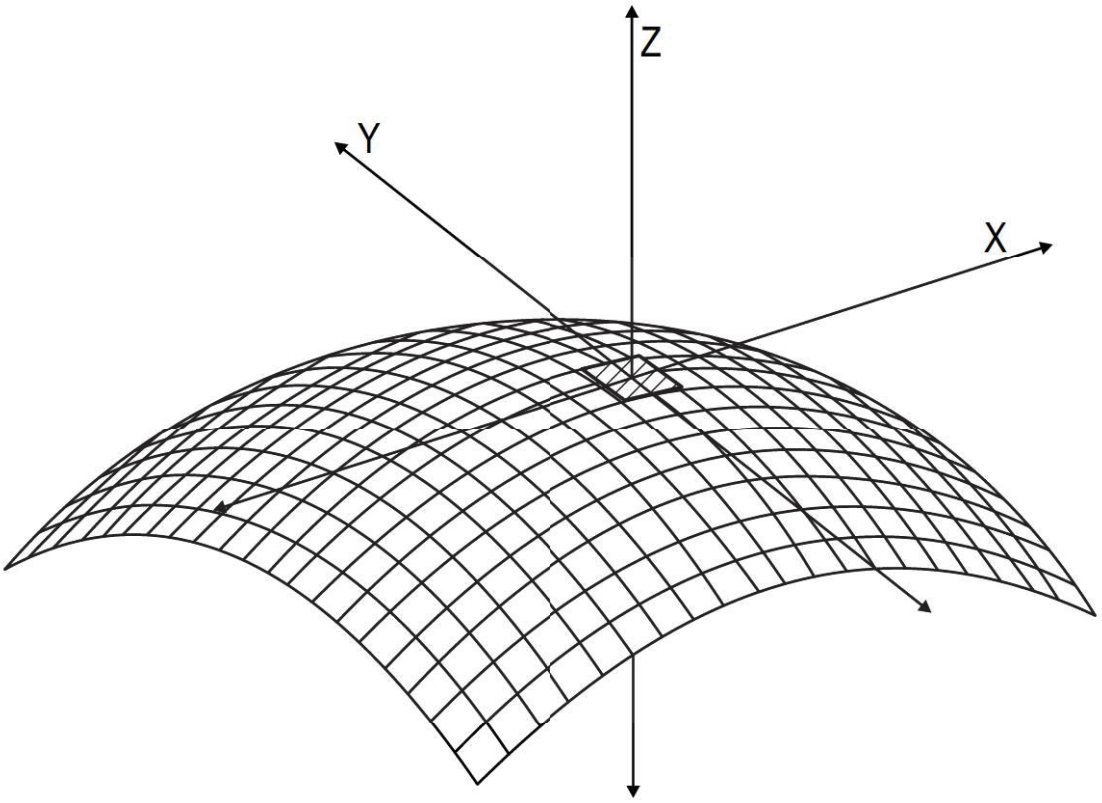



FIG. 3

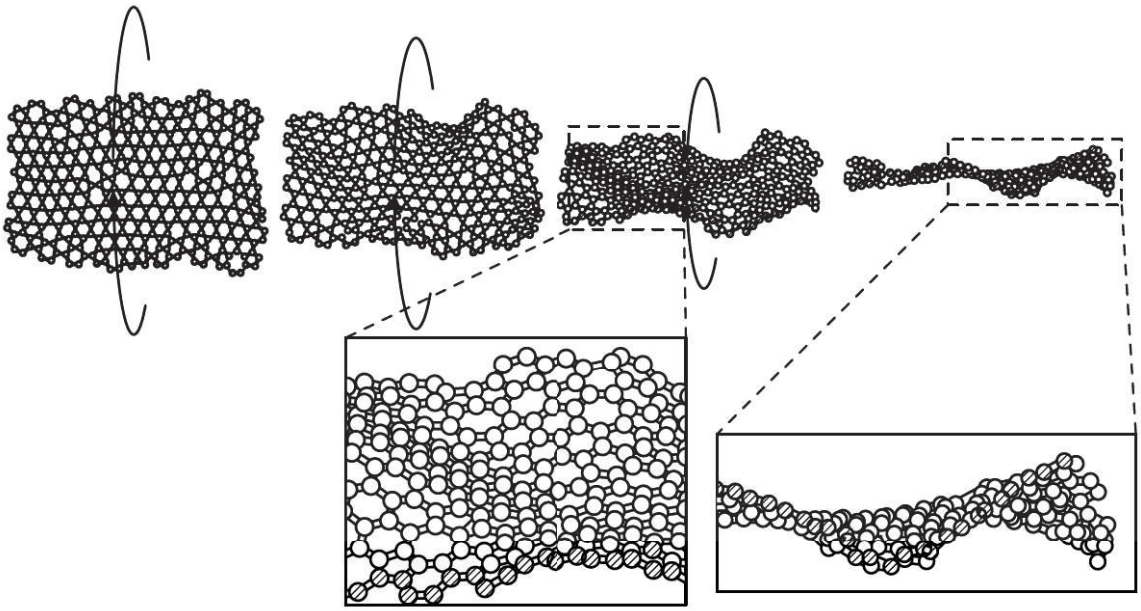


FIG. 4

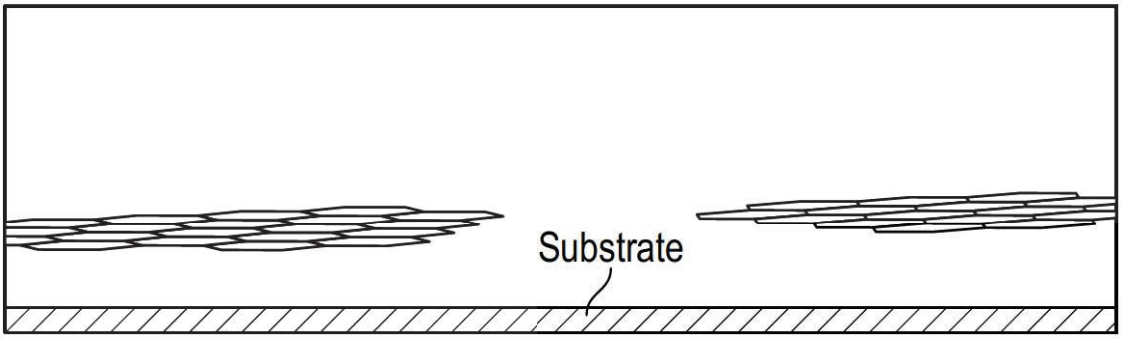



FIG. 5A

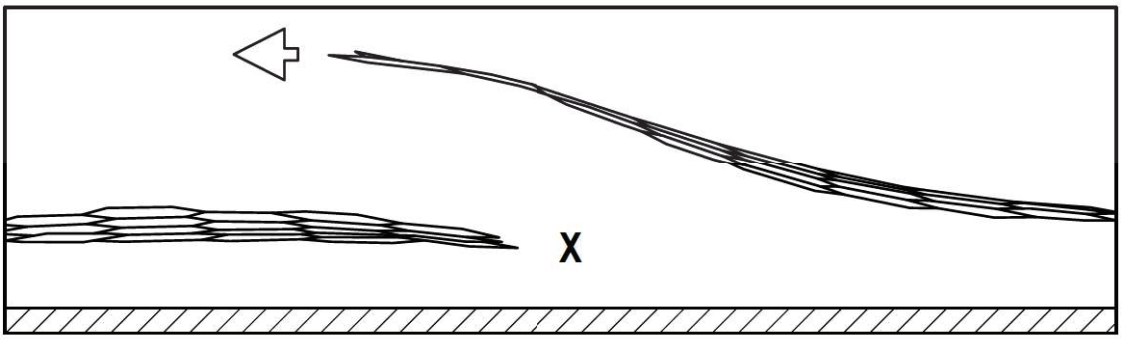



FIG. 5B

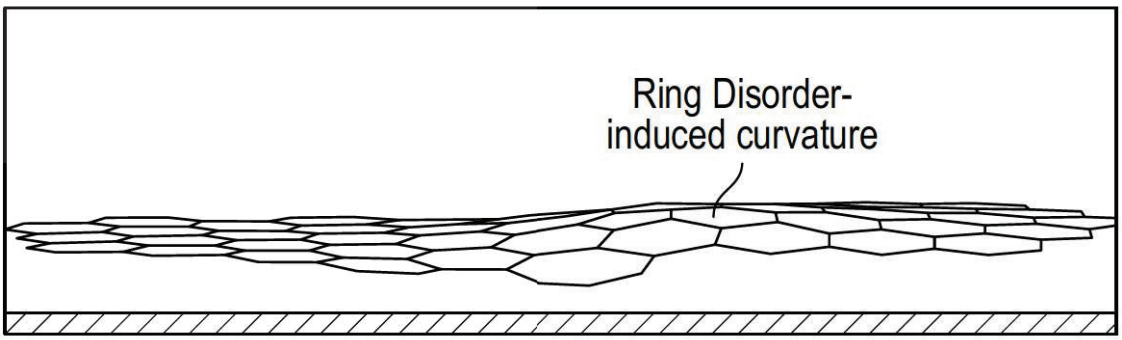



FIG. 5C

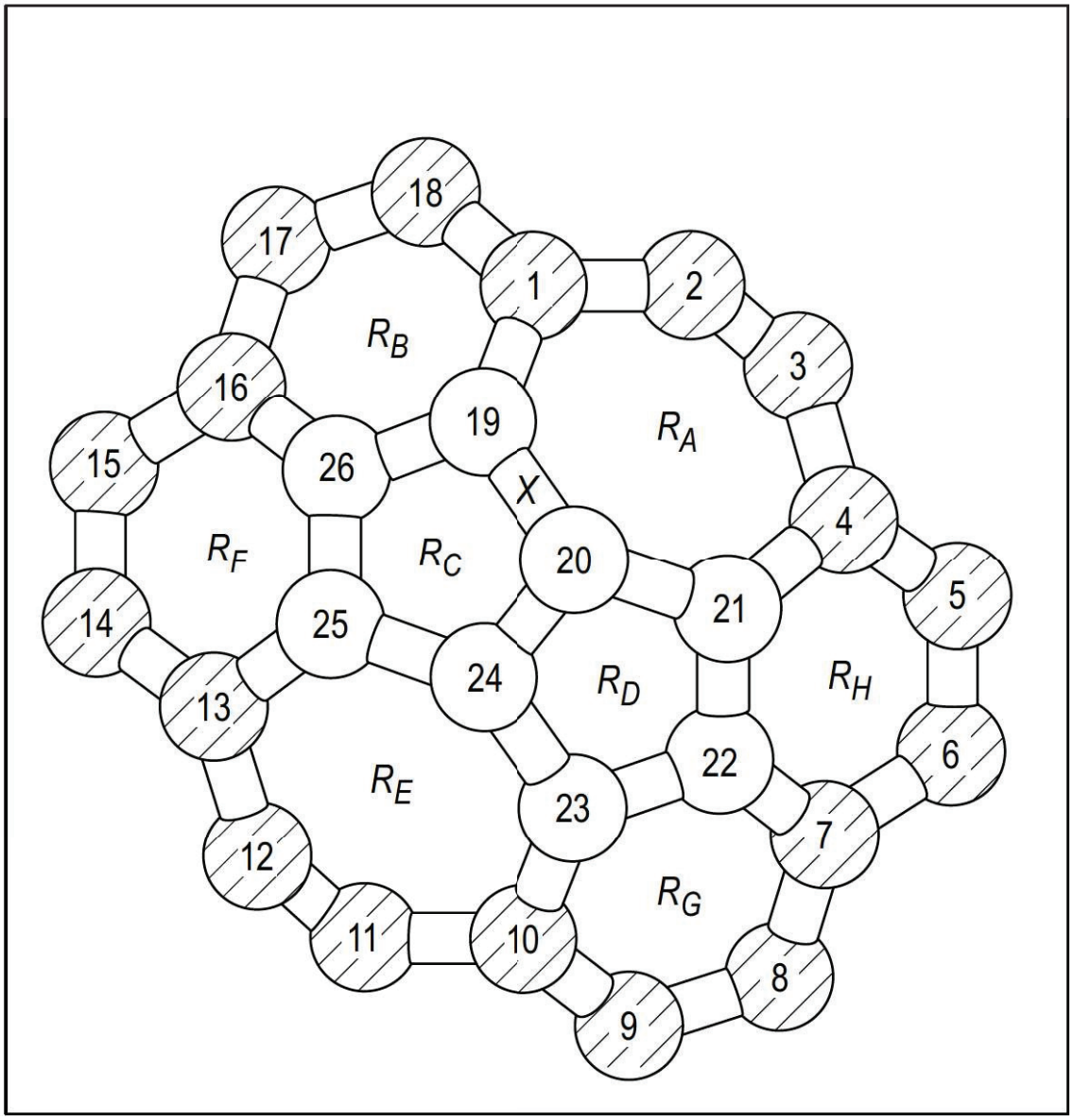

18
17
1
2
$R_B$
3
16
19
$R_A$
15
26
X
4
$R_F$
$R_C$
20
14
25
21
5
24
$R_D$
$R_H$
13
22
6
$R_E$
23
12
7
$R_G$
11
10
8
9

FIG. 6A

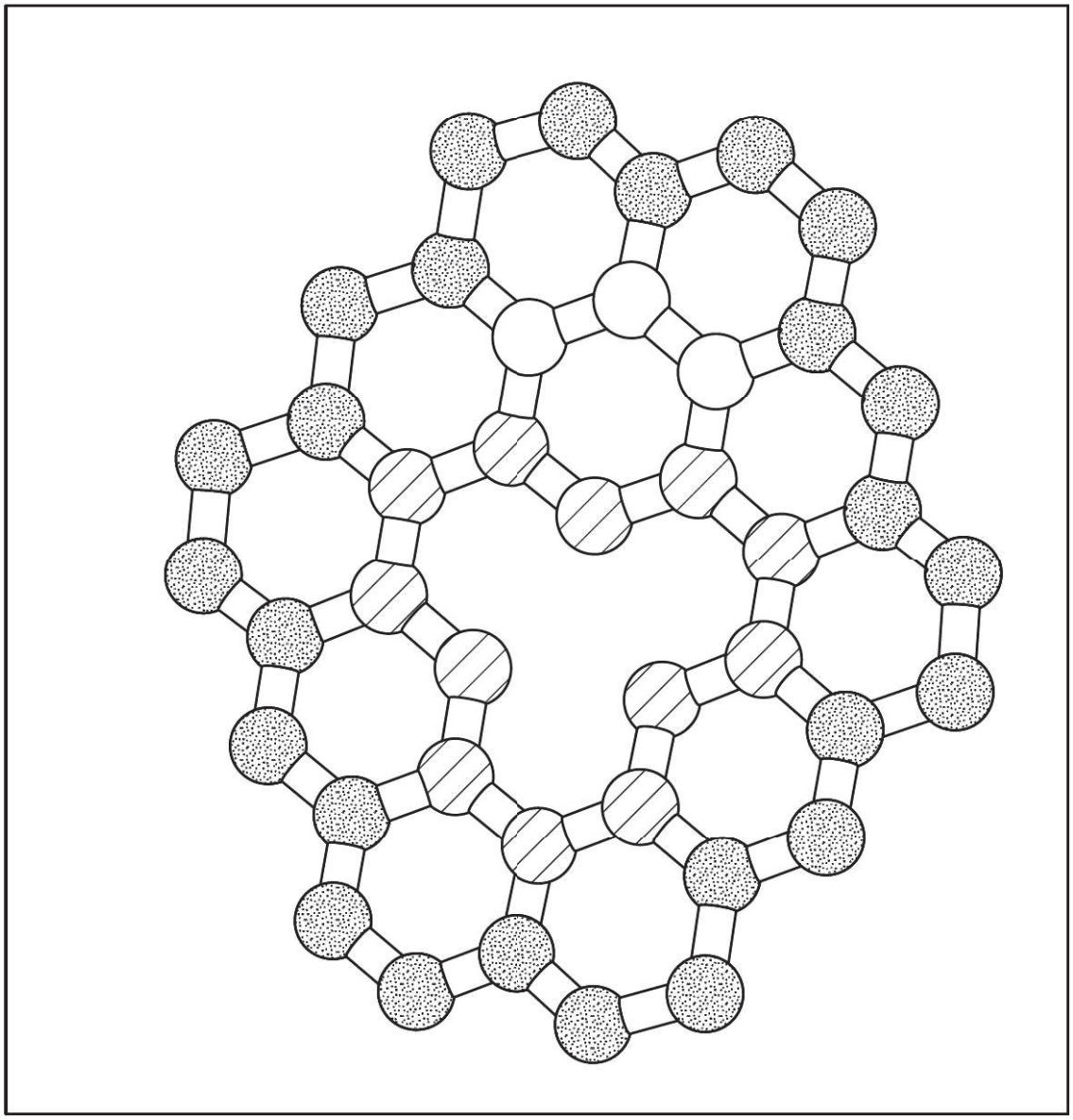


FIG. 6B

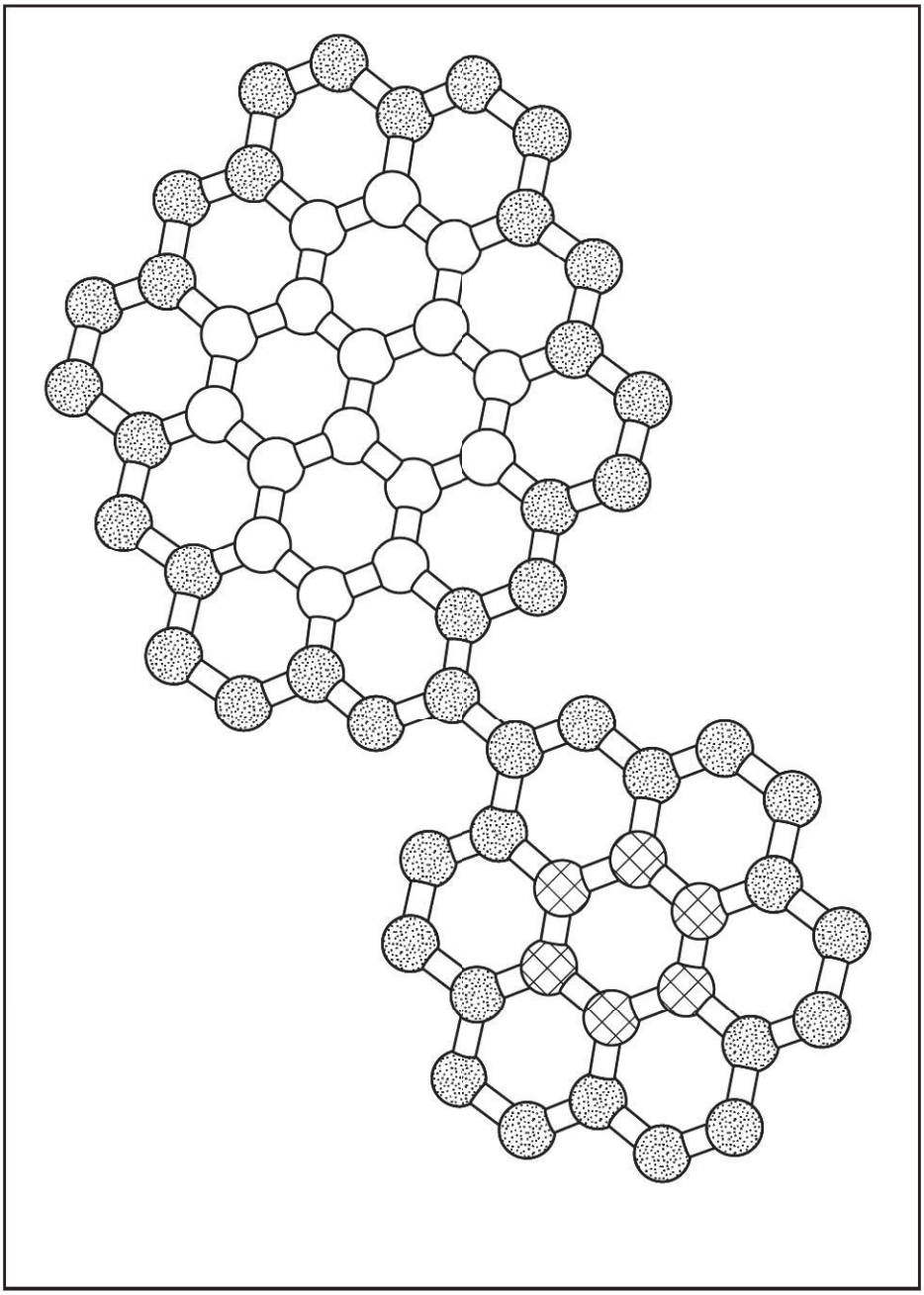


FIG. 6C

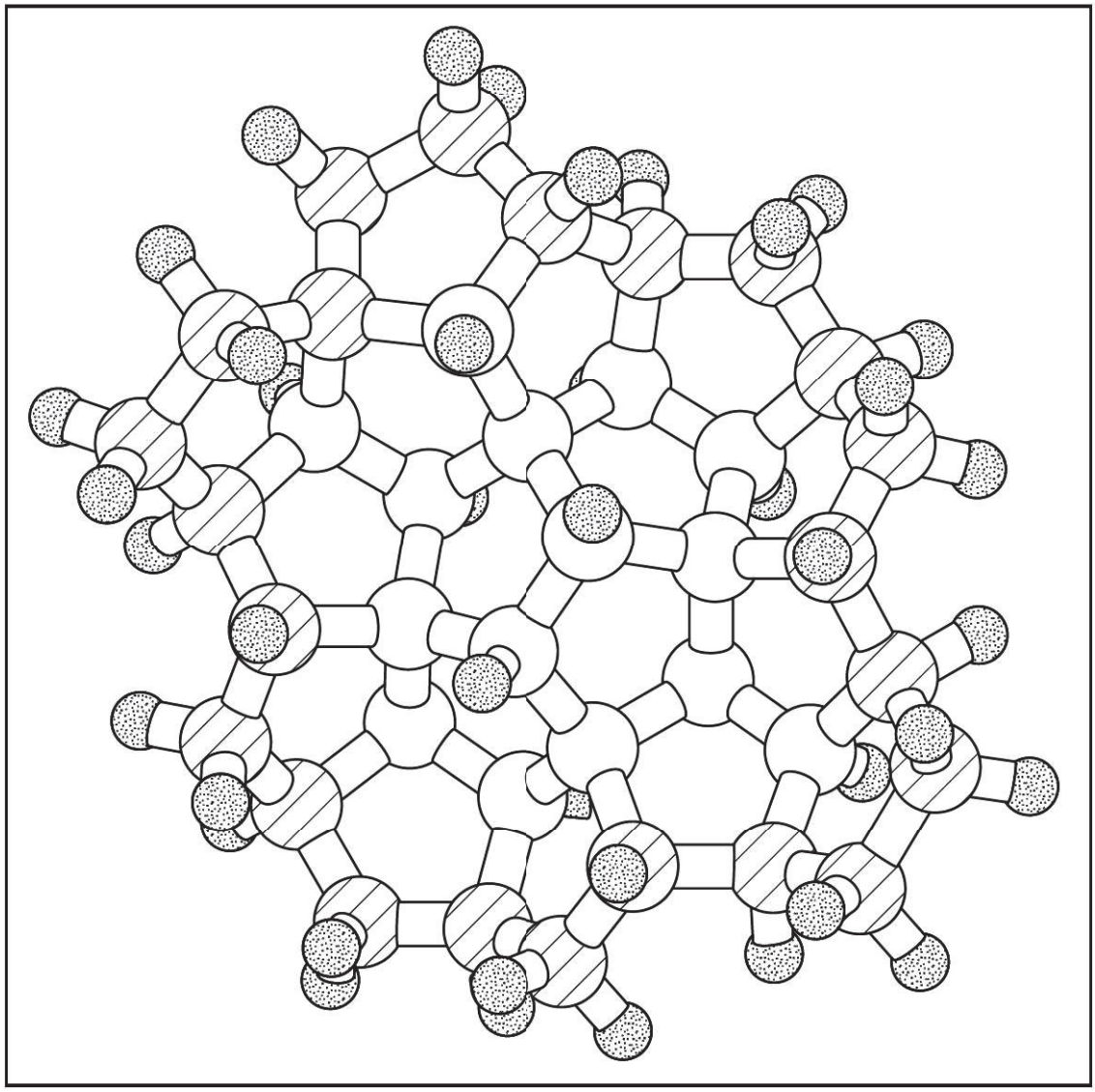


FIG. 6D

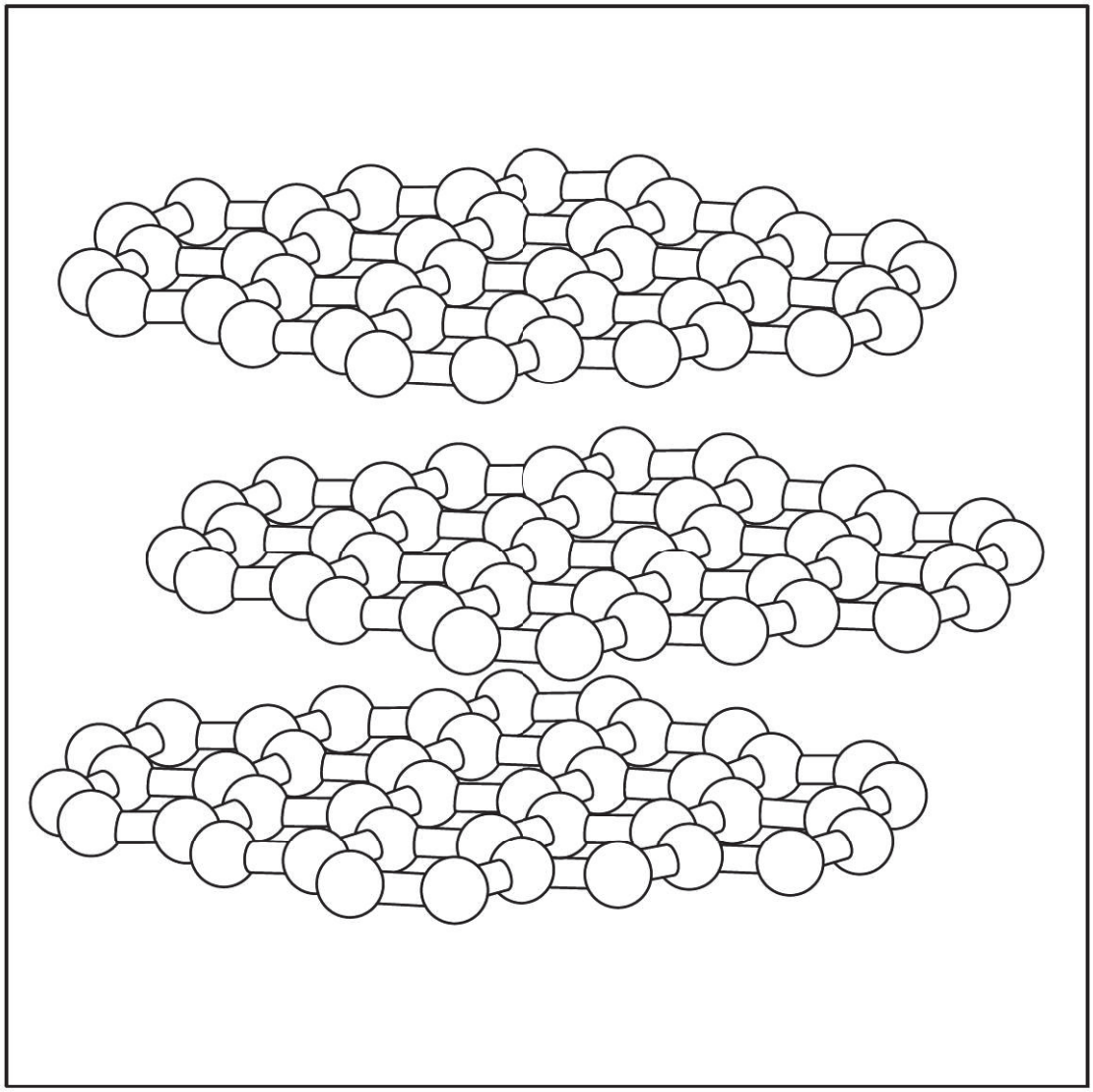


FIG. 6E

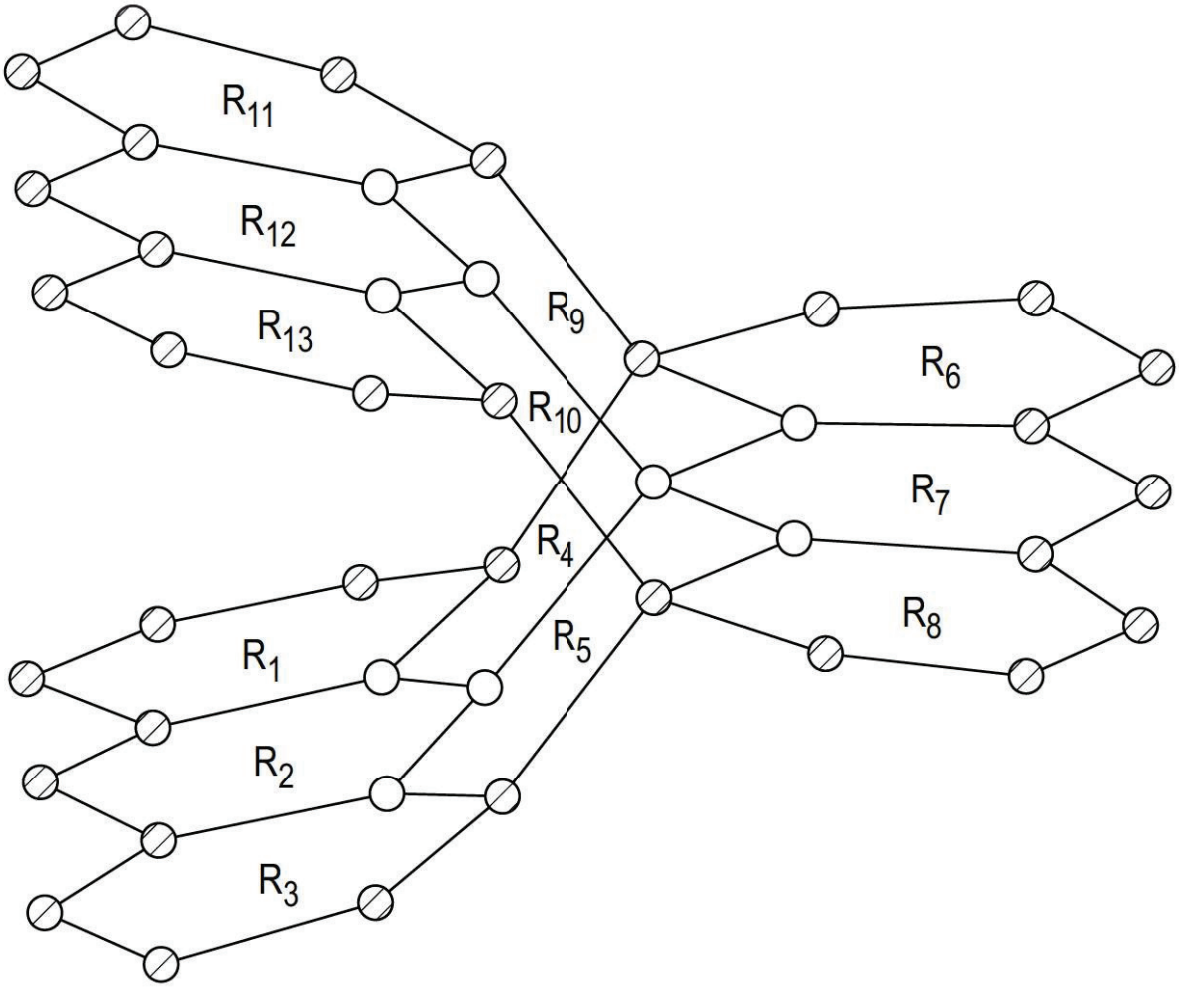



FIG. 7A

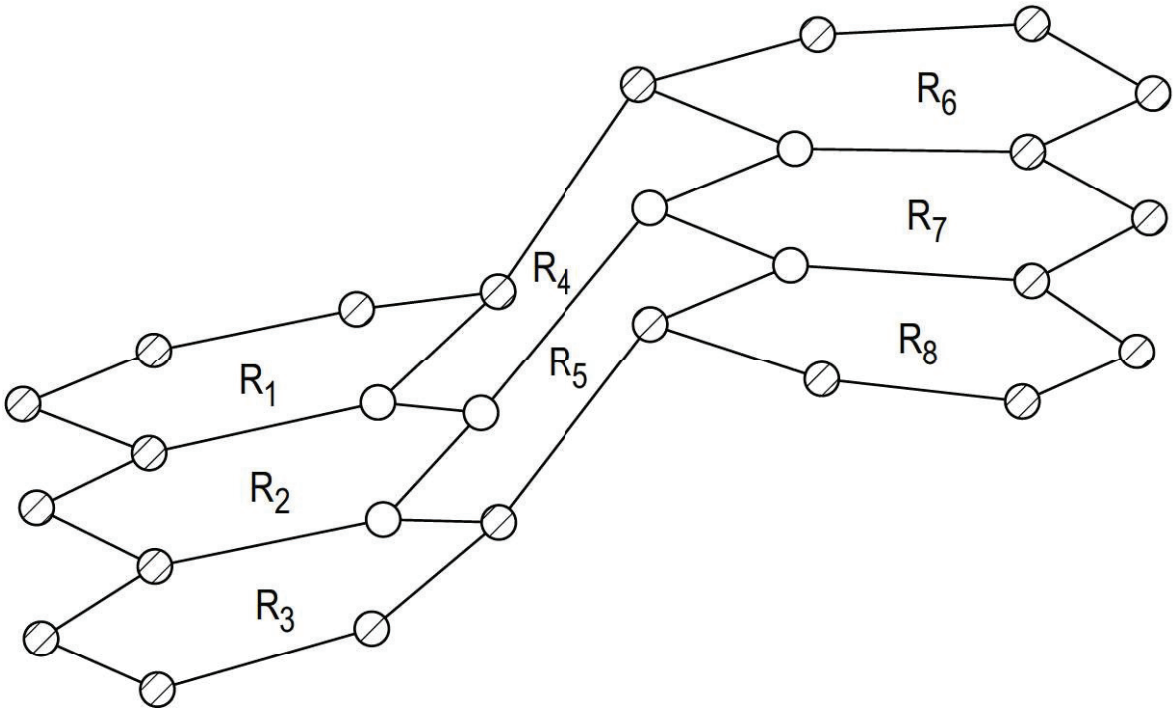



FIG. 7B

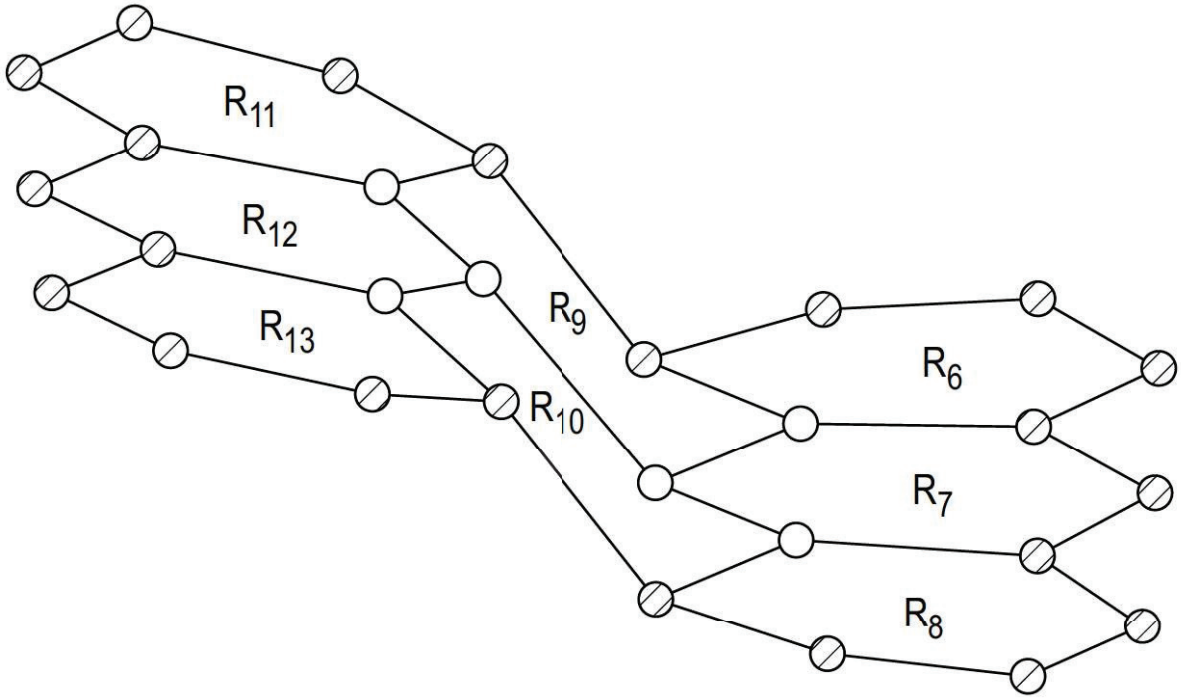



FIG. 7C

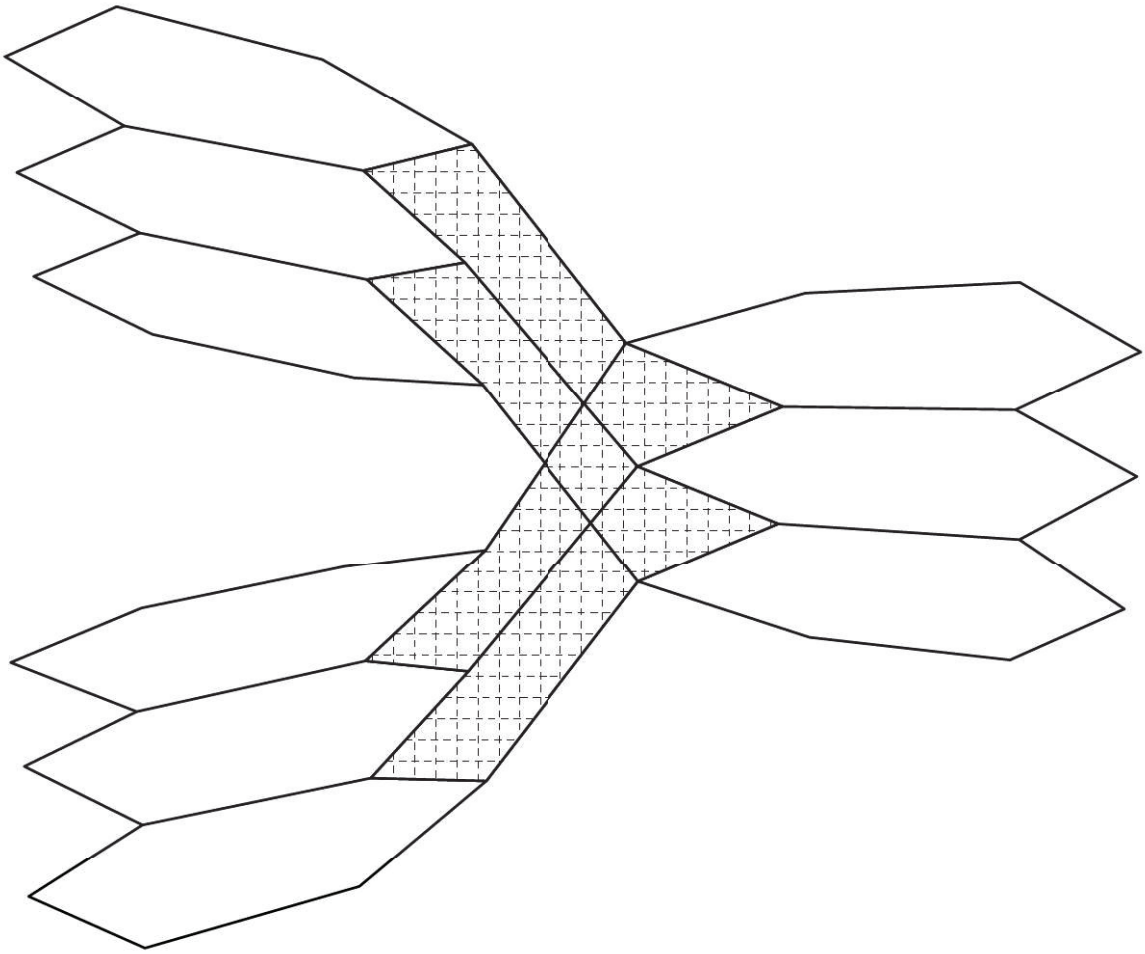


FIG. 7D

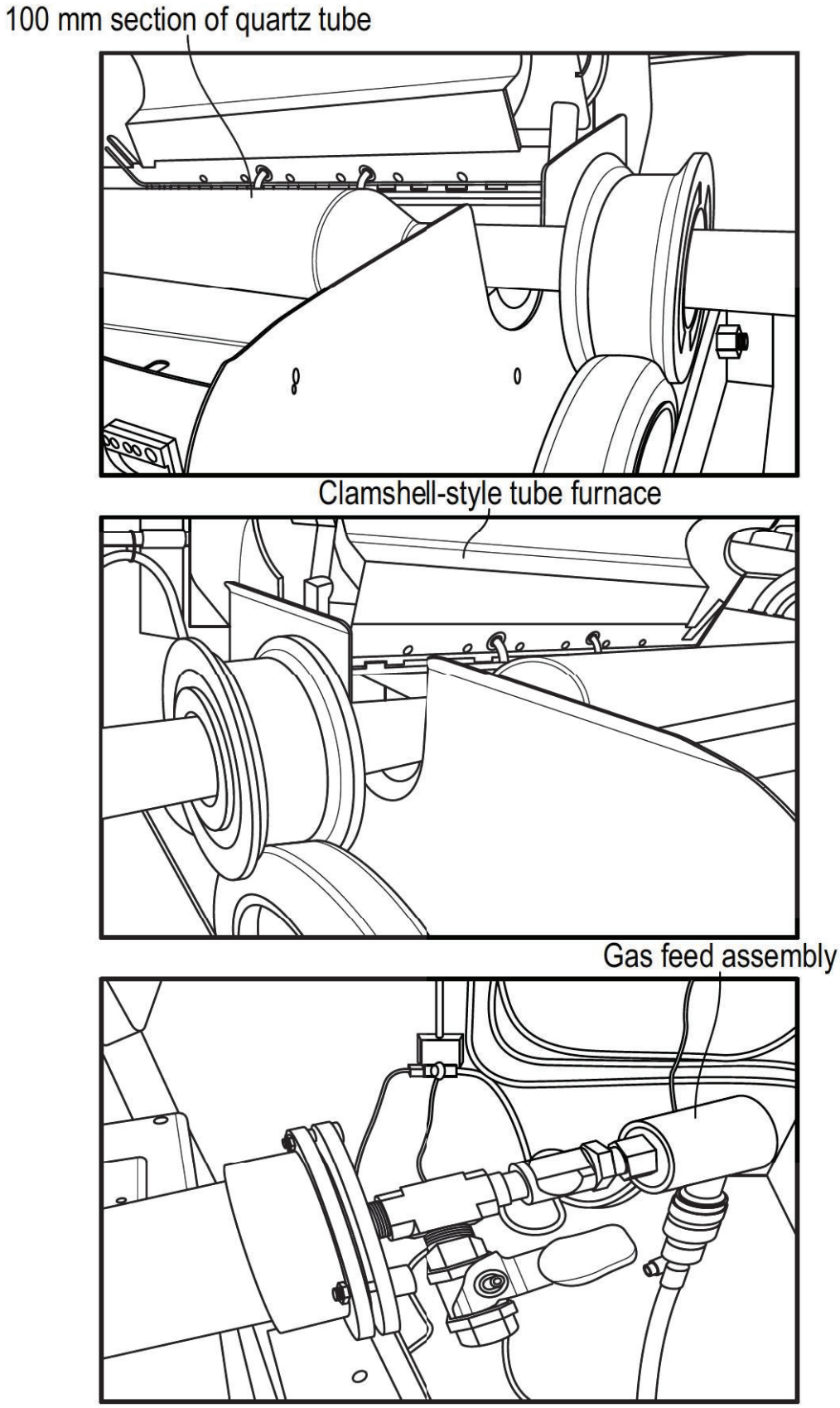

100 mm section of quartz tube
Clamshell-style tube furnace
Gas feed assembly

FIG. 8A

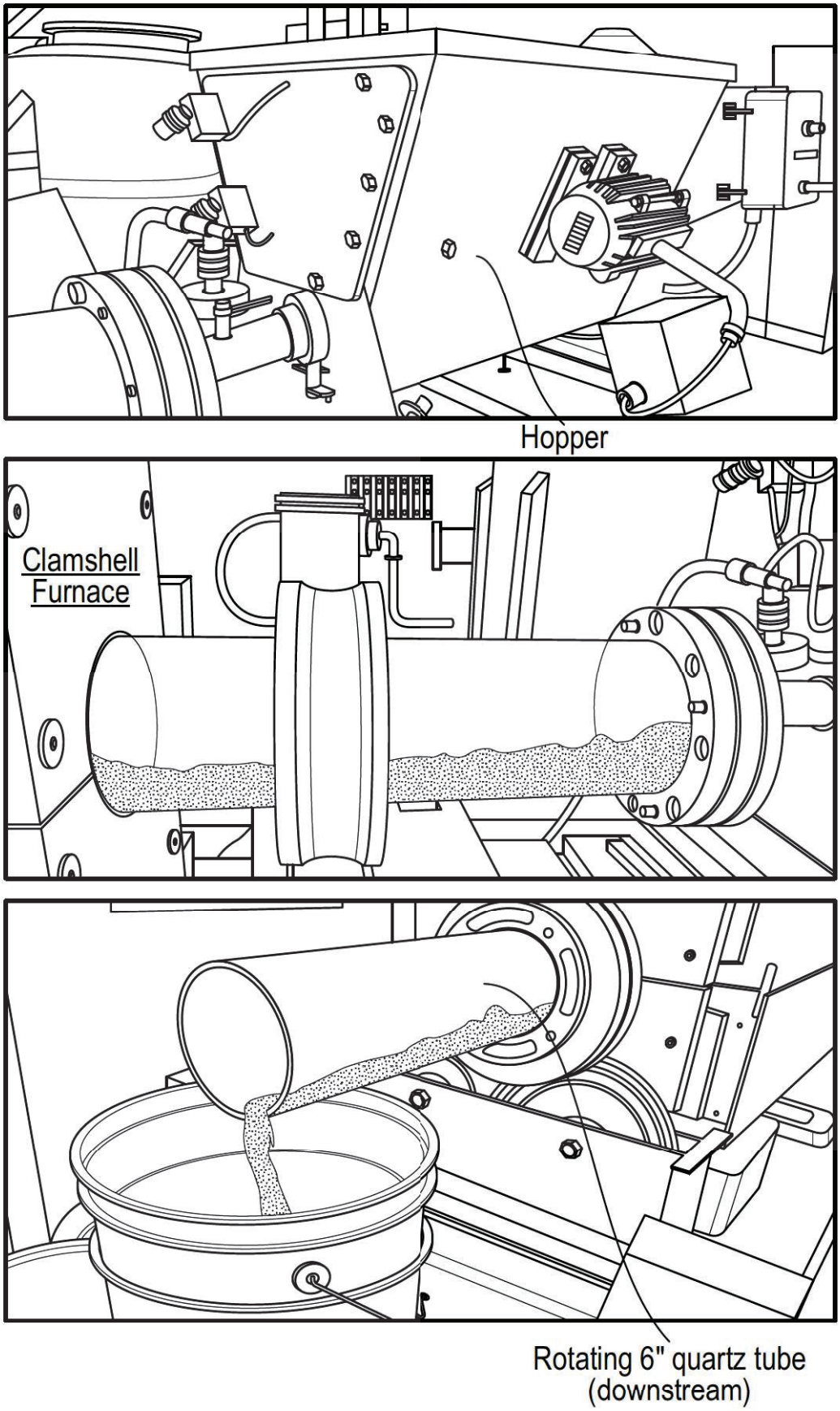

Hopper
Clamshell
Furnace
Rotating 6" quartz tube
(downstream)

FIG. 8B

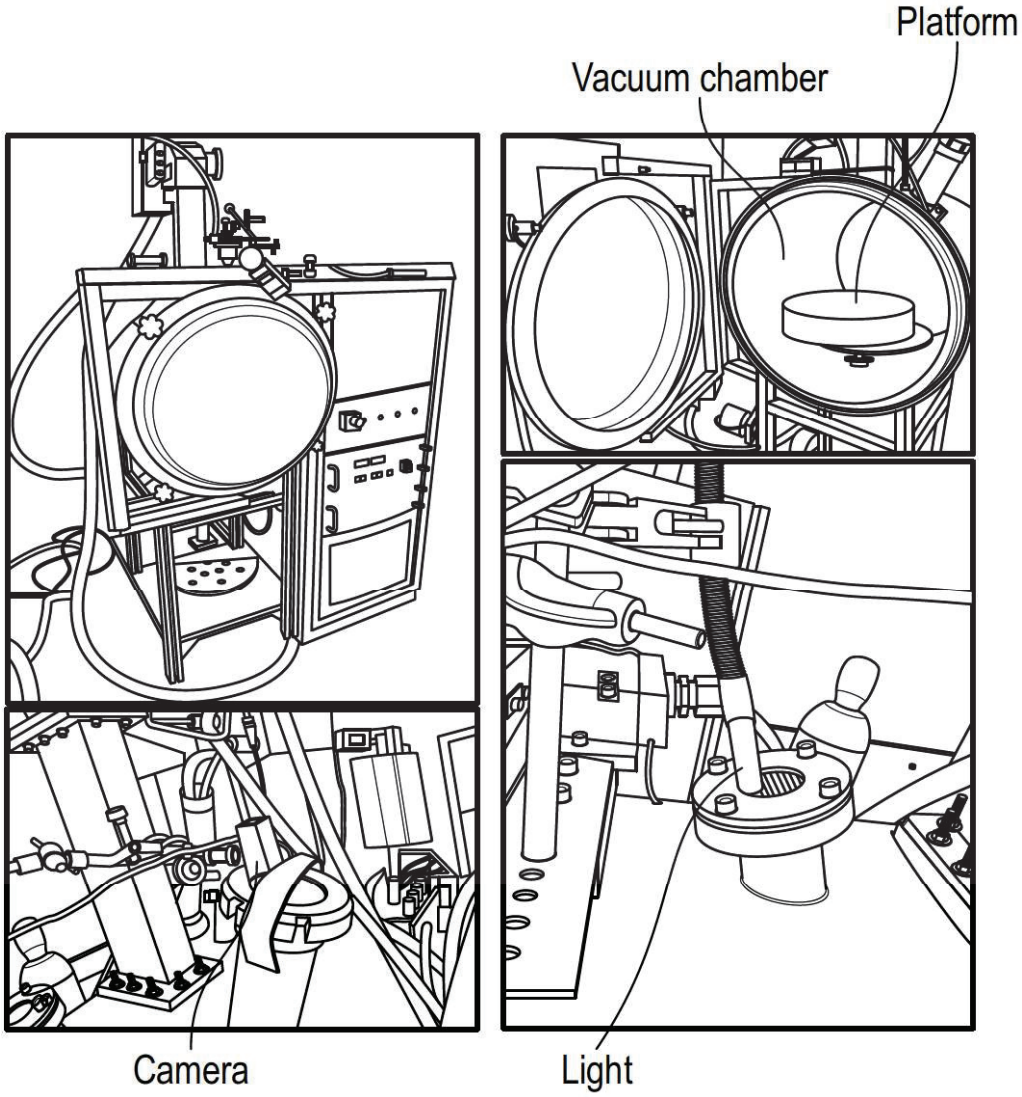



FIG. 8C

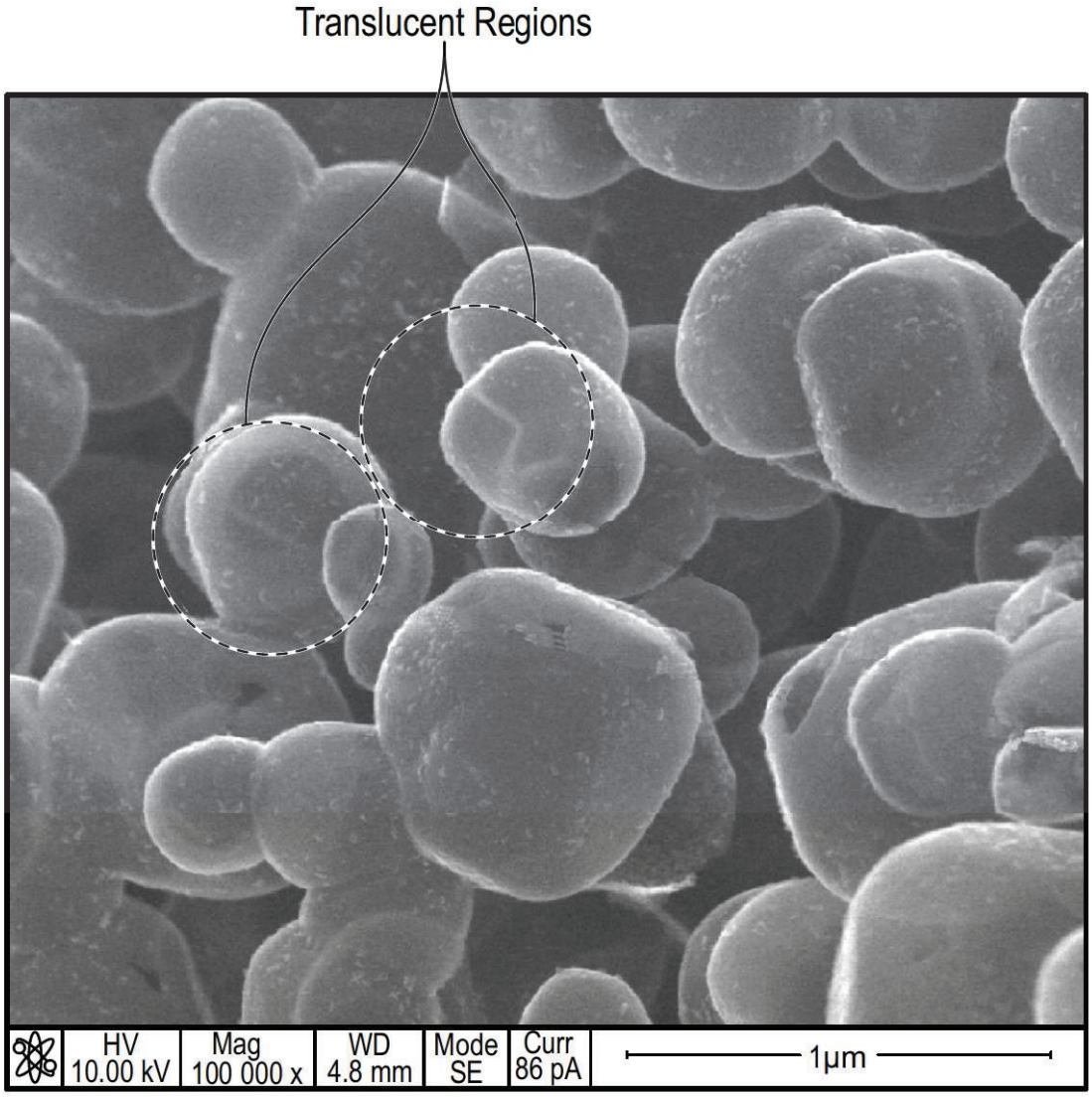

Translucent Regions
HV
10.00 kV
Mag
100 000 x
WD
4.8 mm
Mode
SE
Curr
86 pA
1µm

FIG. 9

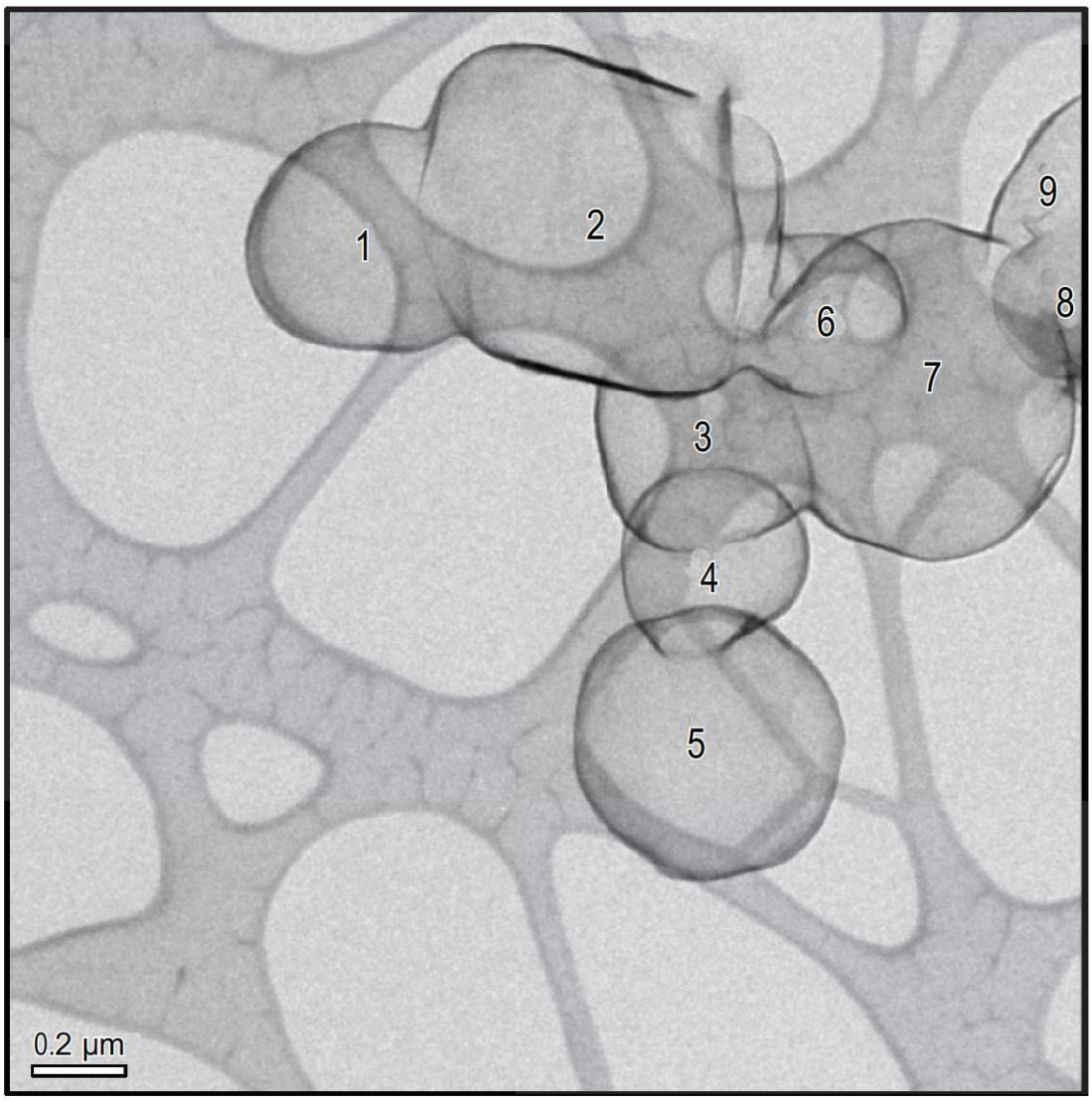



FIG. 10A

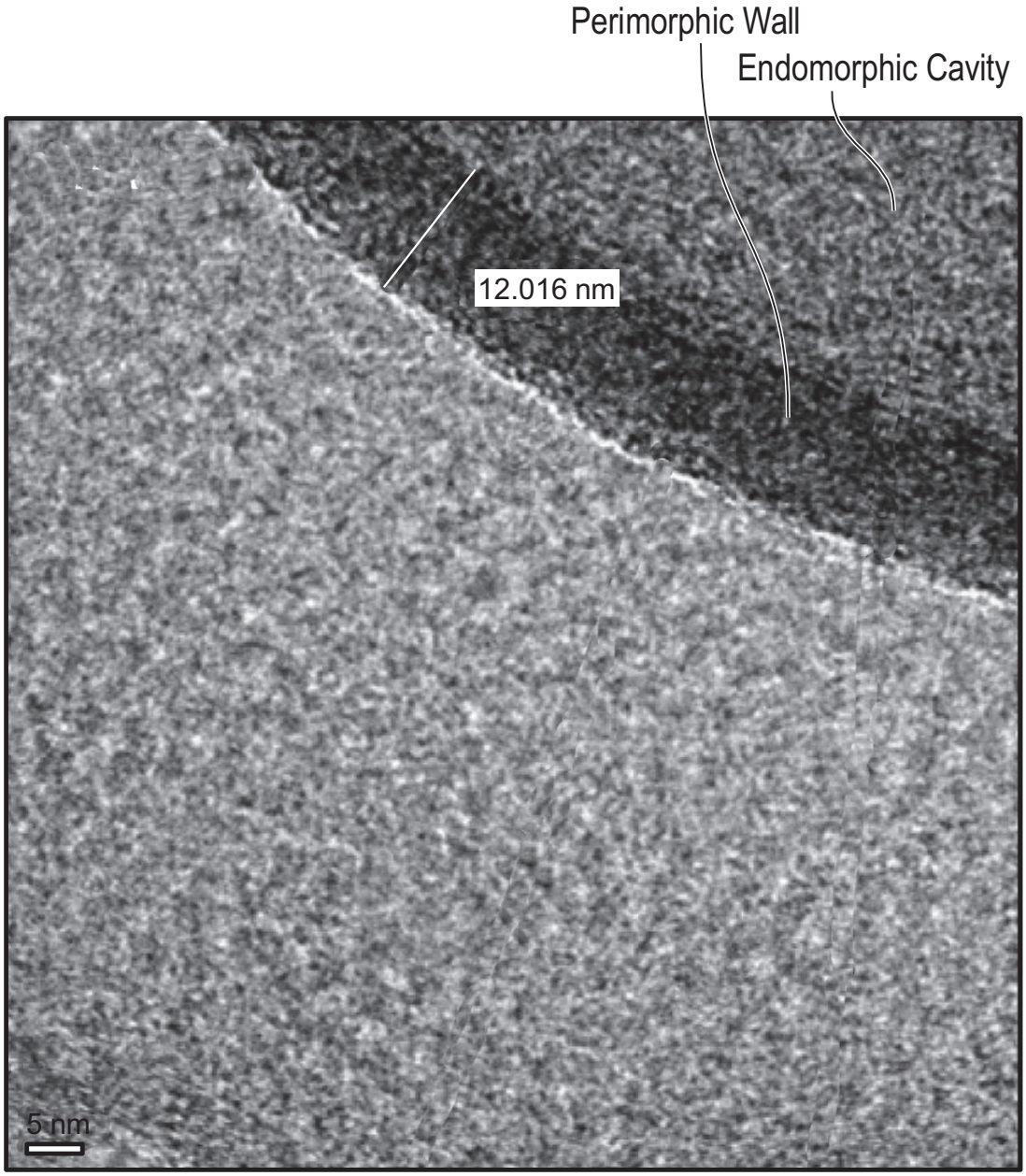



FIG. 10B

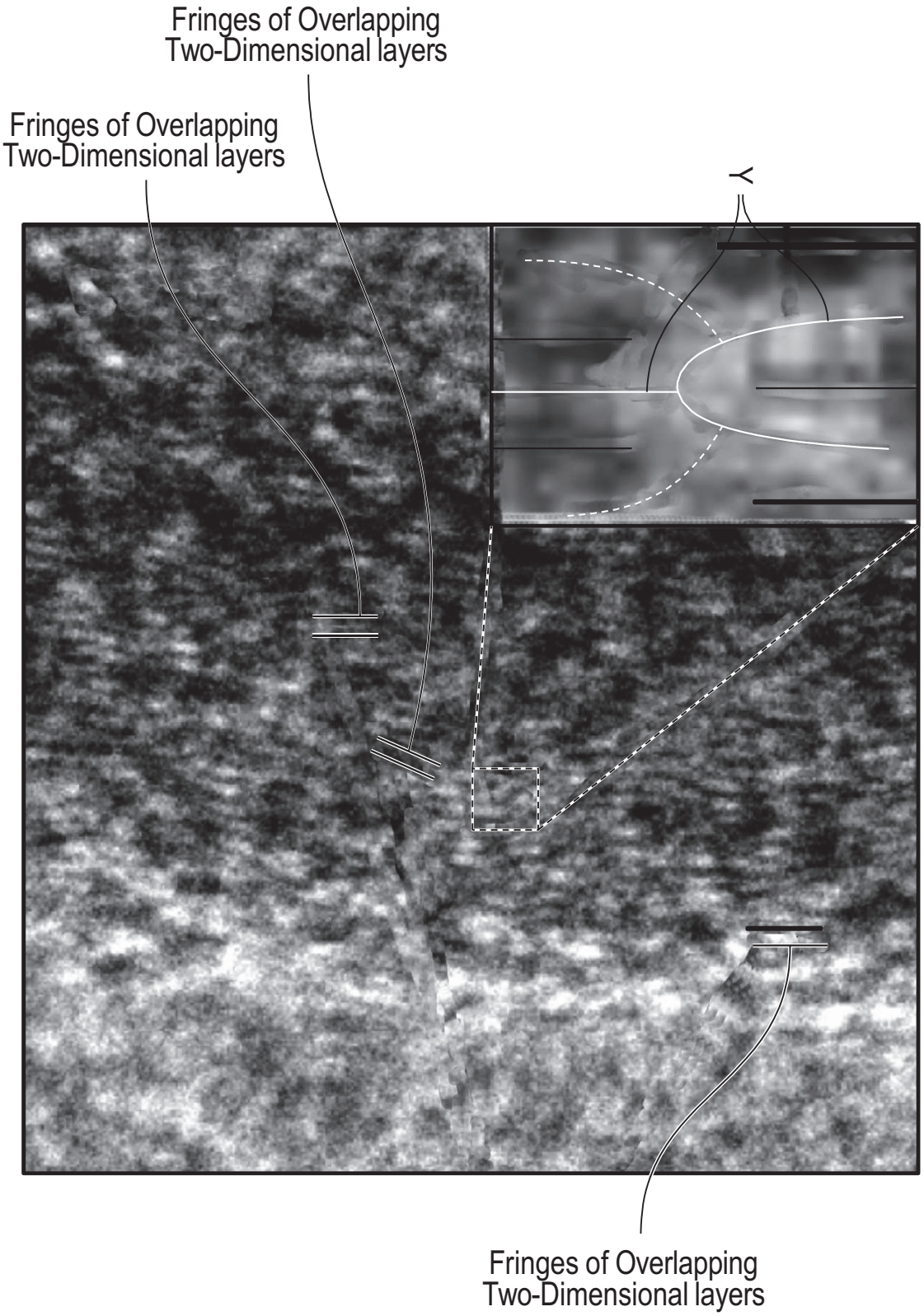

Fringes of Overlapping
Two-Dimensional layers
Fringes of Overlapping
Two-Dimensional layers
Fringes of Overlapping
Two-Dimensional layers

FIG. 10C

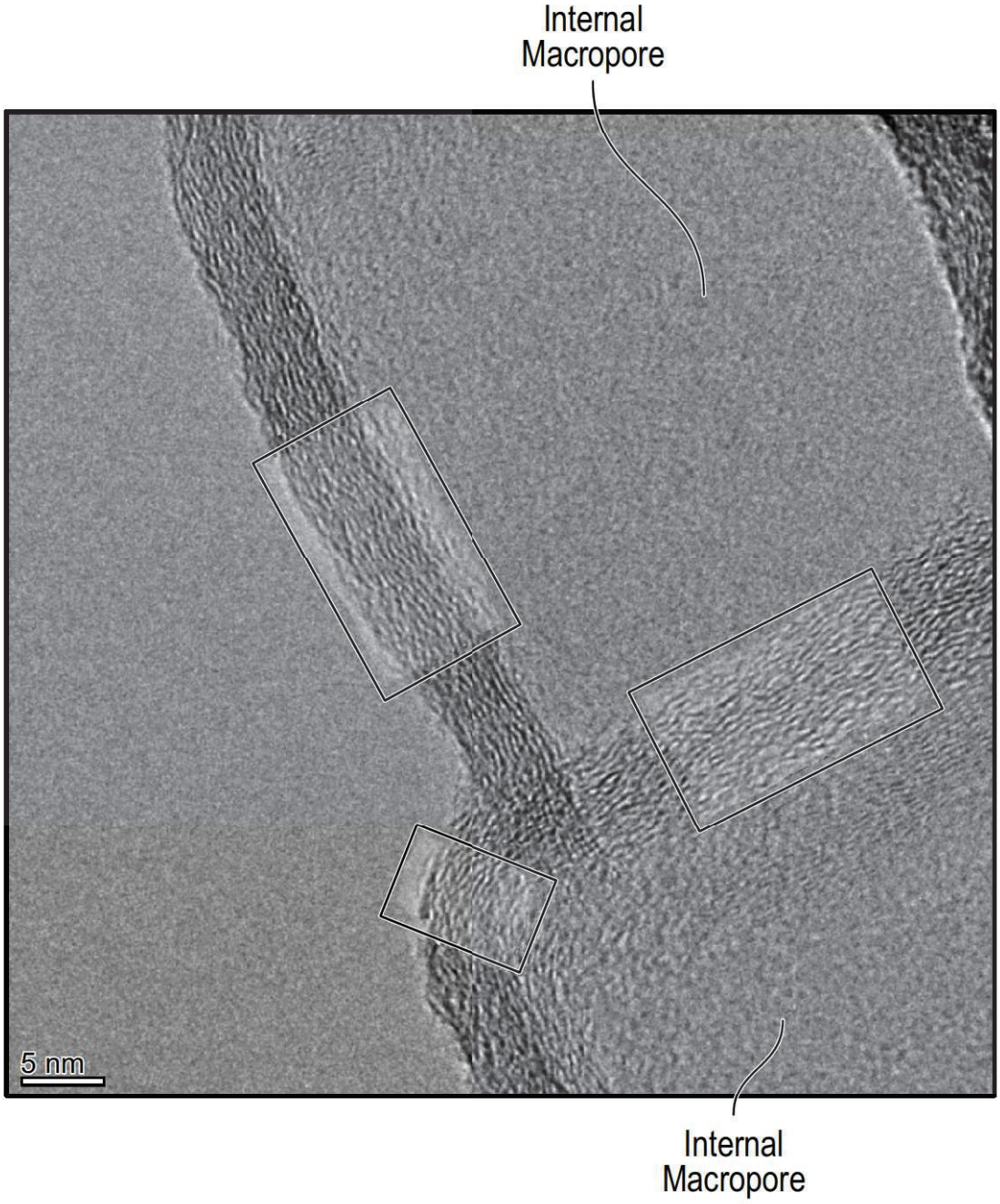



FIG. 11

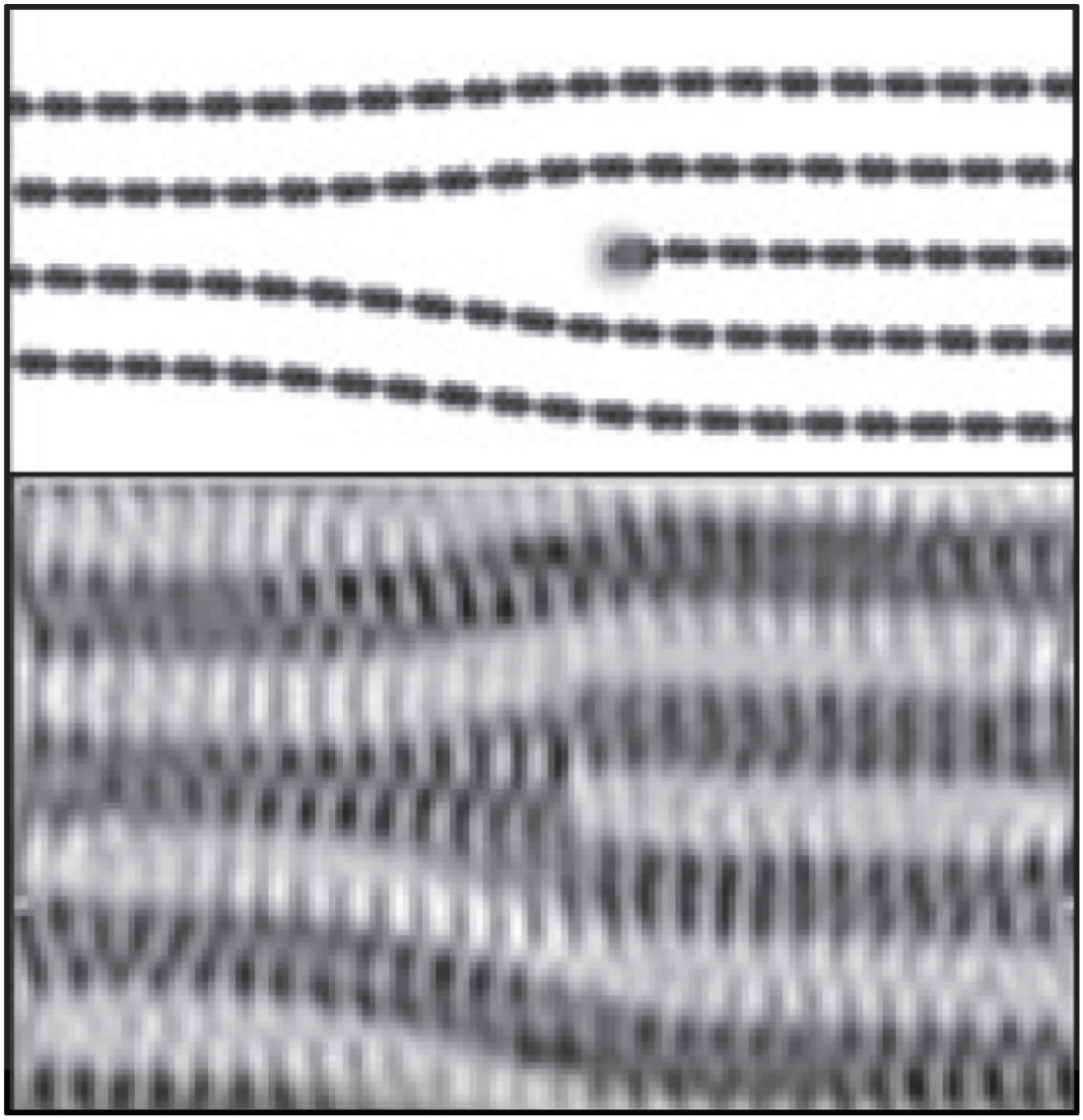


FIG. 12A

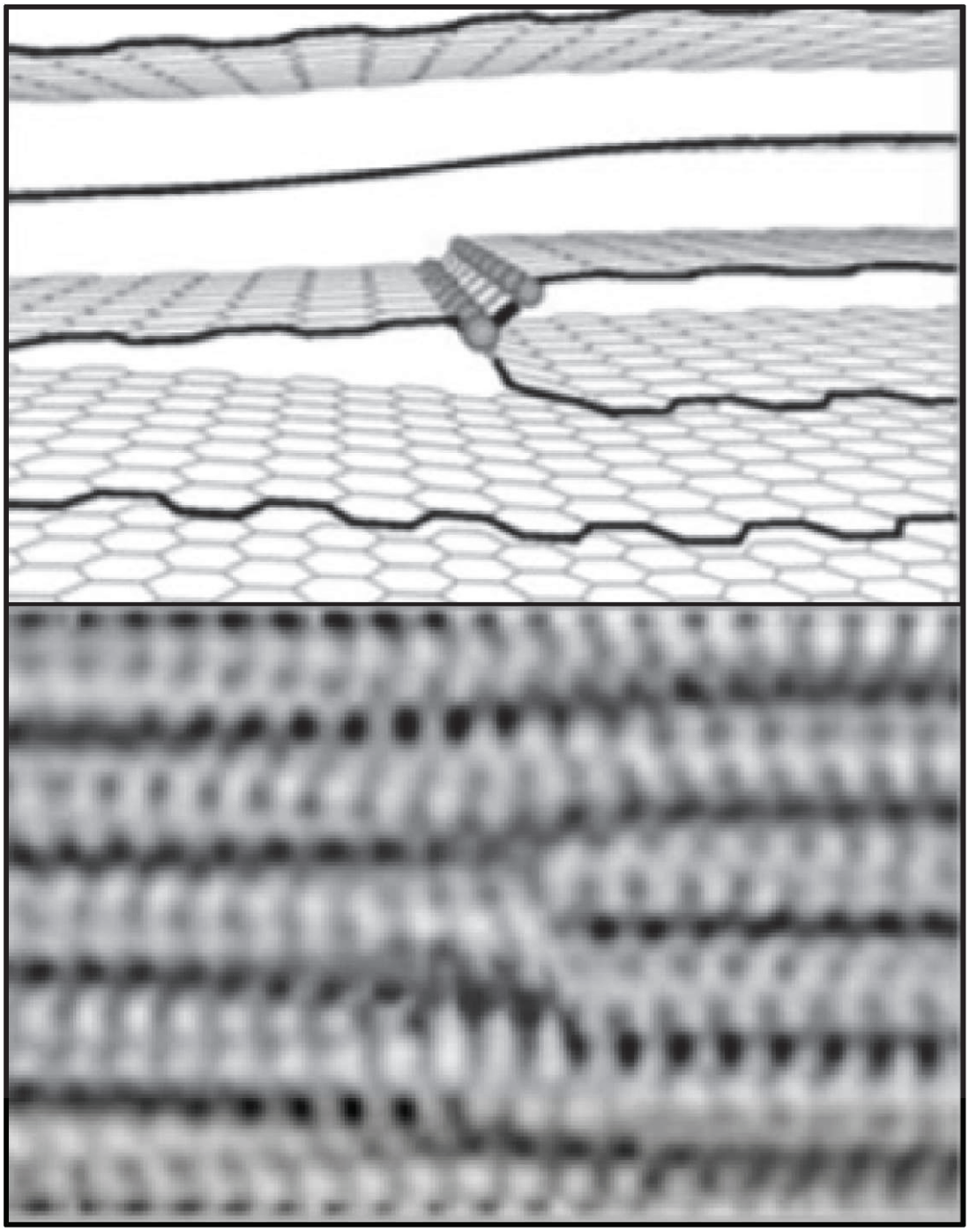


FIG. 12B

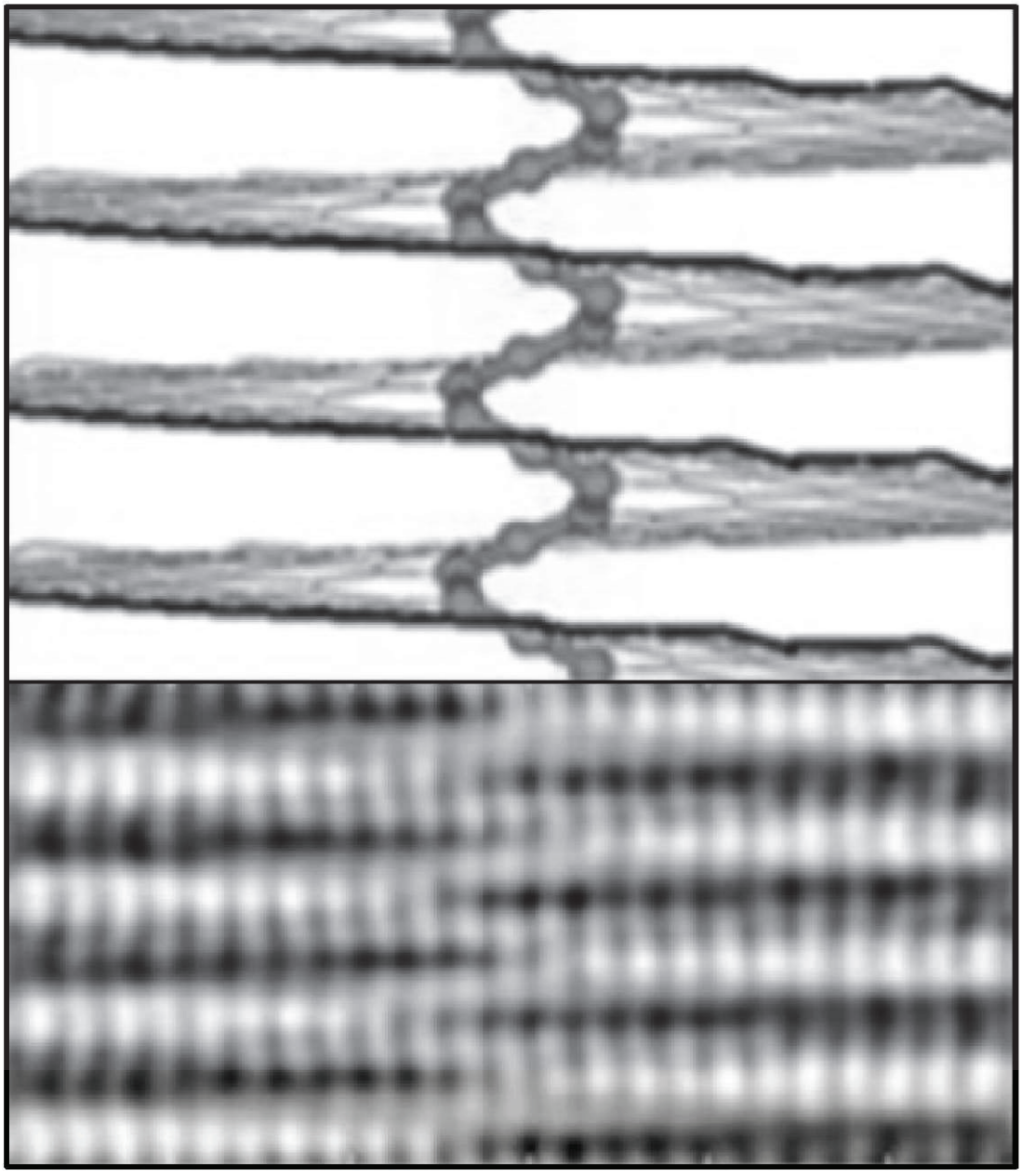


FIG. 12C

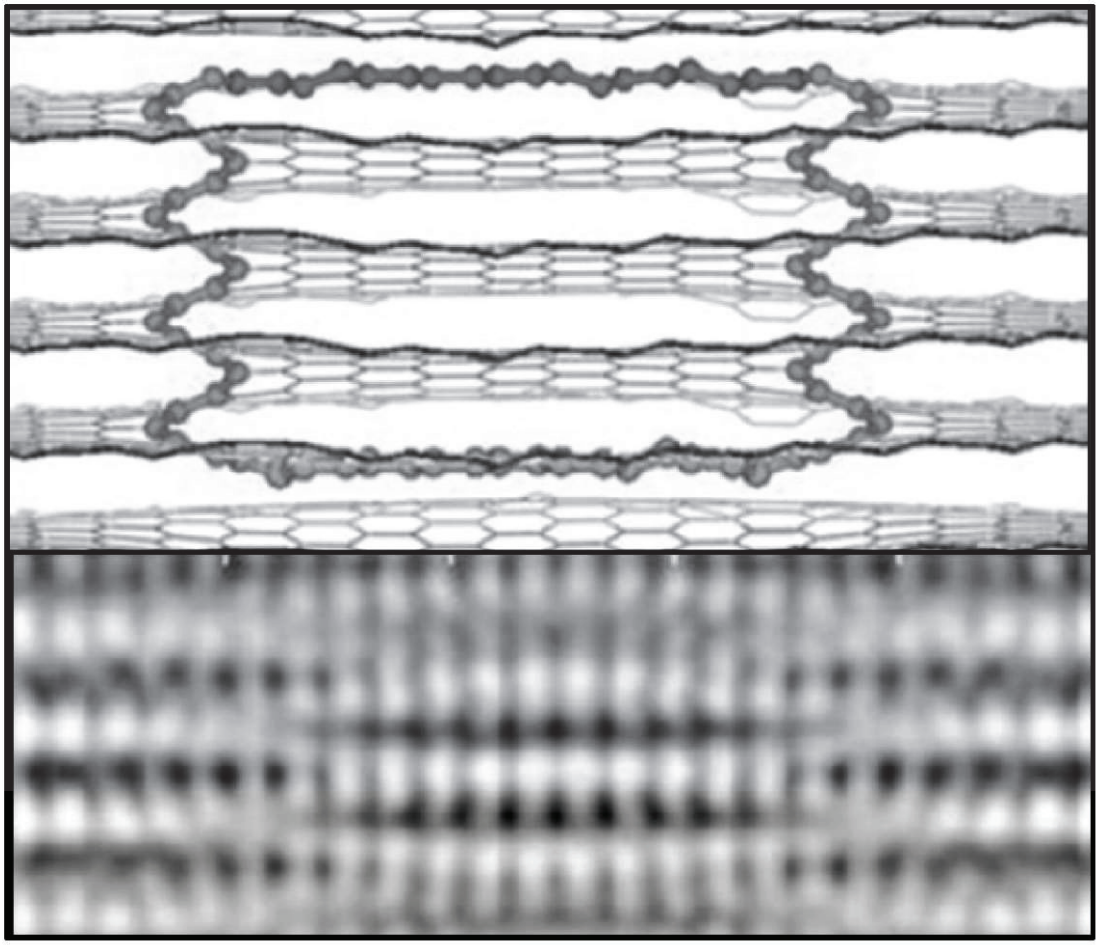


FIG. 12D

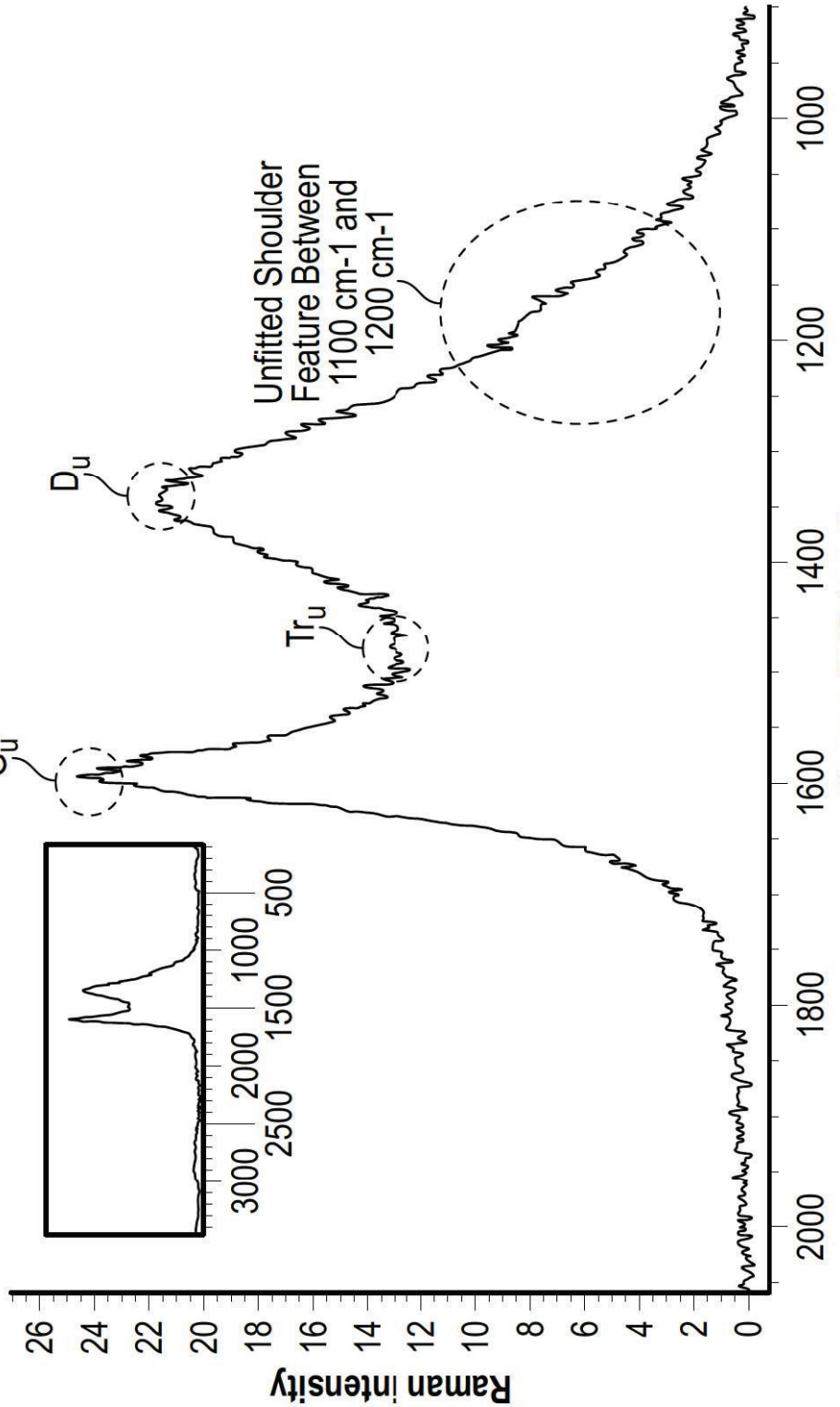

Raman intensity
0
2
4
6
8
10
12
14
16
18
20
22
24
26
2000
1800
1600
1400
1200
1000
Raman Shift (cm-1)
$G_u$
$Tr_u$
$D_u$
Unfitted Shoulder Feature Between 1100 cm-1 and 1200 cm-1
3000
2500
2000
1500
1000
500

FIG. 13

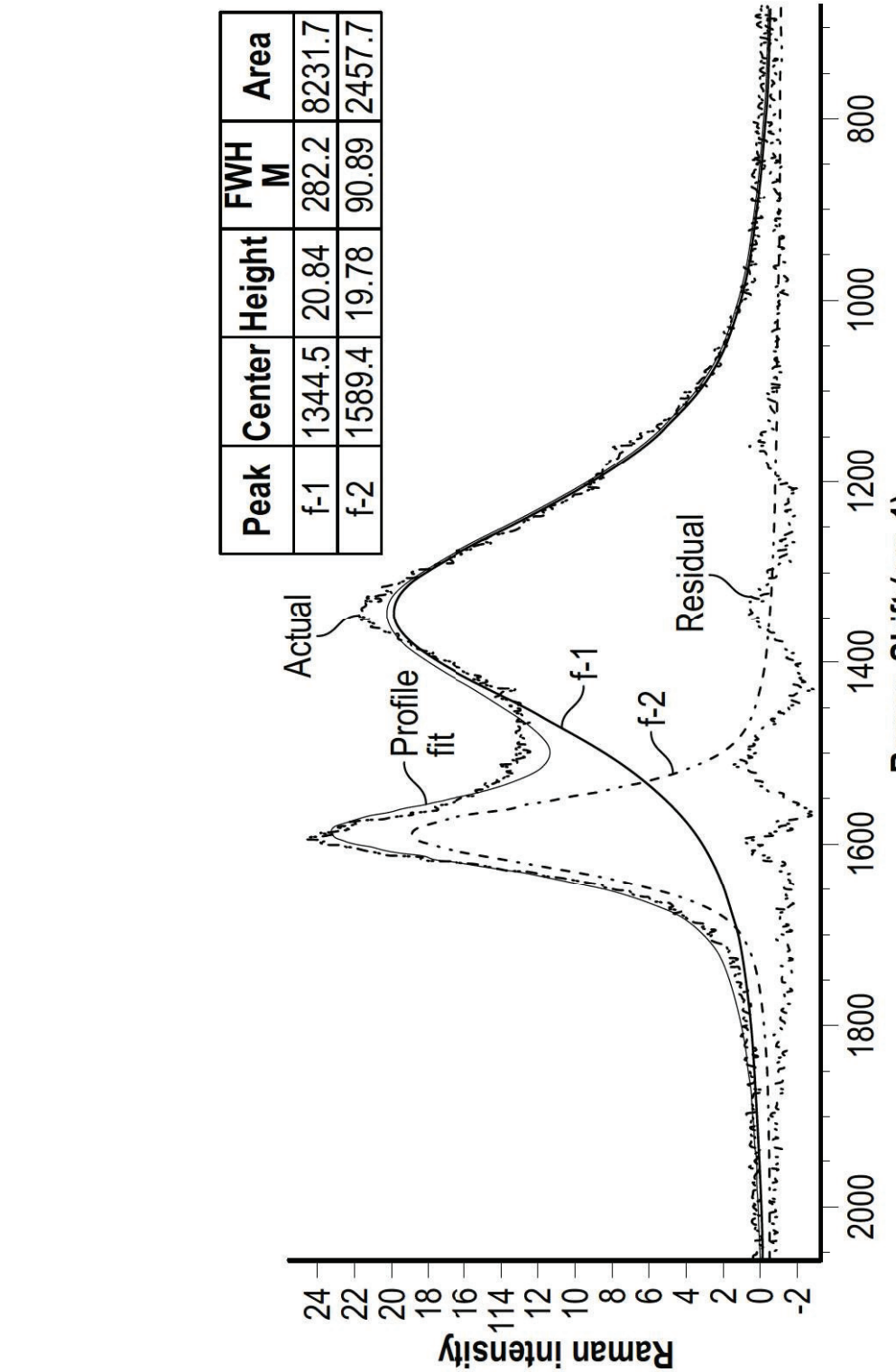

Peak | Center | Height | FWHM | Area
f-1 | 1344.5 | 20.84 | 282.2 | 8231.7
f-2 | 1589.4 | 19.78 | 90.89 | 2457.7
Actual
Profile fit
f-1
f-2
Residual
Raman intensity
Raman Shift (cm-1)
24
22
20
18
16
14
12
10
8
6
4
2
0
-2
2000
1800
1600
1400
1200
1000
800

FIG. 14

| Peak # | Center | Height | FWHM | Area |
|---|---|---|---|---|
| f-1 | 1339.8 | 21.78 | 252..5 | 8397.8 |
| f-2 | 1566.5 | 9.047 | 146.9 | 1415.1 |
| f-3 | 1596.8 | 12.57 | 57.89 | 927.91 |

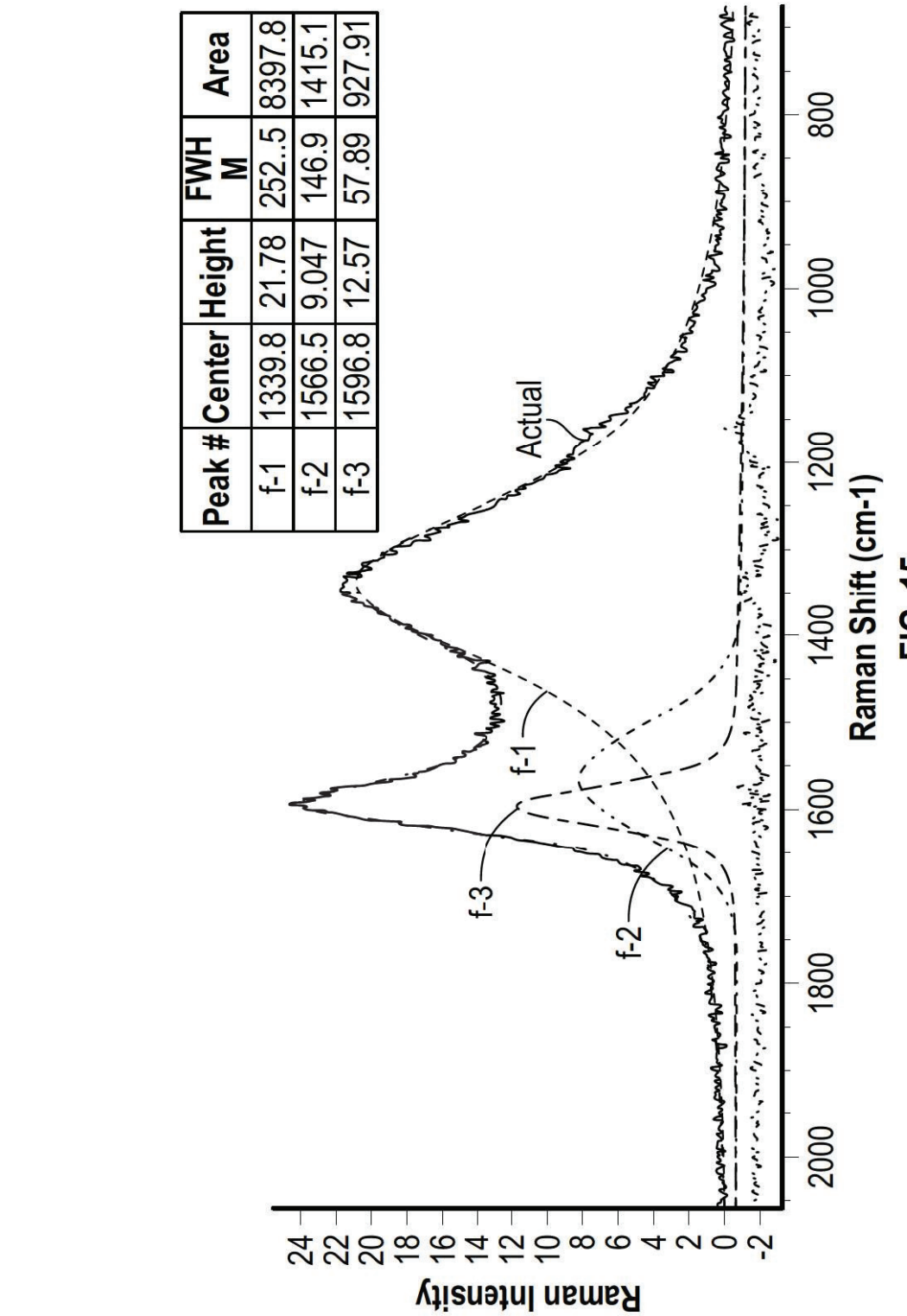



FIG. 15

| Peak # | Center | Height | FWHM | Gauss | Area |
|---|---|---|---|---|---|
| f-1 | 1185 | 6.35 | 180.0 | .720 | 1375 |
| f-2 | 1343 | 19.33 | 167.2 | .999 | 3440 |
| f-3 | 1514 | 8.99 | 153.8 | .889 | 1548 |
| f-4 | 1596 | 19.51 | 77.1 | .118 | 2266 |

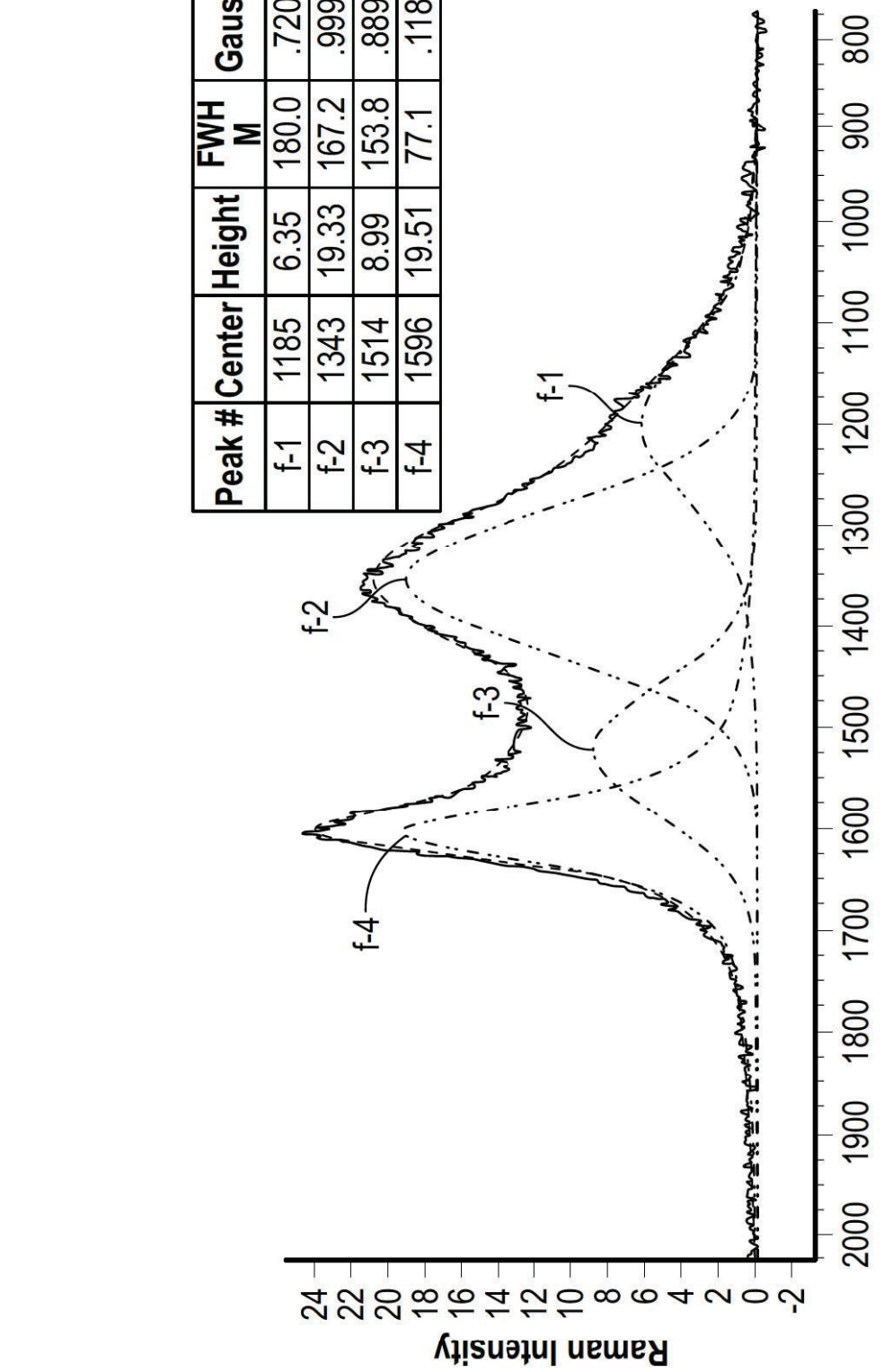



FIG. 16

| Peak # | Center | Height | FWHM | Gauss | Area |
|---|---|---|---|---|---|
| f-1 | 1180 | 1.29 | 167.1 | .606 | 272 |
| f-2 | 1349 | 4.76 | 154.3 | .639 | 914 |
| f-3 | 1482 | 2.41 | 153.4 | .552 | 477 |
| f-4 | 1596 | 5.29 | 99.5 | .409 | 717 |

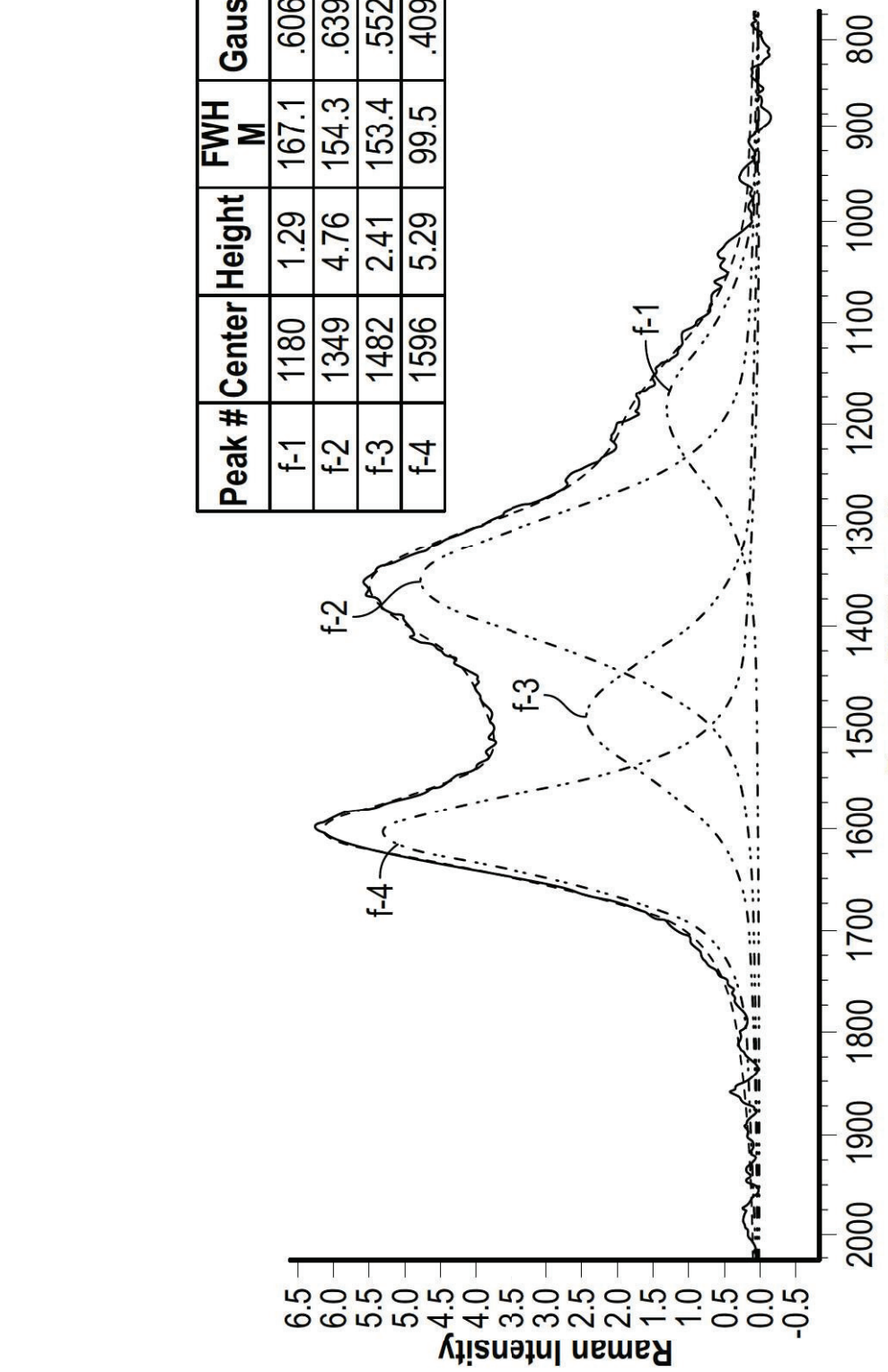



FIG. 17

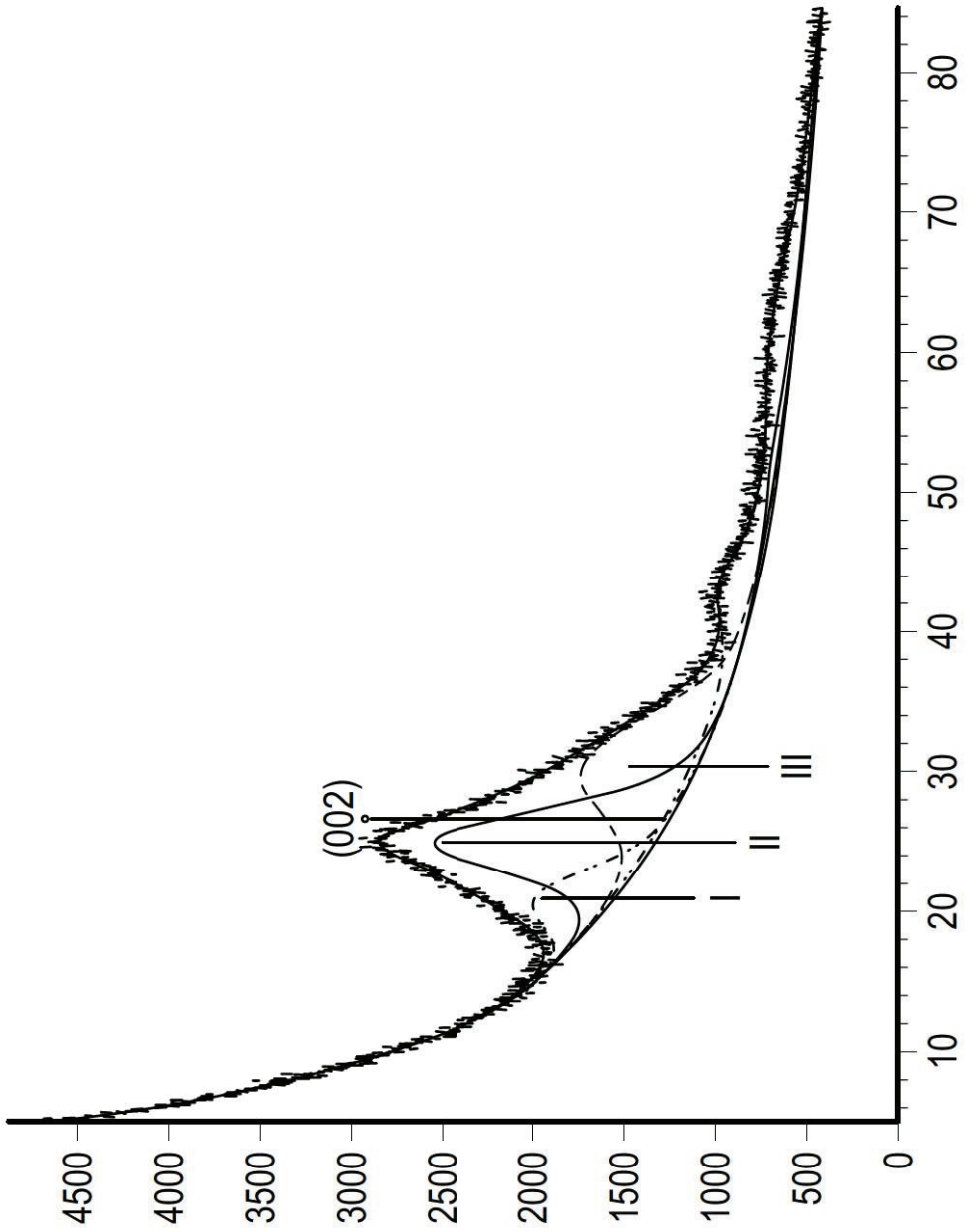

4500
4000
3500
3000
2500
2000
1500
1000
500
0
10
20
30
40
50
60
70
80
(002)
I
II
III

FIG. 18

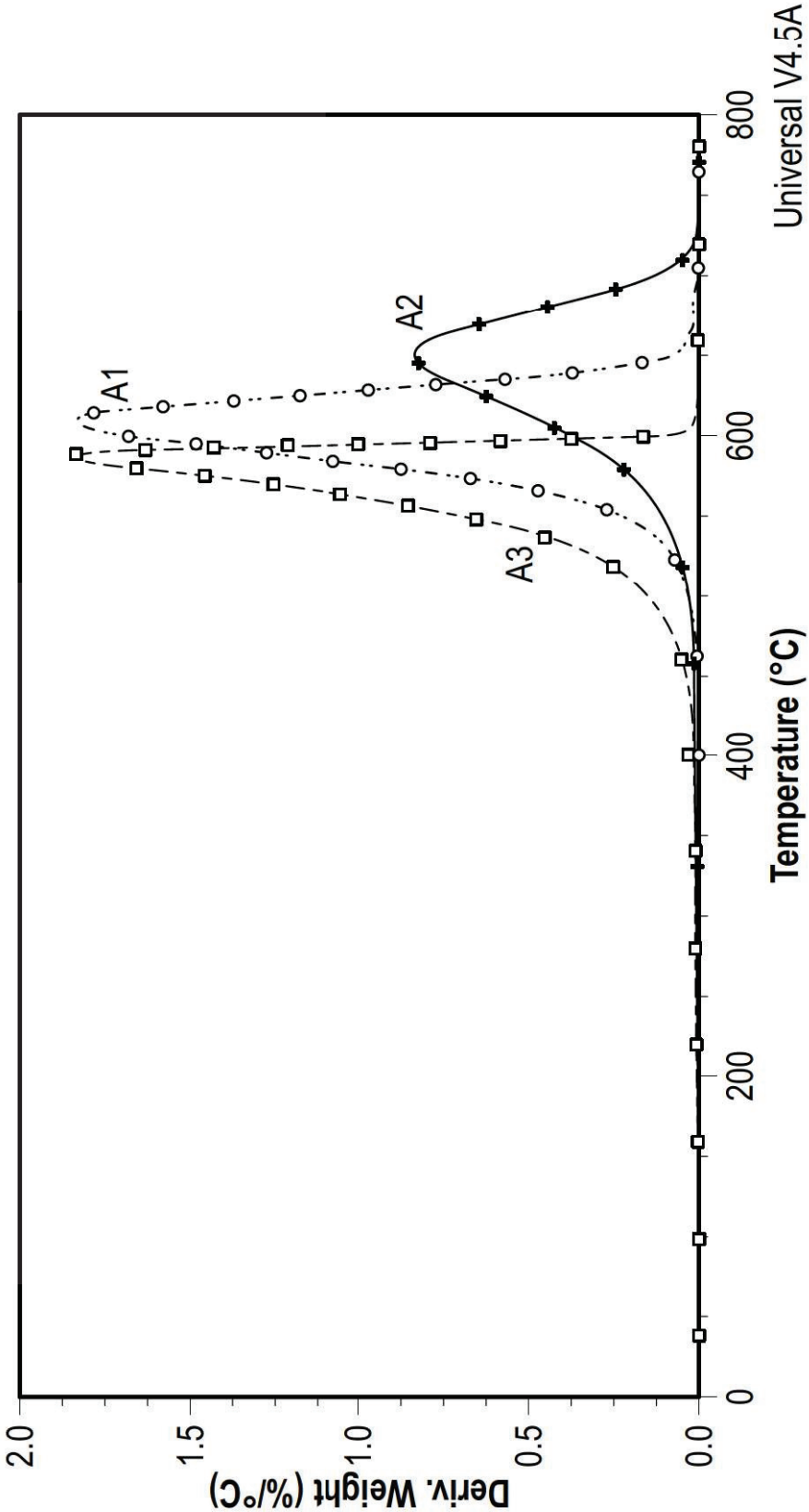

Deriv. Weight (%/°C)
2.0
1.5
1.0
0.5
0.0
0
200
400
600
800
Temperature (°C)
Universal V4.5A
A1
A2
A3

FIG. 19

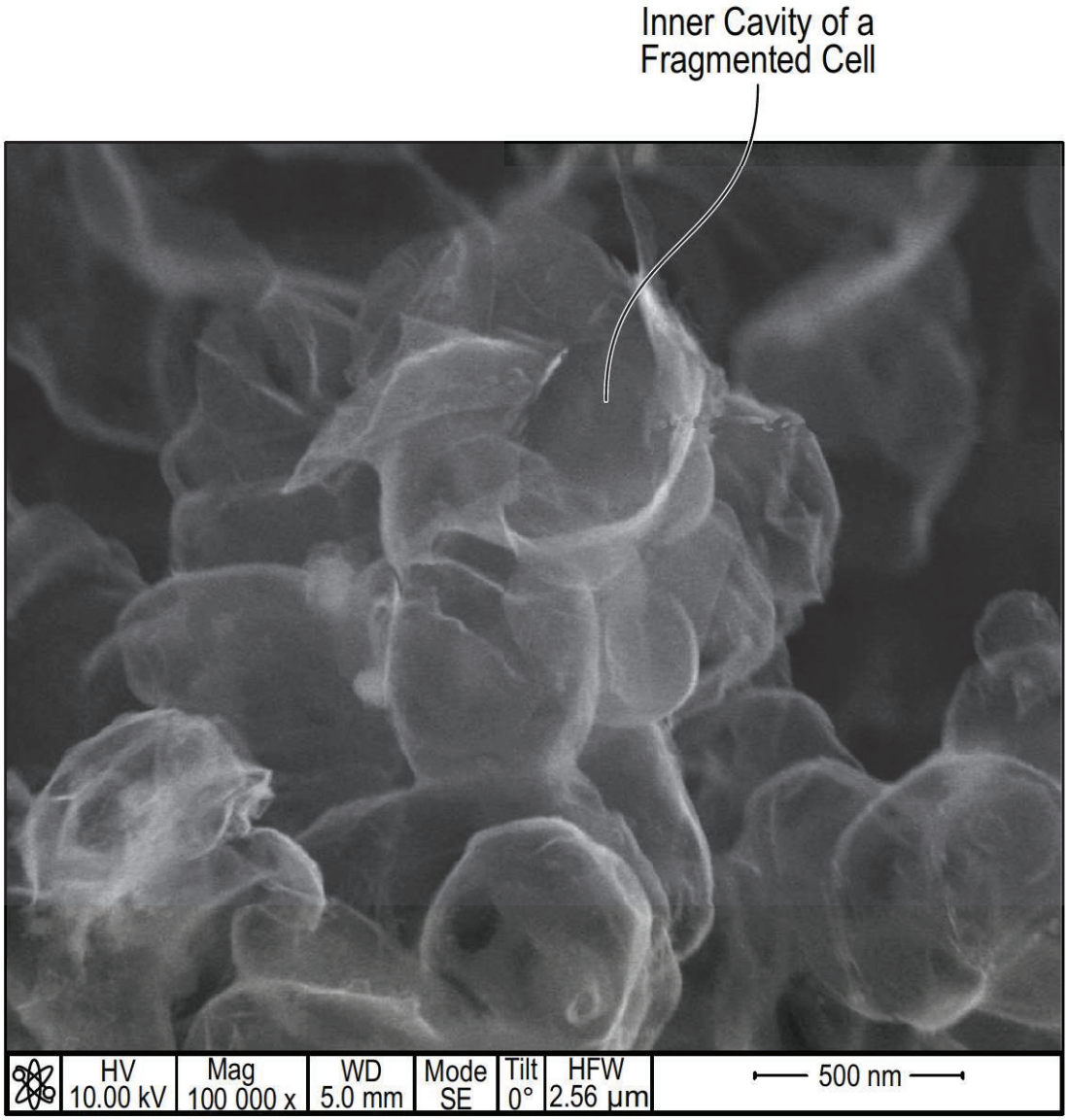

Inner Cavity of a
Fragmented Cell
HV
10.00 kV
Mag
100 000 x
WD
5.0 mm
Mode
SE
Tilt
0°
HFW
2.56 µm
500 nm

FIG. 20

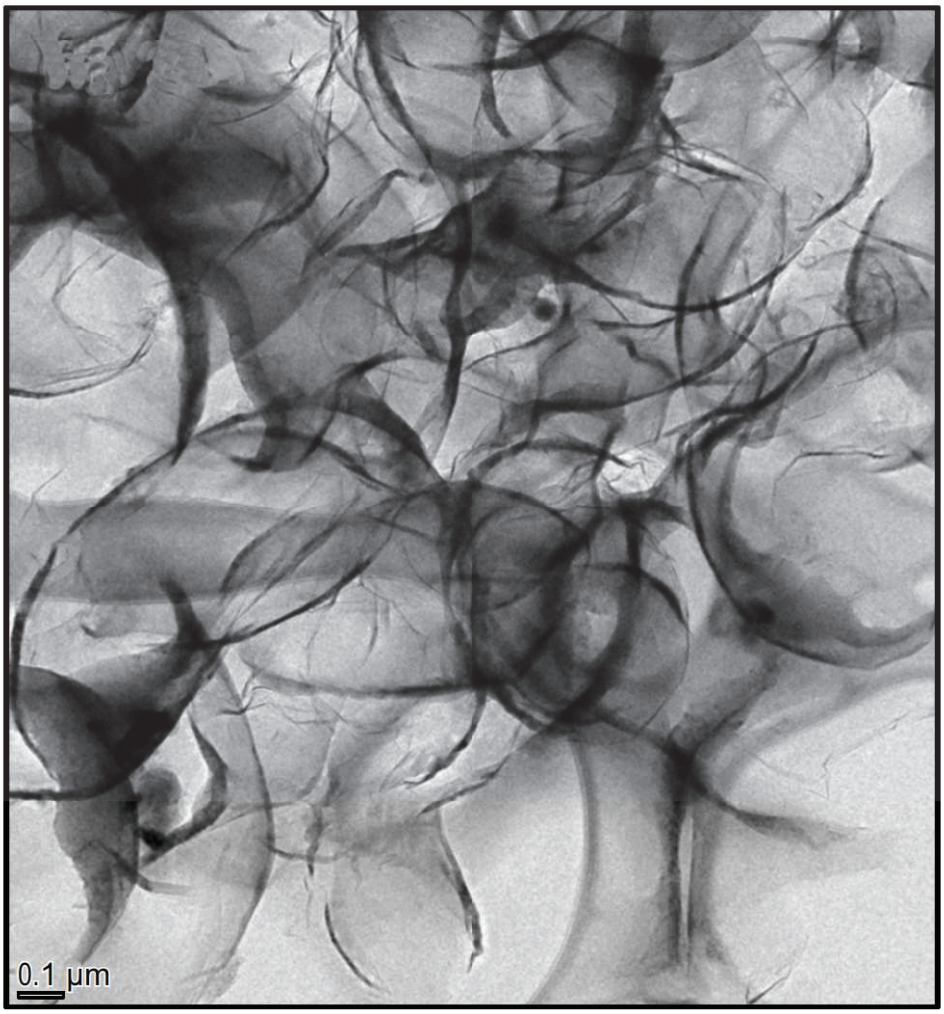



FIG. 21A




FIG. 21B

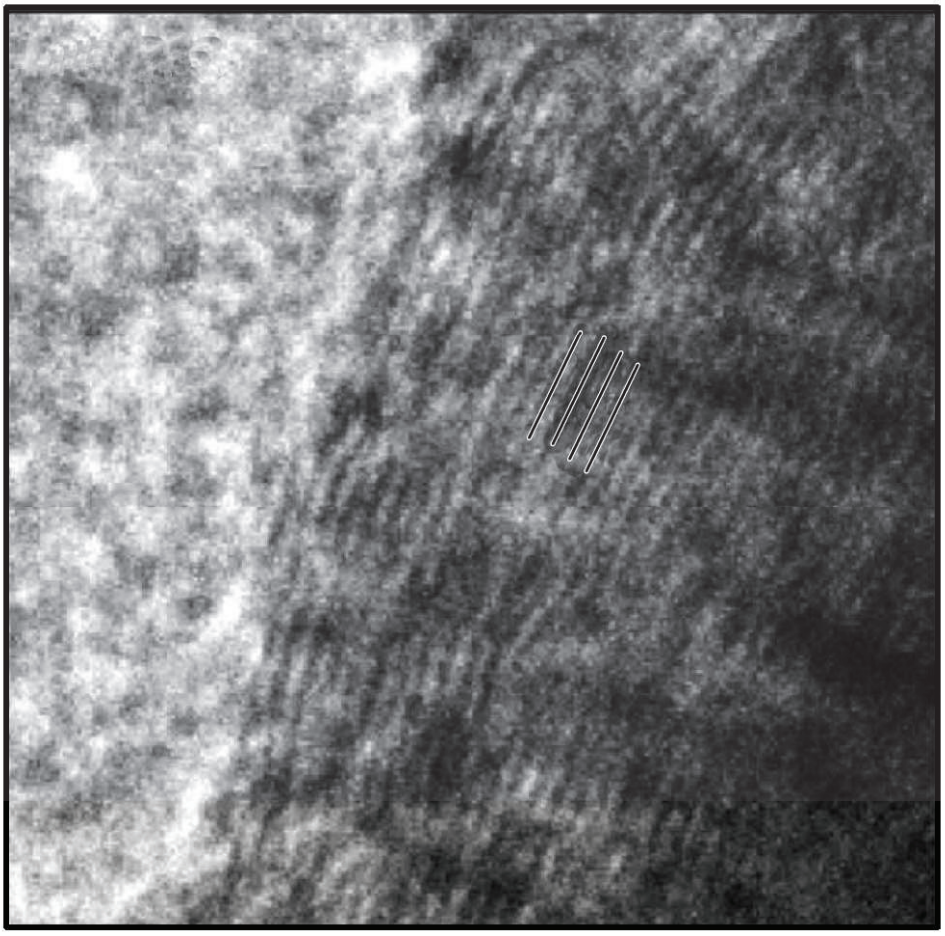


FIG. 21C

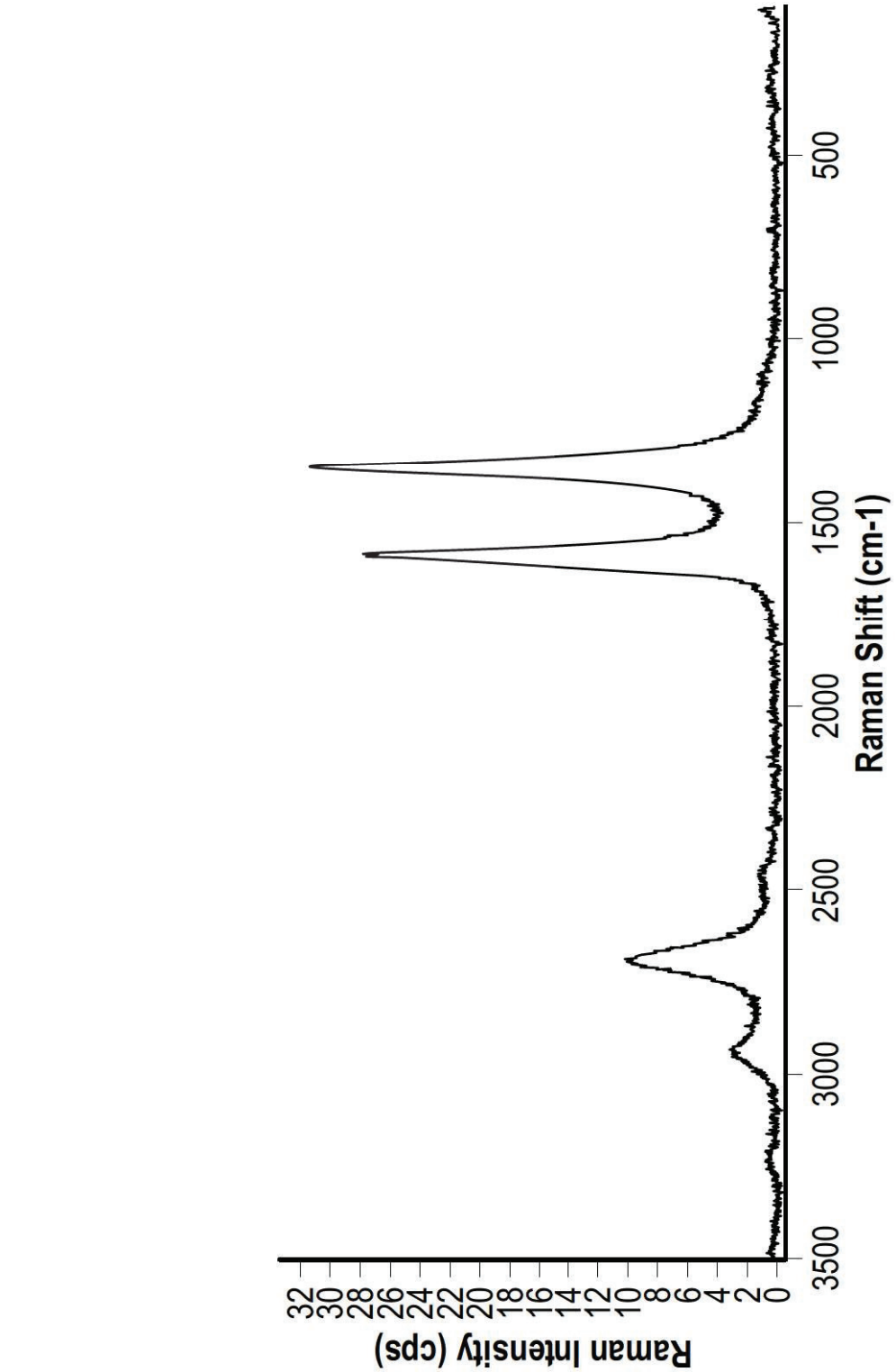

Raman Intensity (cps)
32
30
28
26
24
22
20
18
16
14
12
10
8
6
4
2
0
3500
3000
2500
2000
1500
1000
500
Raman Shift (cm-1)

FIG. 22

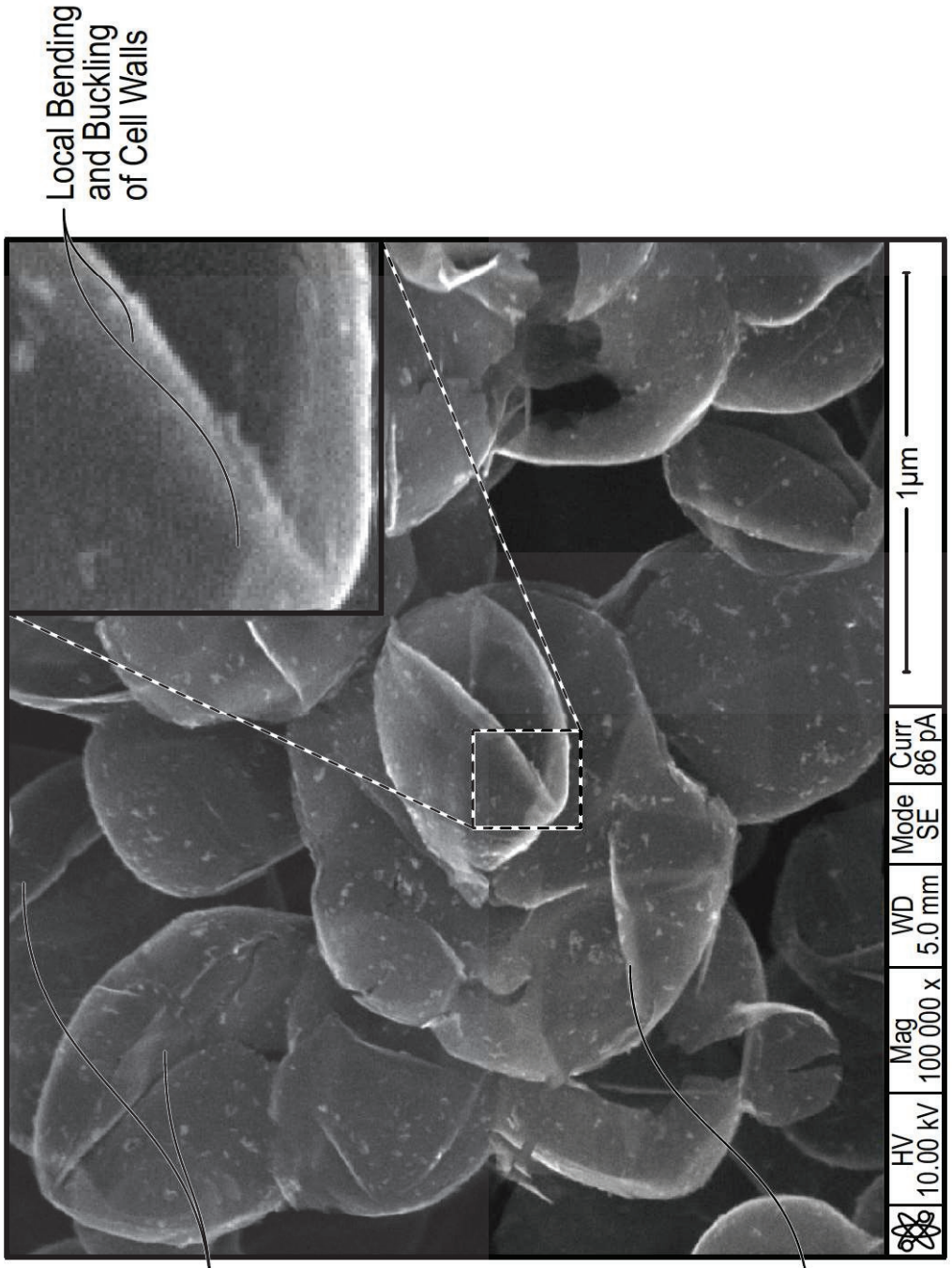

Local Bending and Buckling of Cell Walls
Recurring Linear Features Observed Post-Compression
Recurring Linear Features Observed Post-Compression
HV 10.00 kV
Mag 100 000 x
WD 5.0 mm
Mode SE
Curr 86 pA
1µm

FIG. 23

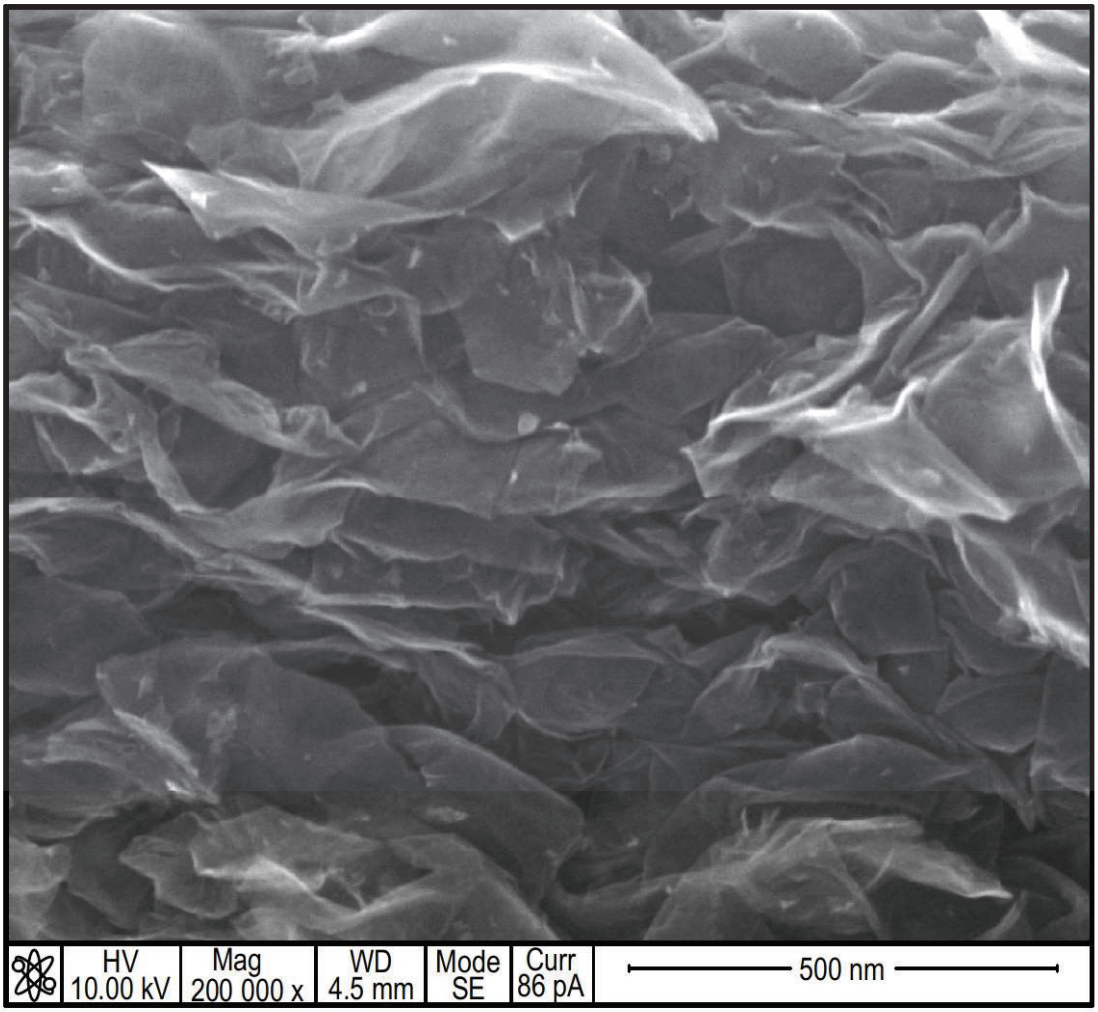



FIG. 24

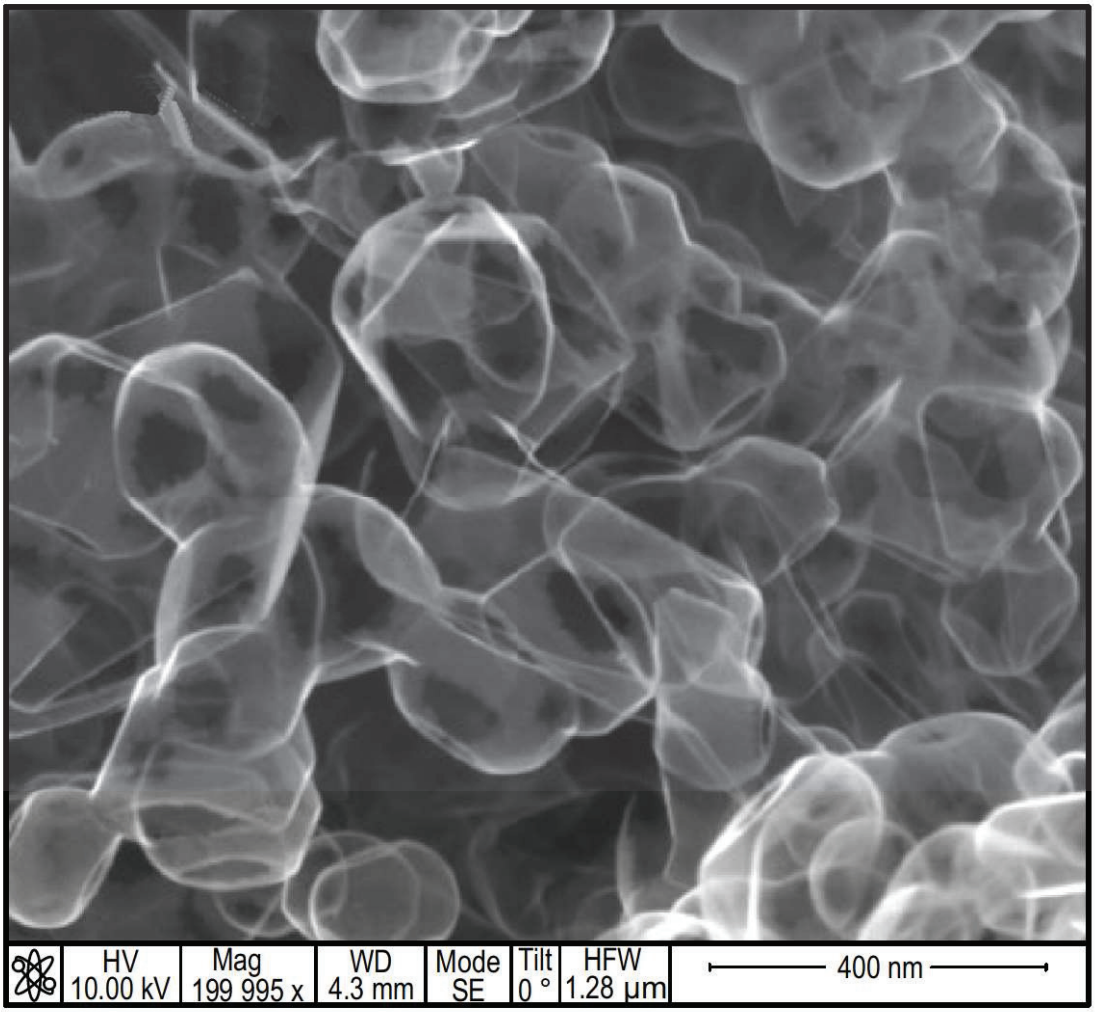



FIG. 25A

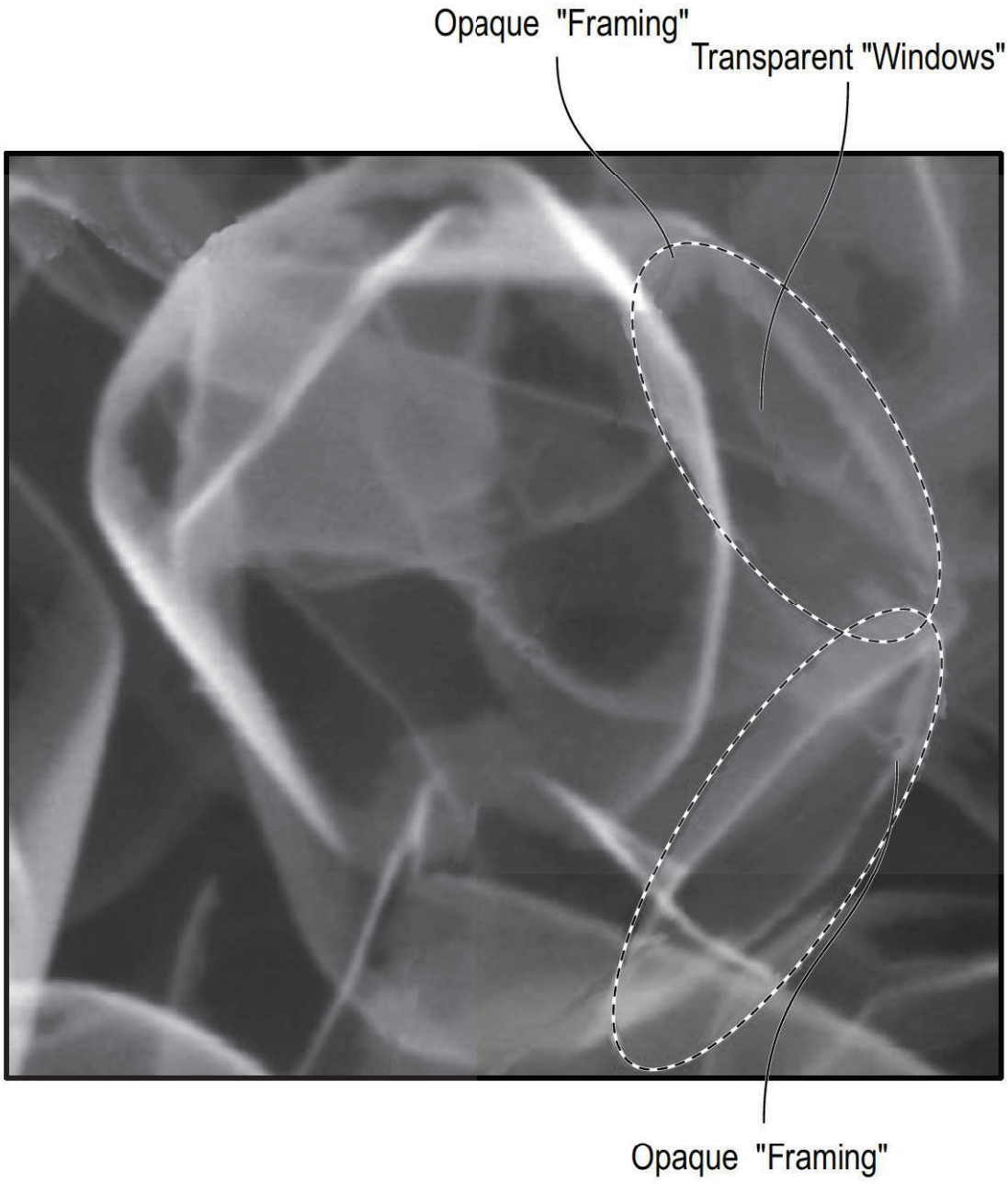



FIG. 25B

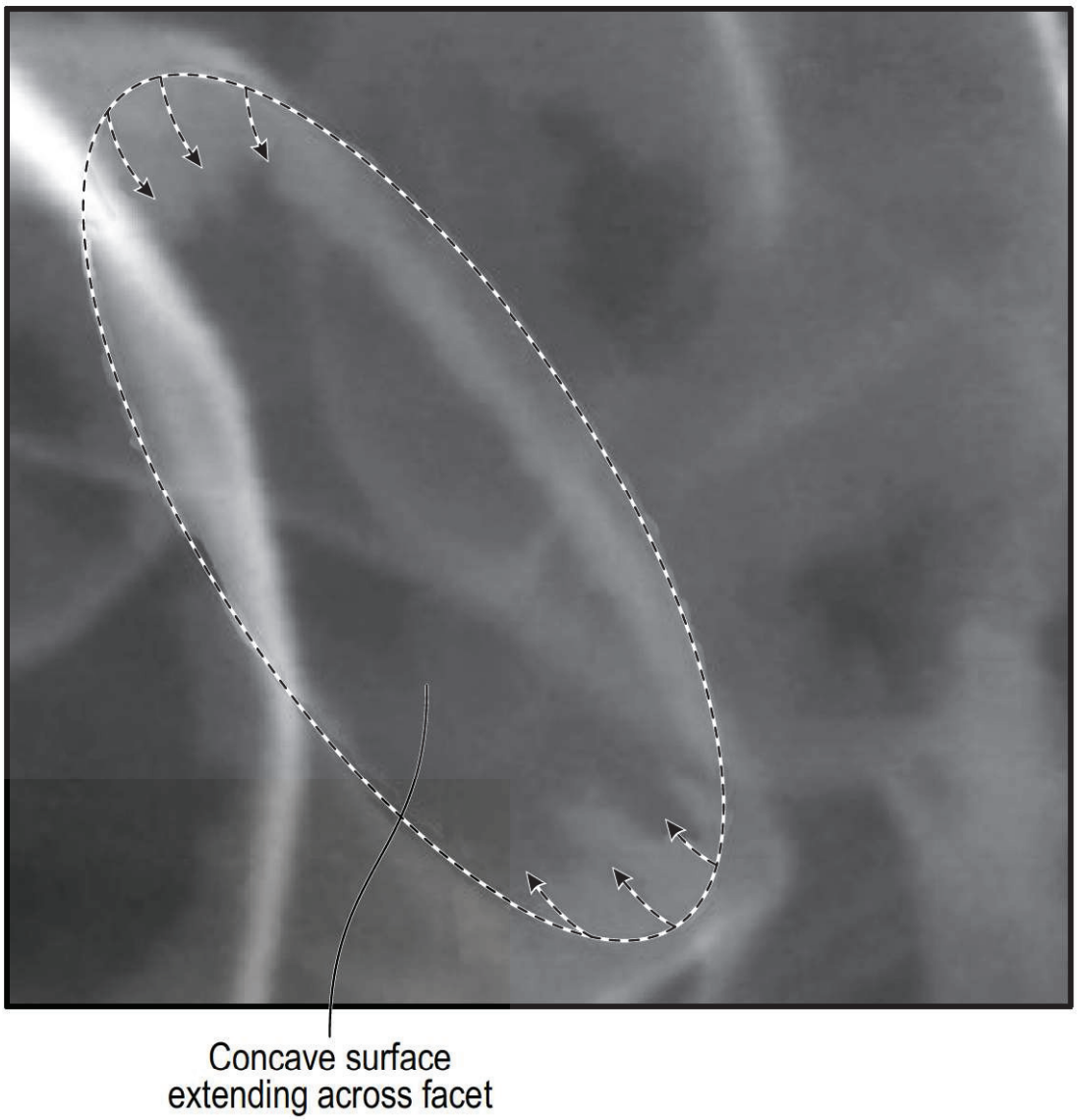



FIG. 25C

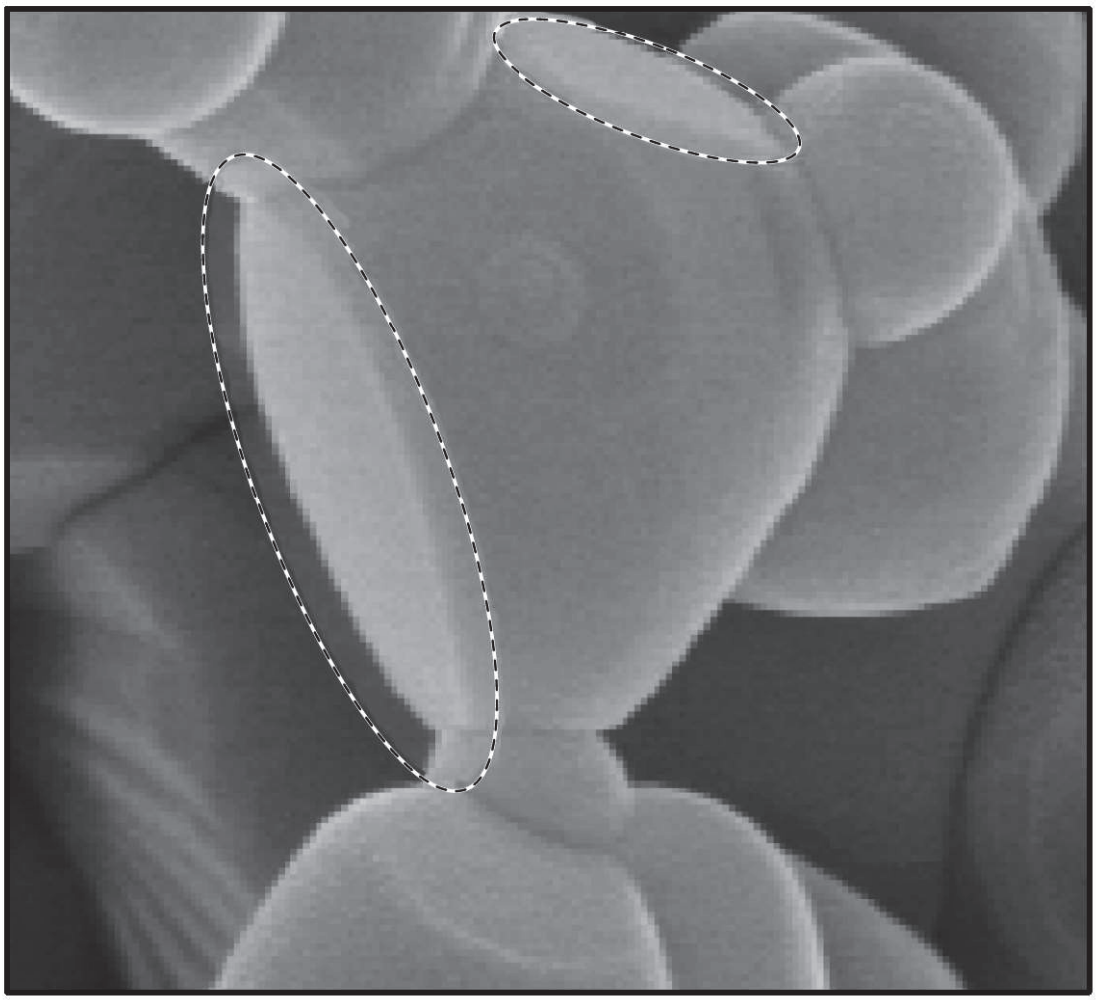


FIG. 26

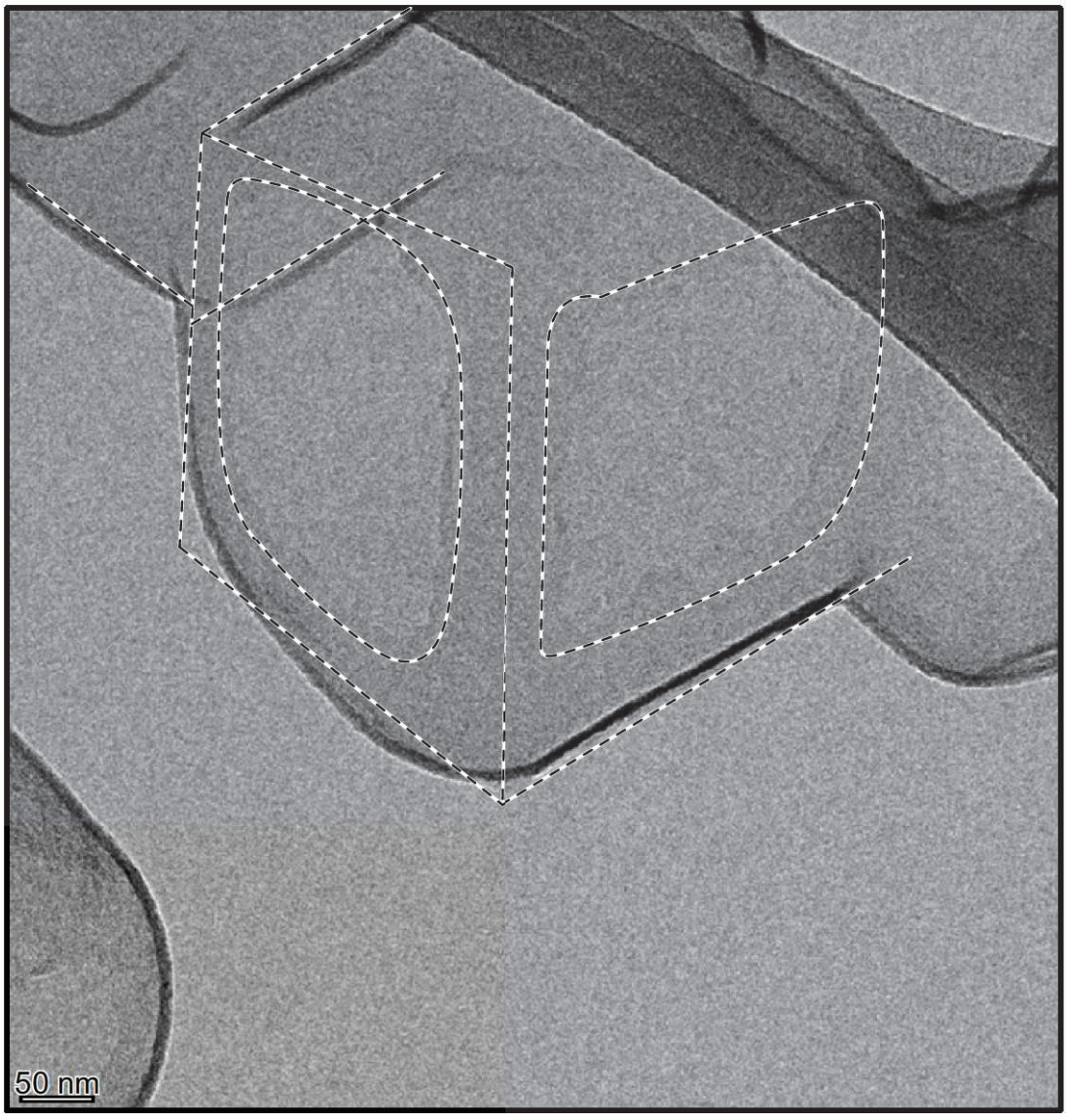



FIG. 27A

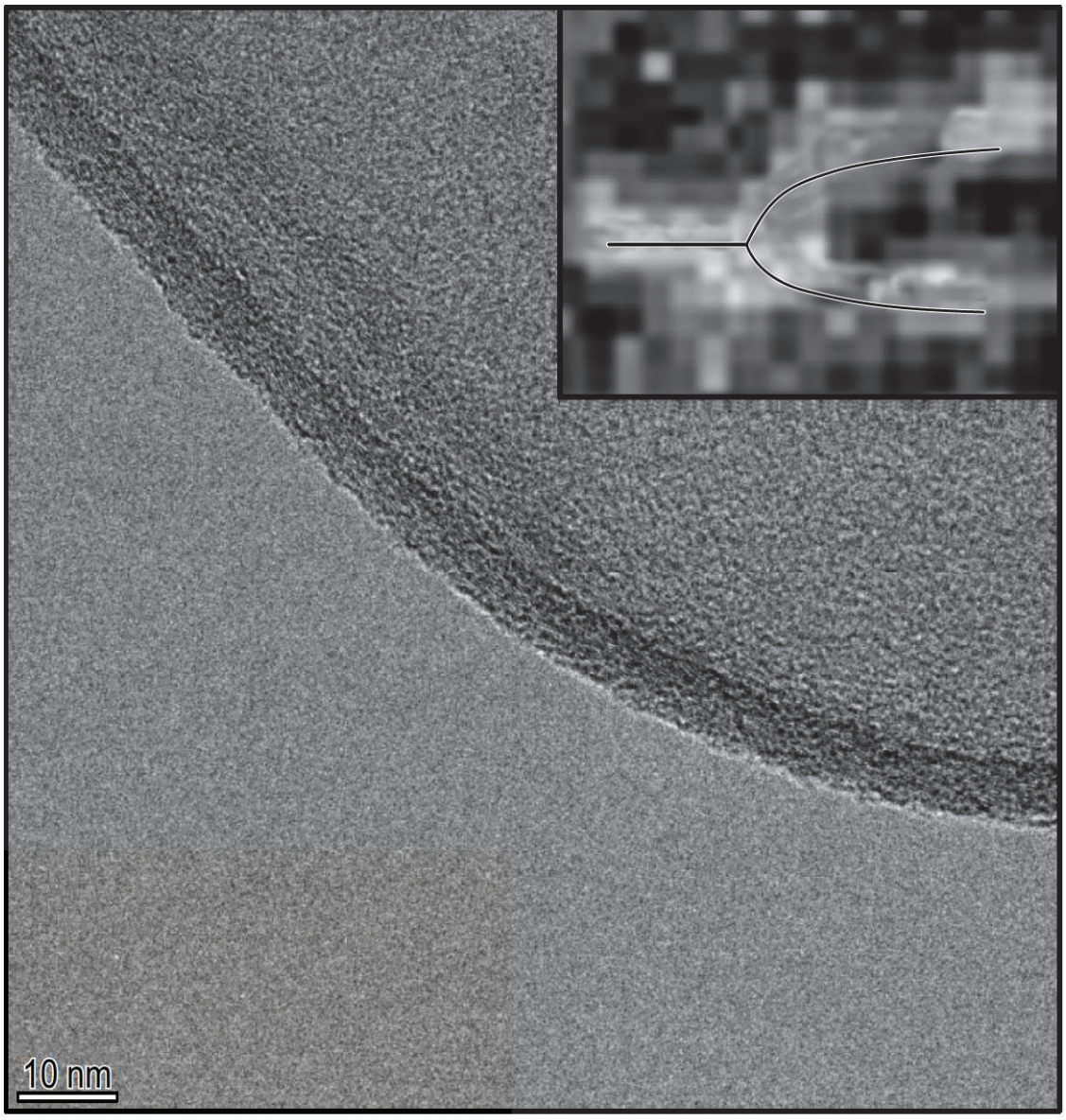



FIG. 27B

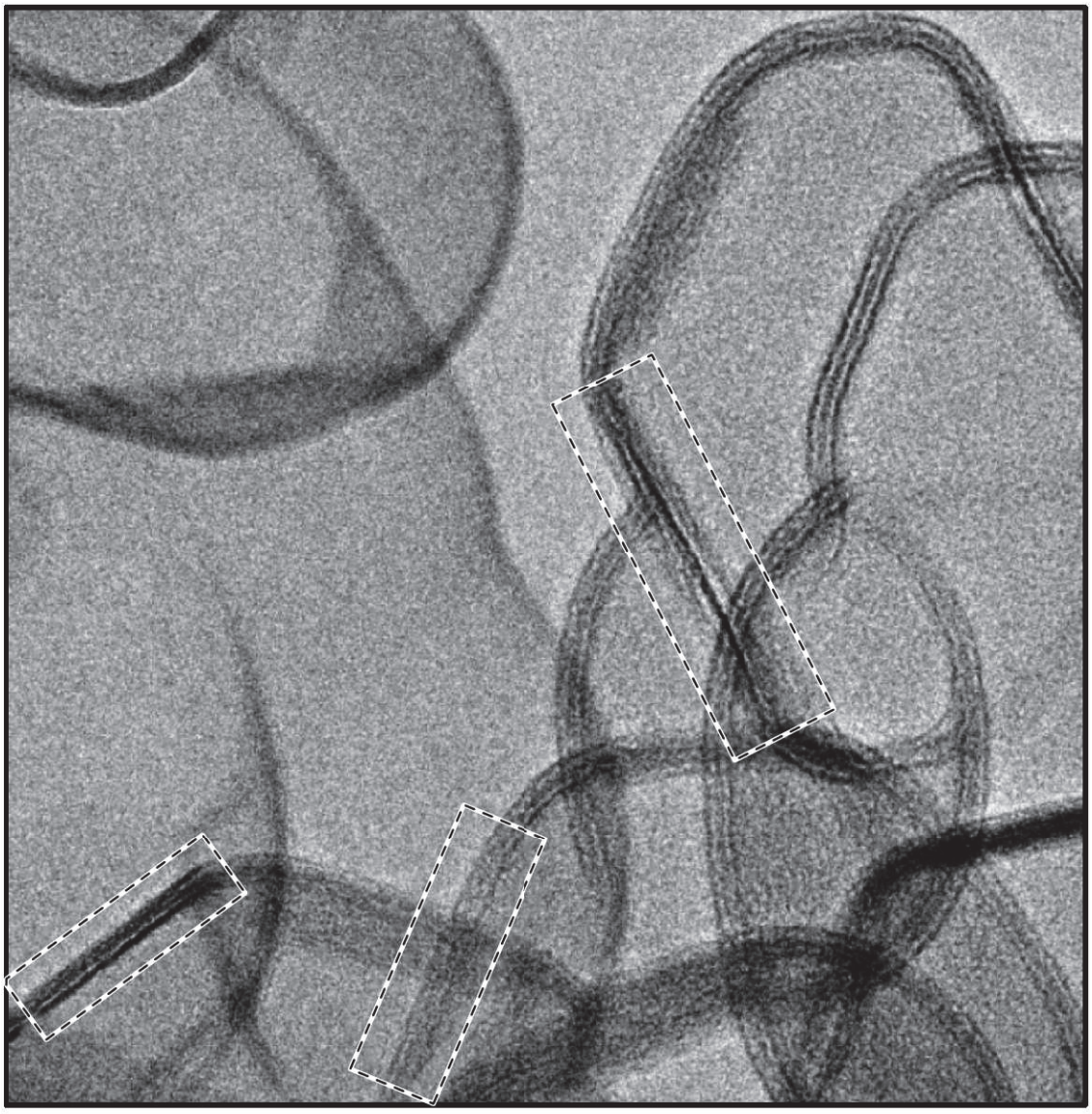


FIG. 27C

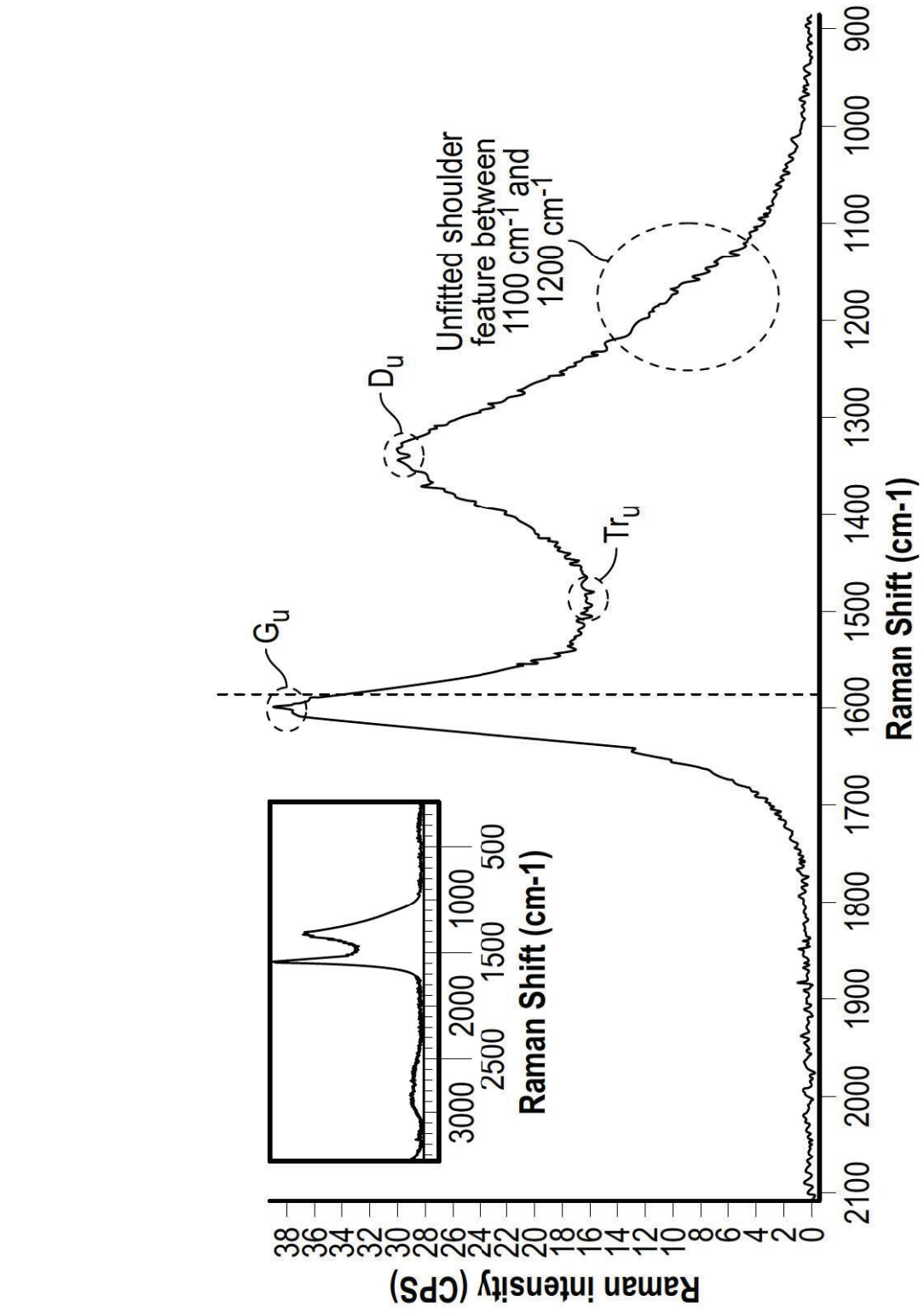

Raman intensity (CPS)
0
2
4
6
8
10
12
14
16
18
20
22
24
26
28
30
32
34
36
38
2100
2000
1900
1800
1700
1600
1500
1400
1300
1200
1100
1000
900
Raman Shift (cm-1)
$G_u$
$D_u$
$Tr_u$
Unfitted shoulder feature between 1100 cm-1 and 1200 cm-1
3000
2500
2000
1500
1000
500
Raman Shift (cm-1)

FIG. 28

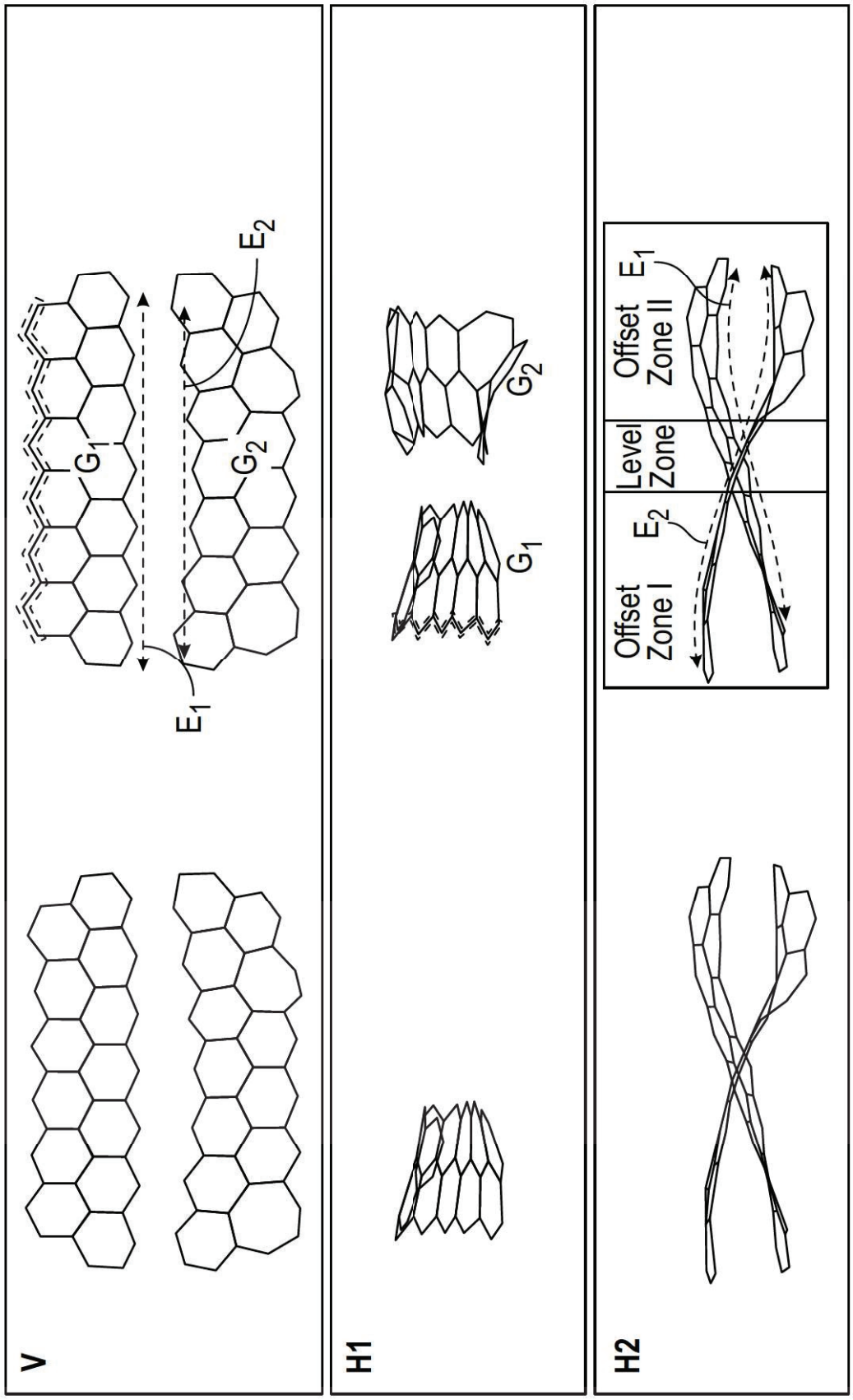



FIG. 29

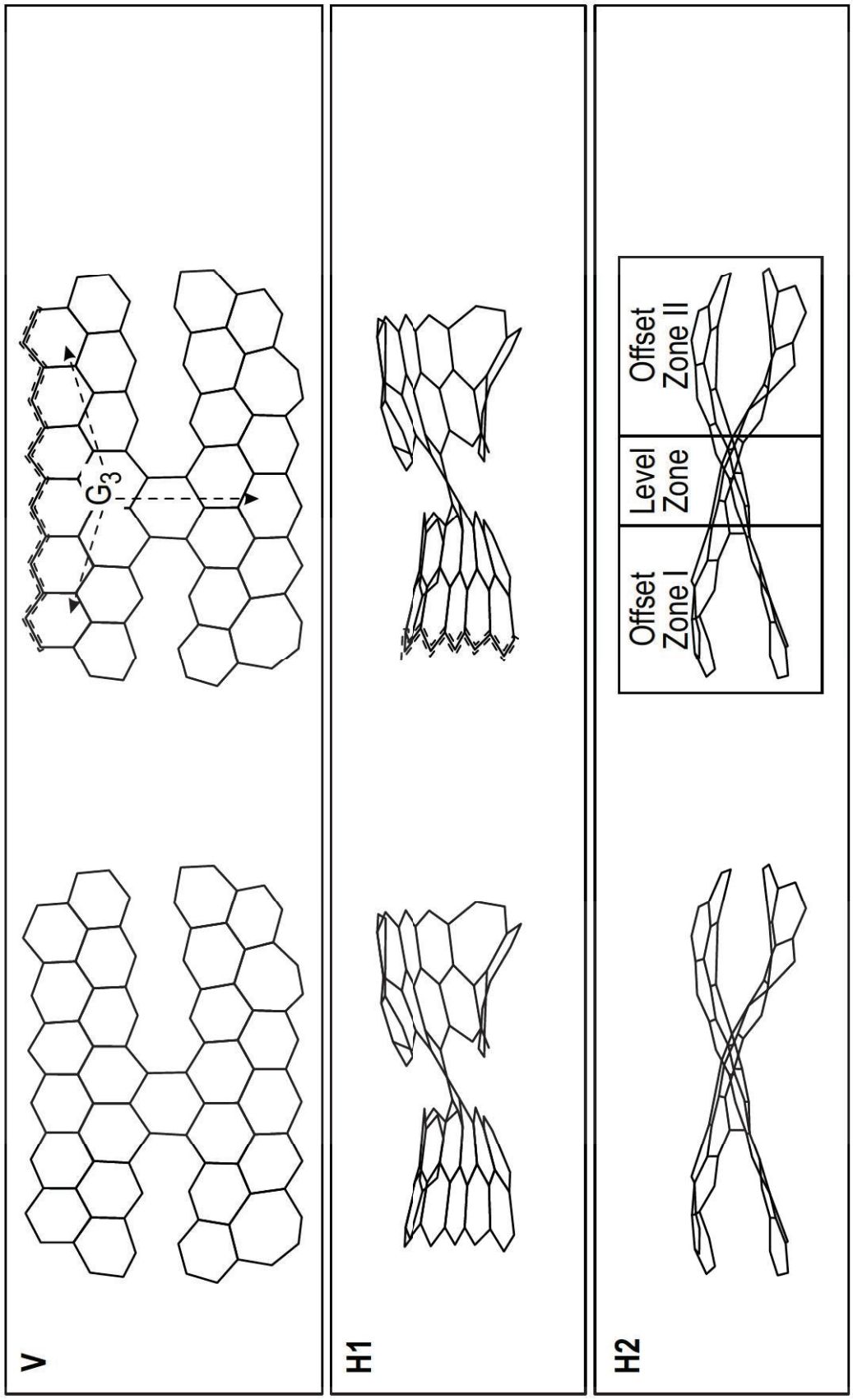



FIG. 30

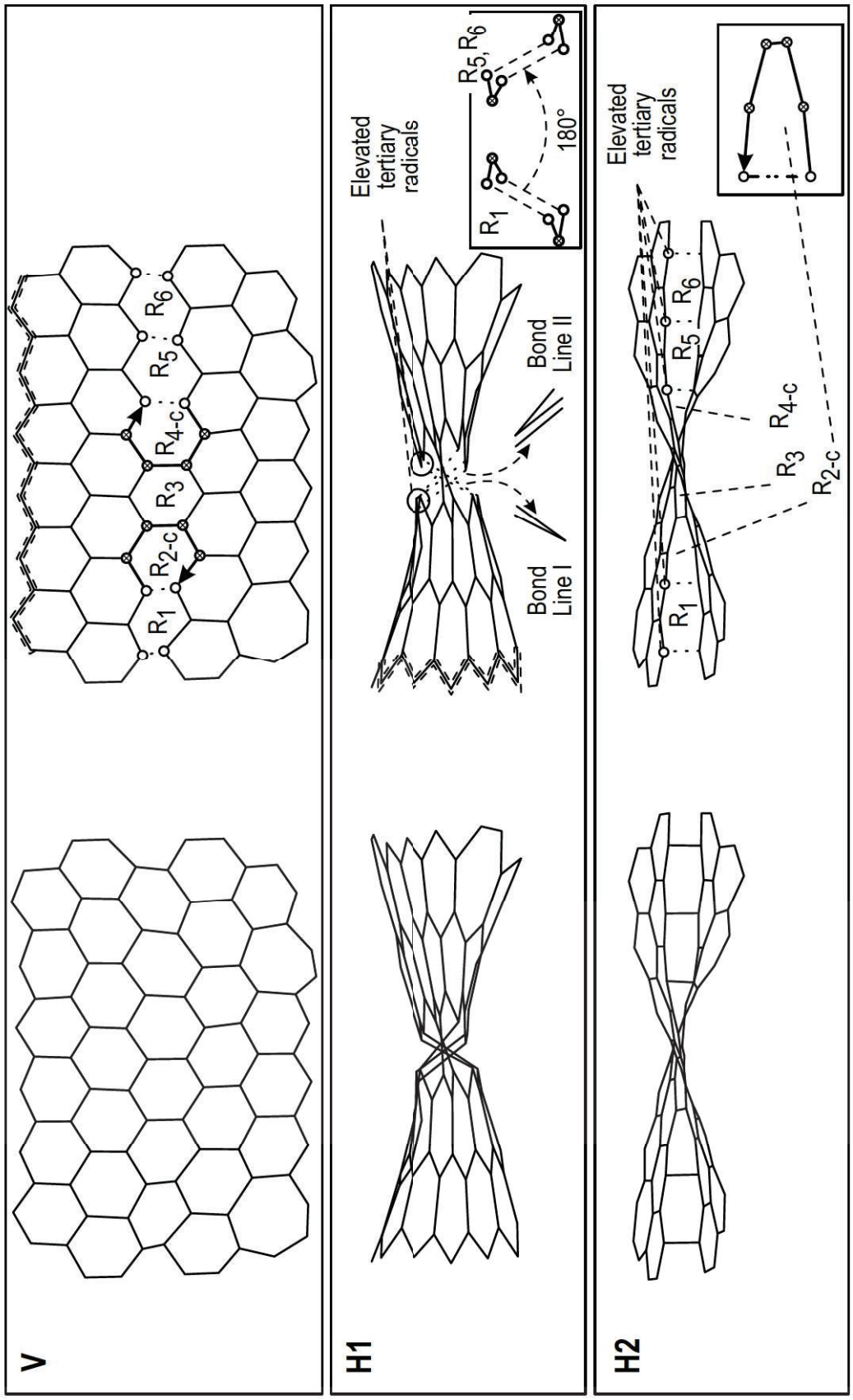

V
H1
H2
R1
R2-c
R3
R4-c
R5
R6
Elevated tertiary radicals
Bond Line I
Bond Line II
180°

FIG. 31

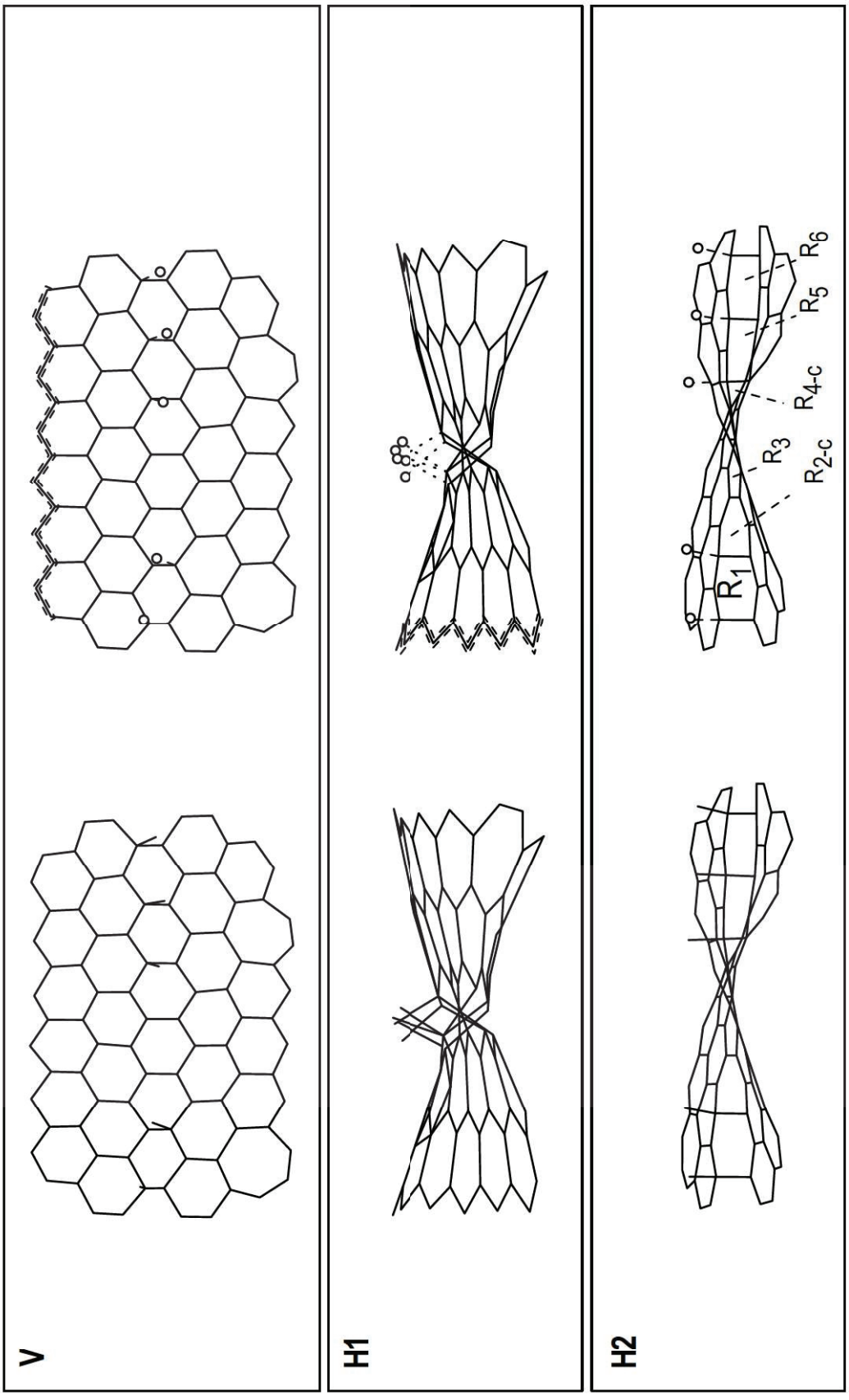



FIG. 32

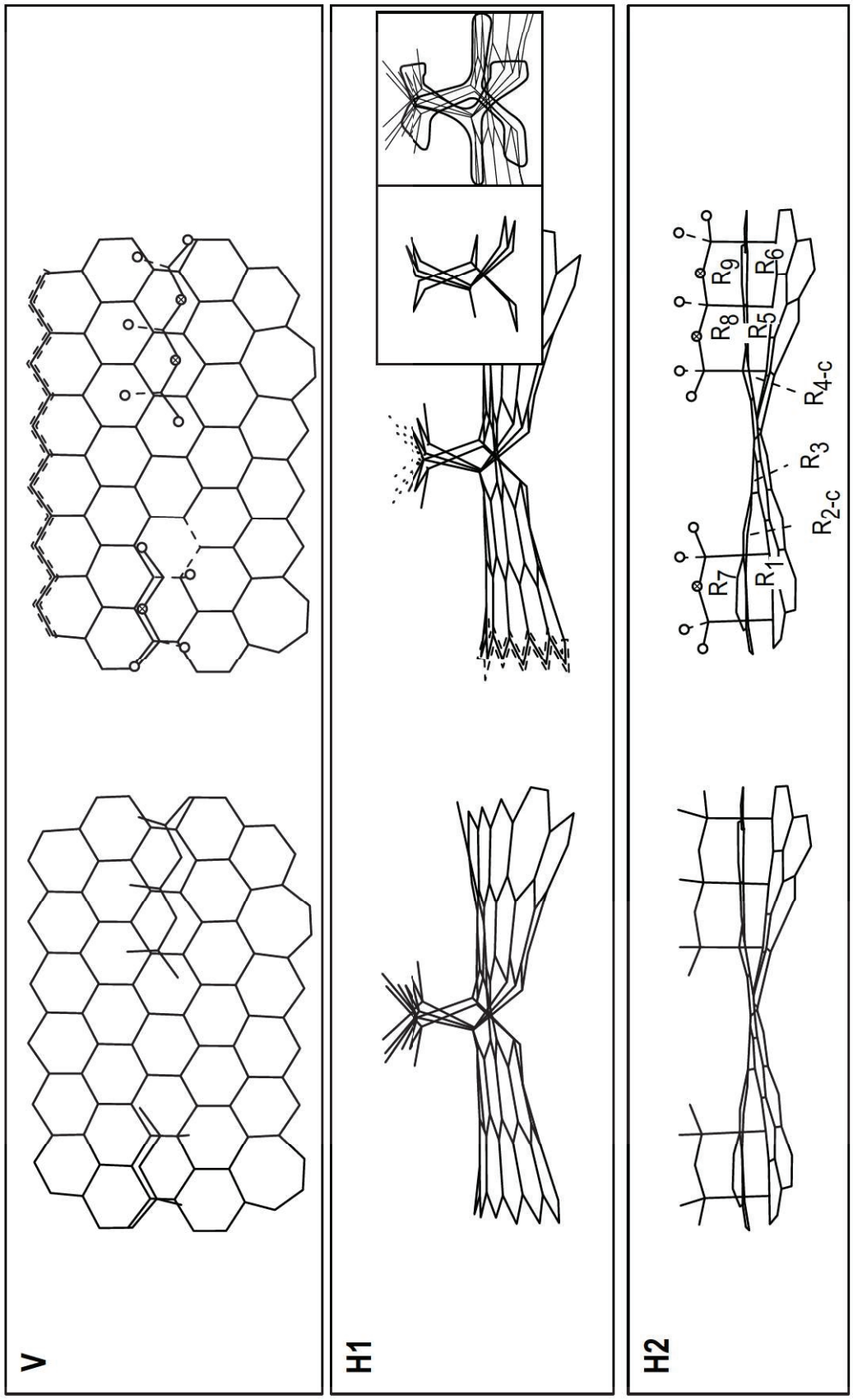



FIG. 33

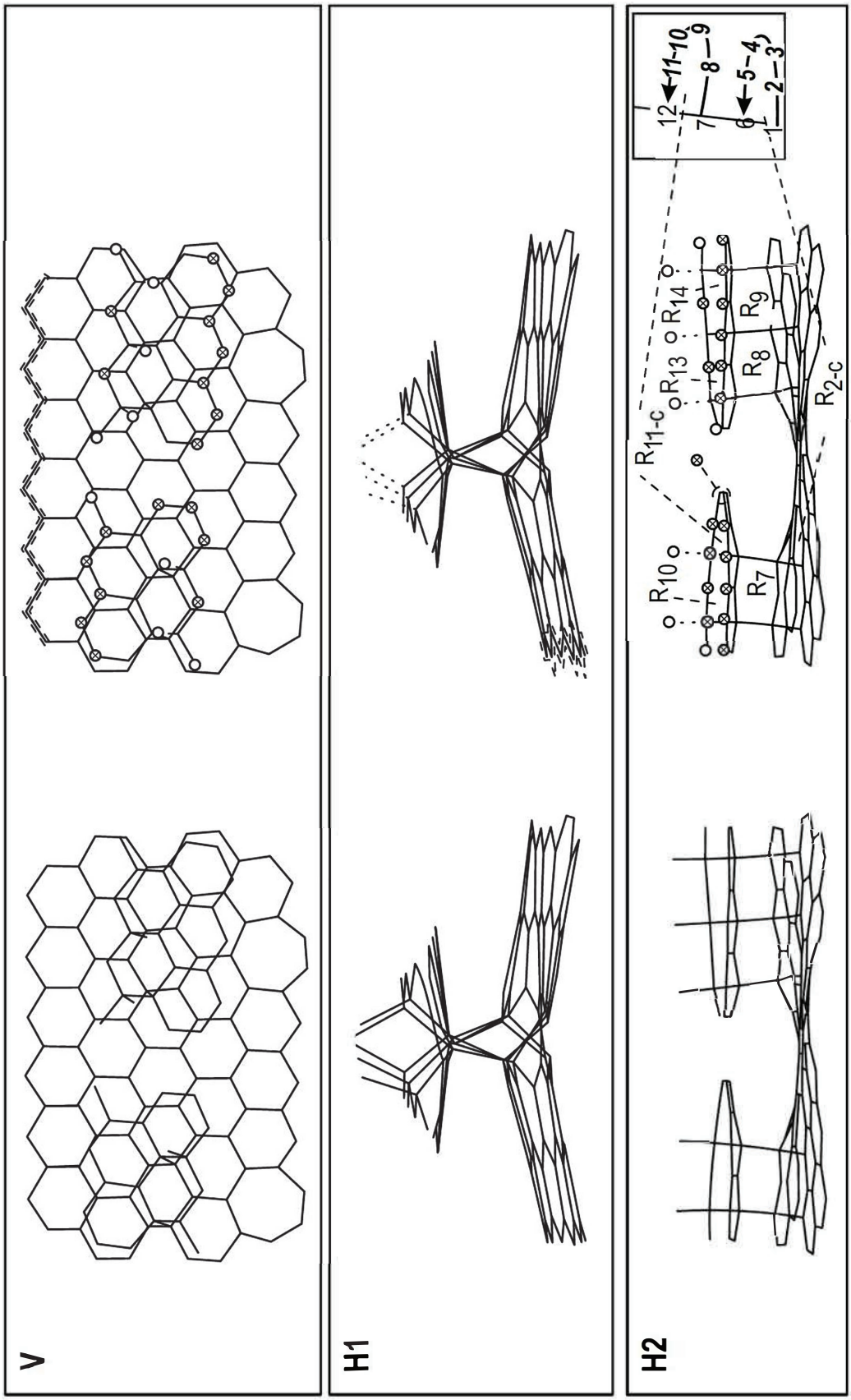



FIG. 34

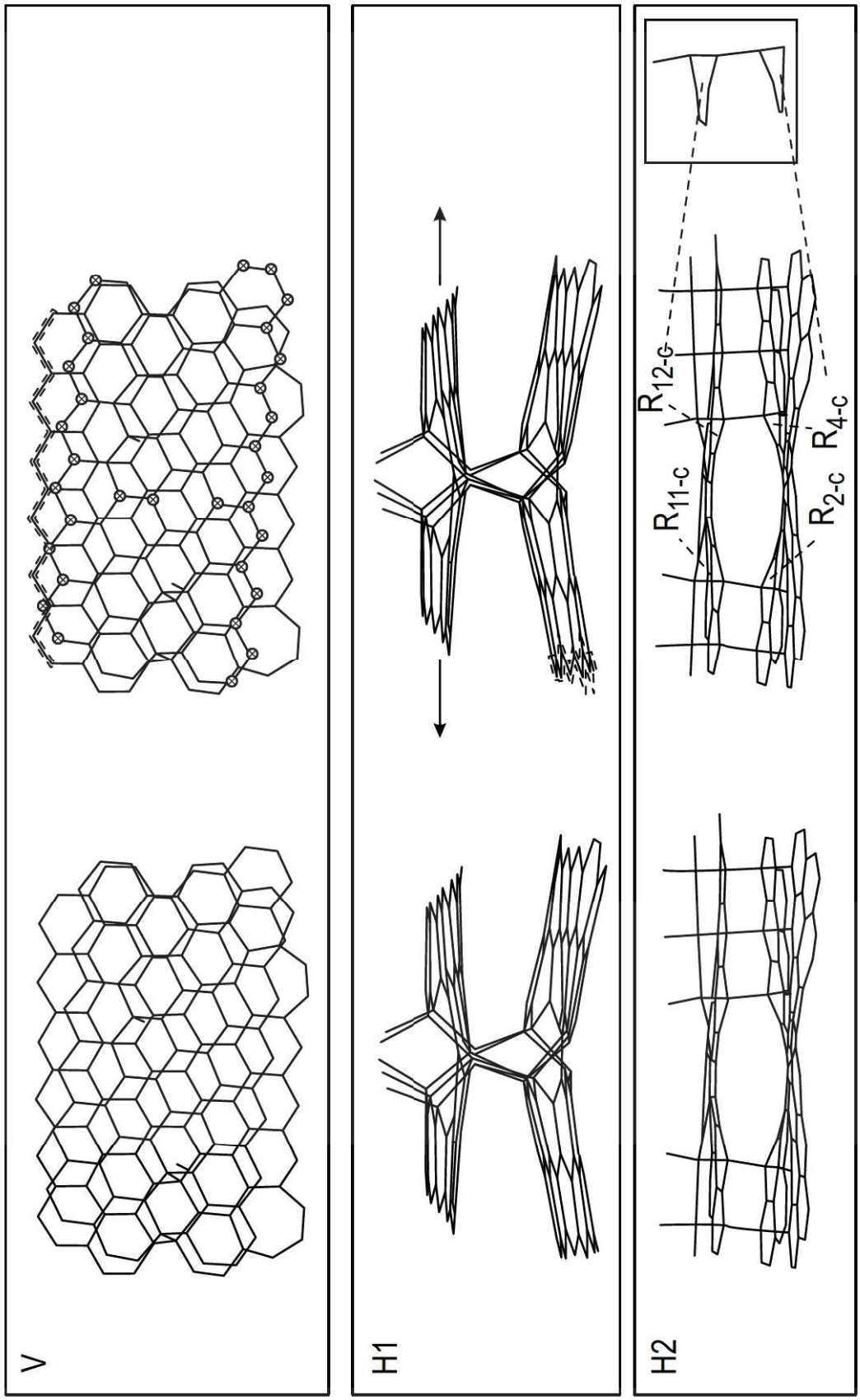



FIG. 35

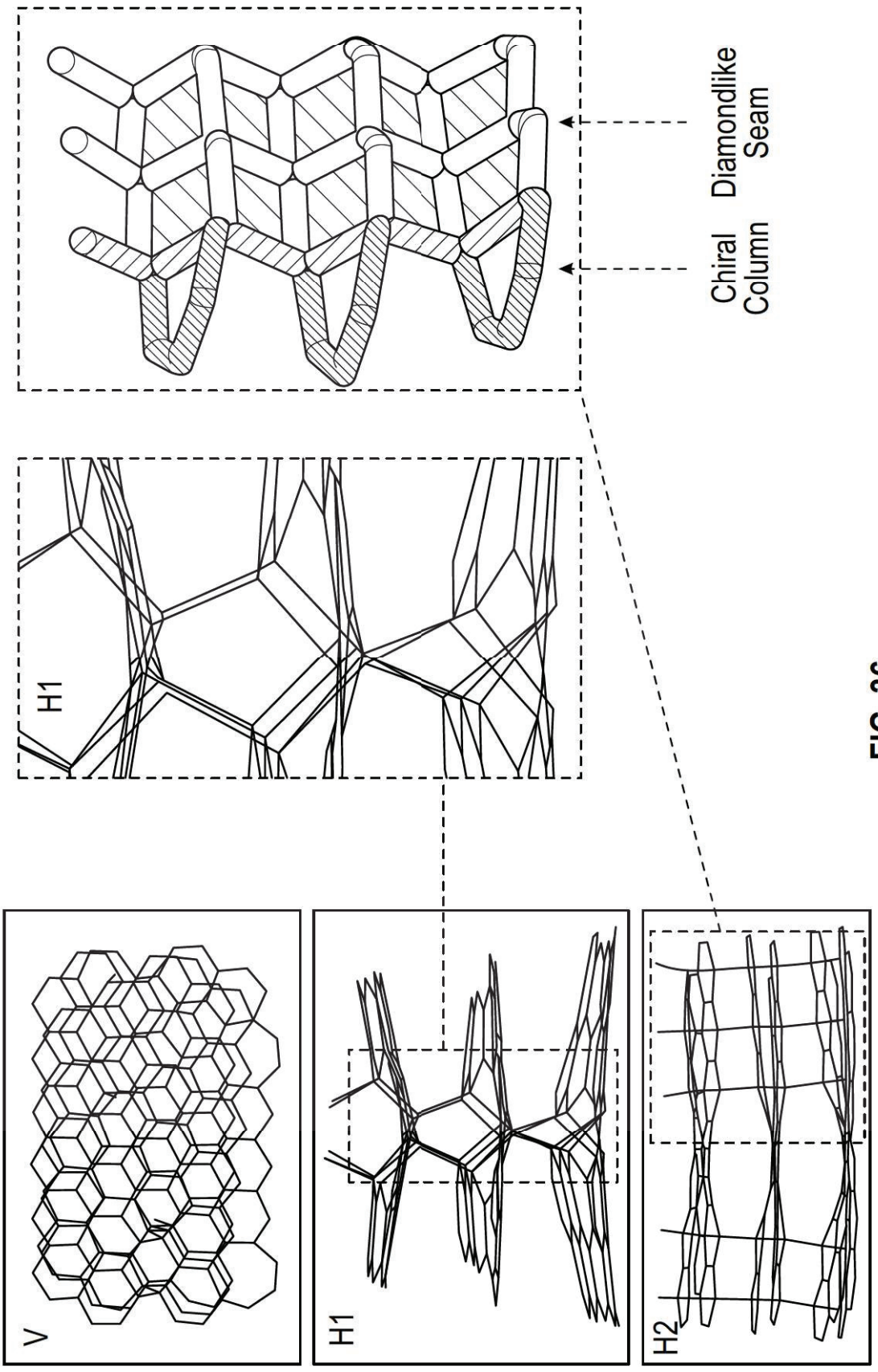



FIG. 36

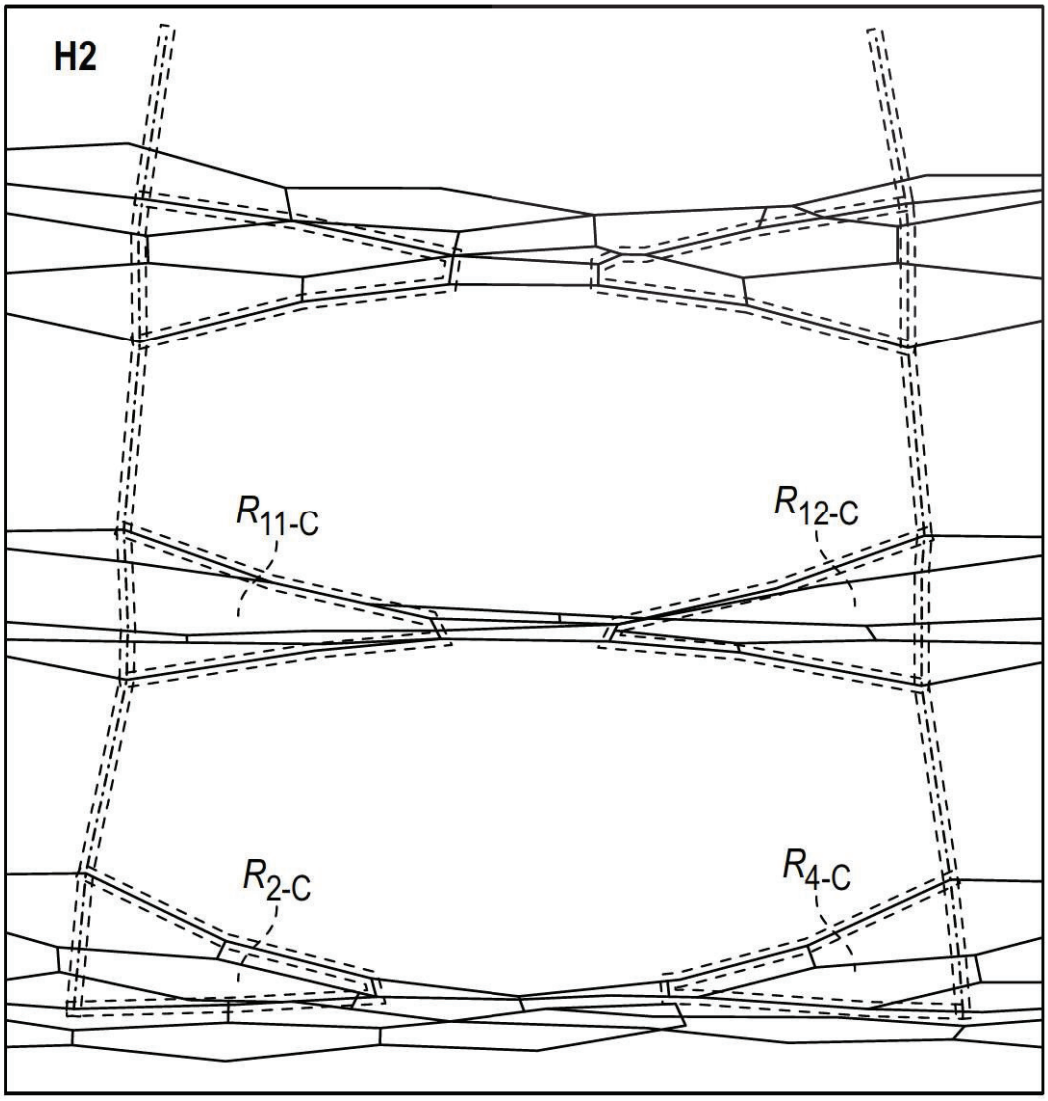



FIG. 37A

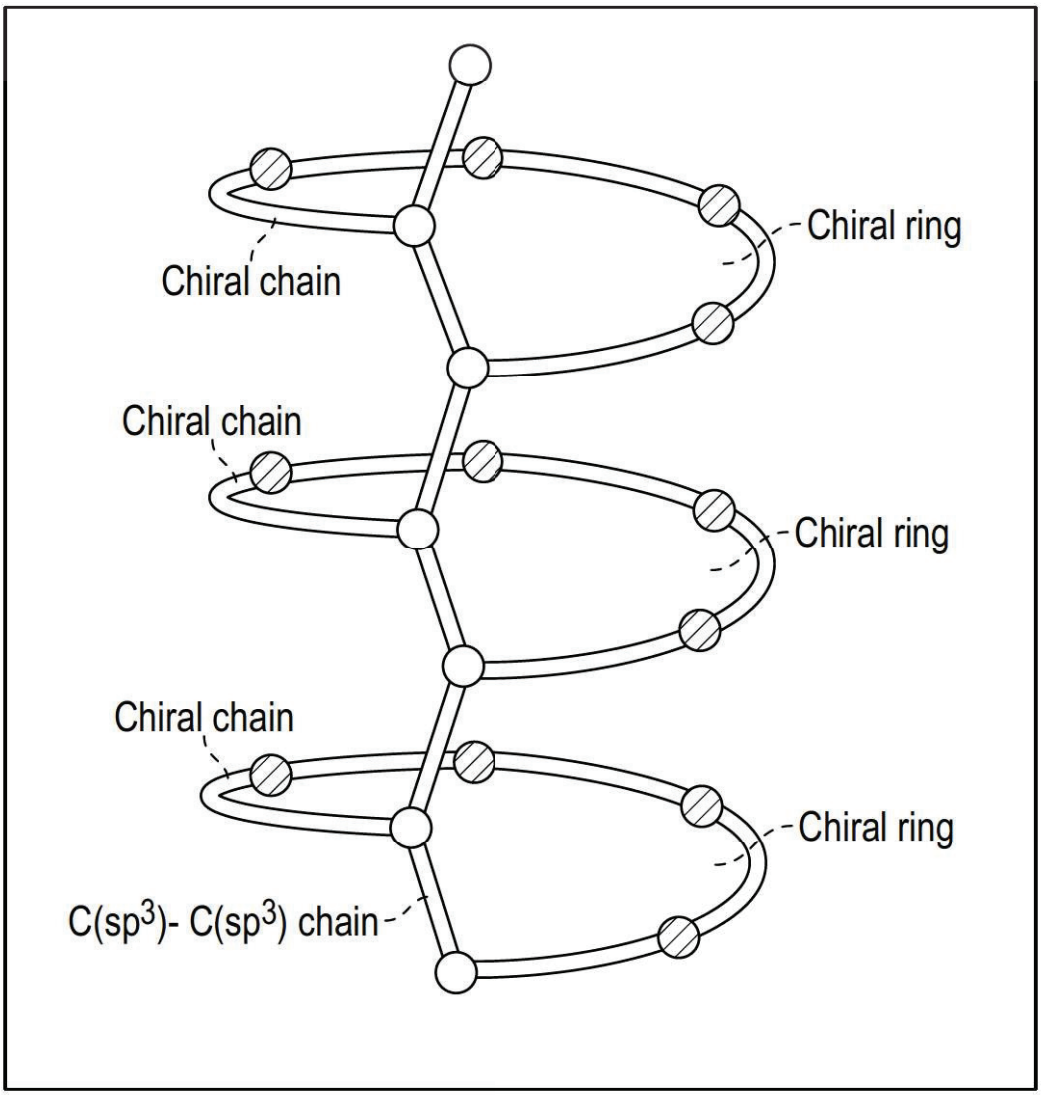

Chiral chain
Chiral ring
Chiral chain
Chiral ring
Chiral chain
Chiral ring
C(sp3)- C(sp3) chain

FIG. 37B

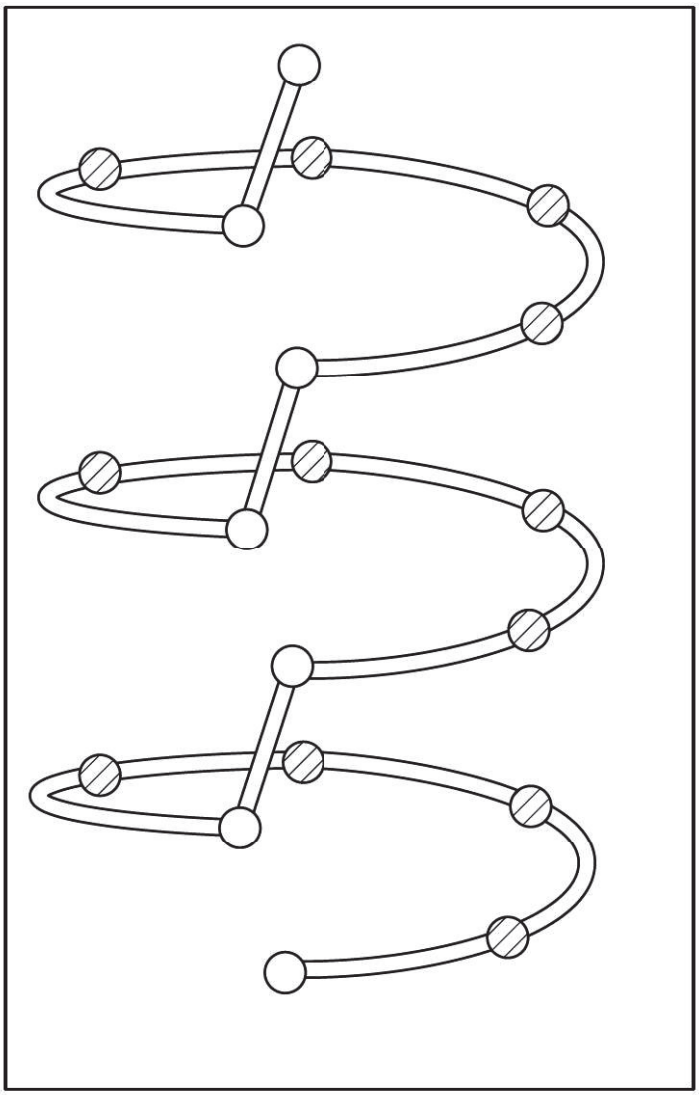


FIG. 37C

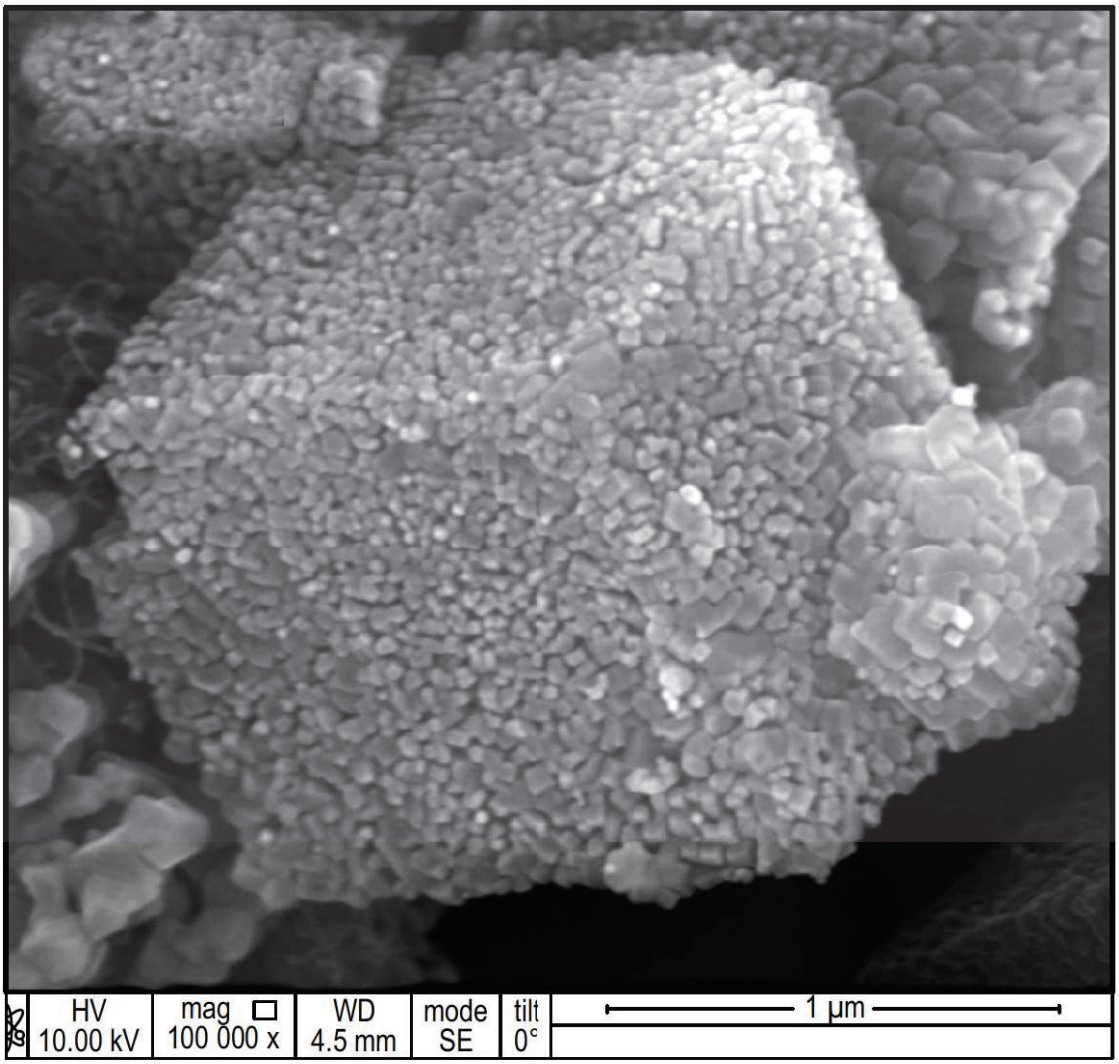



FIG. 38A

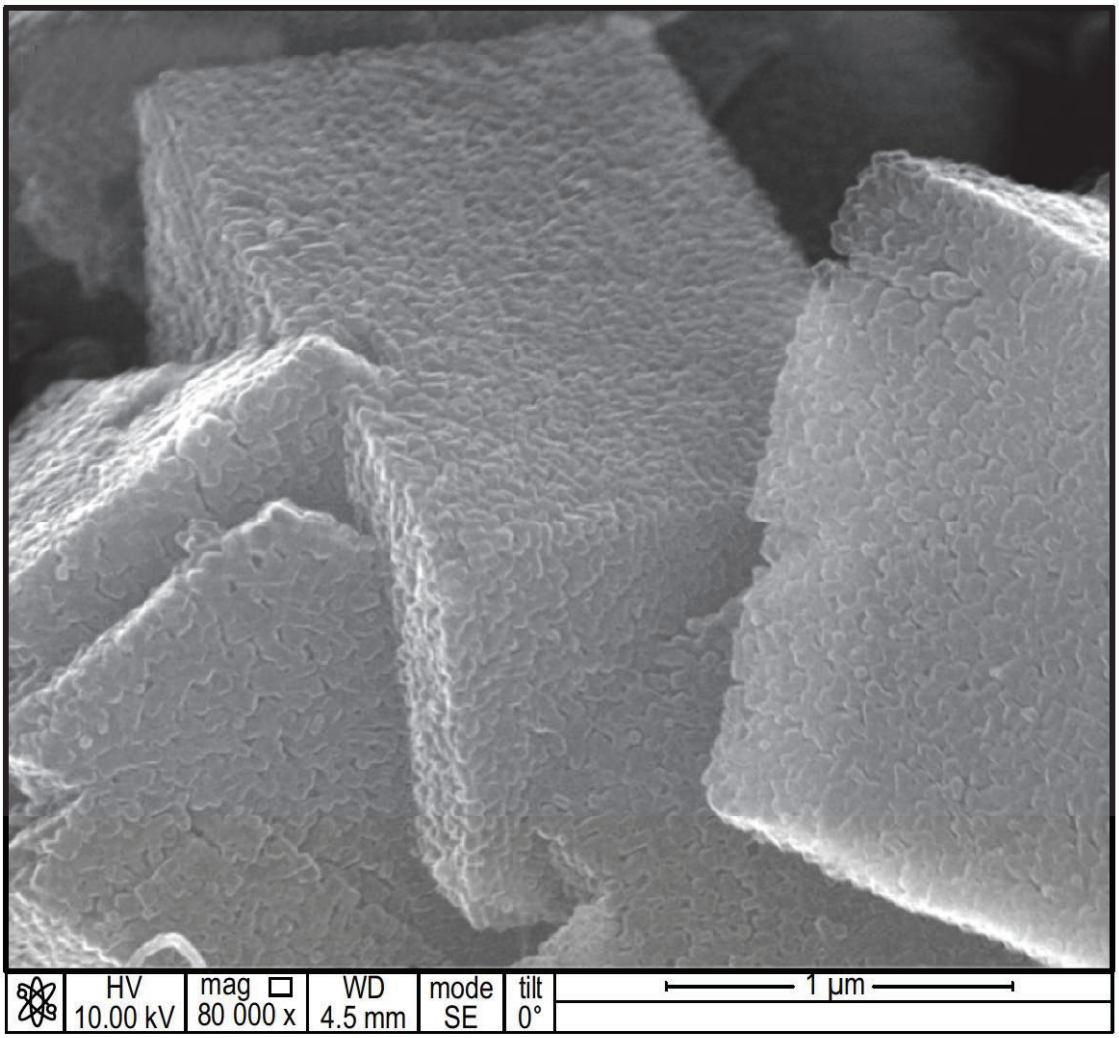



FIG. 38B

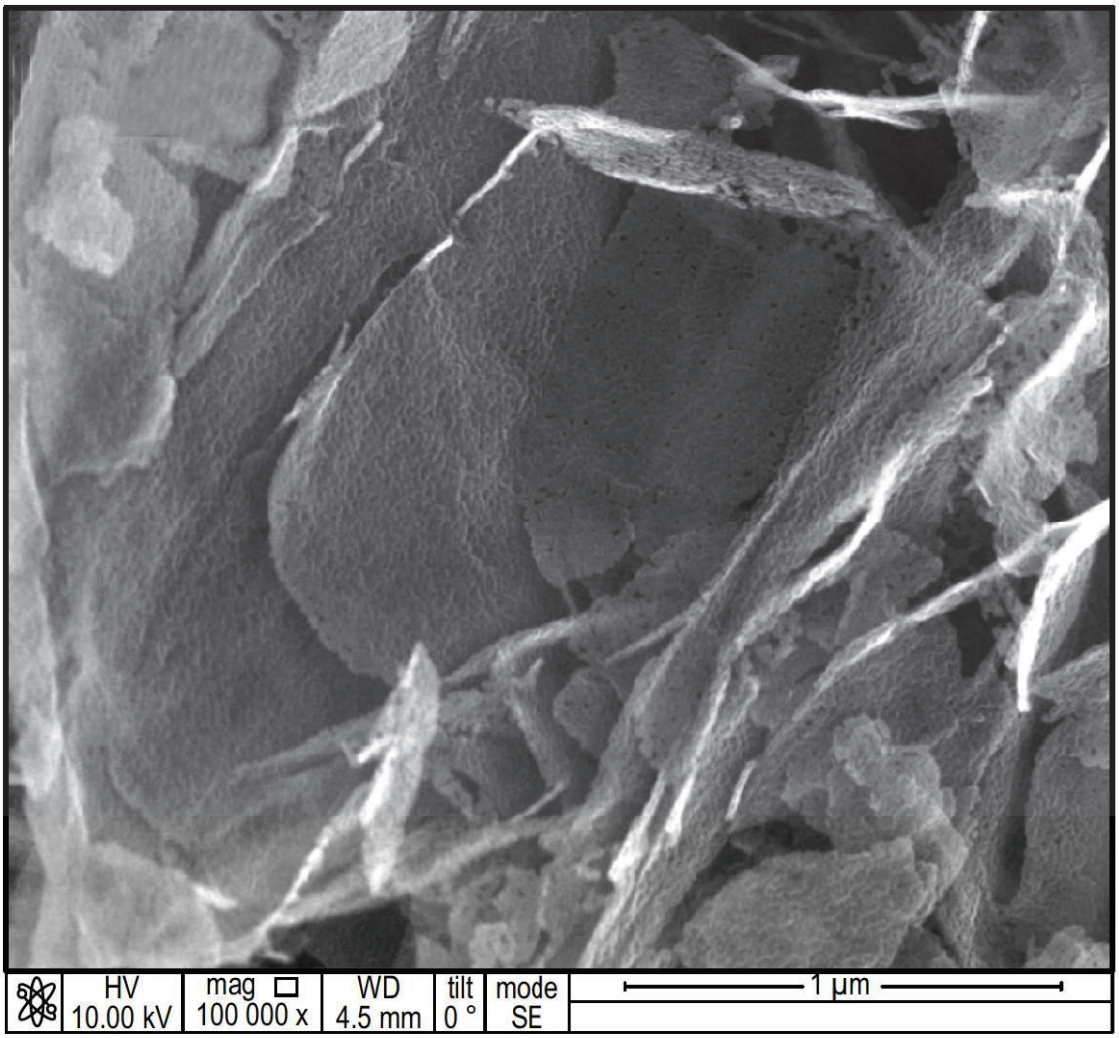



FIG. 38C

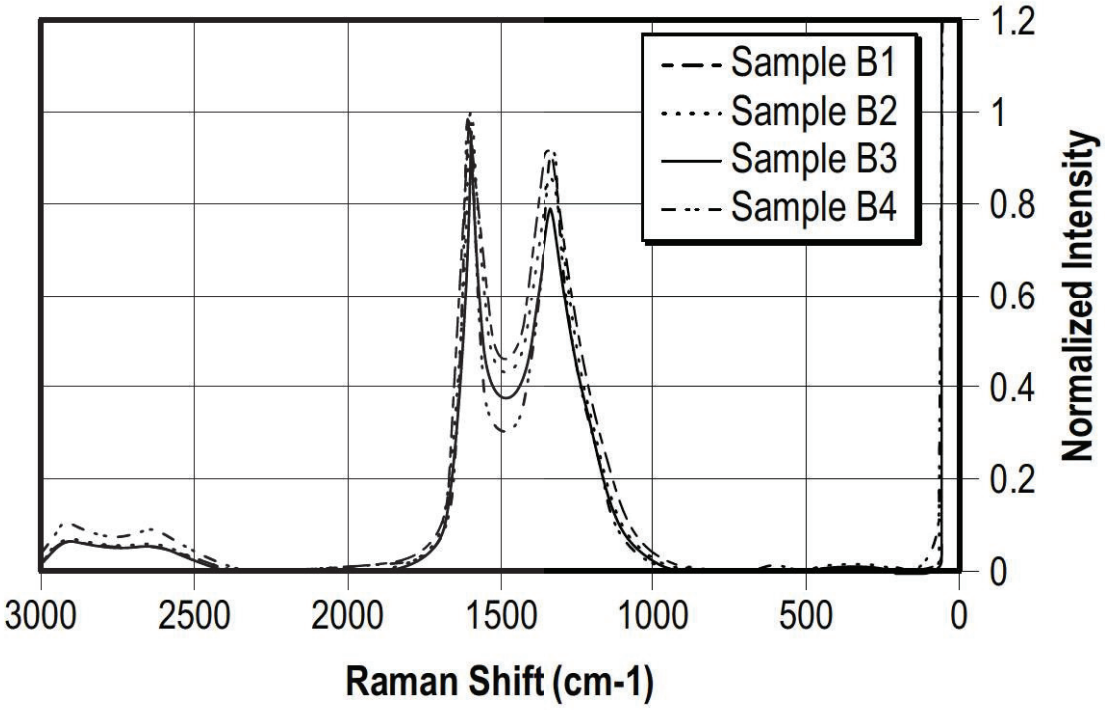

Sample B1
Sample B2
Sample B3
Sample B4
1.2
1
0.8
0.6
0.4
0.2
0
Normalized Intensity
3000
2500
2000
1500
1000
500
0
Raman Shift (cm-1)

FIG. 39A

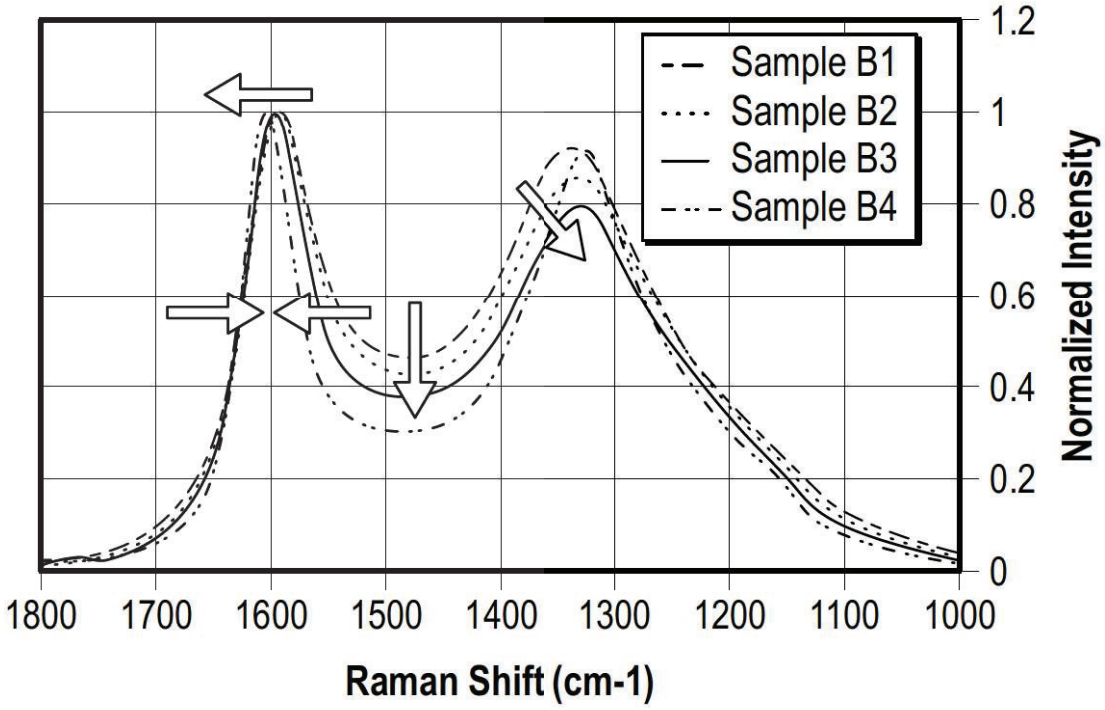

Sample B1
Sample B2
Sample B3
Sample B4
1.2
1
0.8
0.6
0.4
0.2
0
Normalized Intensity
1800
1700
1600
1500
1400
1300
1200
1100
1000
Raman Shift (cm-1)

FIG. 39B

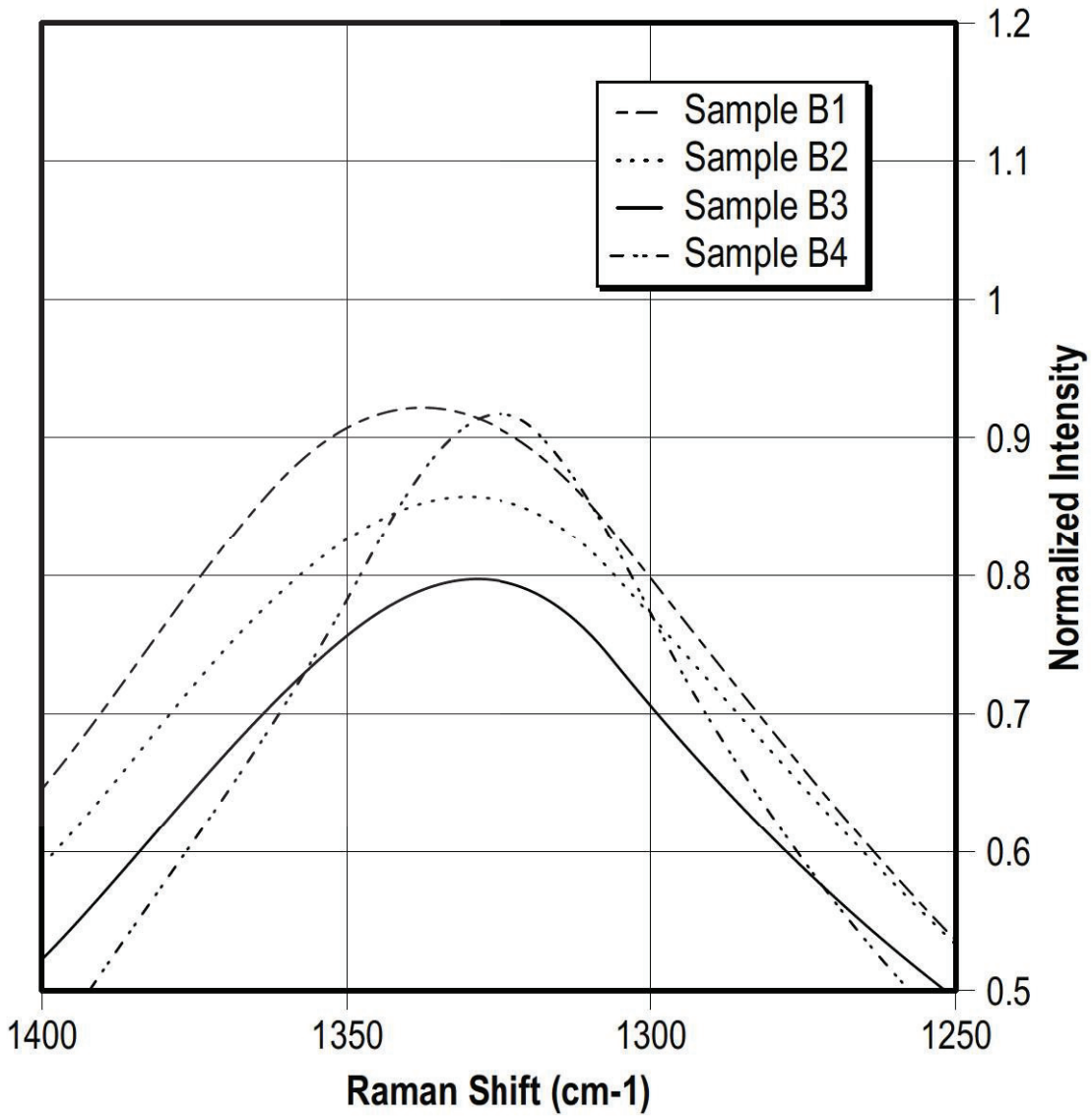

Sample B1
Sample B2
Sample B3
Sample B4
1.2
1.1
1
0.9
0.8
0.7
0.6
0.5
Normalized Intensity
1400
1350
1300
1250
Raman Shift (cm-1)

FIG. 39C

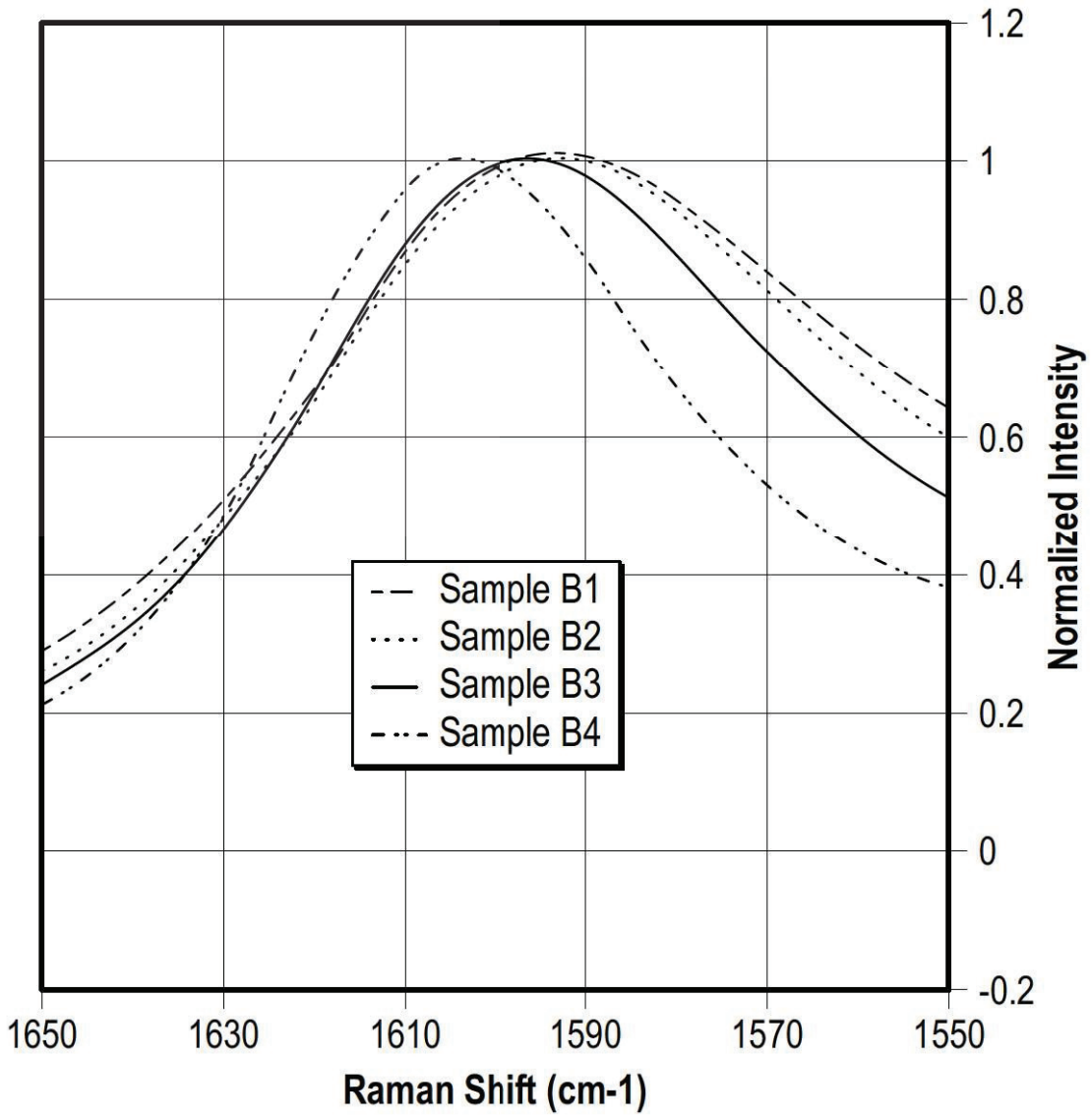

1.2
1
0.8
0.6
0.4
0.2
0
-0.2
Normalized Intensity
Sample B1
Sample B2
Sample B3
Sample B4
1650
1630
1610
1590
1570
1550
Raman Shift (cm-1)

FIG. 39D

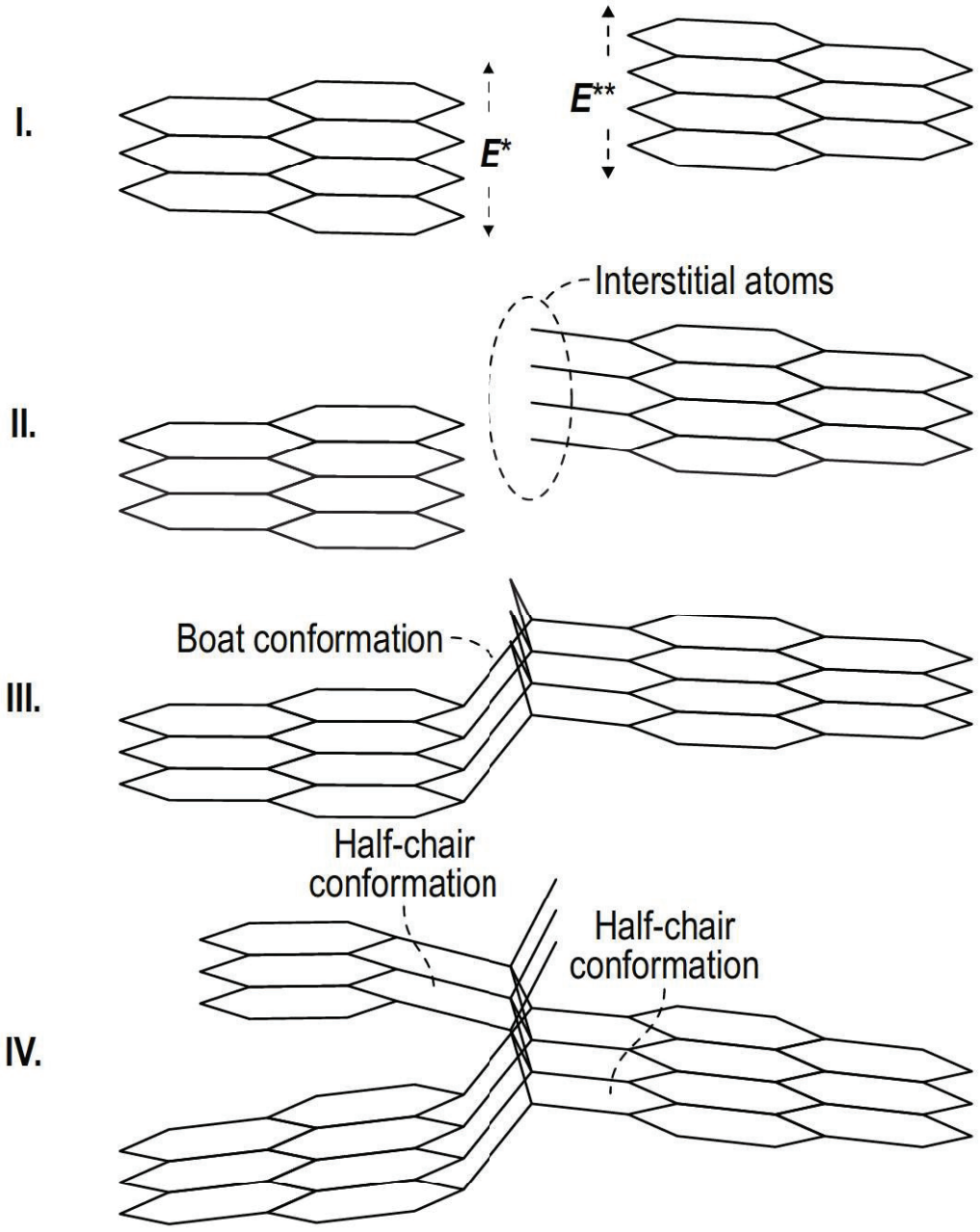

I.
E*
E**
II.
Interstitial atoms
III.
Boat conformation
IV.
Half-chair conformation
Half-chair conformation

FIG. 40

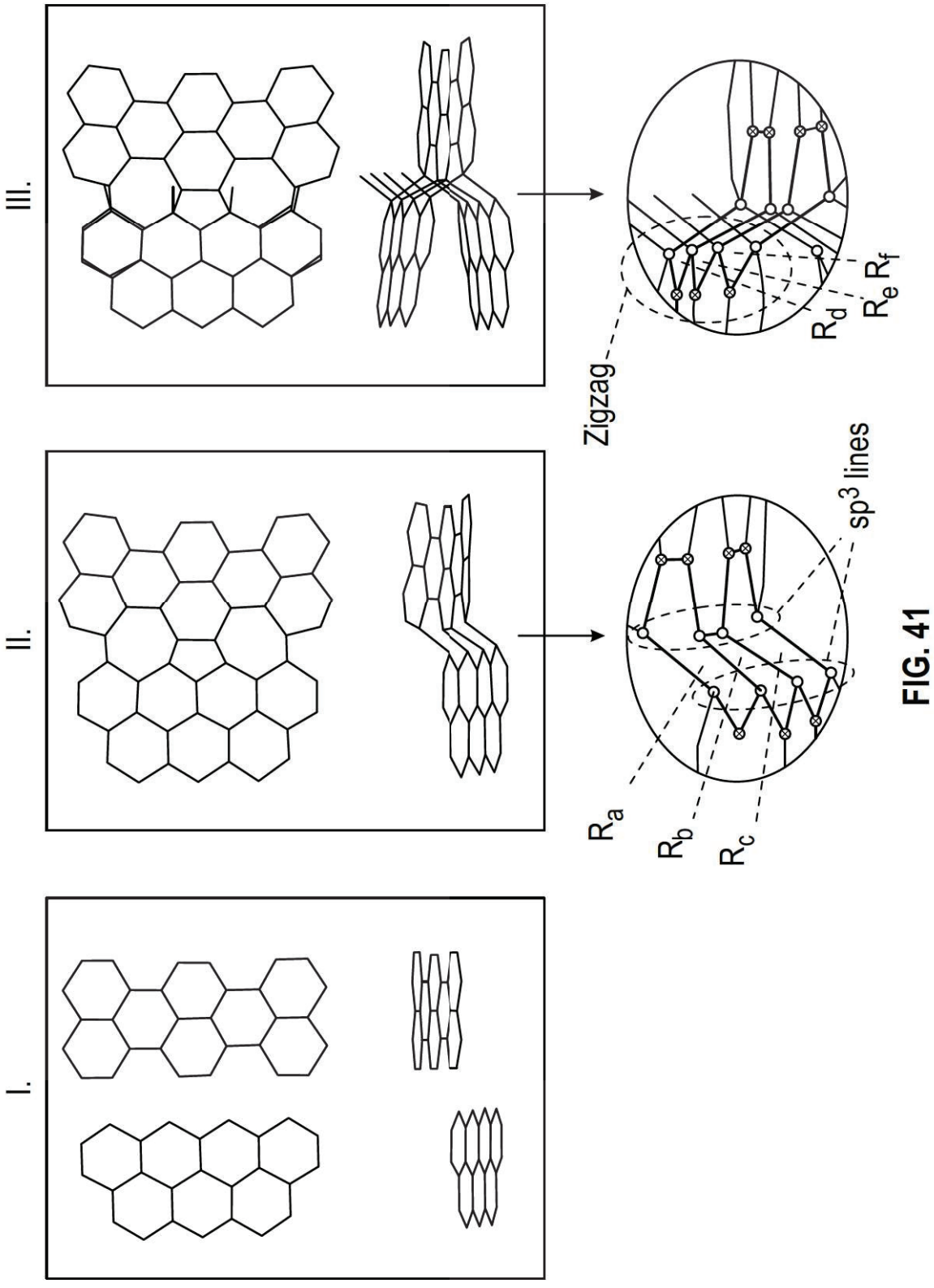



FIG. 41

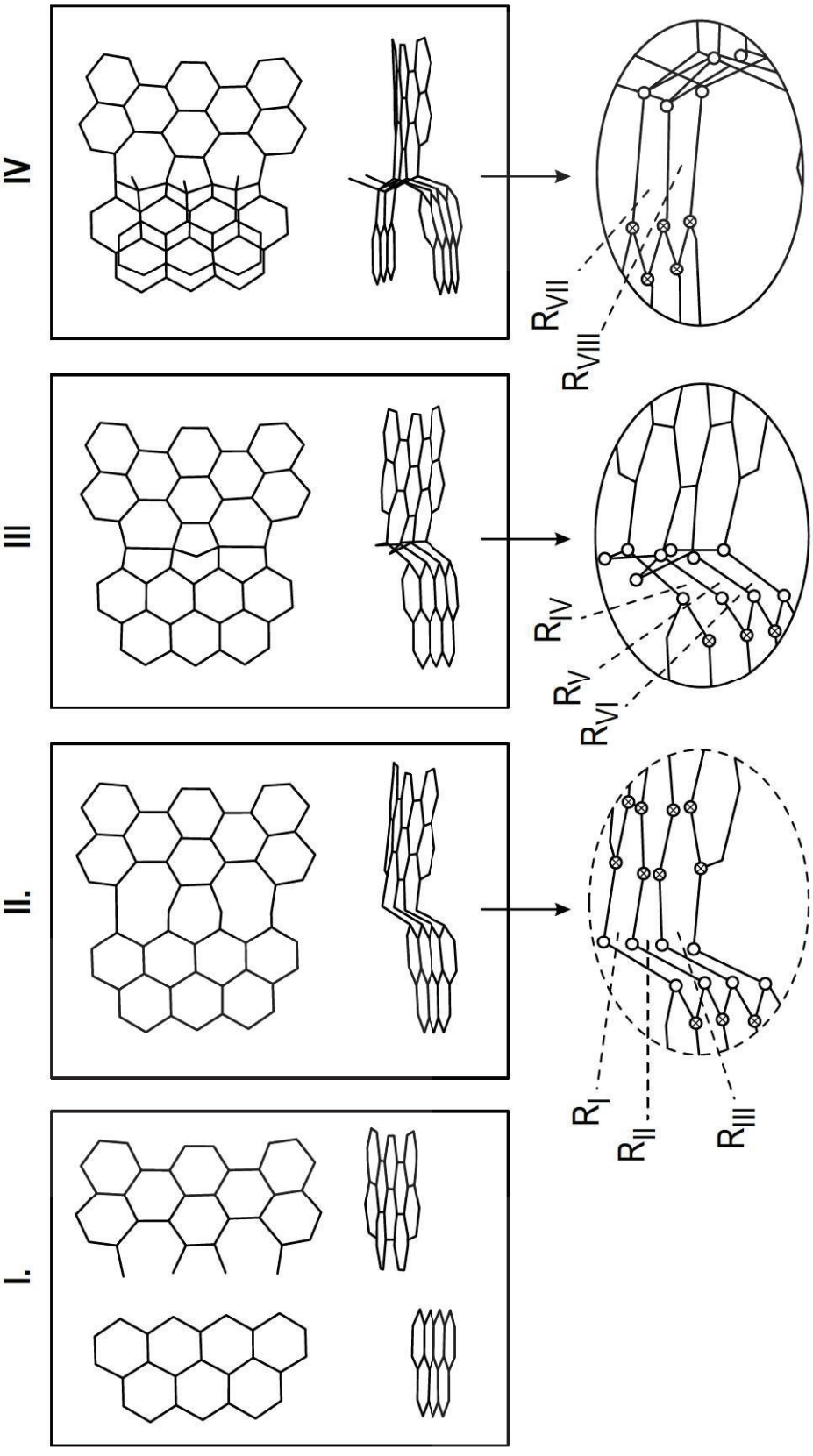



FIG. 42

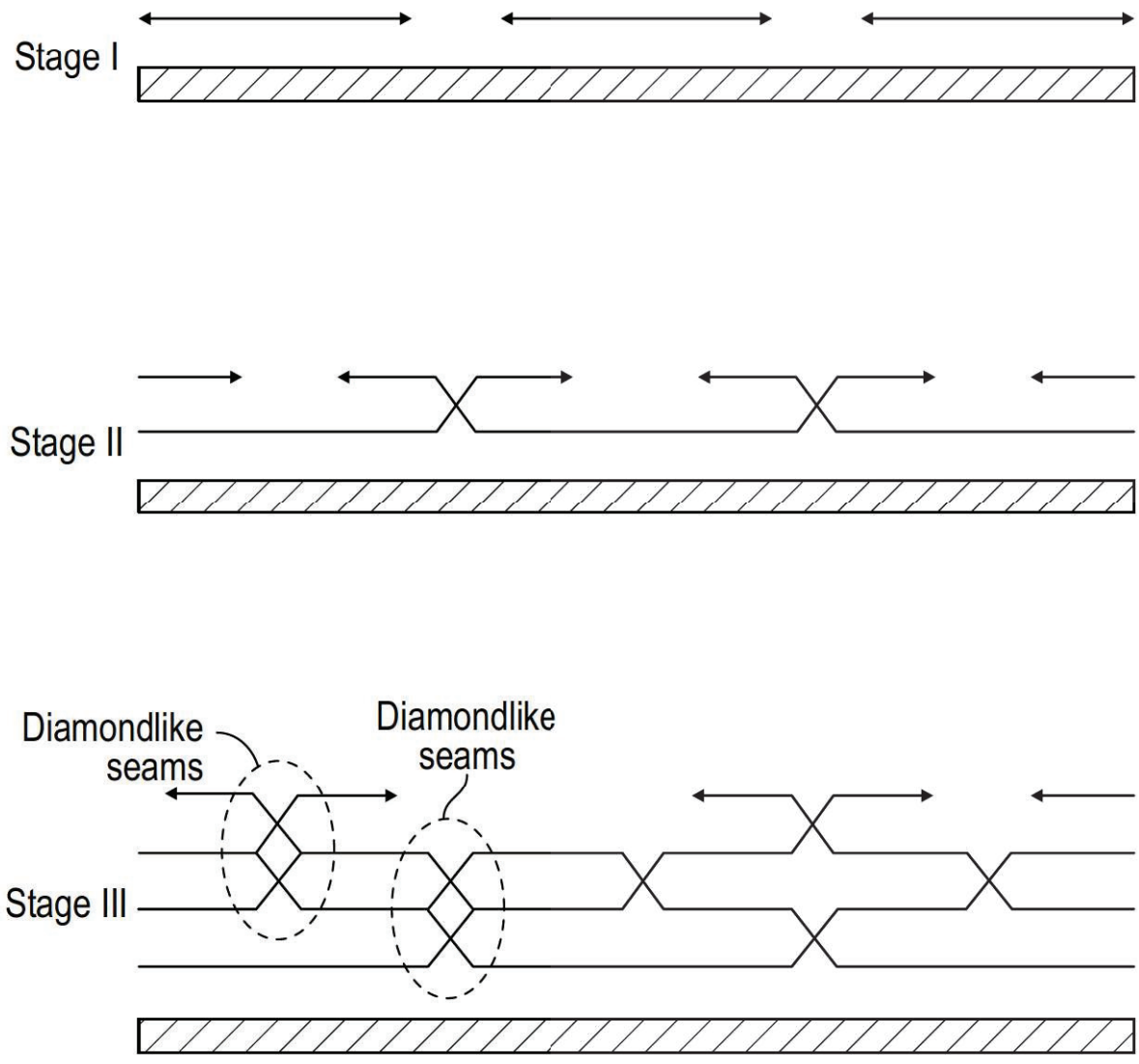

Stage I
Stage II
Diamondlike seams
Diamondlike seams
Stage III

FIG. 43

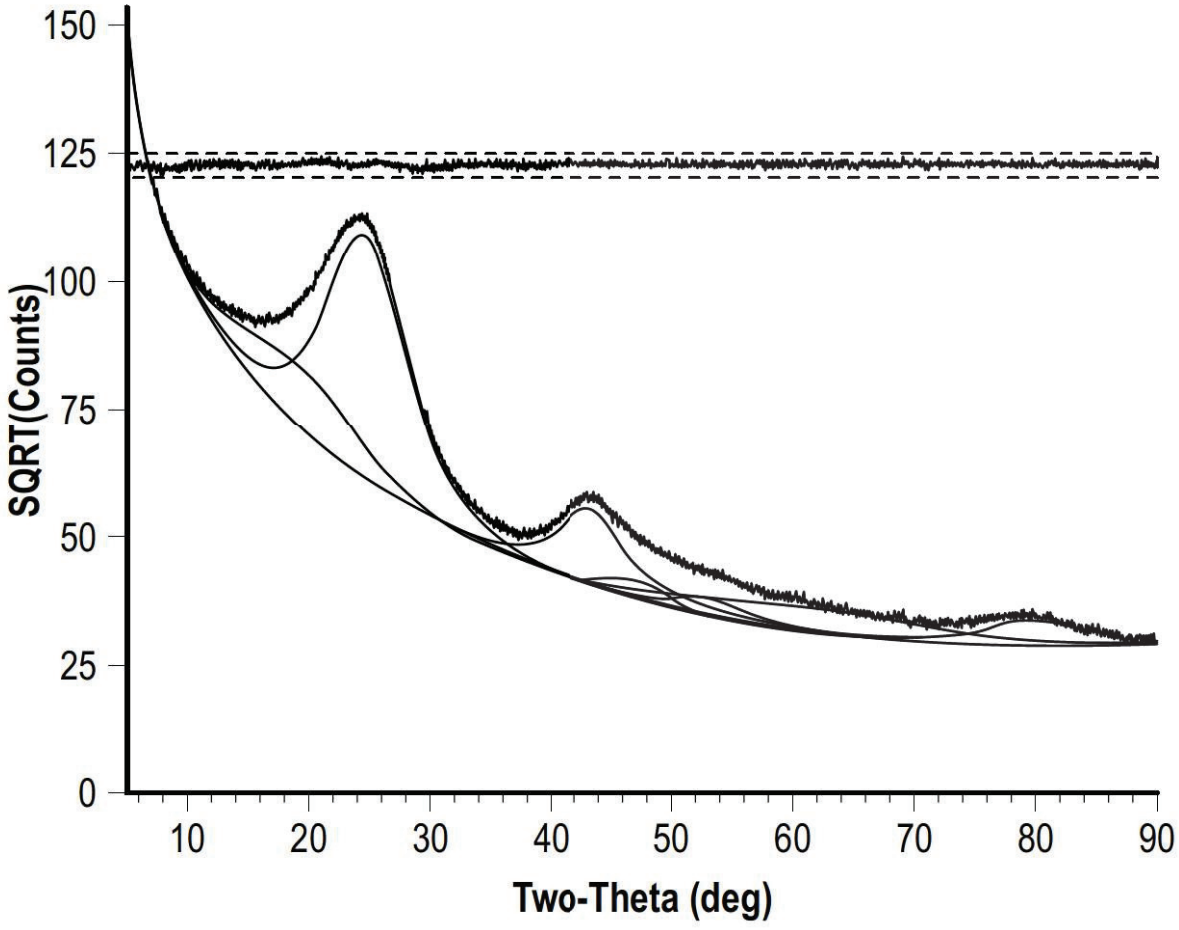

150
125
100
75
50
25
0
SQRT(Counts)
10
20
30
40
50
60
70
80
90
Two-Theta (deg)

FIG. 44



460°C 400°C

FIG. 45

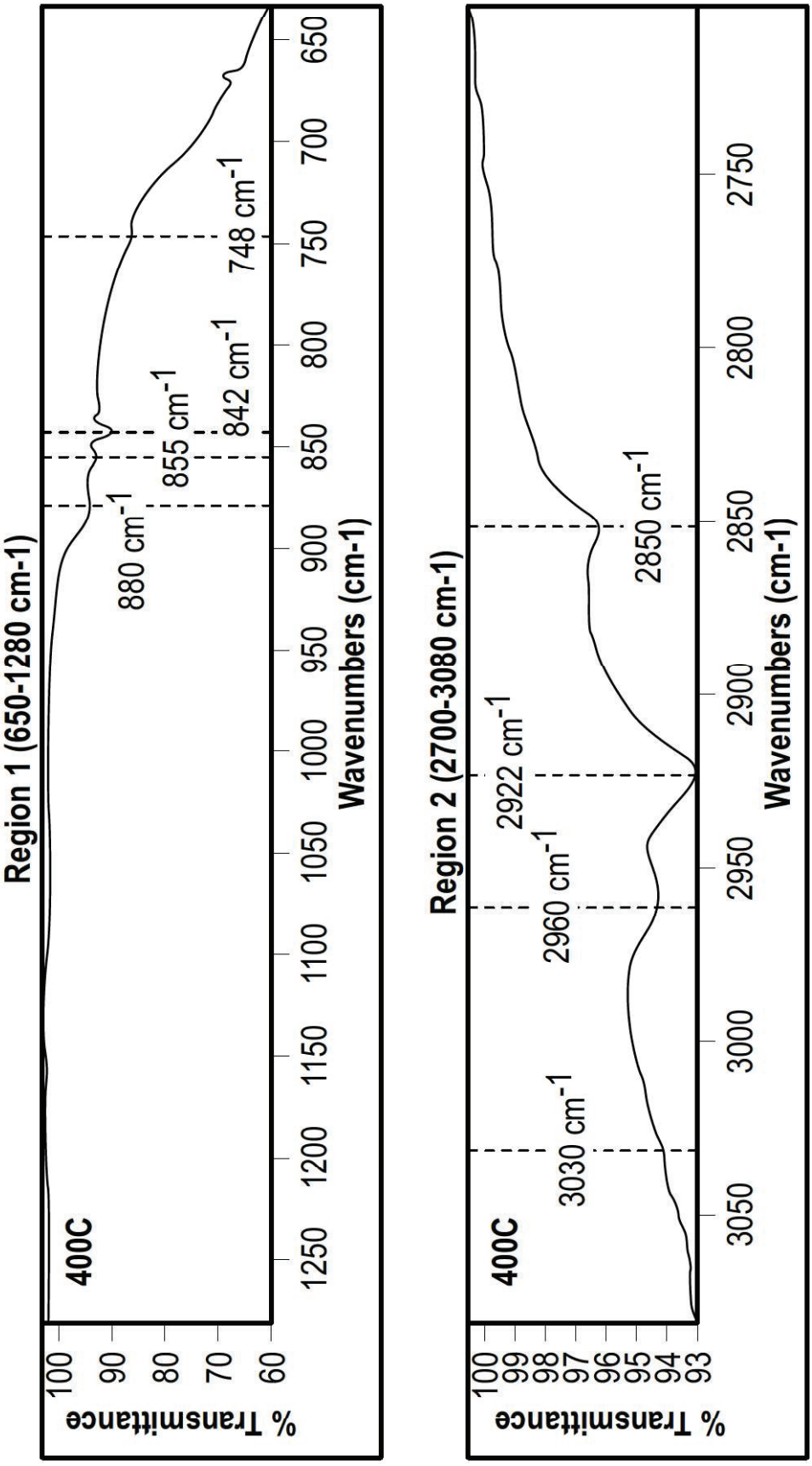

Region 1 (650-1280 cm-1)
400C
% Transmittance
100
90
80
70
60
1250
1200
1150
1100
1050
1000
950
900
850
800
750
700
650
Wavenumbers (cm-1)
880 cm-1
855 cm-1
842 cm-1
748 cm-1
Region 2 (2700-3080 cm-1)
400C
% Transmittance
100
99
98
97
96
95
94
93
3050
3000
2950
2900
2850
2800
2750
Wavenumbers (cm-1)
3030 cm-1
2960 cm-1
2922 cm-1
2850 cm-1

FIG. 46A

| | Region 1 | | | | Region 2 | | | |
|---|---|---|---|---|---|---|---|---|
| Peak pos. ($cm^{-1}$) | 880 | 855 | 842 | 748 | 3030 | 2960 | 2922 | 2850 |
| | X | X | X | X | X | X | X | X |
| Peak Assignment | geminal disub alkene | | | mono/orthodi -sub aromatic | sp2 C-H stretch | sp3 C-H stretch | | |
| | sp2 CH bend for aromatics | | | | | | | |
| | sp2 CH bend for alkenes | | | | | | | |



**FIG. 46B**

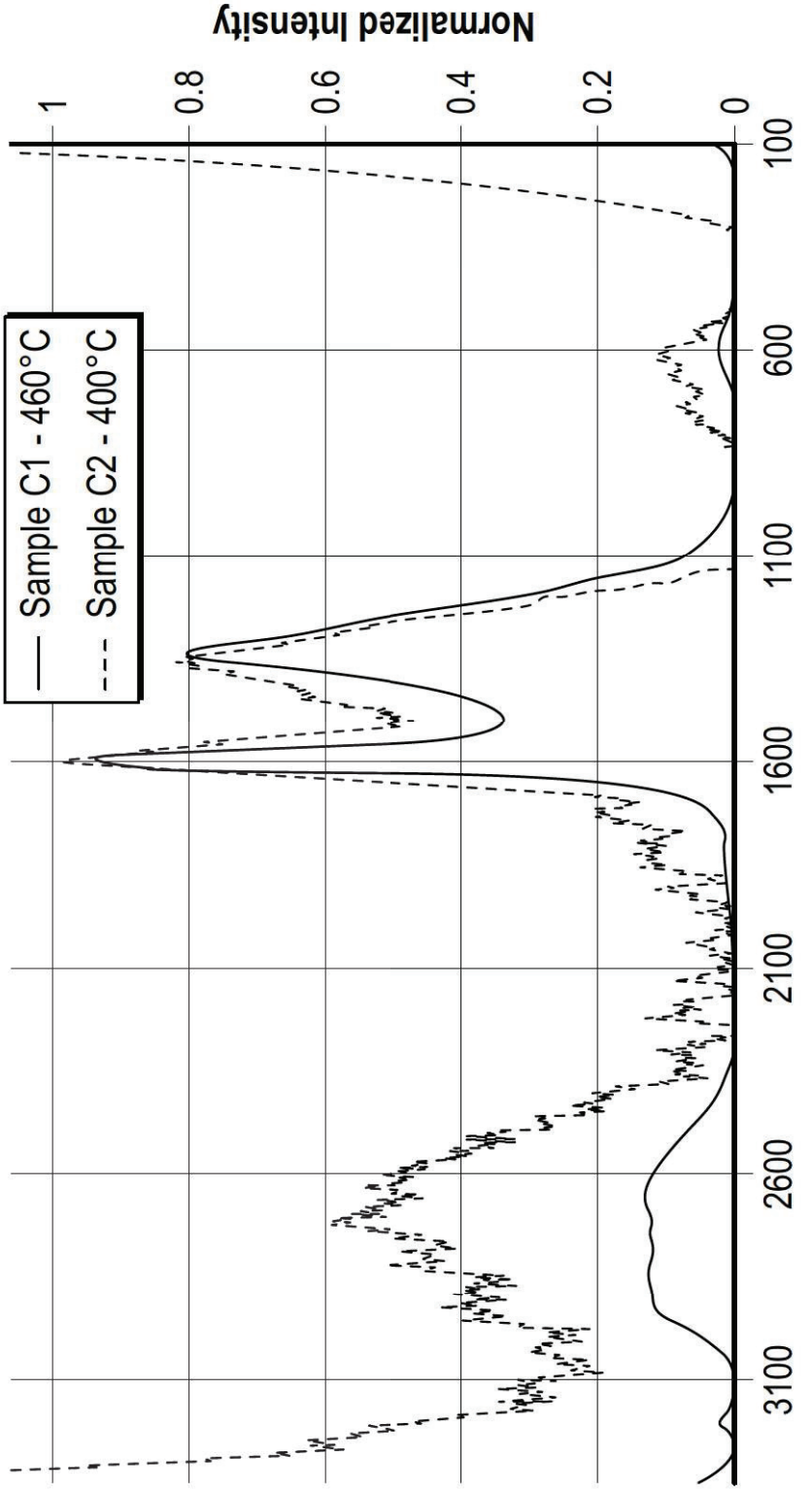

Normalized Intensity
1
0.8
0.6
0.4
0.2
0
Sample C1 - 460°C
Sample C2 - 400°C
100
600
1100
1600
2100
2600
3100
Raman Shift (cm-1)

FIG. 47

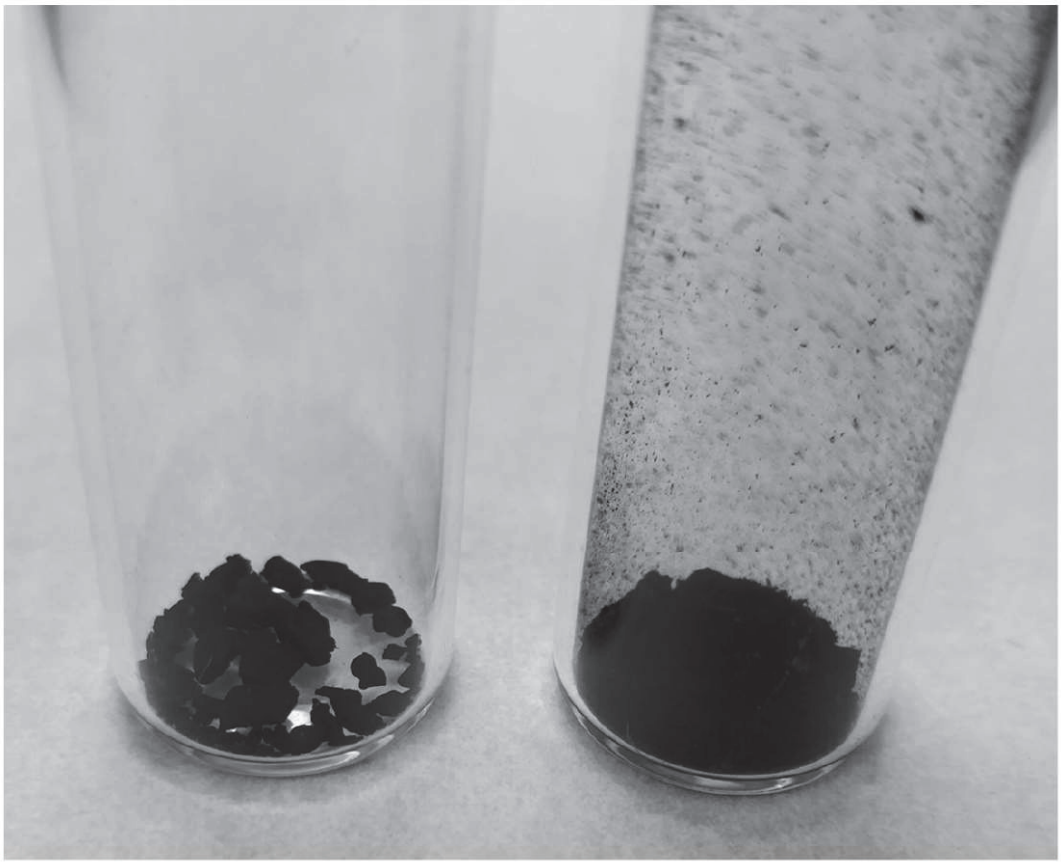


FIG. 48

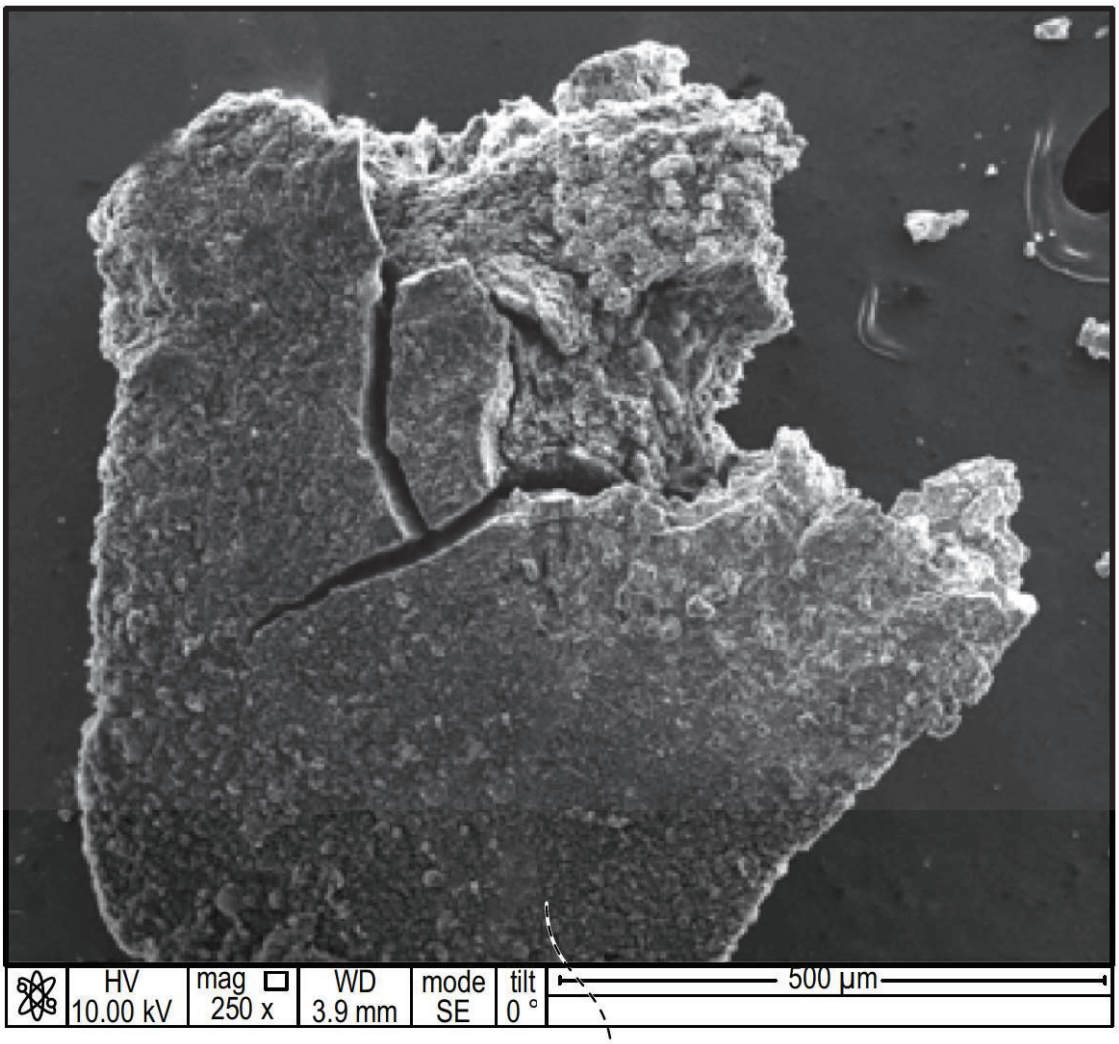

HV
10.00 kV
mag
250 x
WD
3.9 mm
mode
SE
tilt
0 °
500 µm
Dense, macroscopic granules

**FIG. 49A**

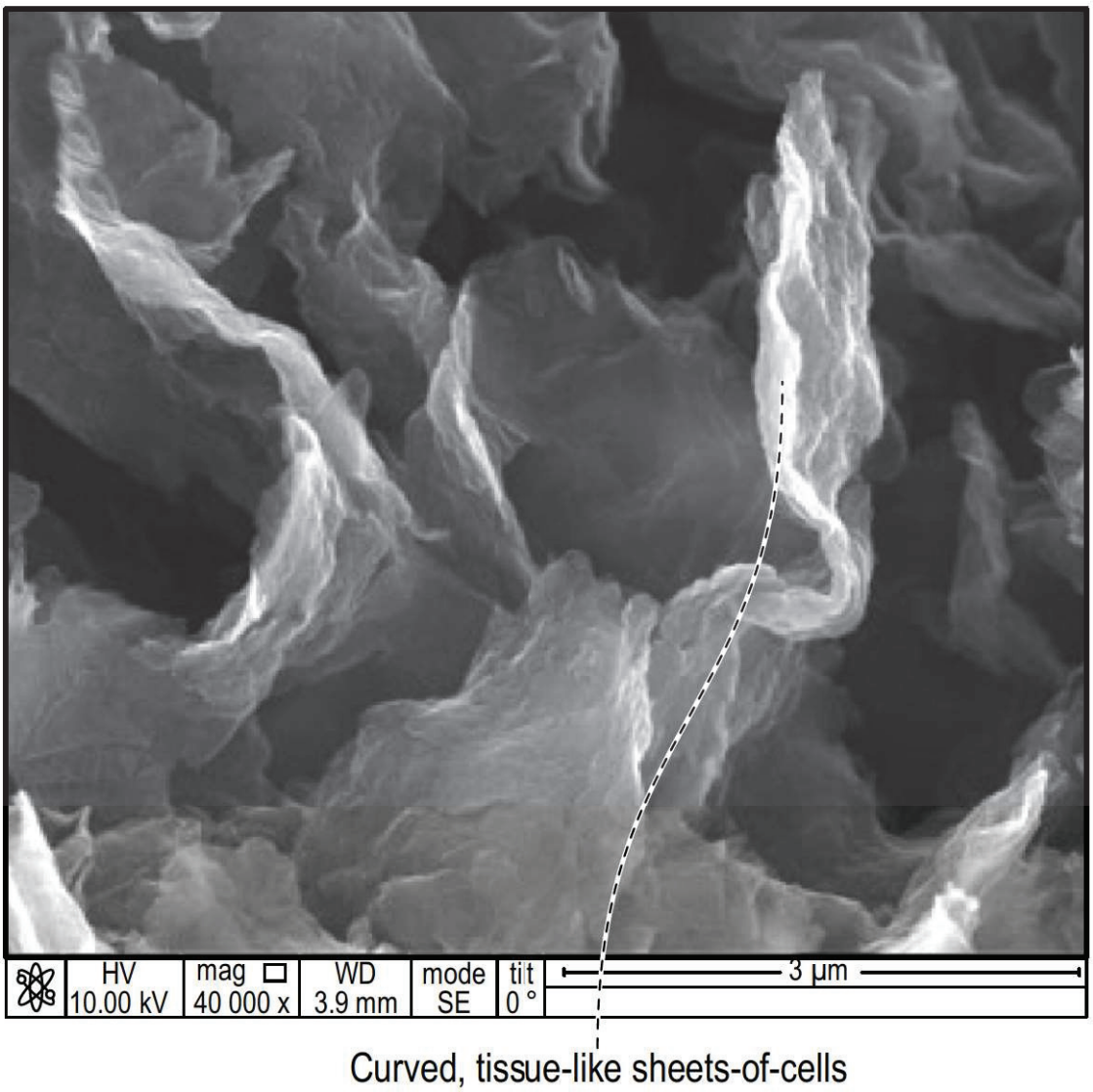

HV
10.00 kV
mag
40 000 x
WD
3.9 mm
mode
SE
tilt
0 °
3 µm
Curved, tissue-like sheets-of-cells

FIG. 49B

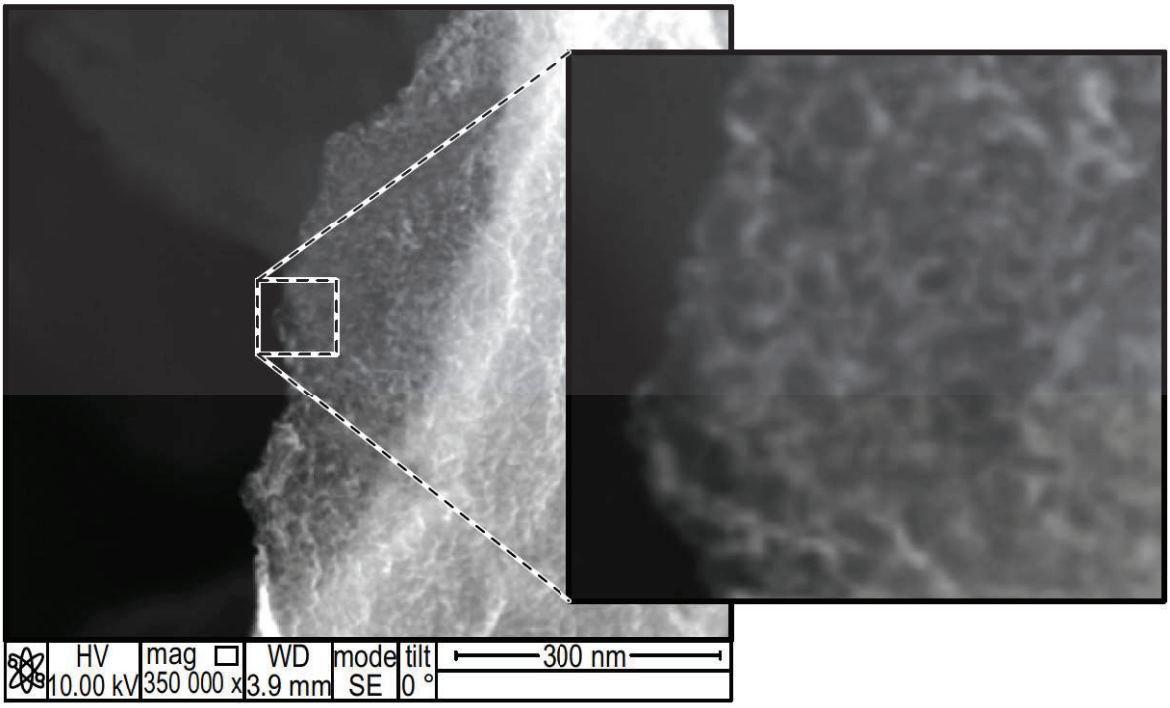



FIG. 49C

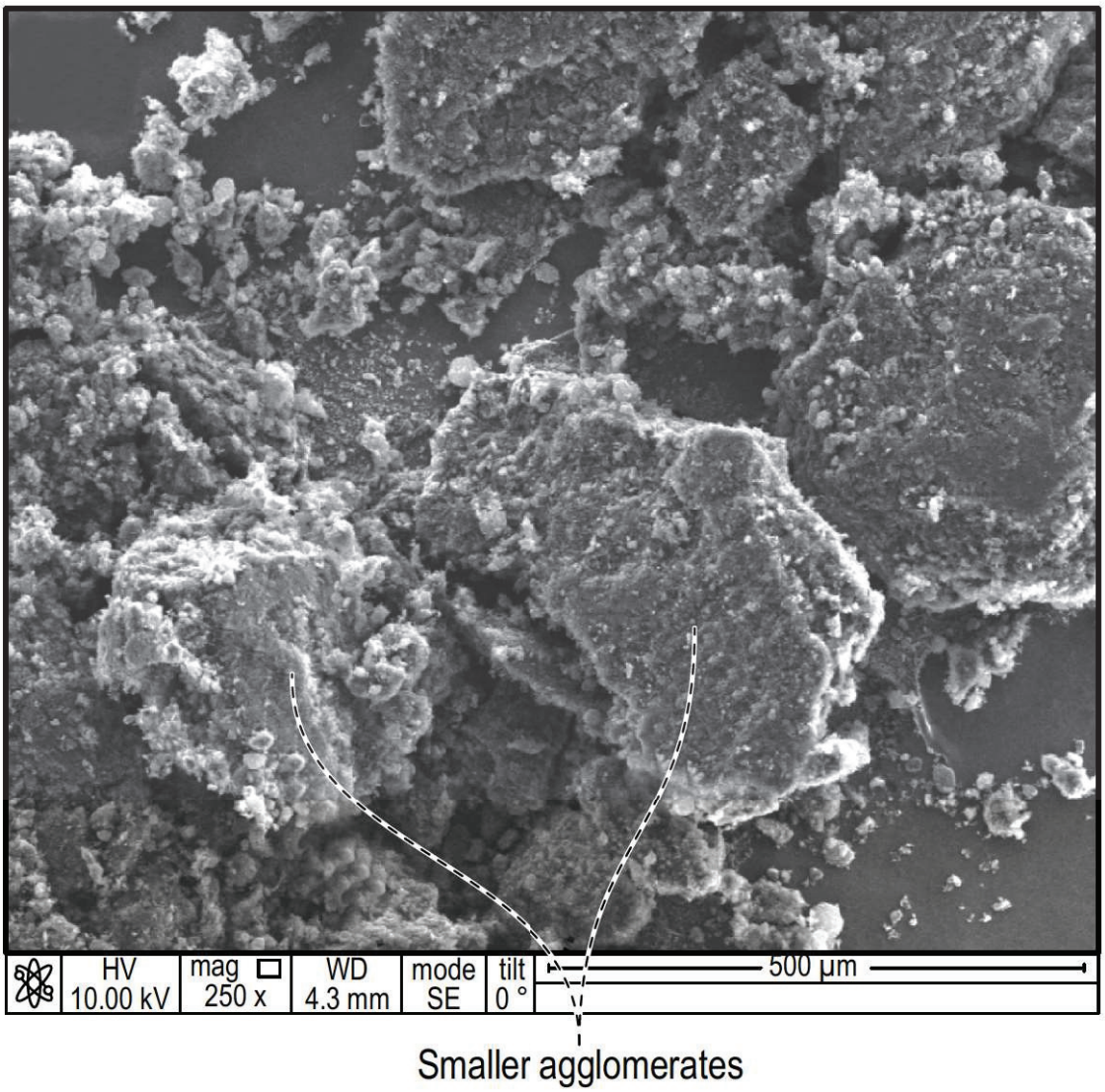

HV
10.00 kV
mag
250 x
WD
4.3 mm
mode
SE
tilt
0 °
500 µm
Smaller agglomerates

FIG. 49D

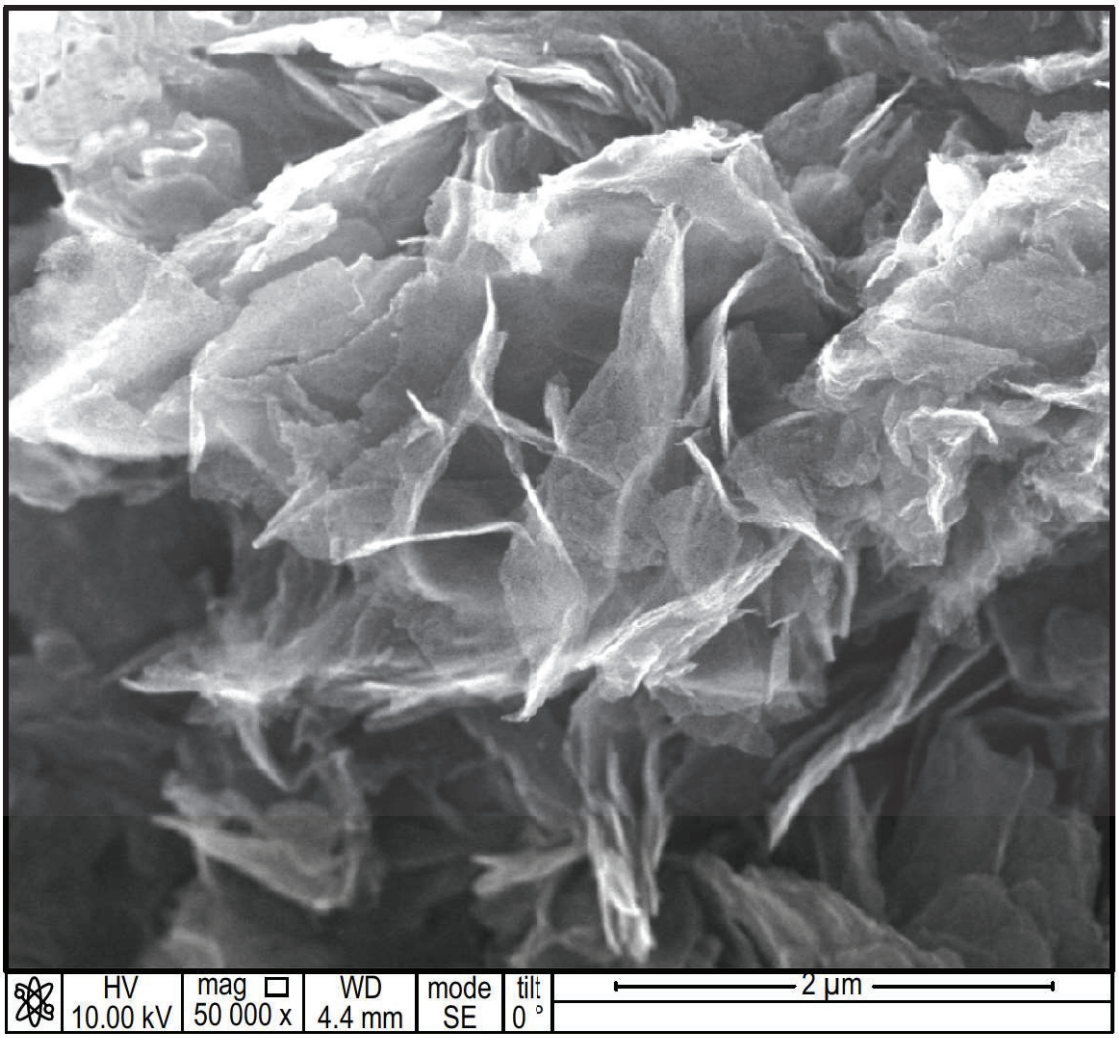



FIG. 49E

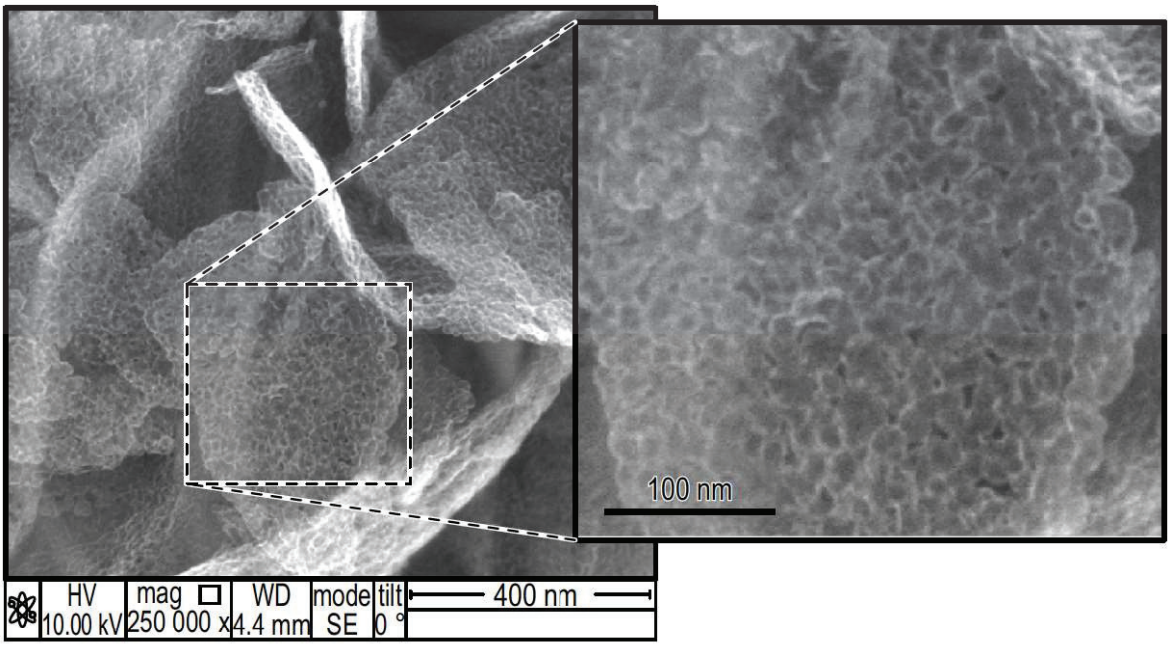



FIG. 49F

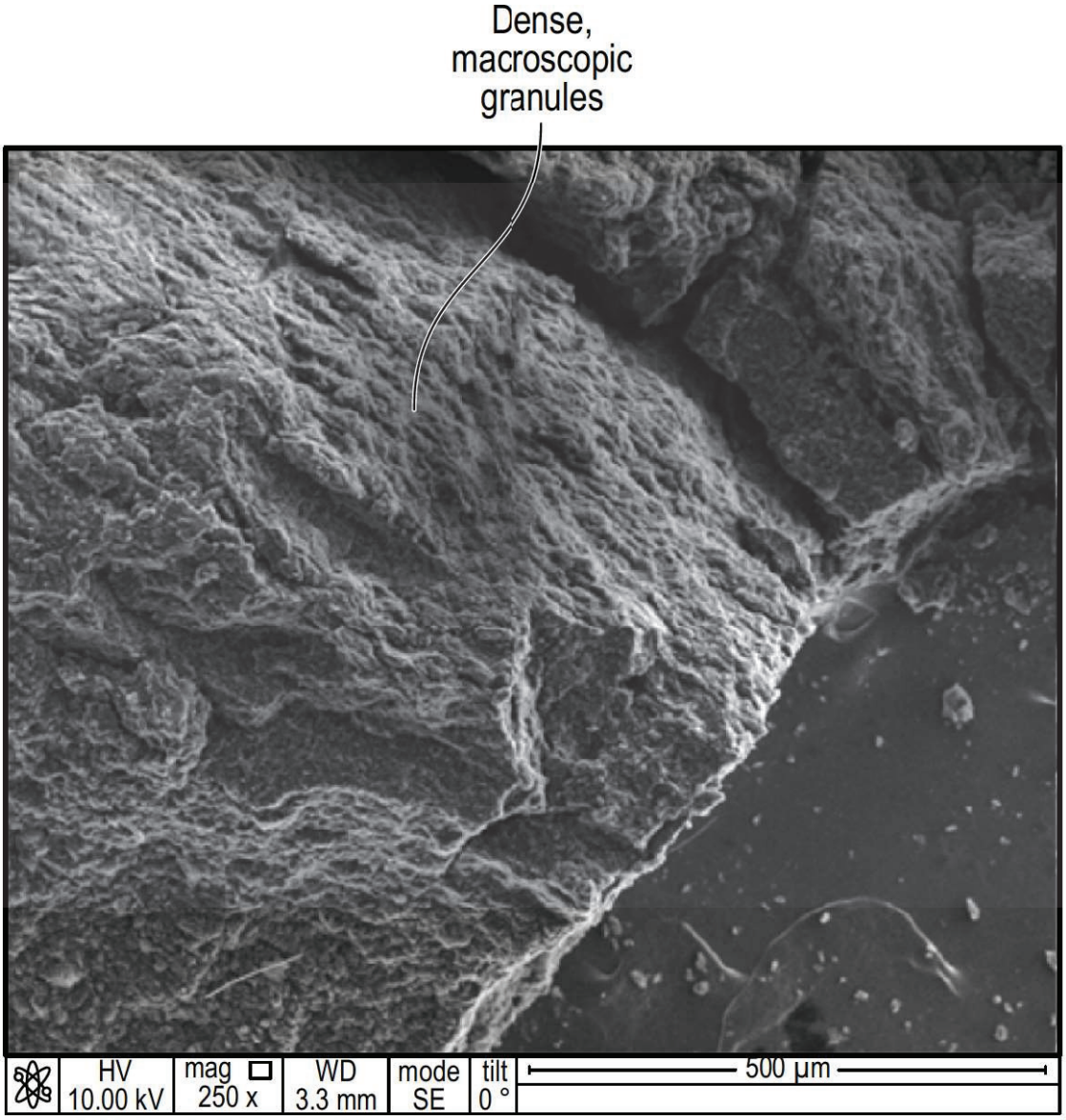

Dense,
macroscopic
granules
HV
10.00 kV
mag
250 x
WD
3.3 mm
mode
SE
tilt
0 °
500 µm

FIG. 50A

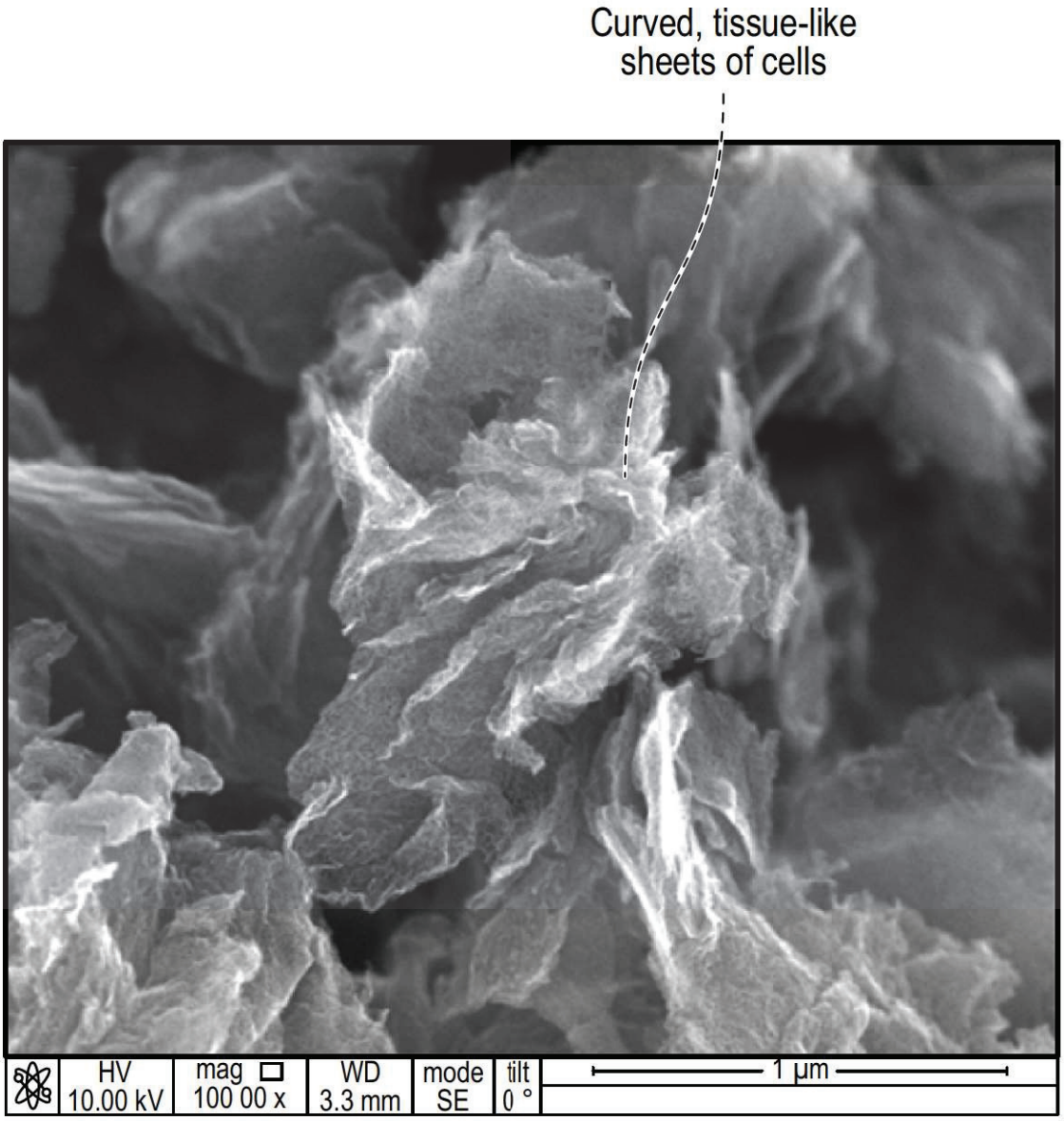

Curved, tissue-like
sheets of cells
HV
10.00 kV
mag
100 00 x
WD
3.3 mm
mode
SE
tilt
0 °
1 µm

FIG. 50B

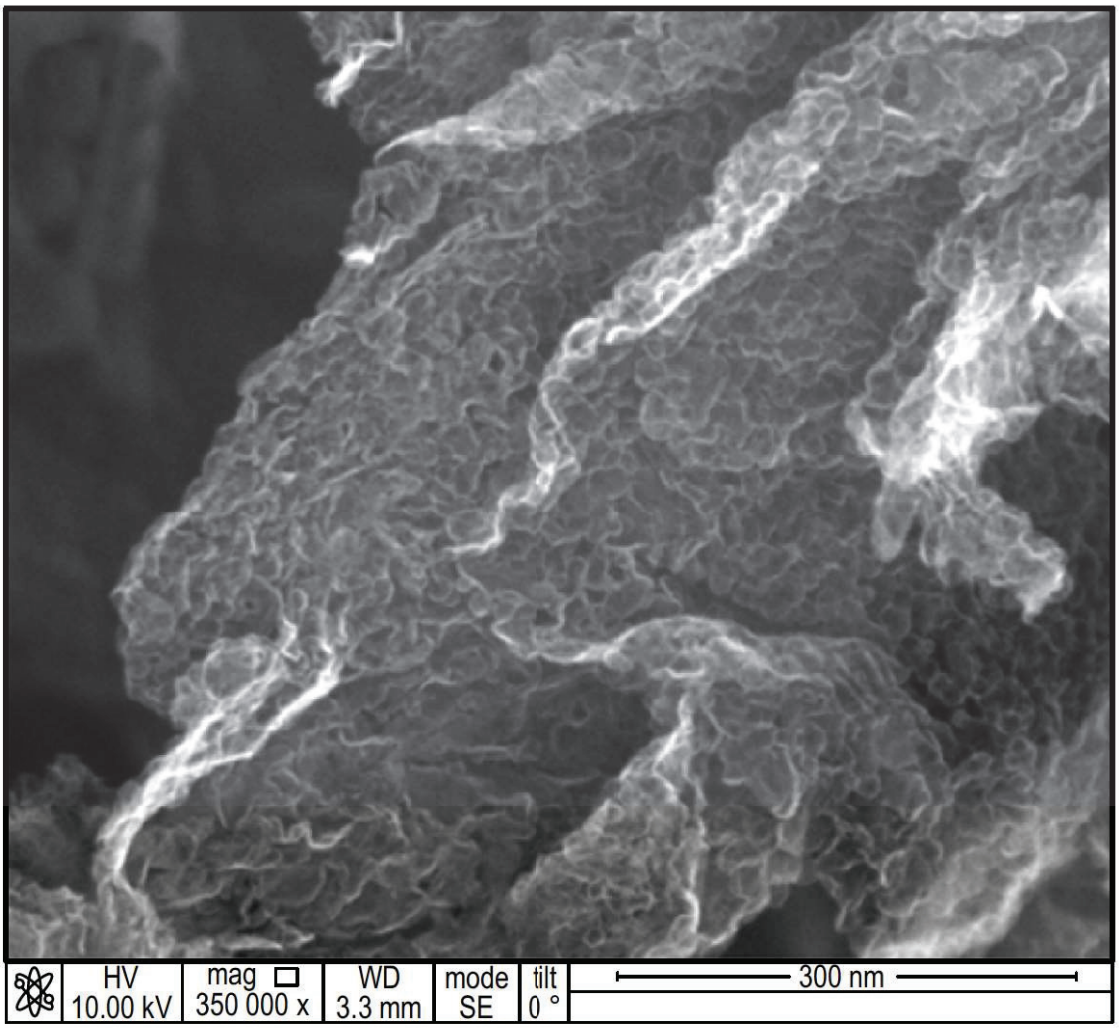



FIG. 50C

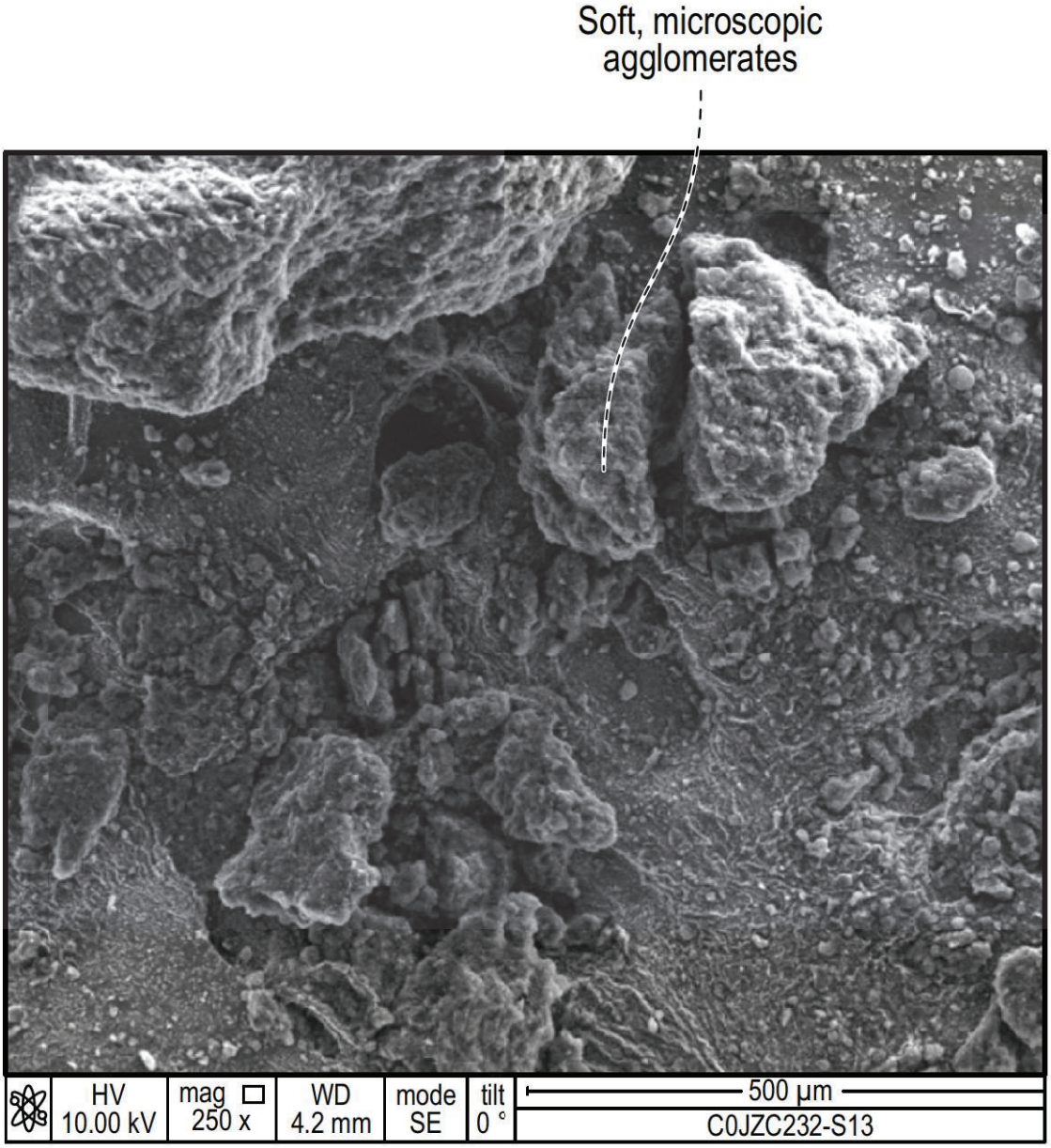

Soft, microscopic agglomerates
HV
10.00 kV
mag
250 x
WD
4.2 mm
mode
SE
tilt
0 °
500 µm
C0JZC232-S13

FIG. 50D

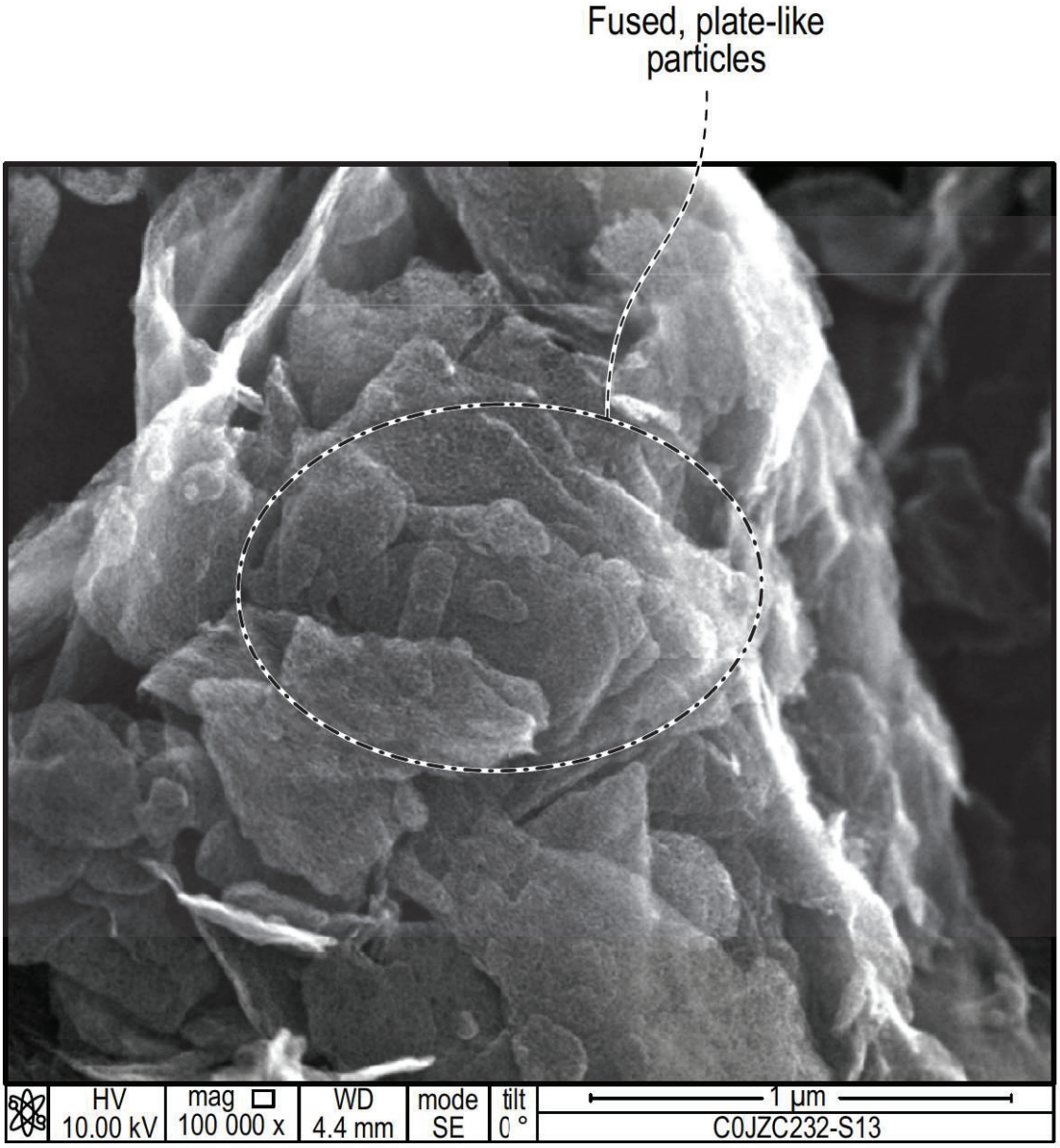

Fused, plate-like particles
HV
10.00 kV
mag
100 000 x
WD
4.4 mm
mode
SE
tilt
0 °
1 µm
C0JZC232-S13

FIG. 50E

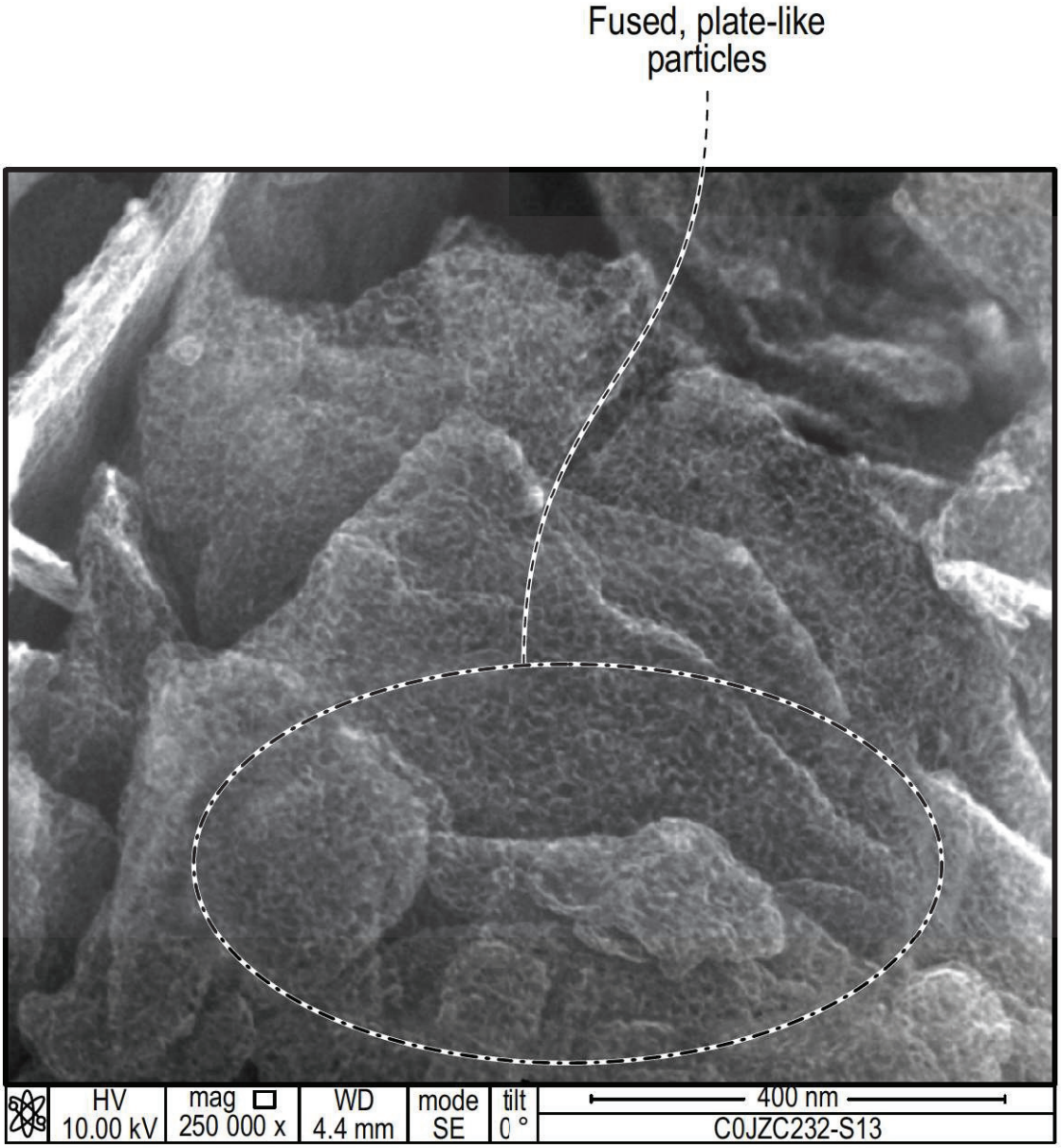

Fused, plate-like particles
HV
10.00 kV
mag
250 000 x
WD
4.4 mm
mode
SE
tilt
0 °
400 nm
C0JZC232-S13

FIG. 50F

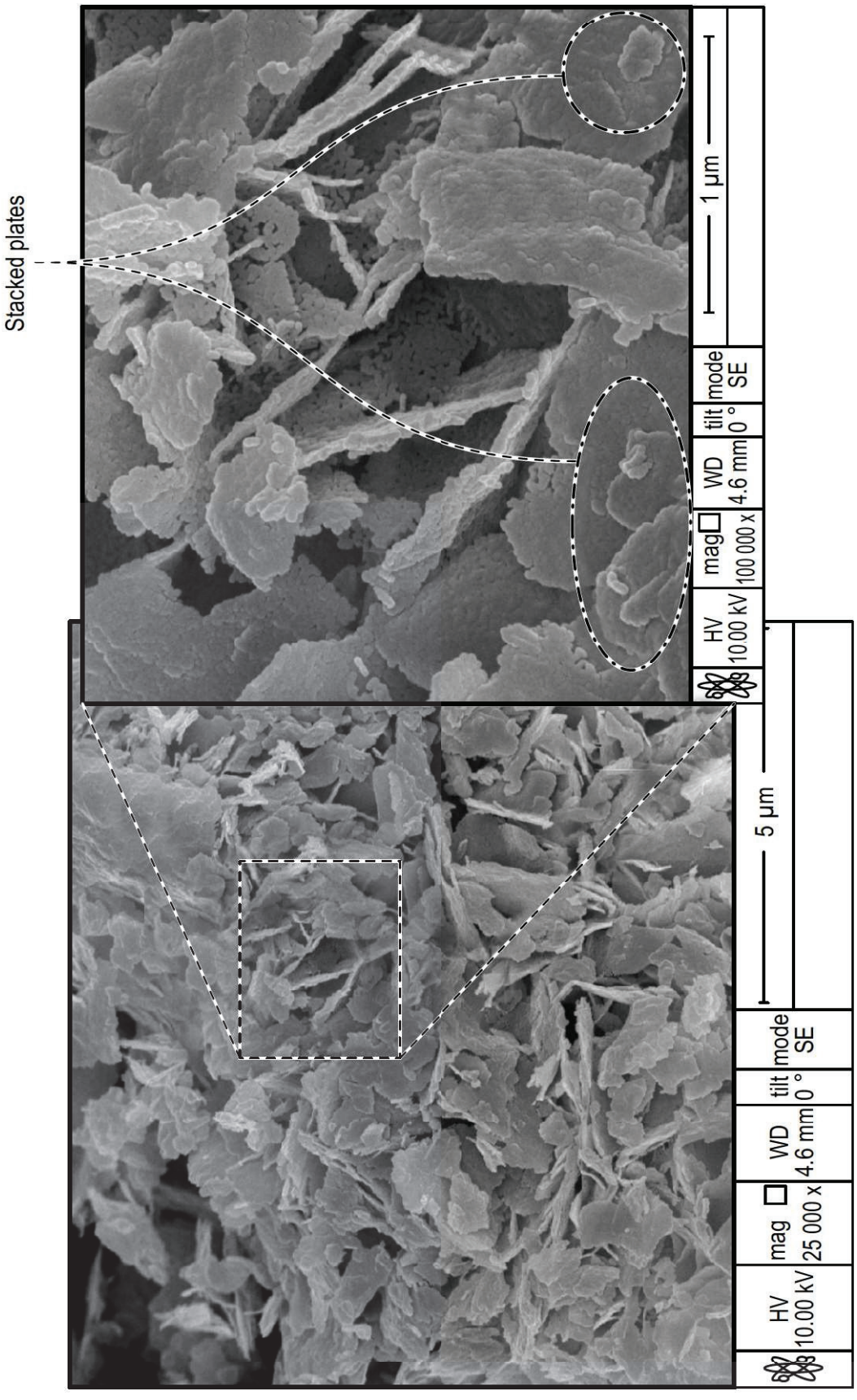

Stacked plates
HV 10.00 kV
mag 25 000 x
WD 4.6 mm
tilt 0 °
mode SE
5 µm
HV 10.00 kV
mag 100 000 x
WD 4.6 mm
tilt 0 °
mode SE
1 µm

FIG. 51

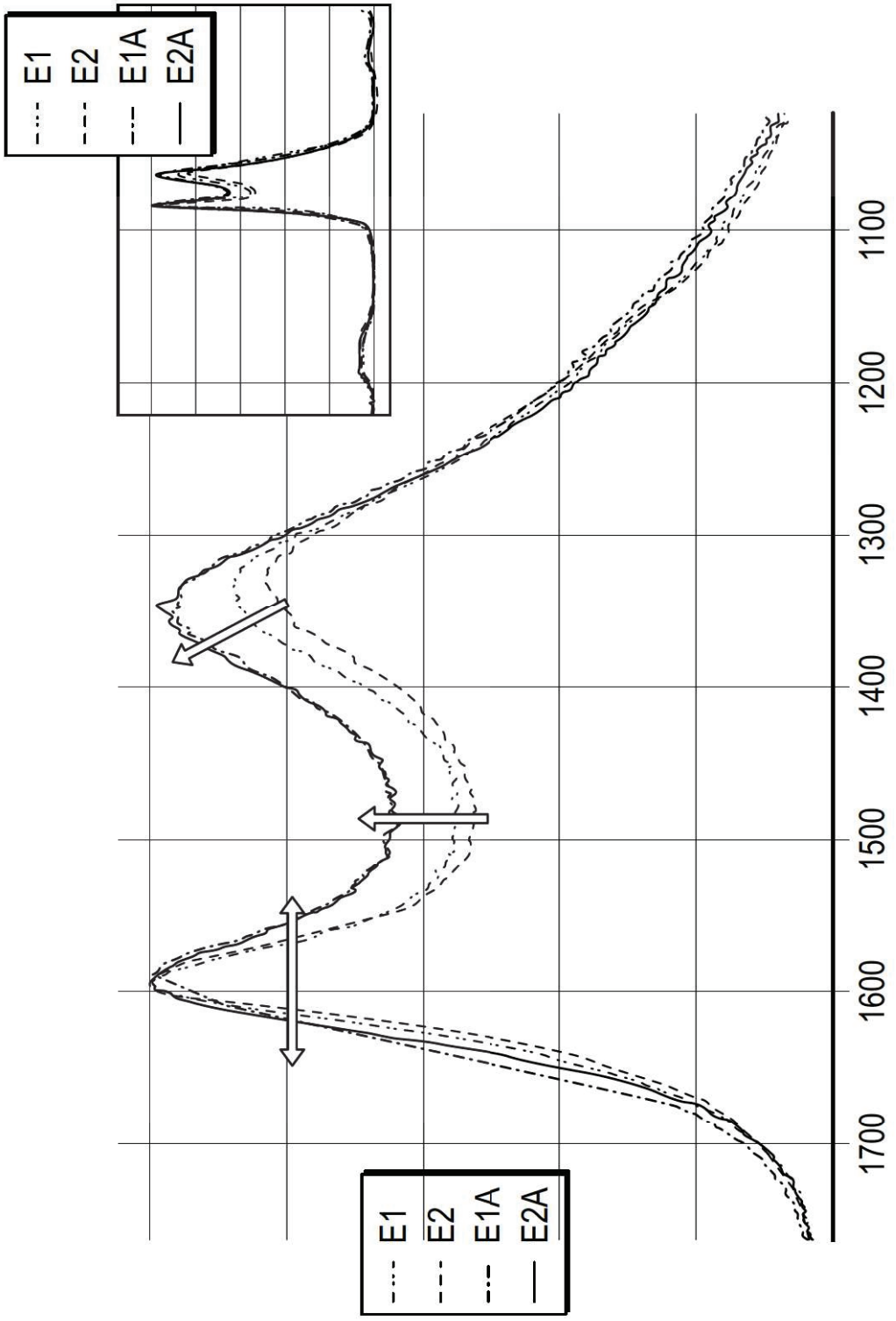



FIG. 52

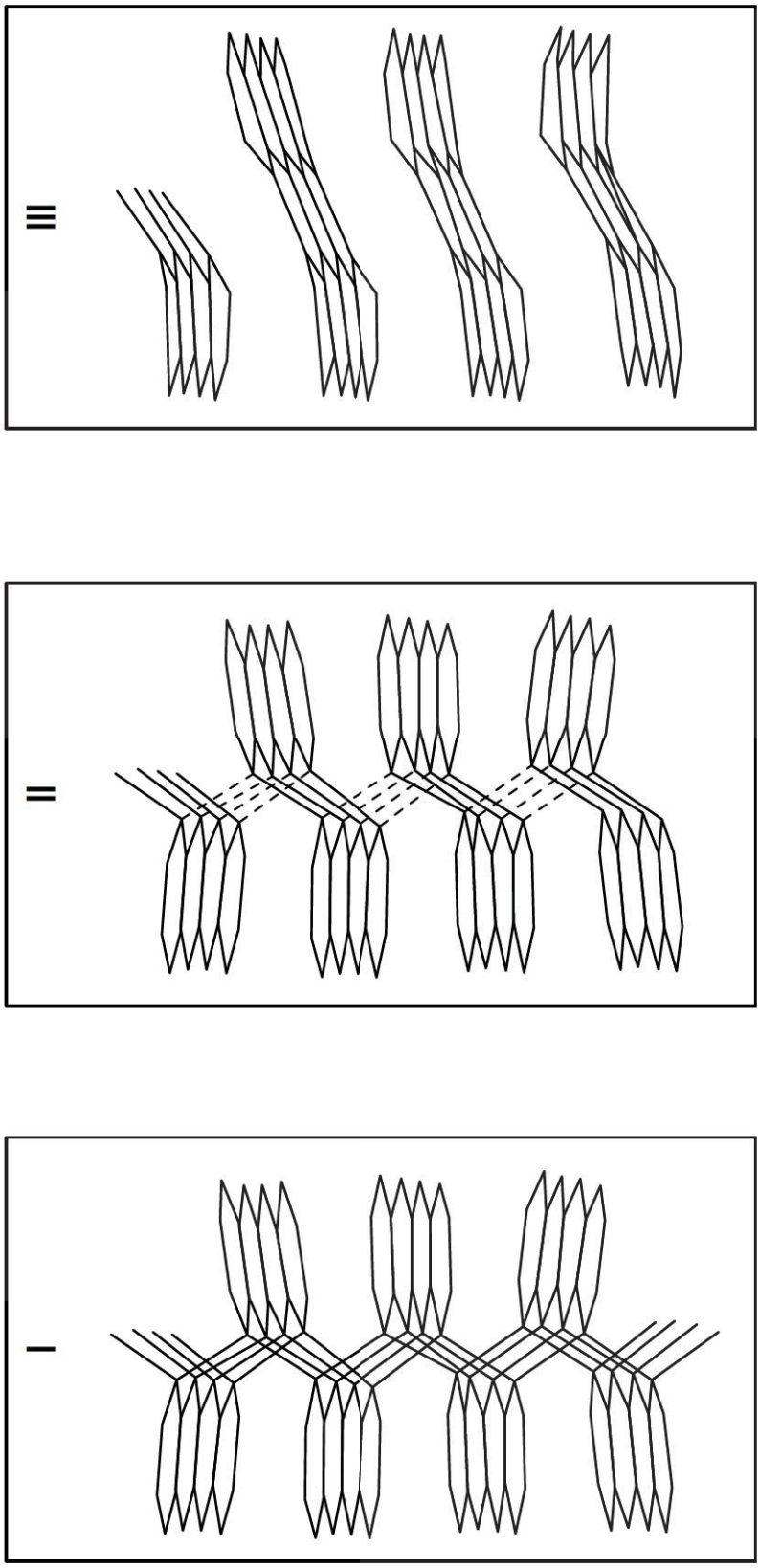



FIG. 53

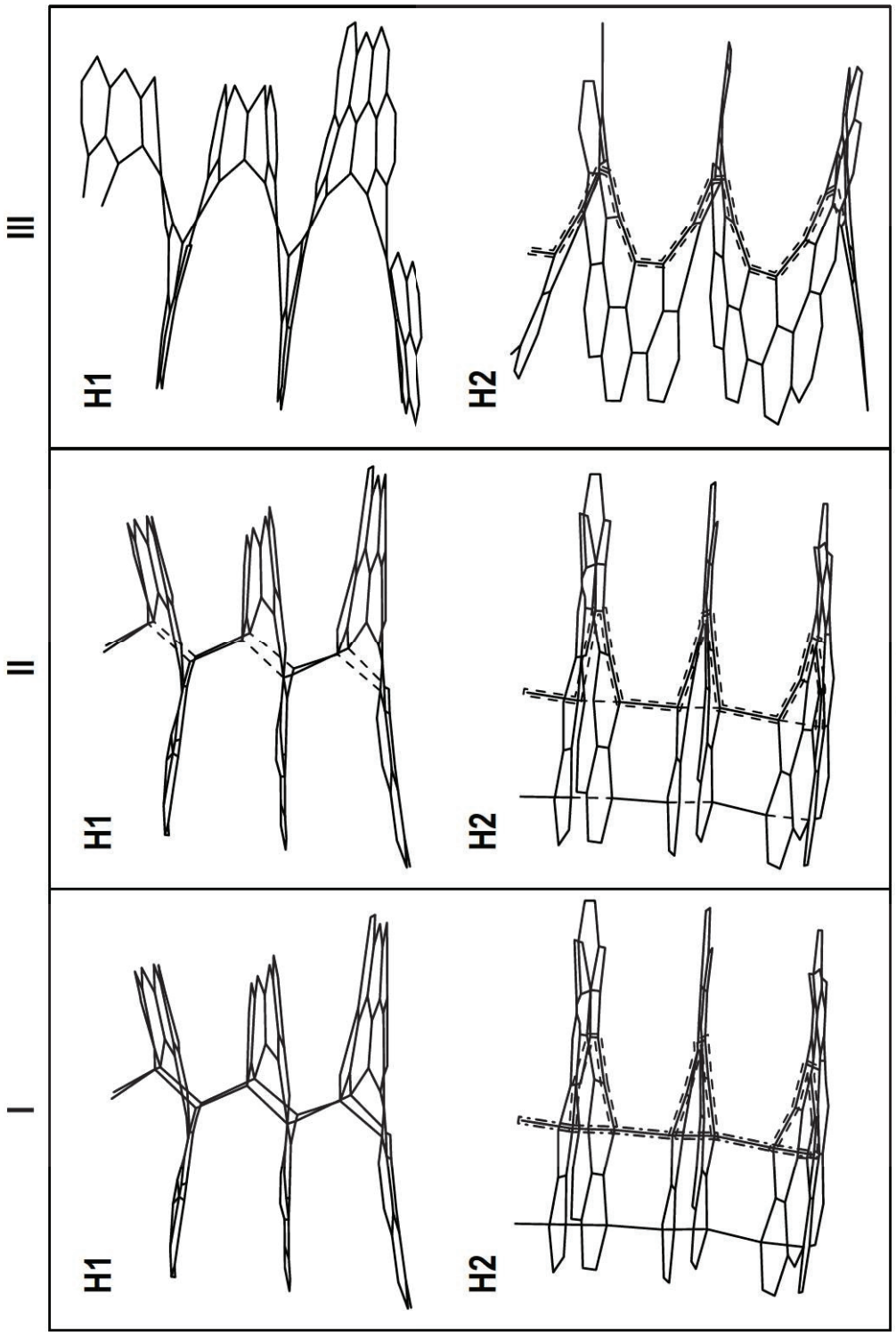



FIG. 54

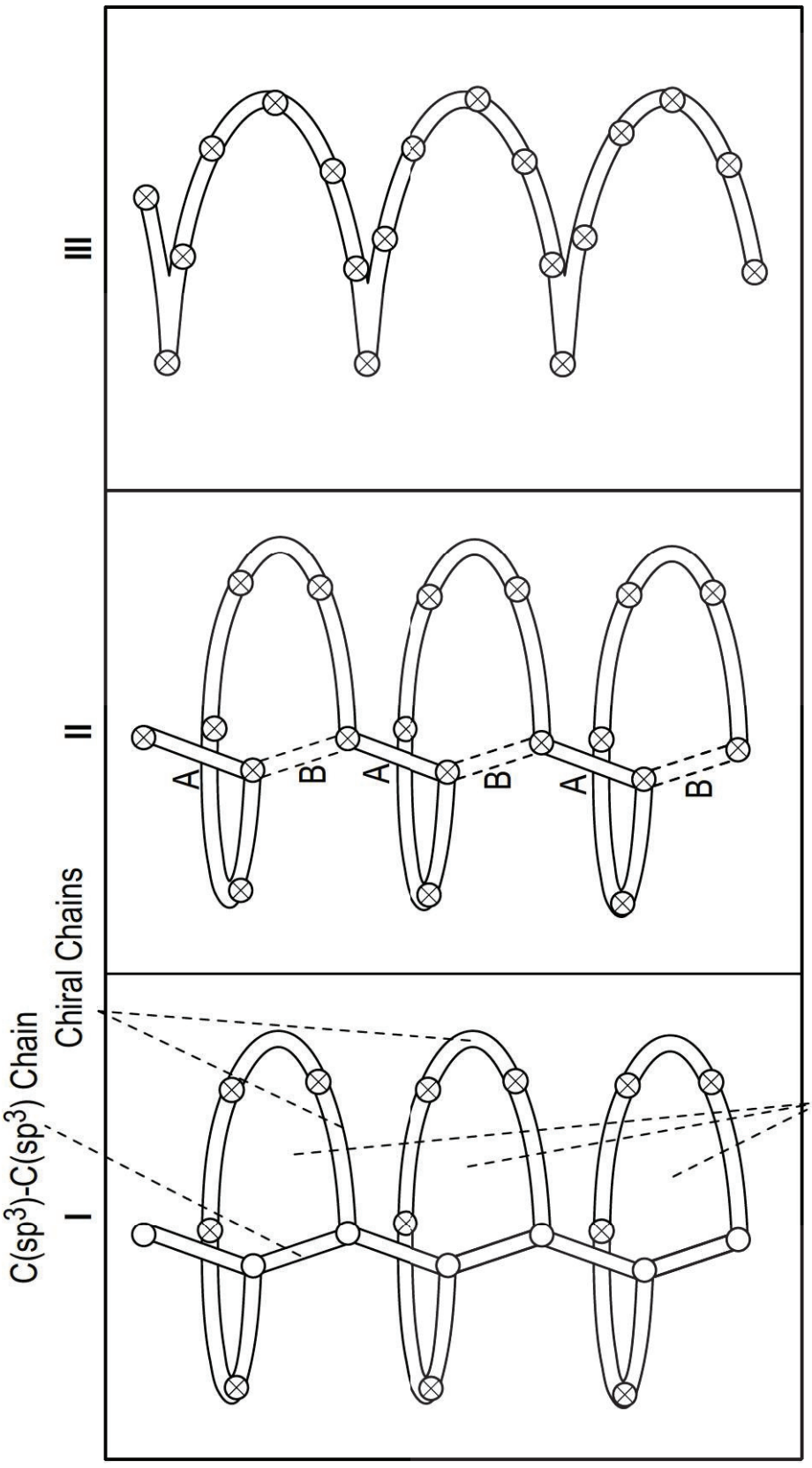



FIG. 55

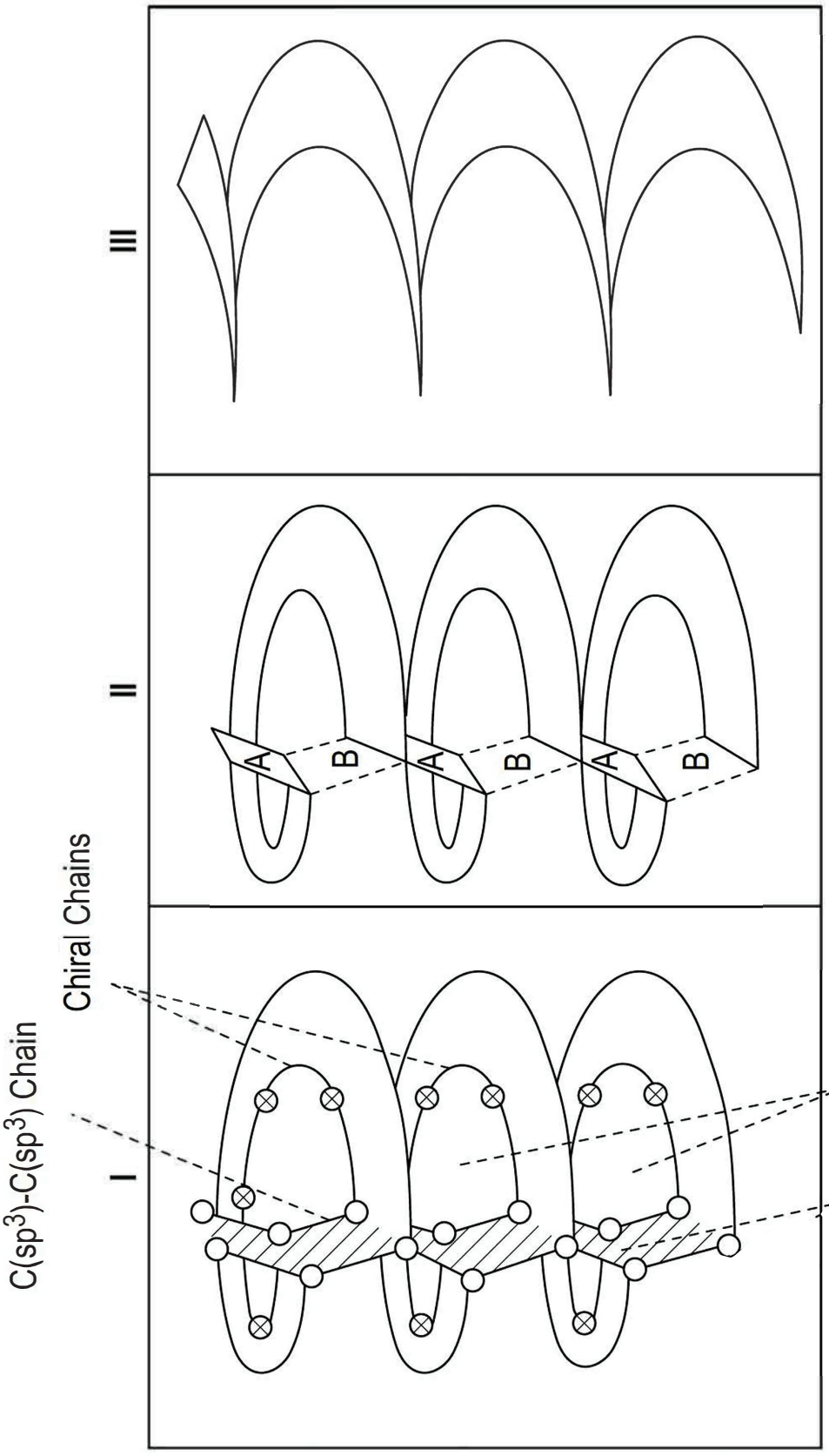

III
II
I
A
B
A
B
A
B
Chiral Chains
C(sp3)-C(sp3) Chain
Seam
Chiral Rings

FIG. 56

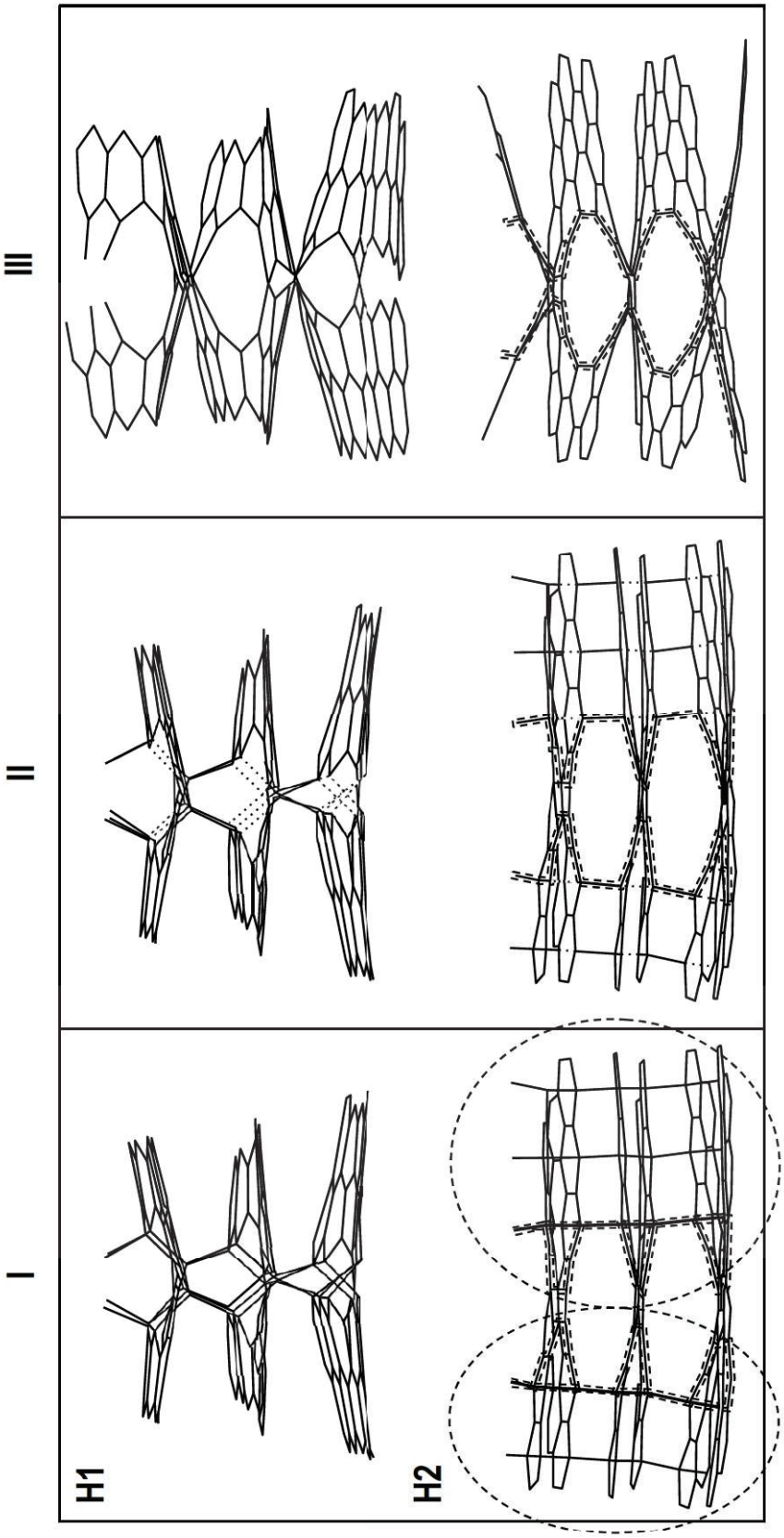



FIG. 57

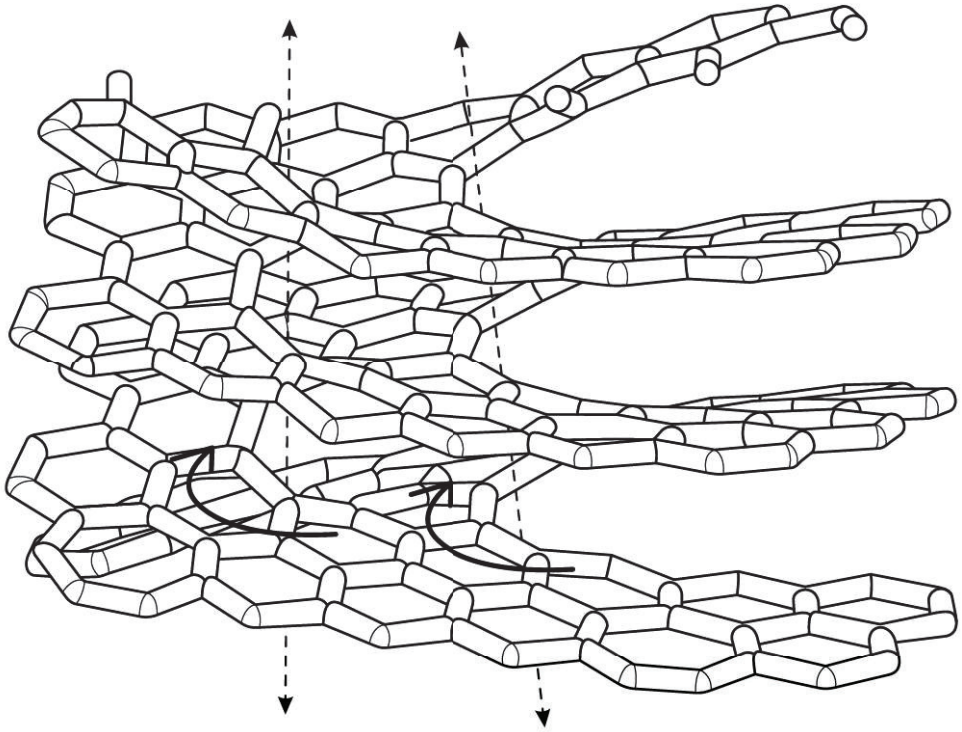


FIG. 58

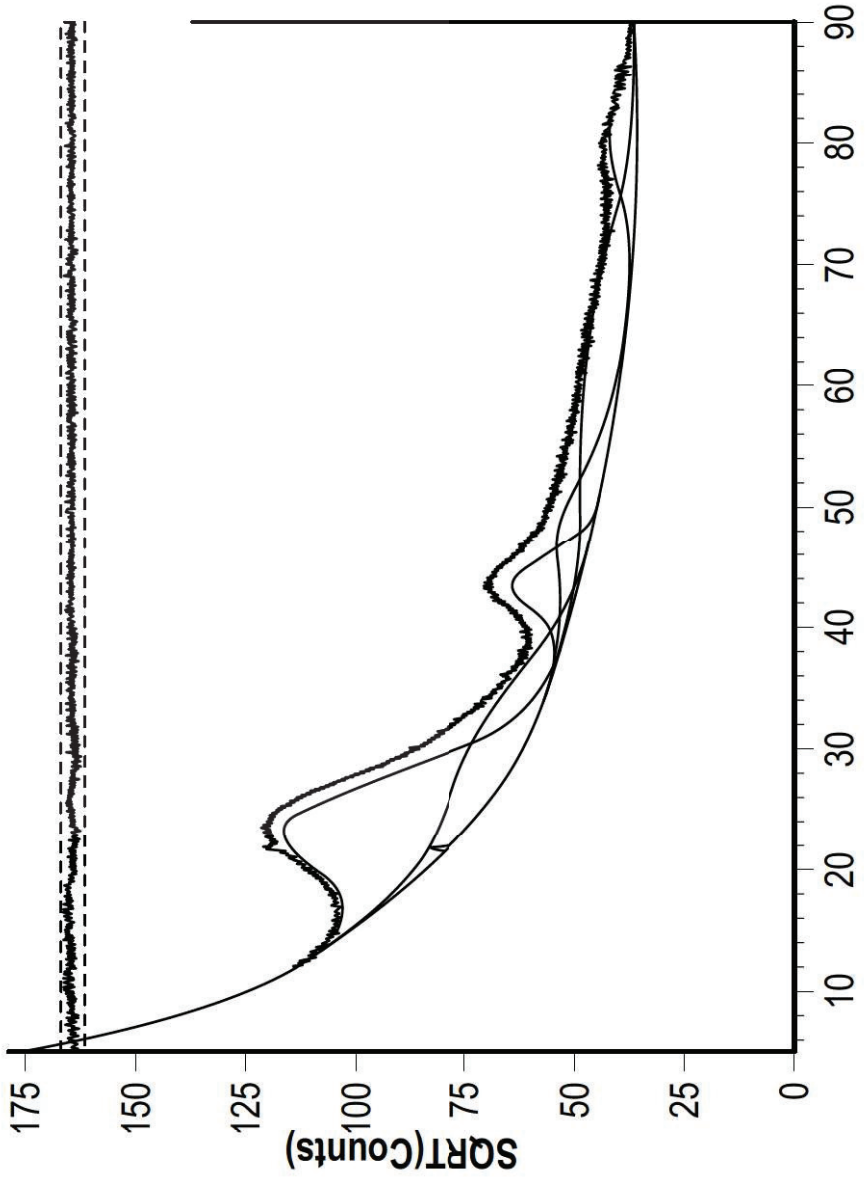

SQRT(Counts)
0
25
50
75
100
125
150
175
10
20
30
40
50
60
70
80
90
Two-Theta (deg)

FIG. 59

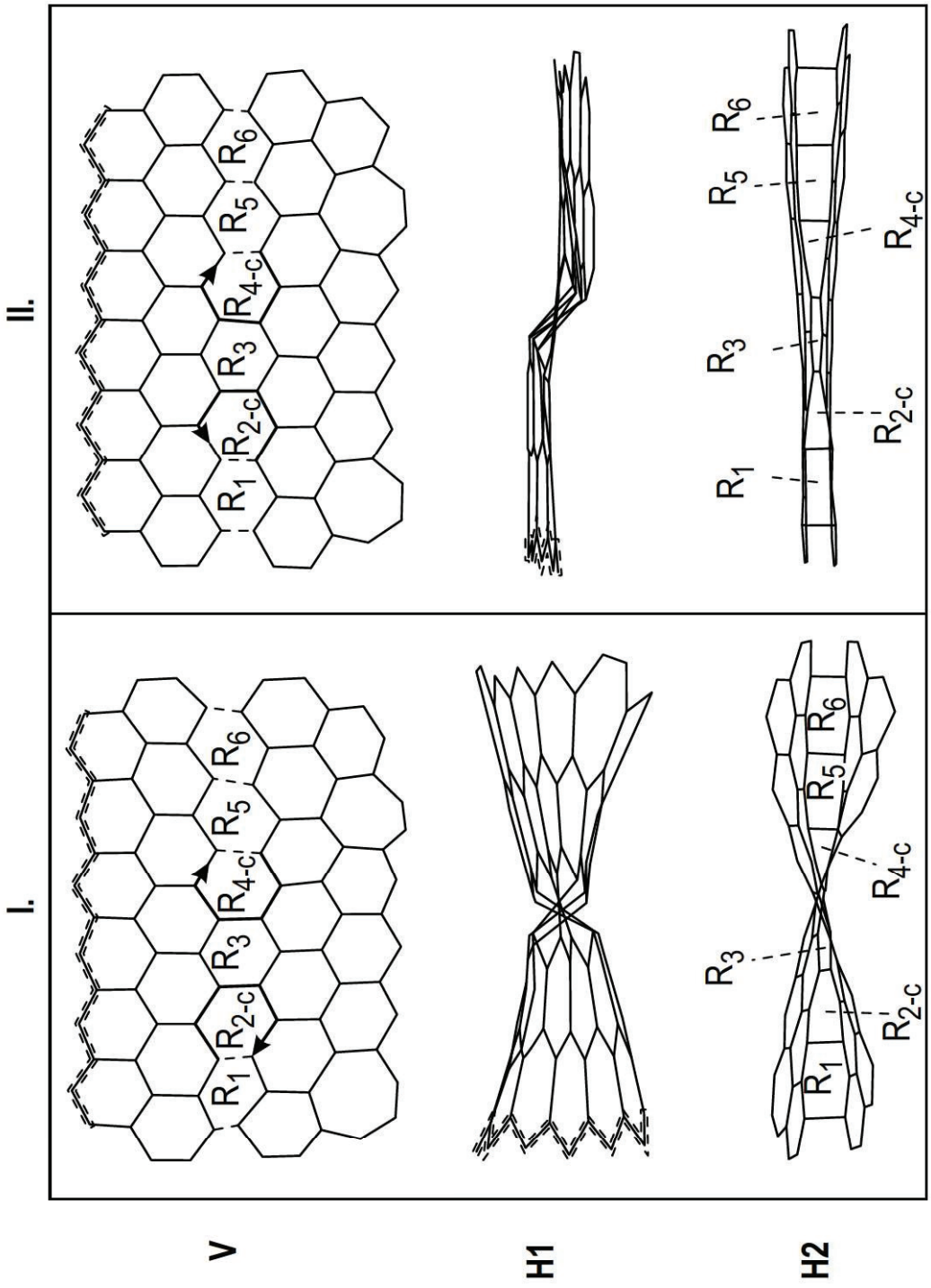



FIG. 60

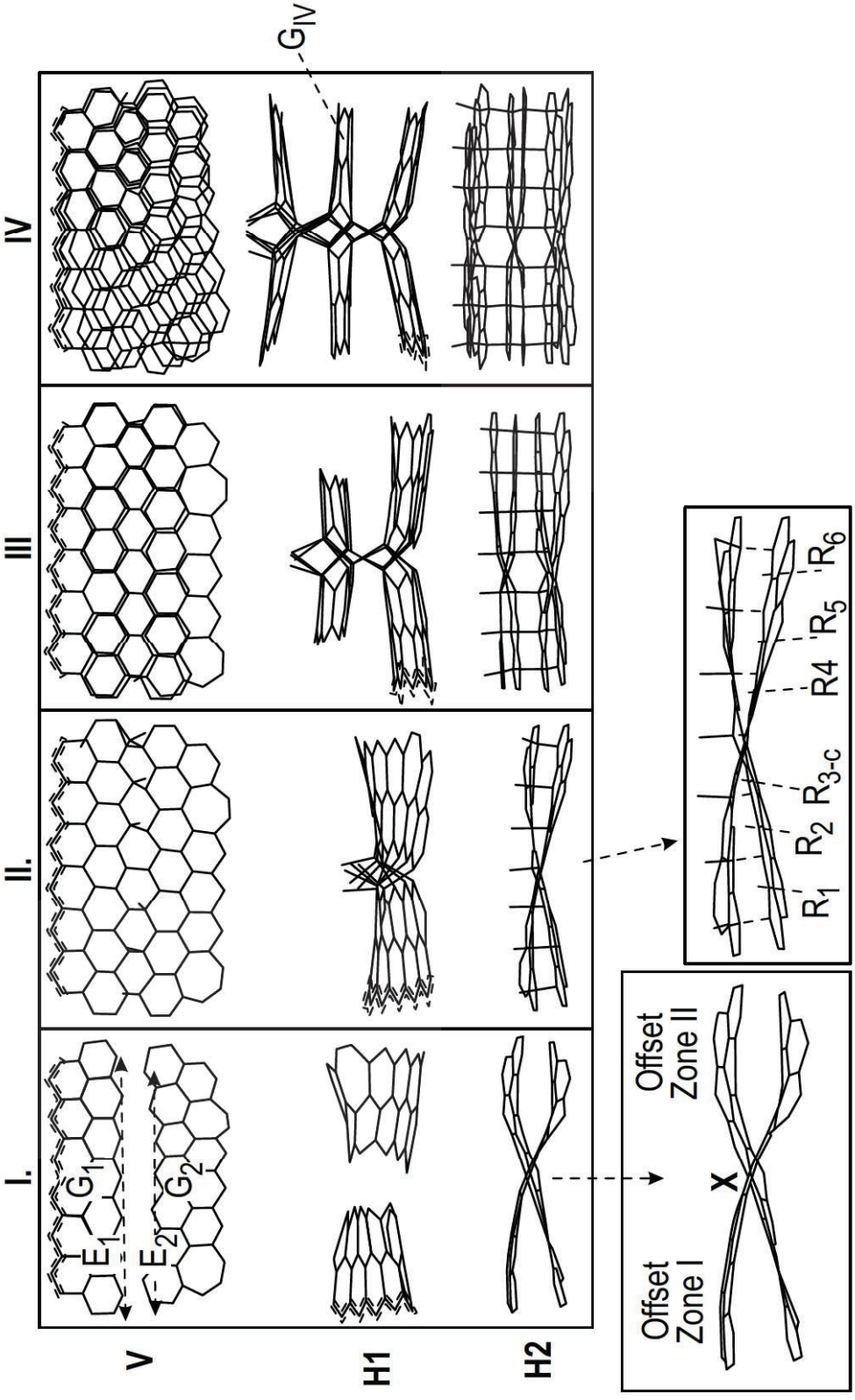

I.
II.
III
IV
V
H1
H2
$G_1$
$E_1$
$E_2$
$G_2$
$G_{IV}$
Offset Zone I
Offset Zone II
X
$R_1'$ $R_2$ $R_{3-c}$ R4 $R_5'$ $R_6'$

FIG. 61

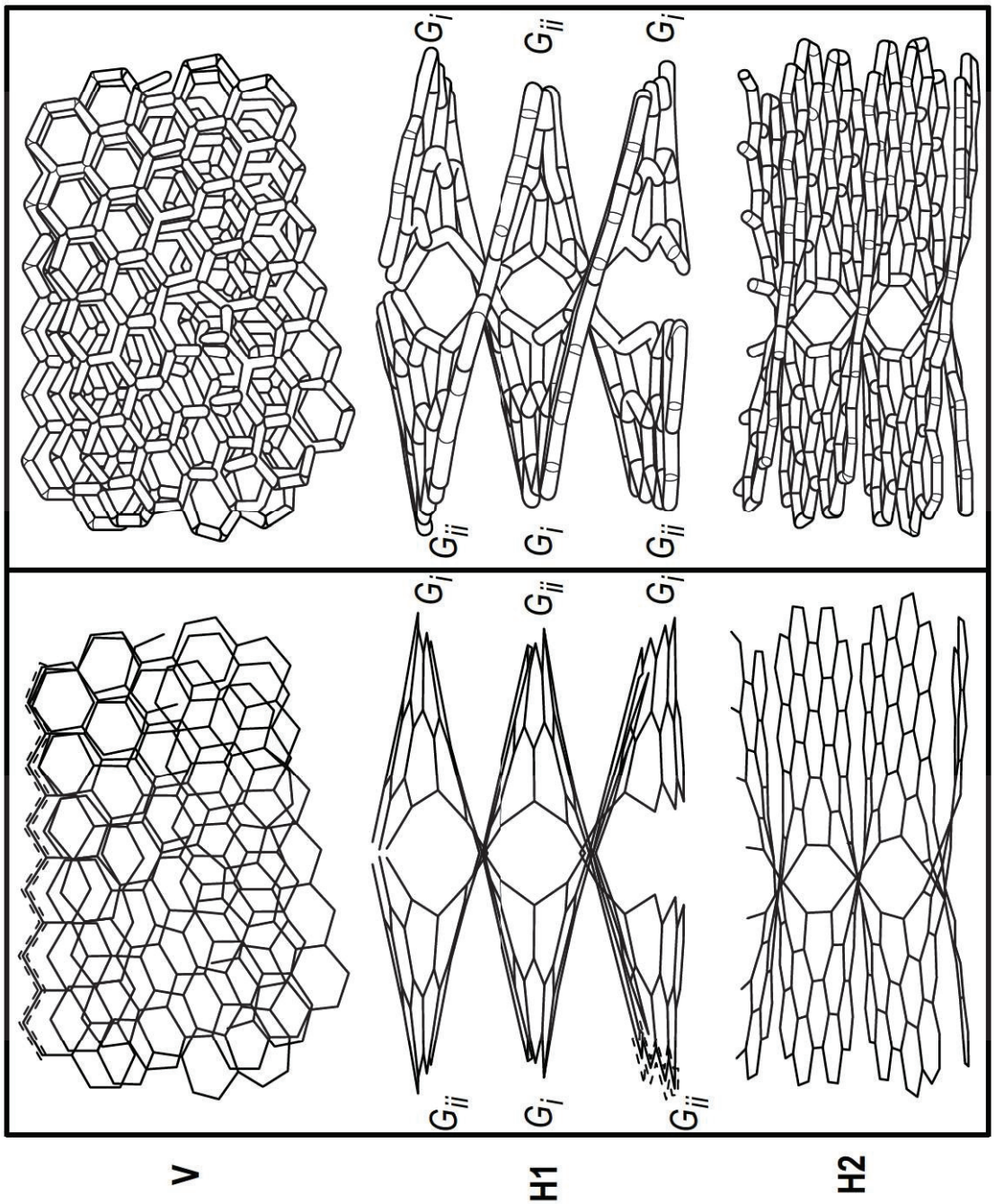
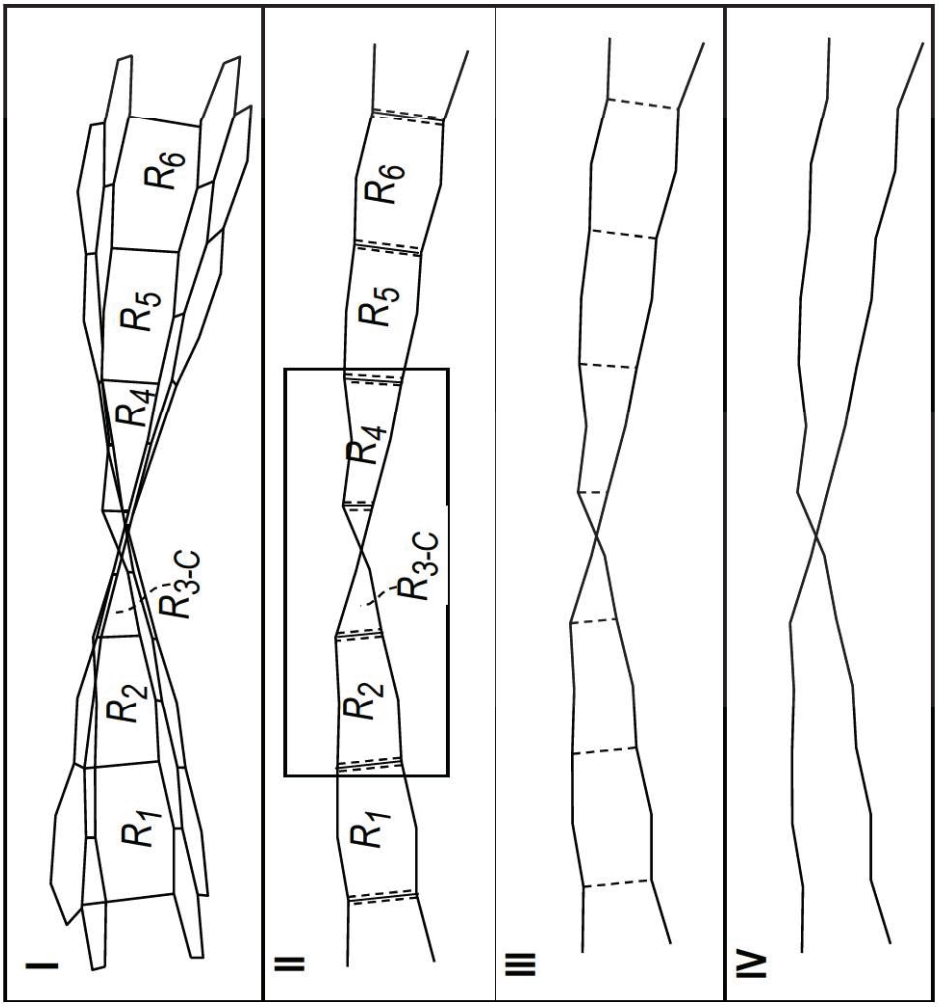



FIG. 62



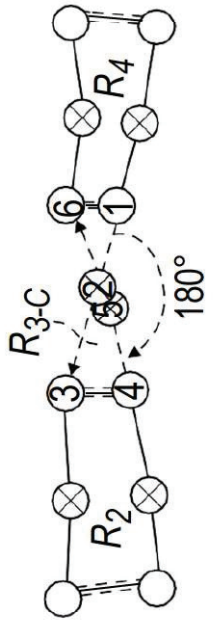




FIG. 63

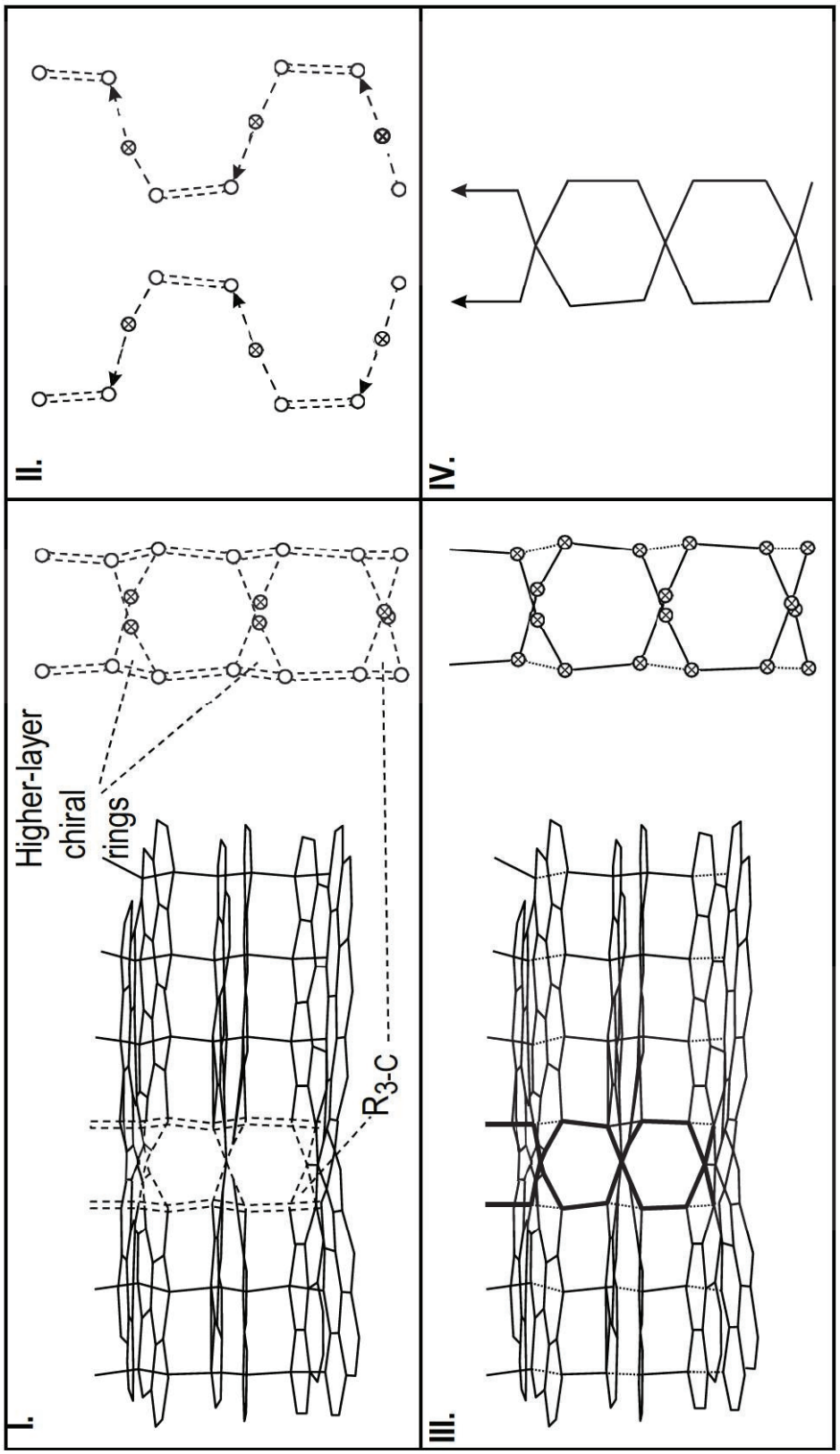



FIG. 64

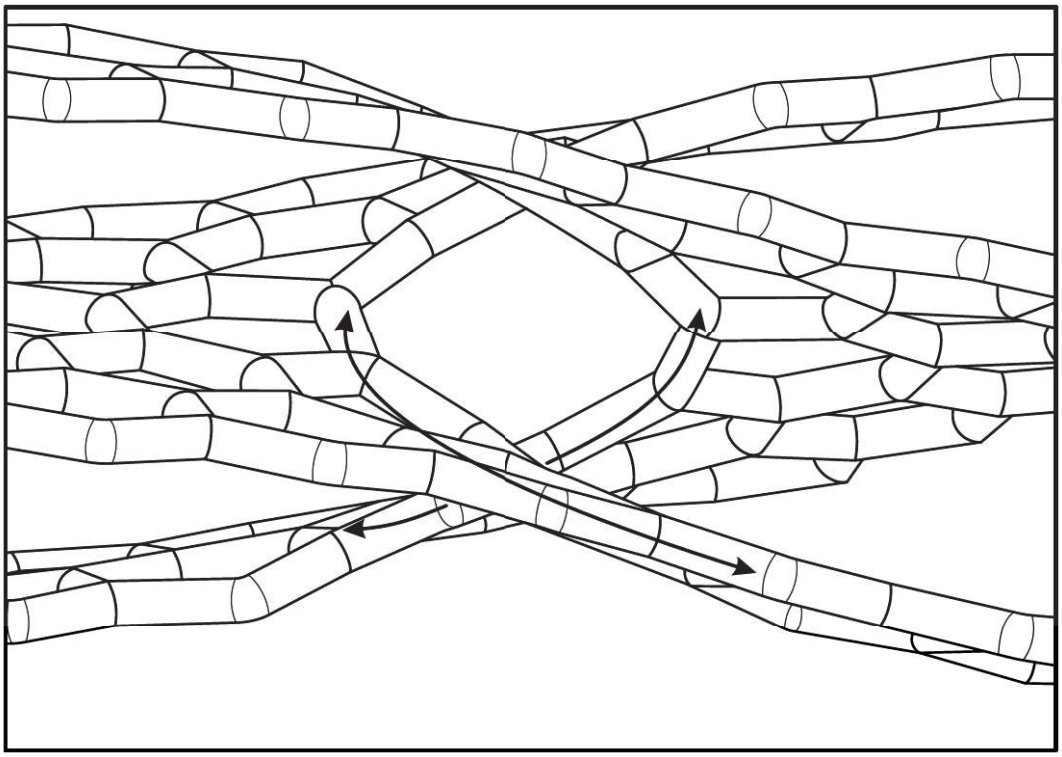


FIG. 65A

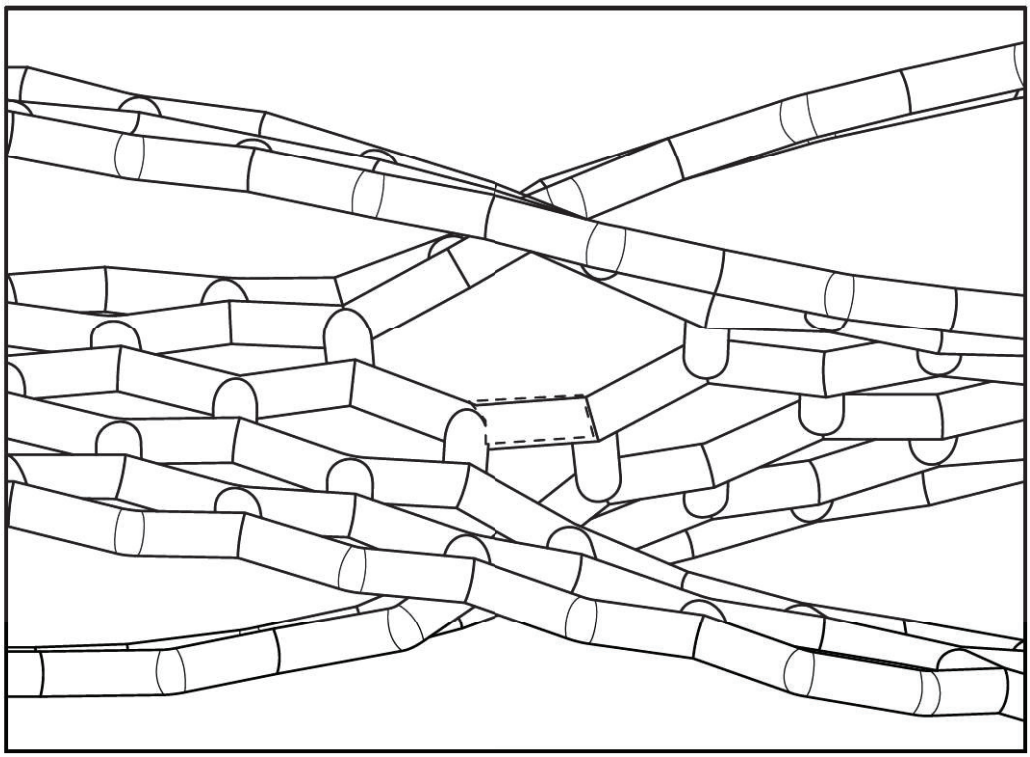


FIG. 65B

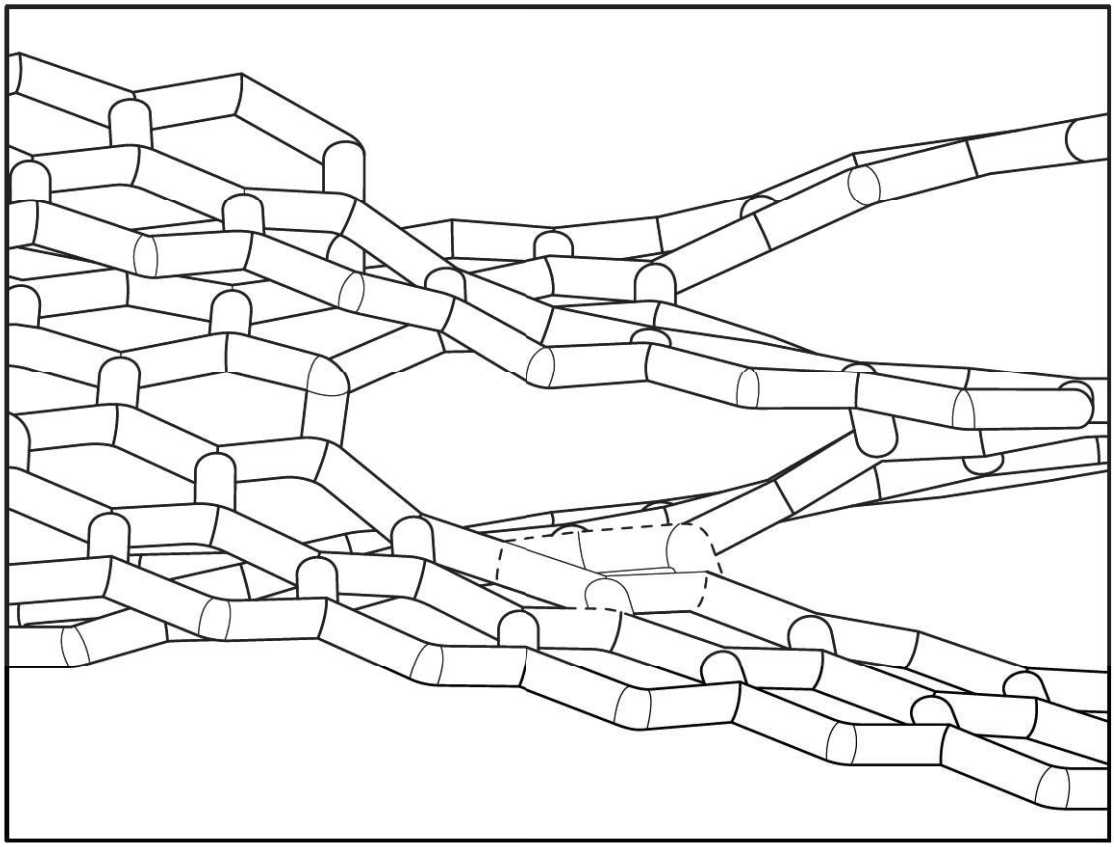


FIG. 65C

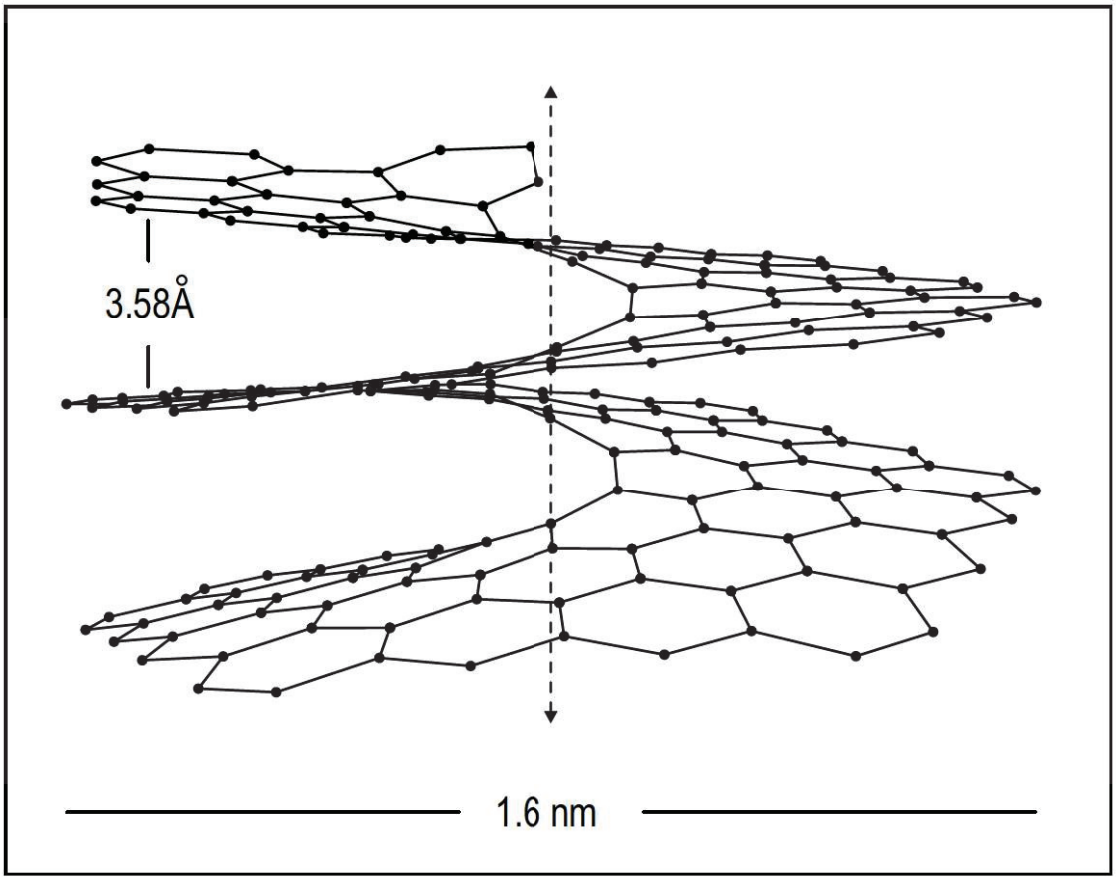



FIG. 66A

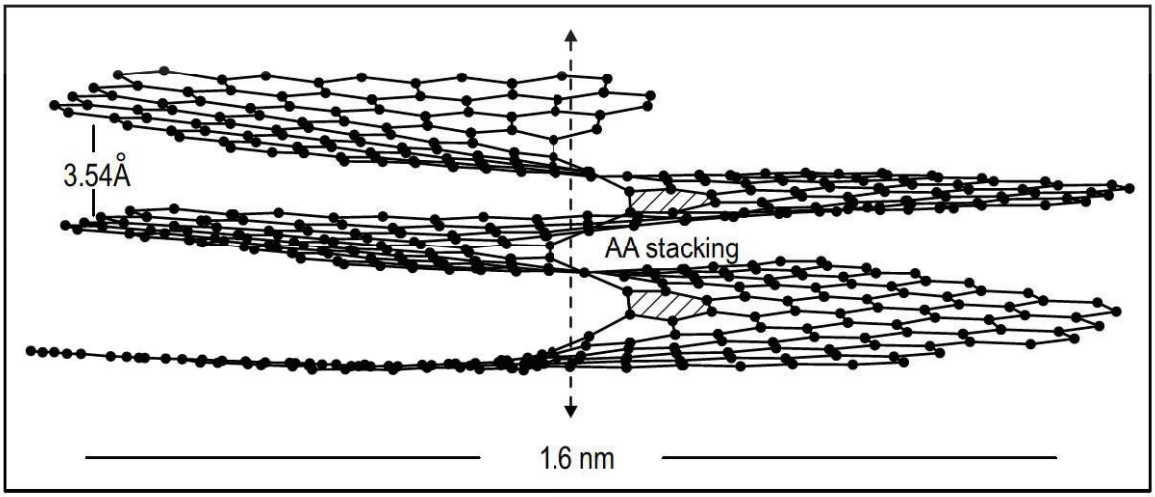



FIG. 66B

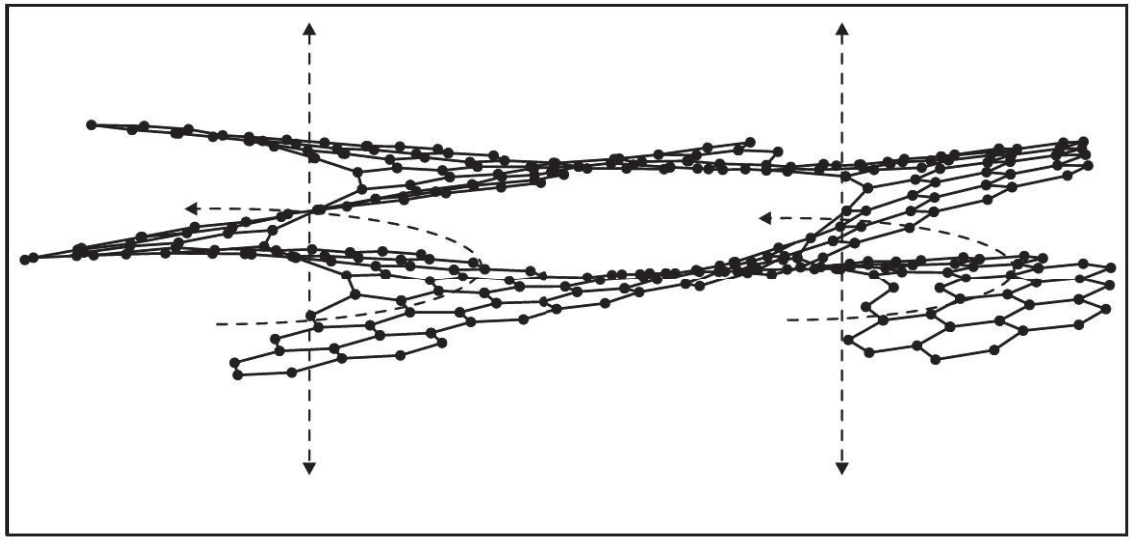


FIG. 66C

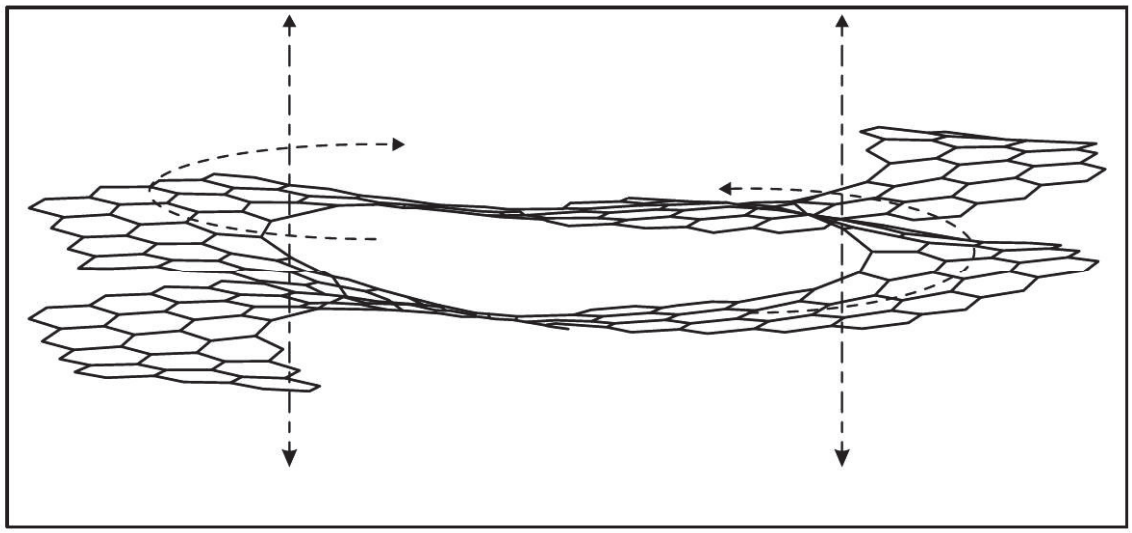


FIG. 66D

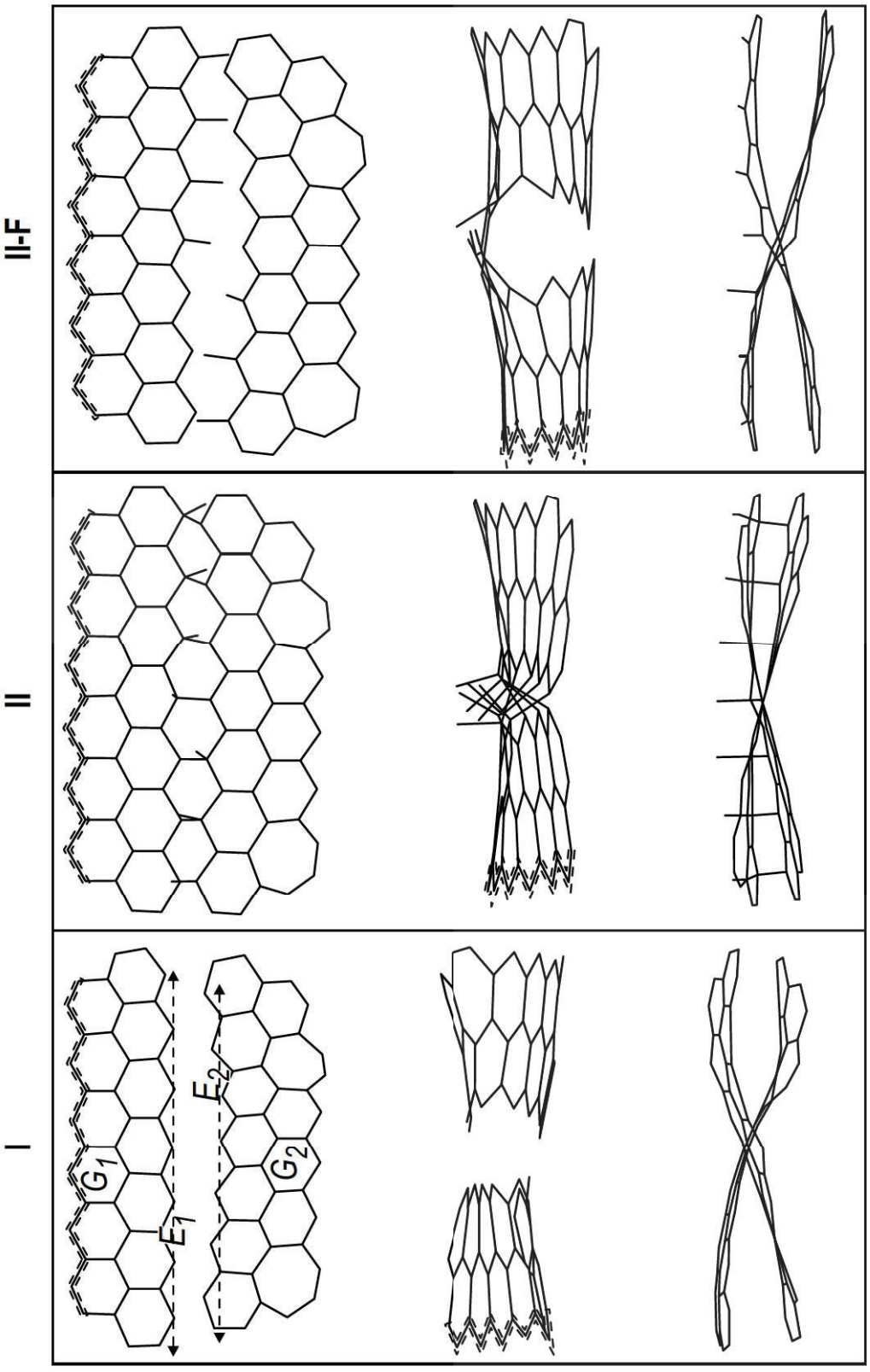



FIG. 67

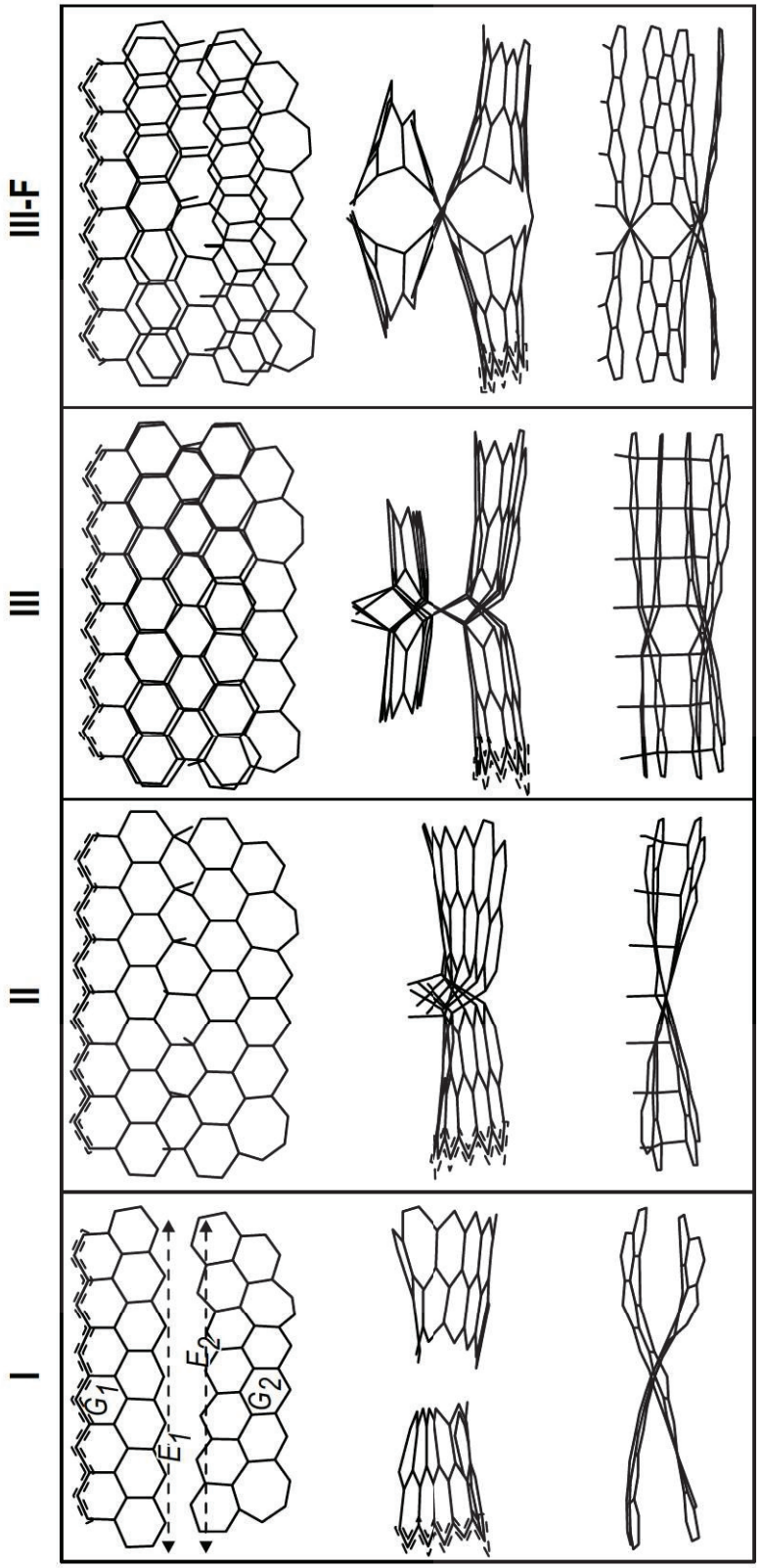



FIG. 68

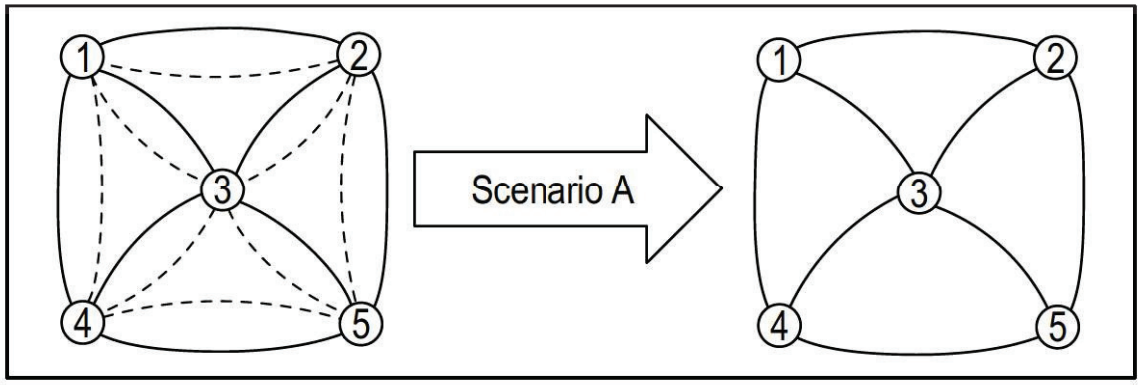



FIG. 69A

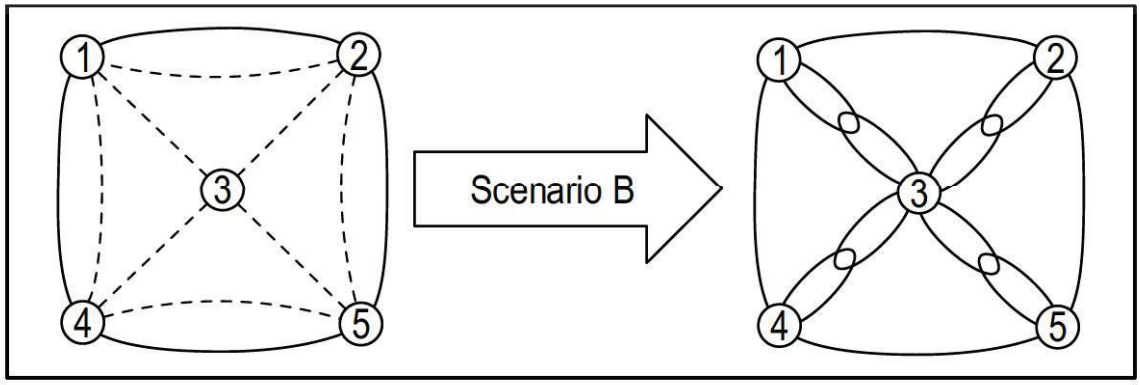



FIG. 69B

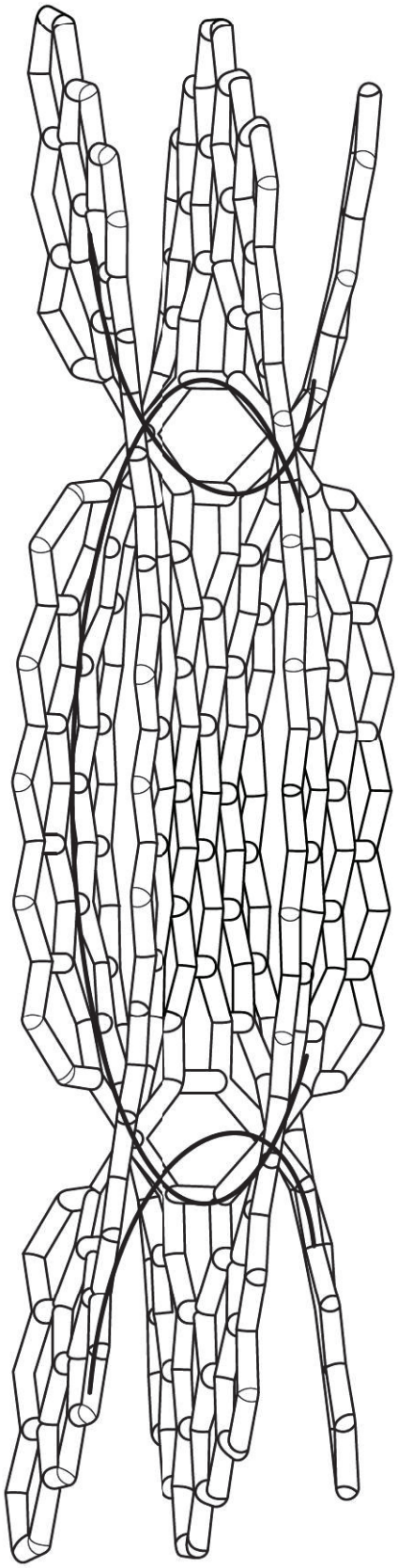


FIG. 70




FIG. 71A

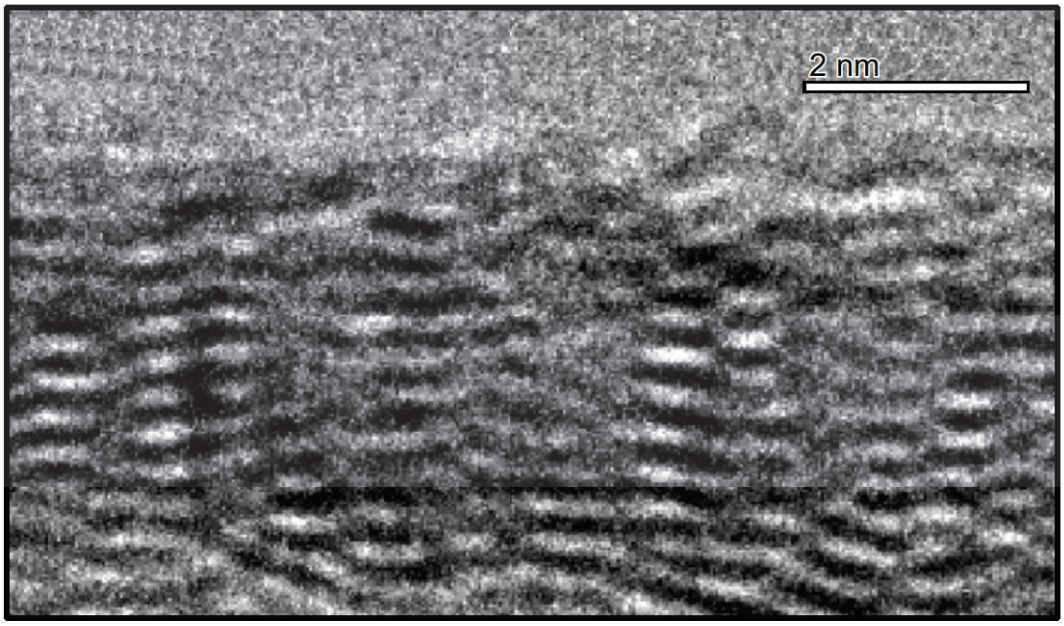



FIG. 71B

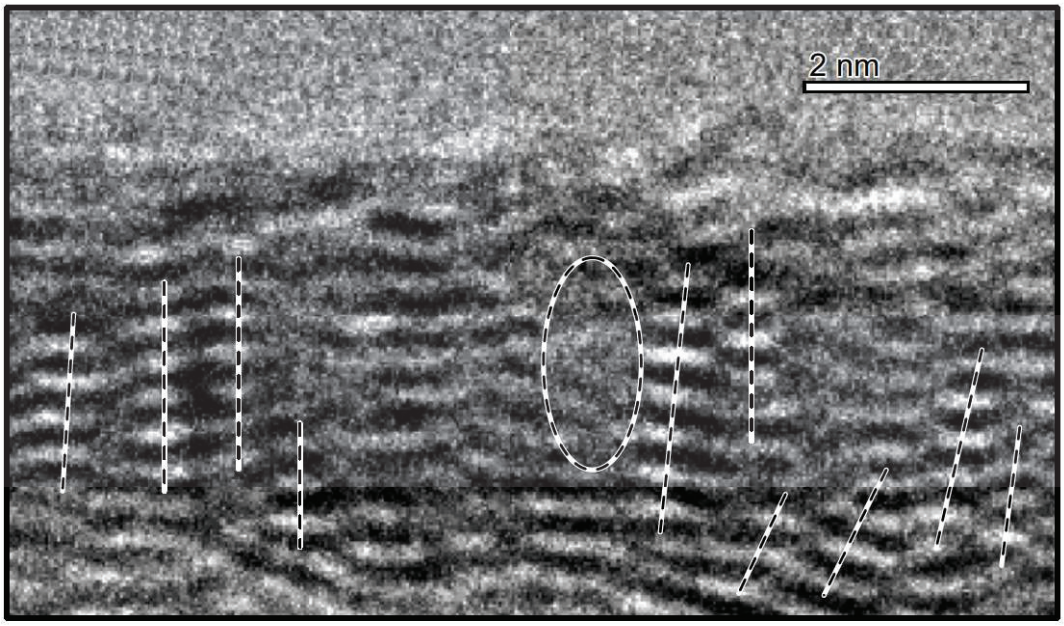



FIG. 71C

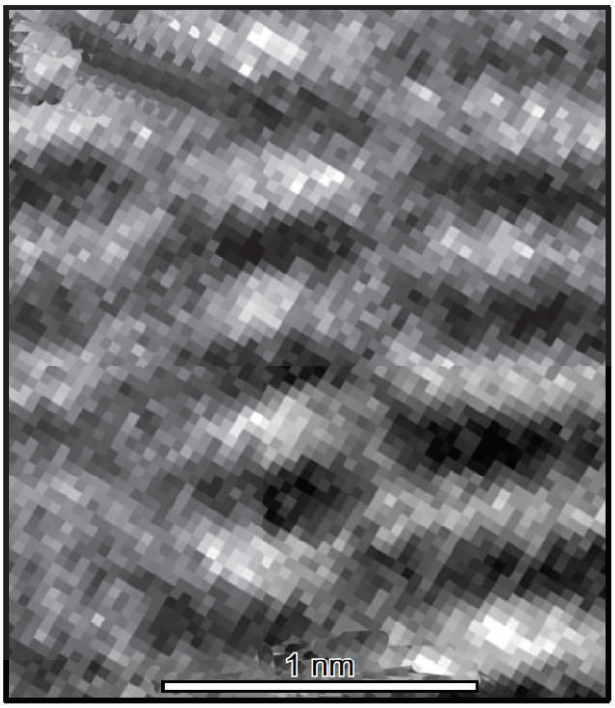



FIG. 71D

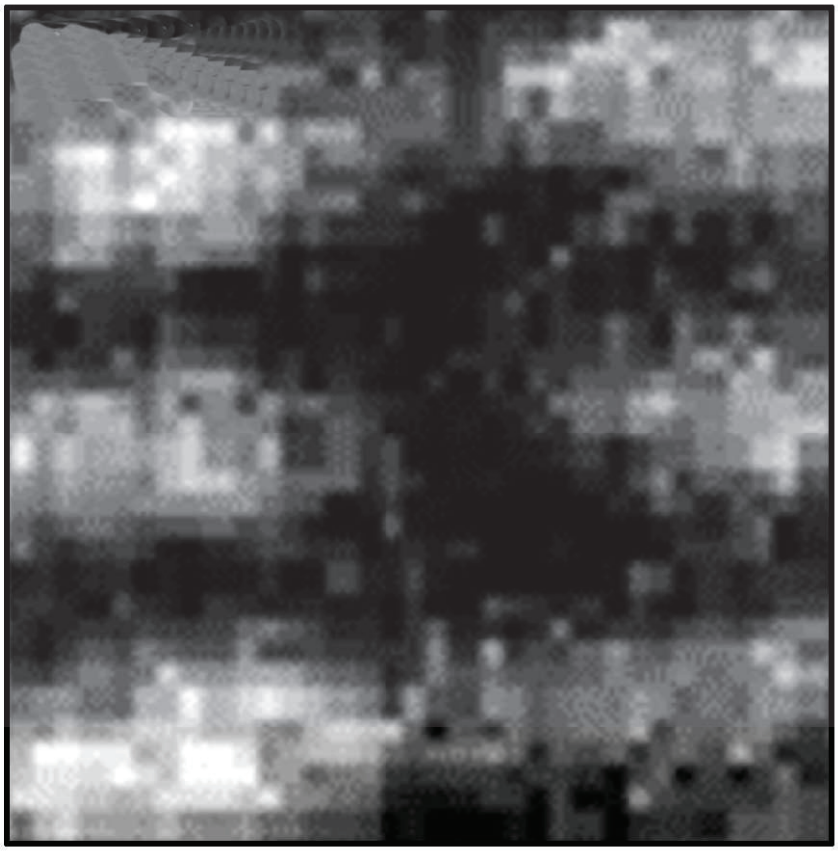


FIG. 71E

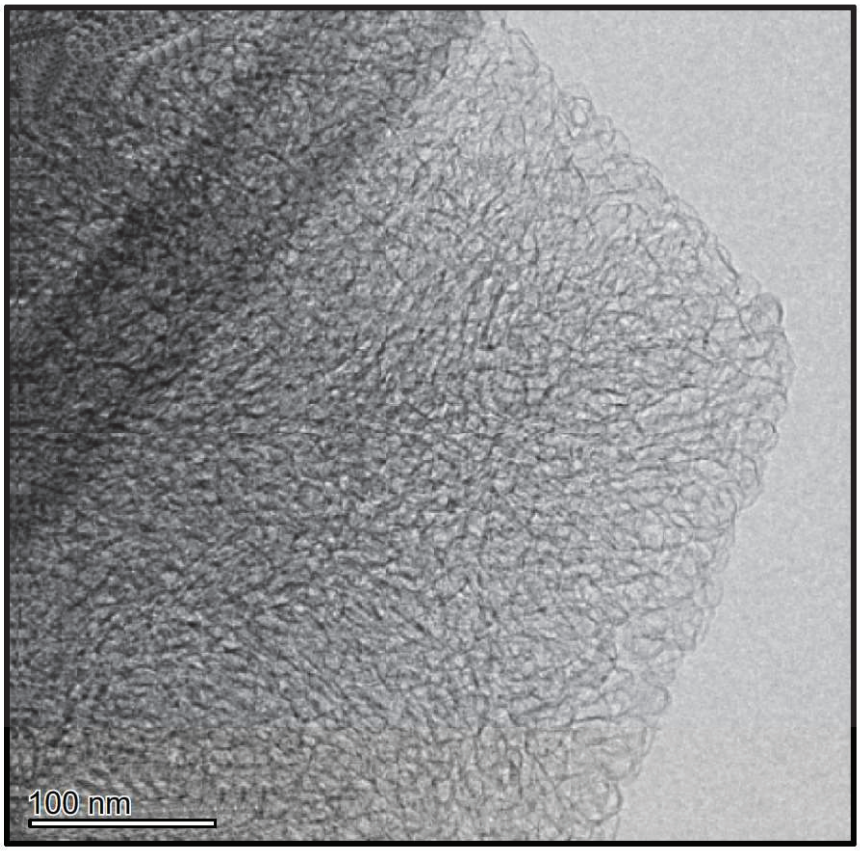



FIG. 72A

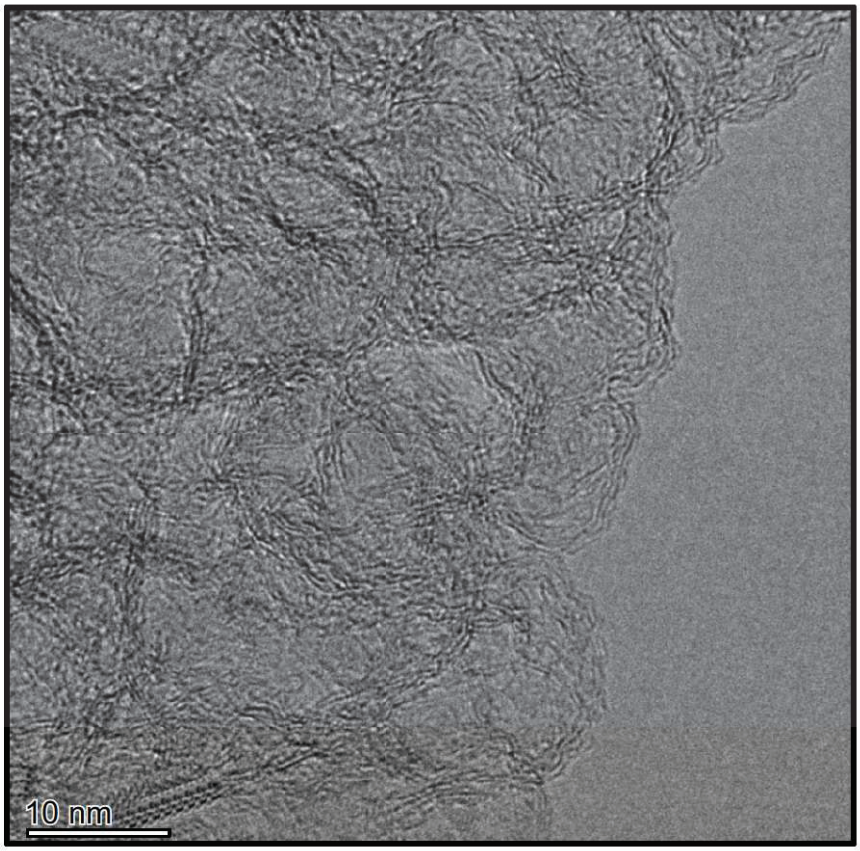



FIG. 72B

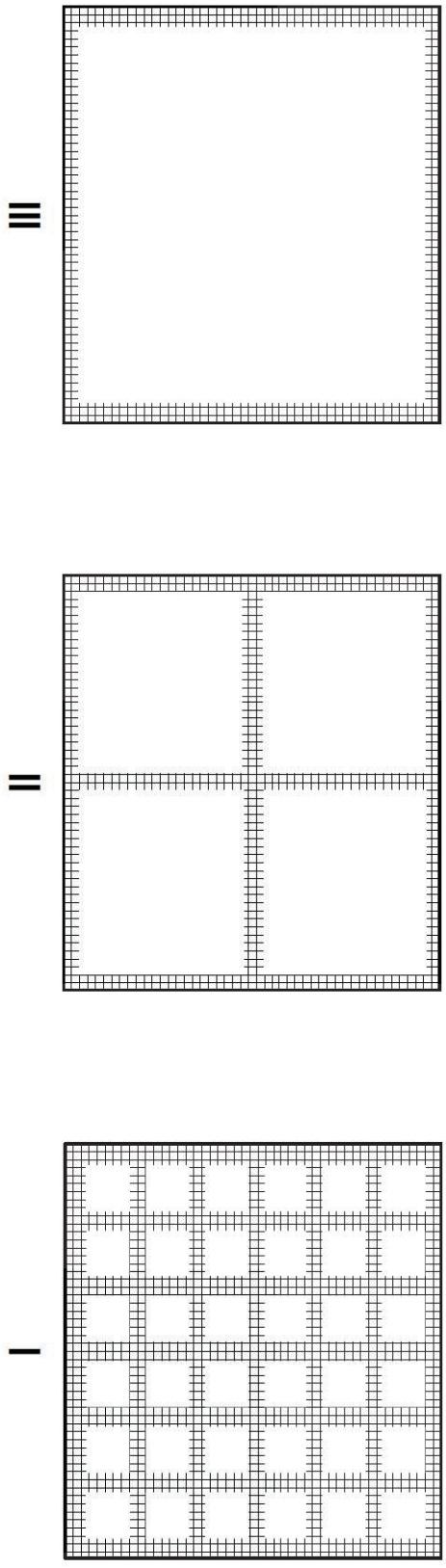



FIG. 73

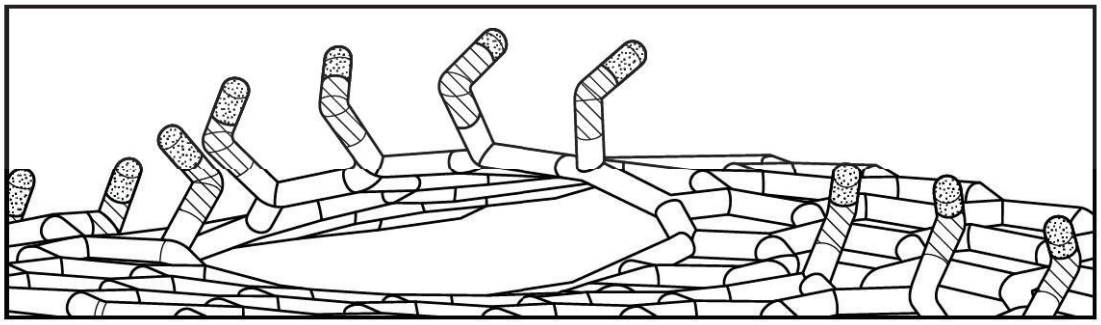


FIG. 74A

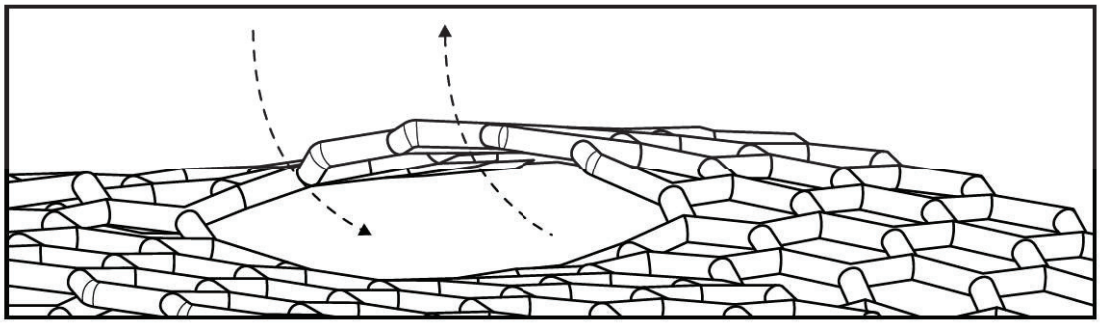


FIG. 74B

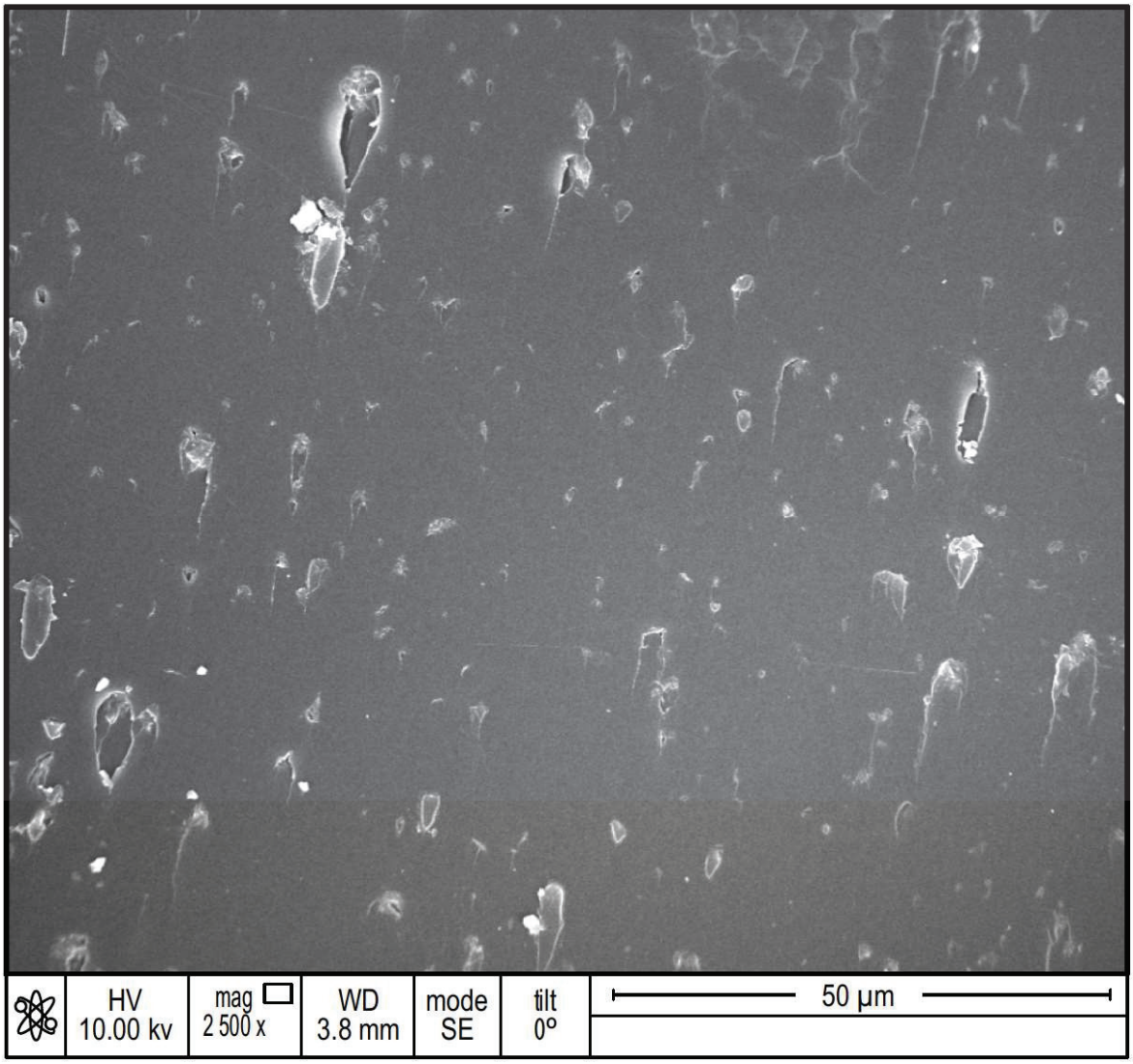



FIG. 75A

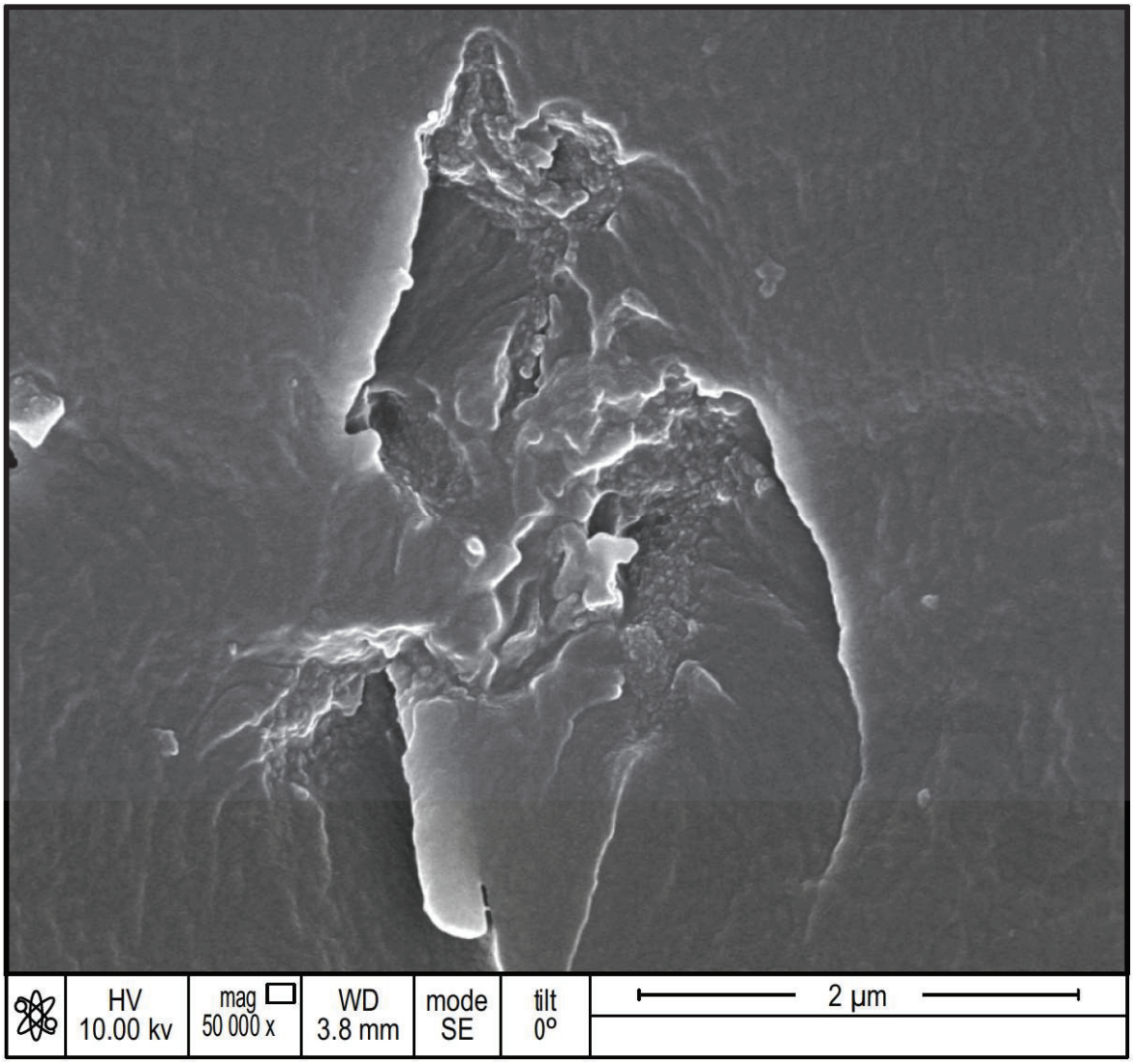



FIG. 75B

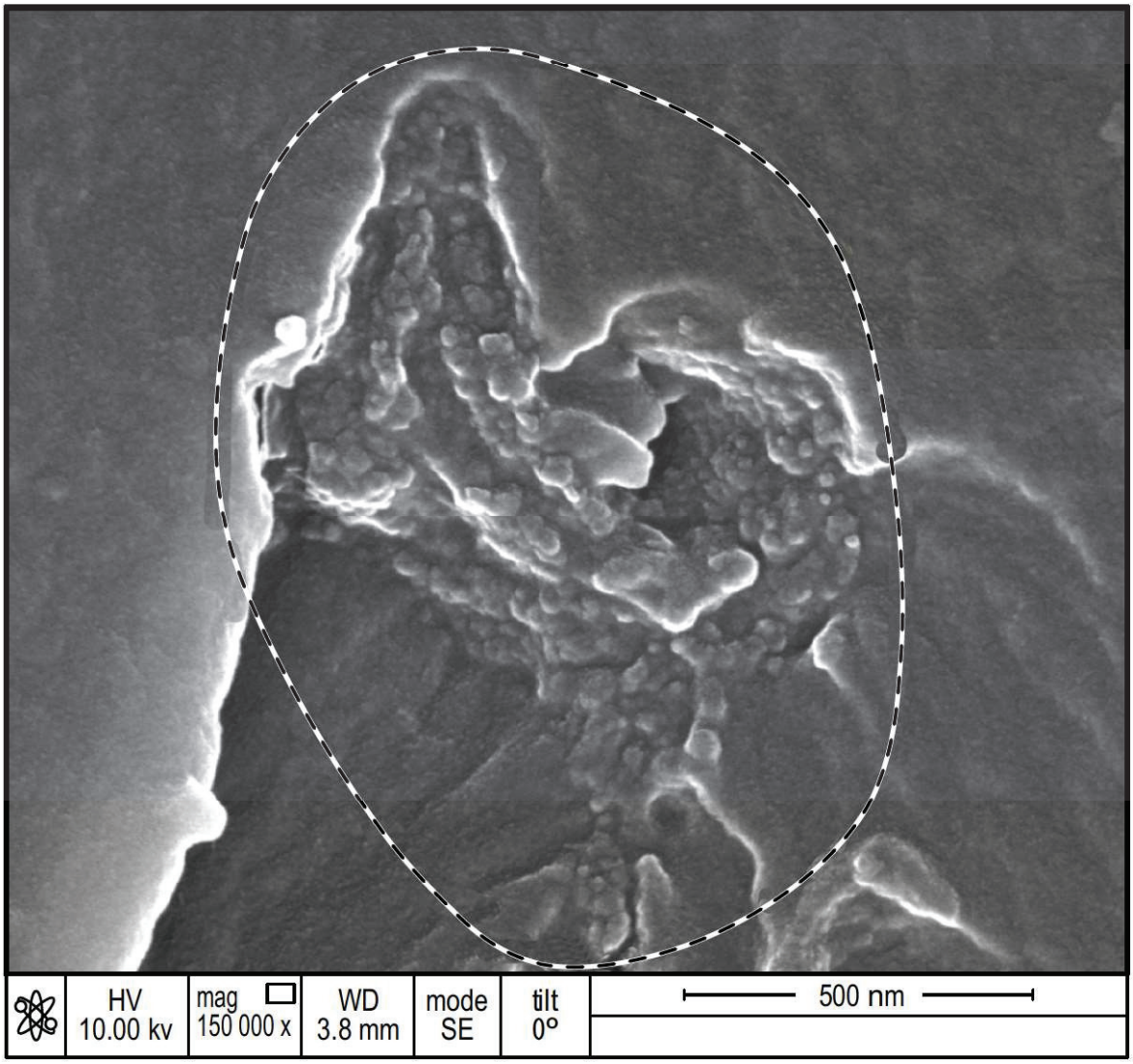



FIG. 75C

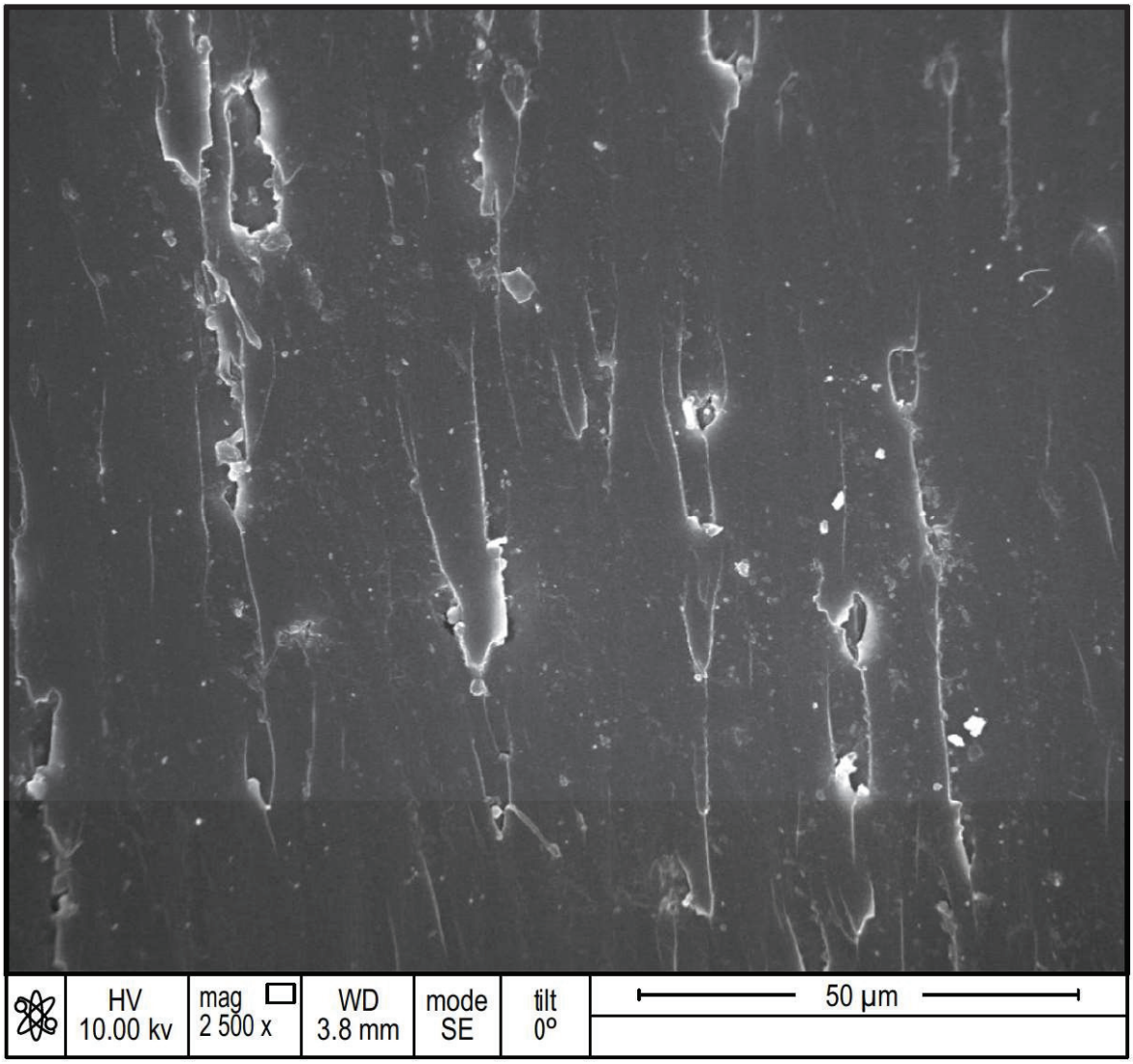



FIG. 76A

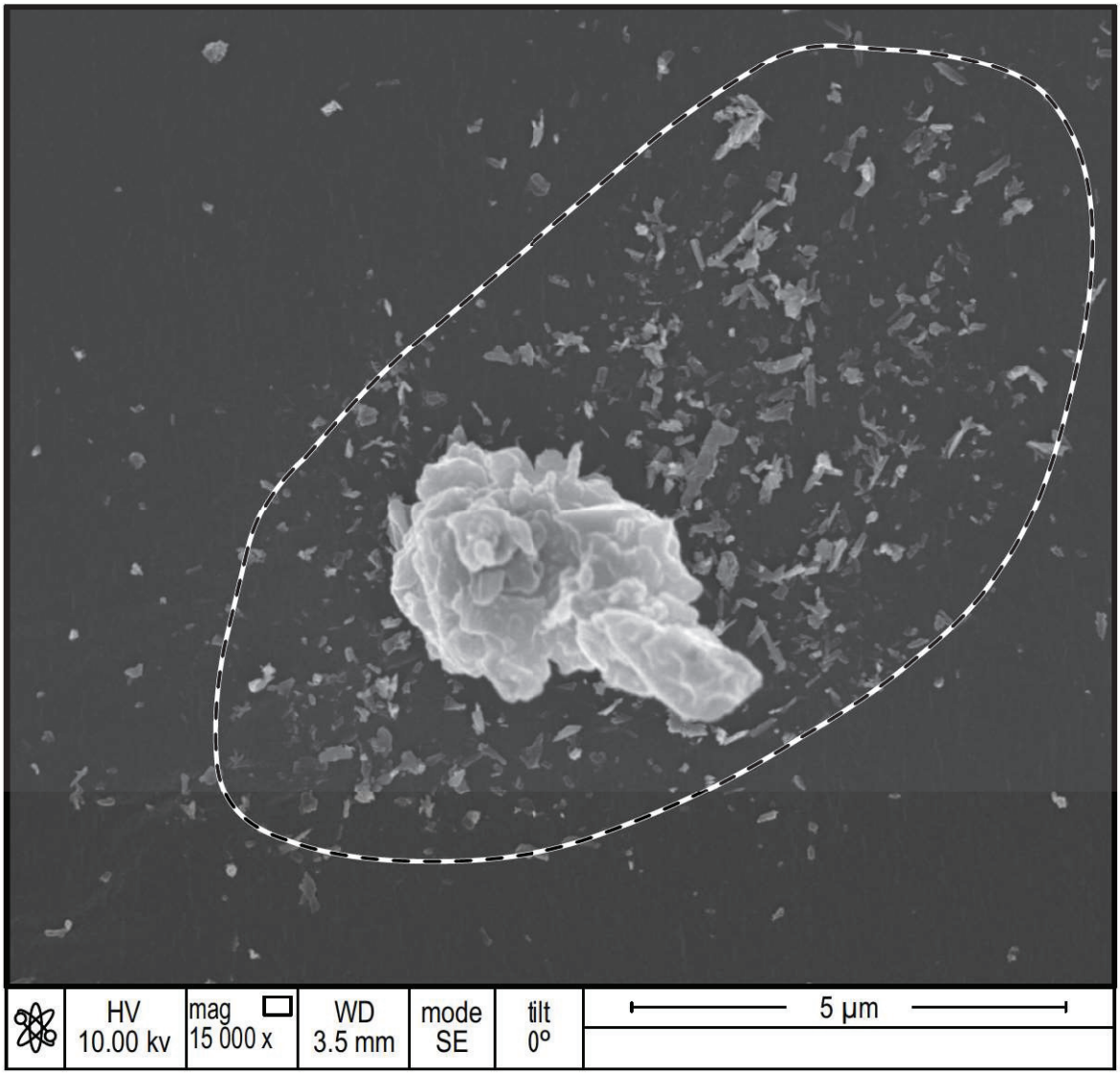



FIG. 76B

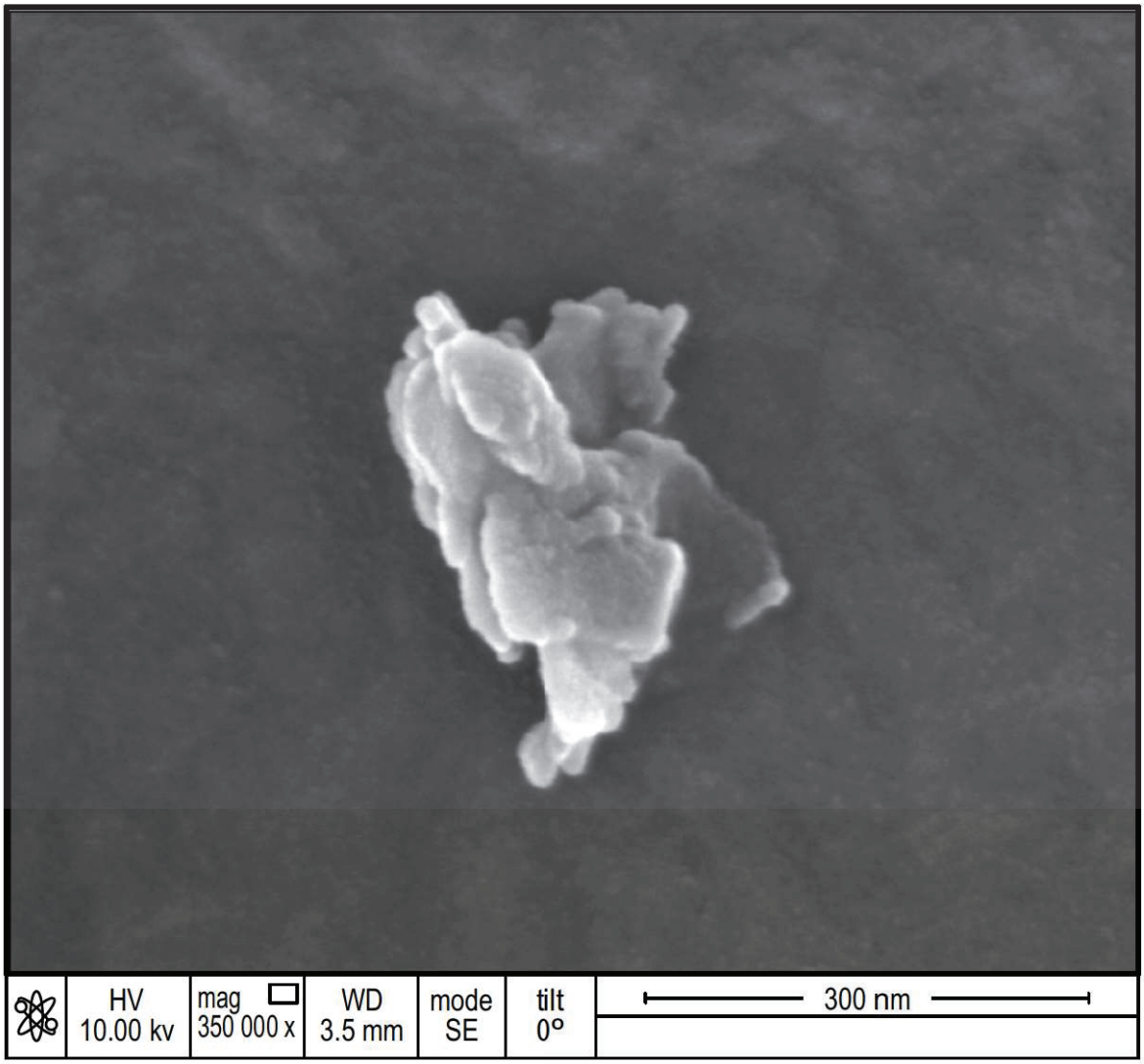



FIG. 76C

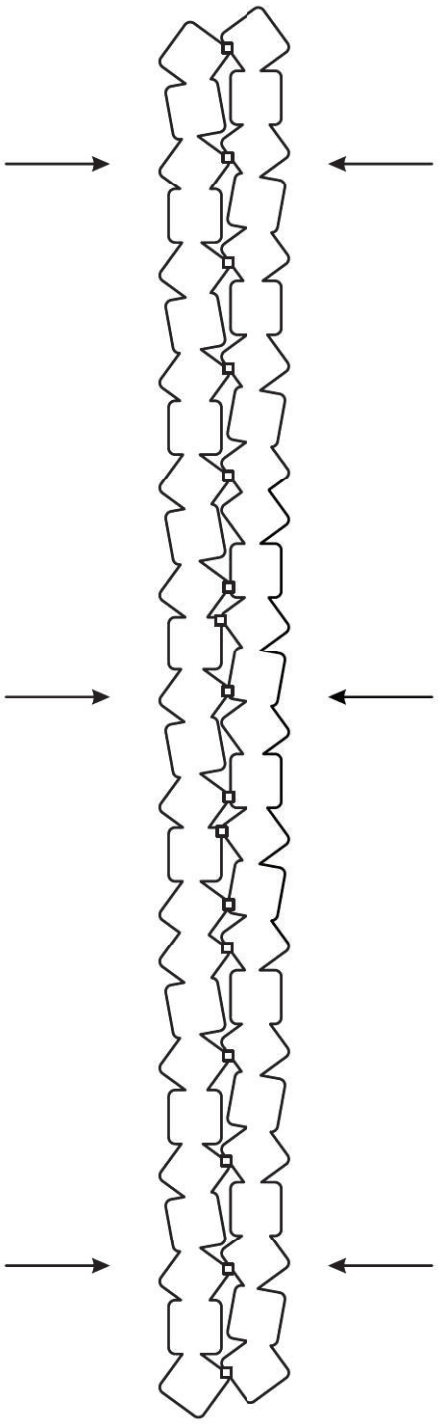


FIG. 77

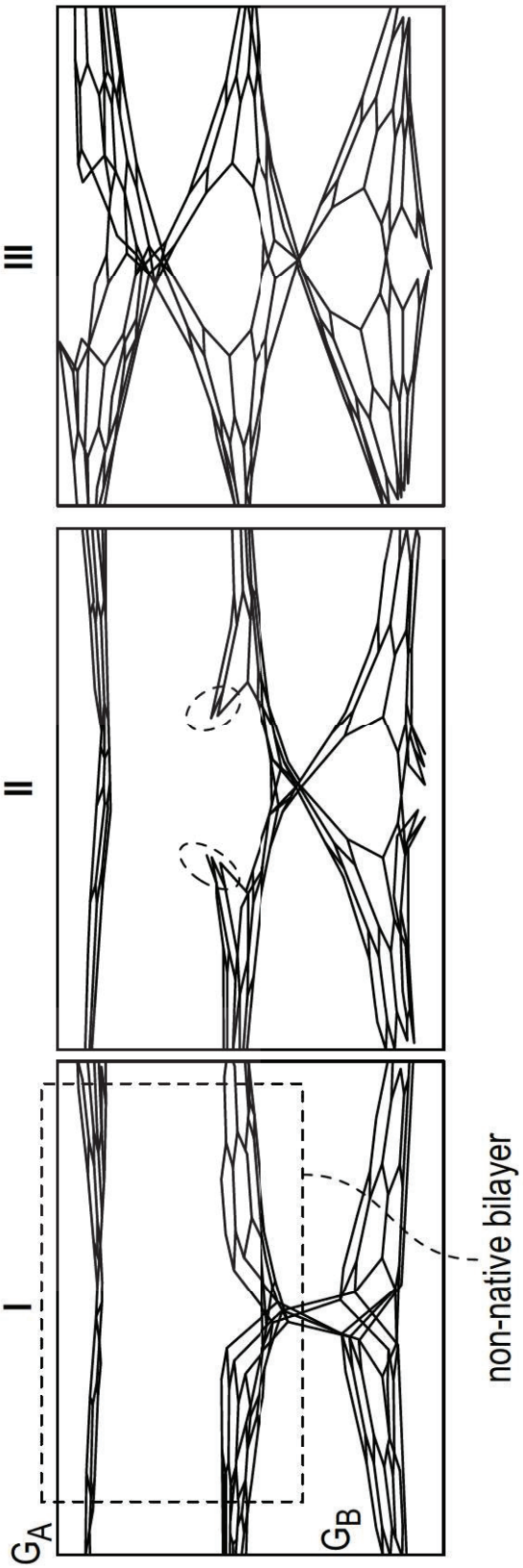



FIG. 78

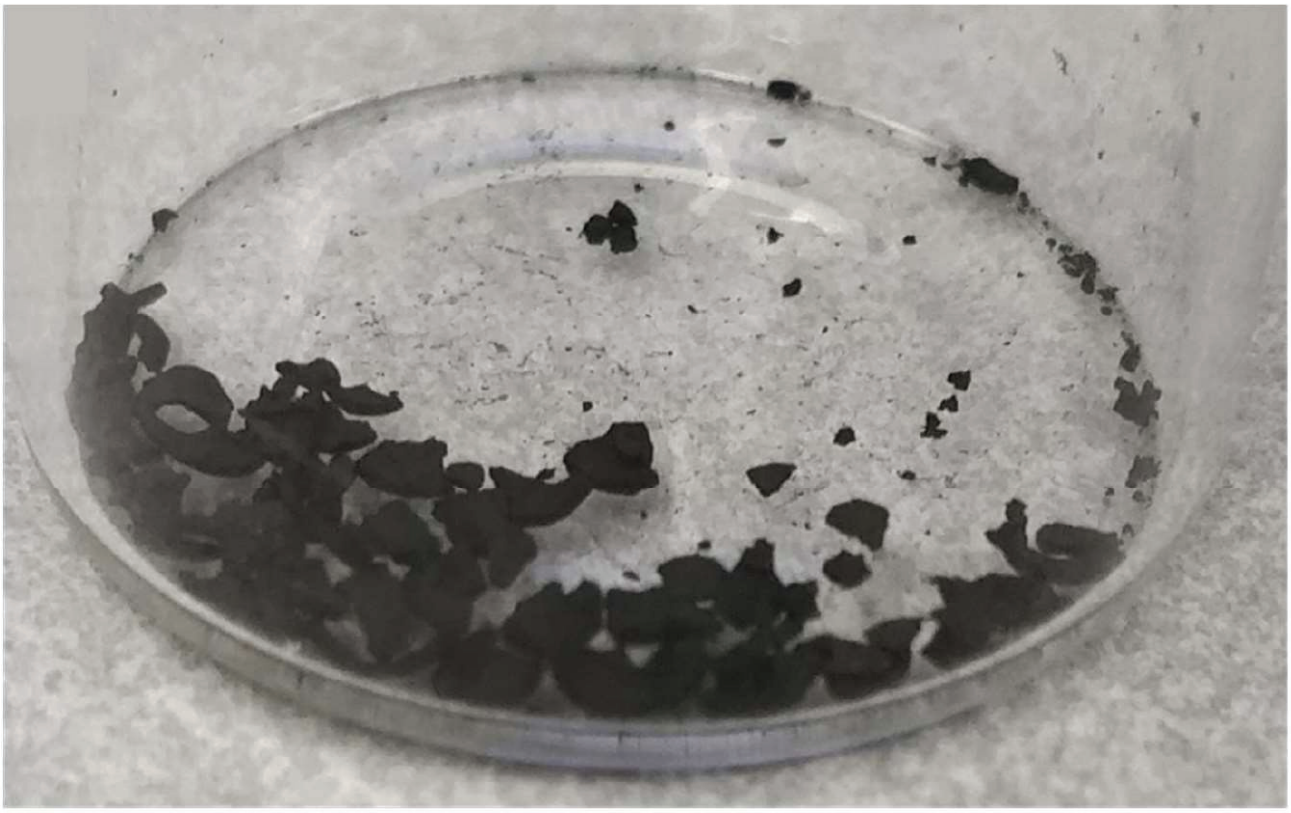


Fig. 79A

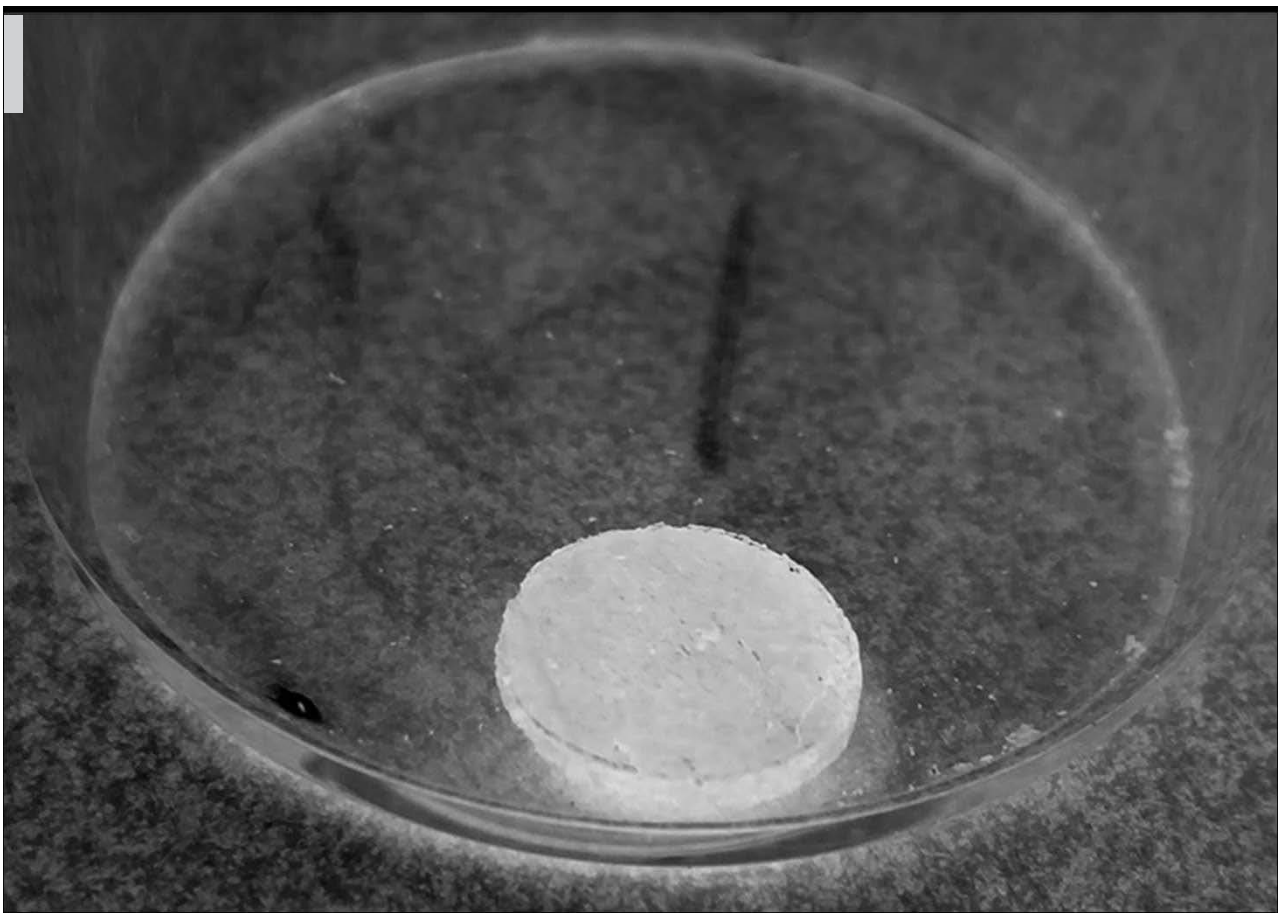


Fig. 79B

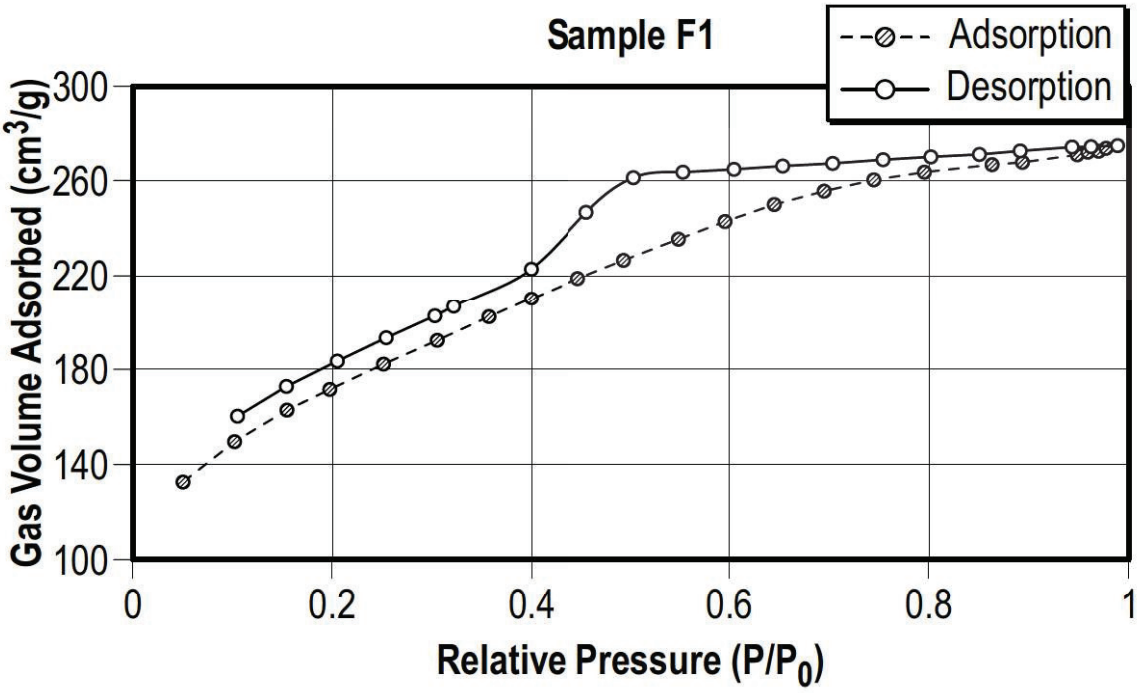

Sample F1
Adsorption
Desorption
Gas Volume Adsorbed (cm3/g)
300
260
220
180
140
100
0
0.2
0.4
0.6
0.8
1
Relative Pressure (P/P0)

FIG. 80A

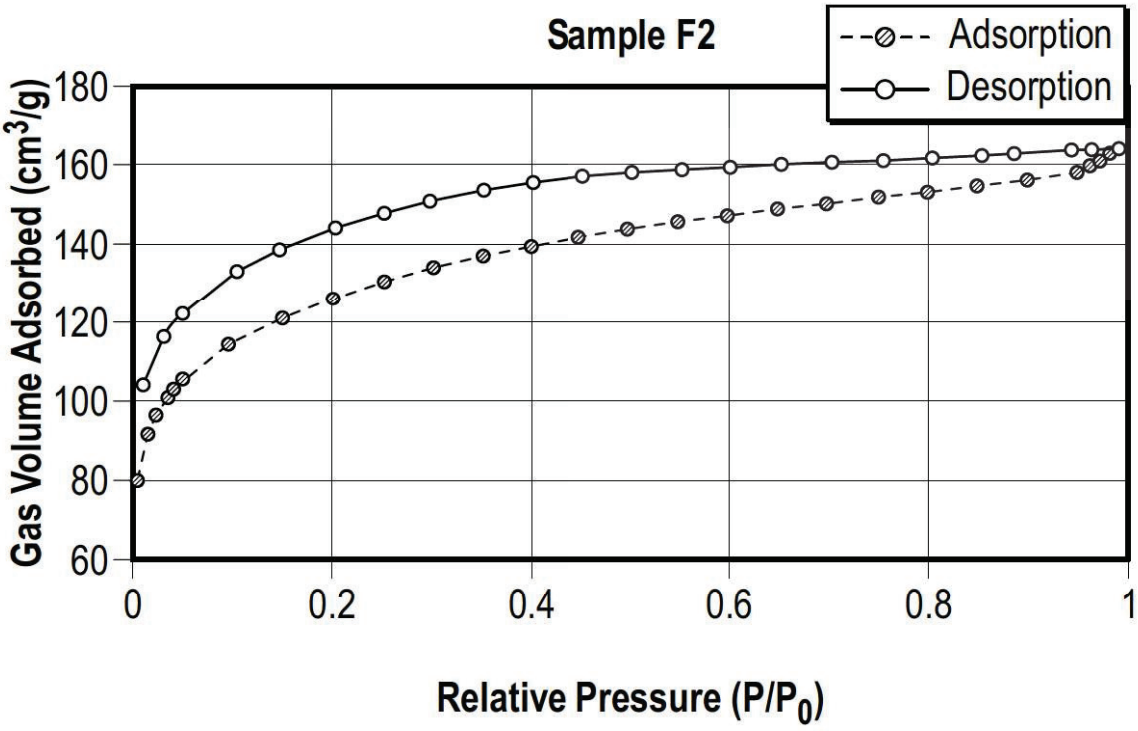

Sample F2
Adsorption
Desorption
Gas Volume Adsorbed (cm3/g)
180
160
140
120
100
80
60
0
0.2
0.4
0.6
0.8
1
Relative Pressure (P/P0)

FIG. 80B

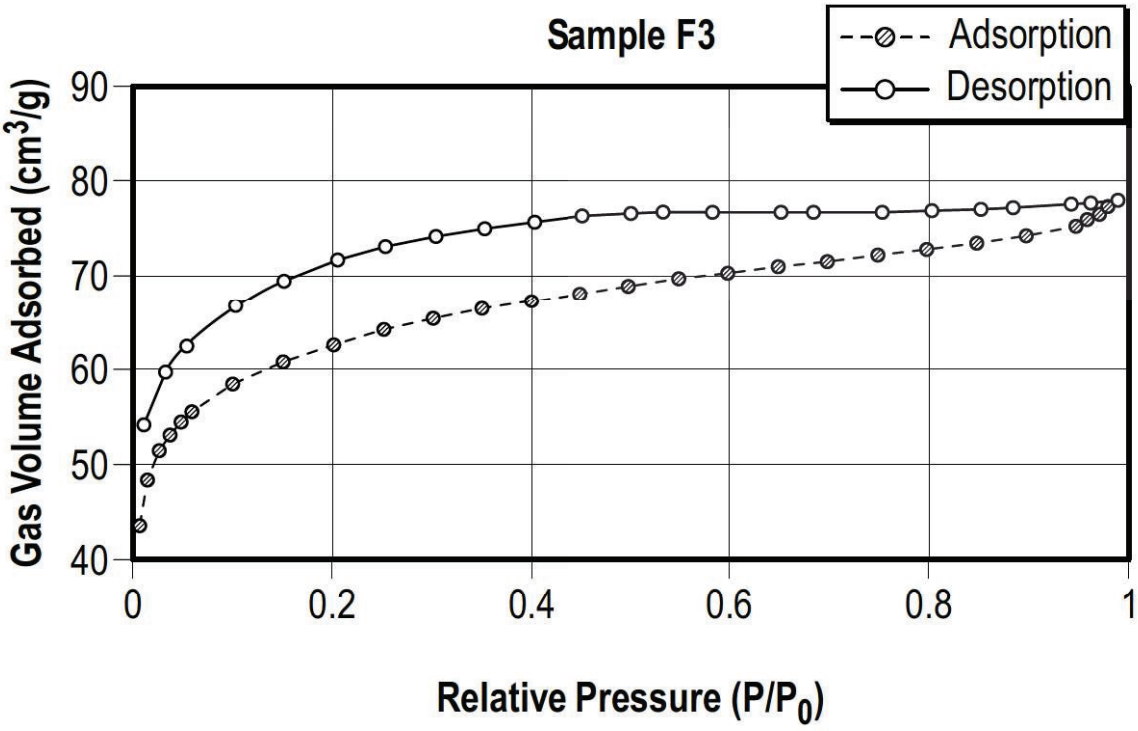

Sample F3
Adsorption
Desorption
Gas Volume Adsorbed (cm3/g)
90
80
70
60
50
40
0
0.2
0.4
0.6
0.8
1
Relative Pressure (P/P0)

FIG. 80C

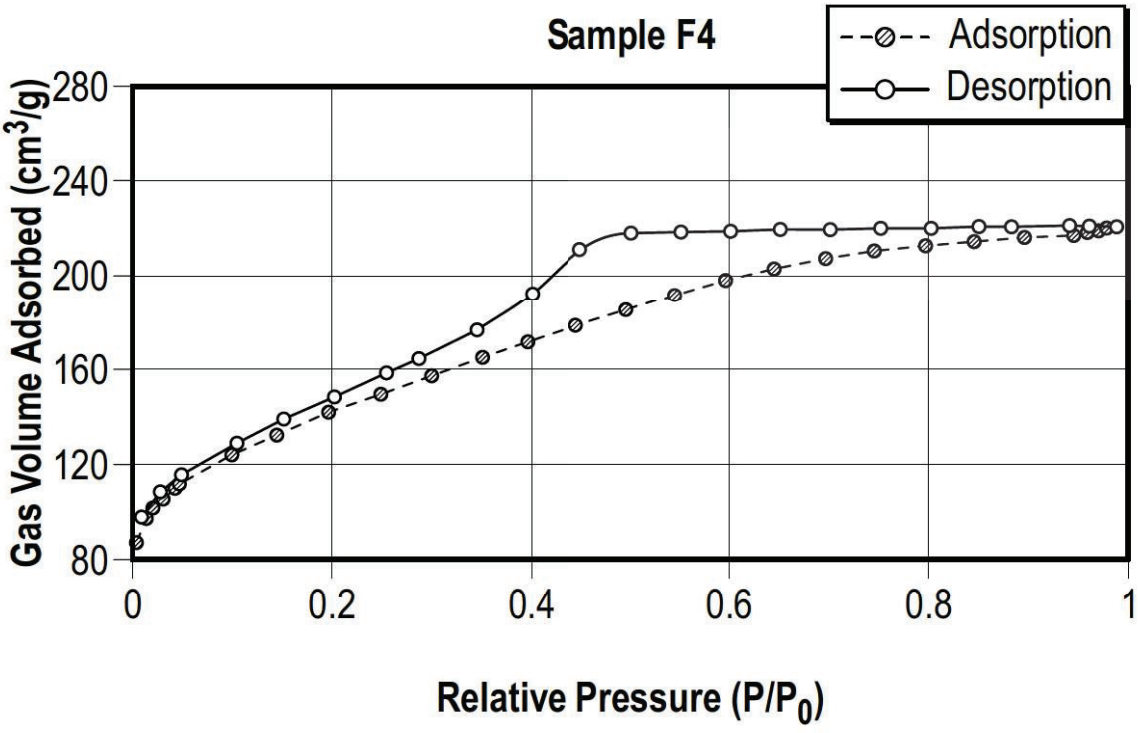

Sample F4
Adsorption
Desorption
Gas Volume Adsorbed (cm3/g)
280
240
200
160
120
80
0
0.2
0.4
0.6
0.8
1
Relative Pressure (P/P0)

FIG. 80D

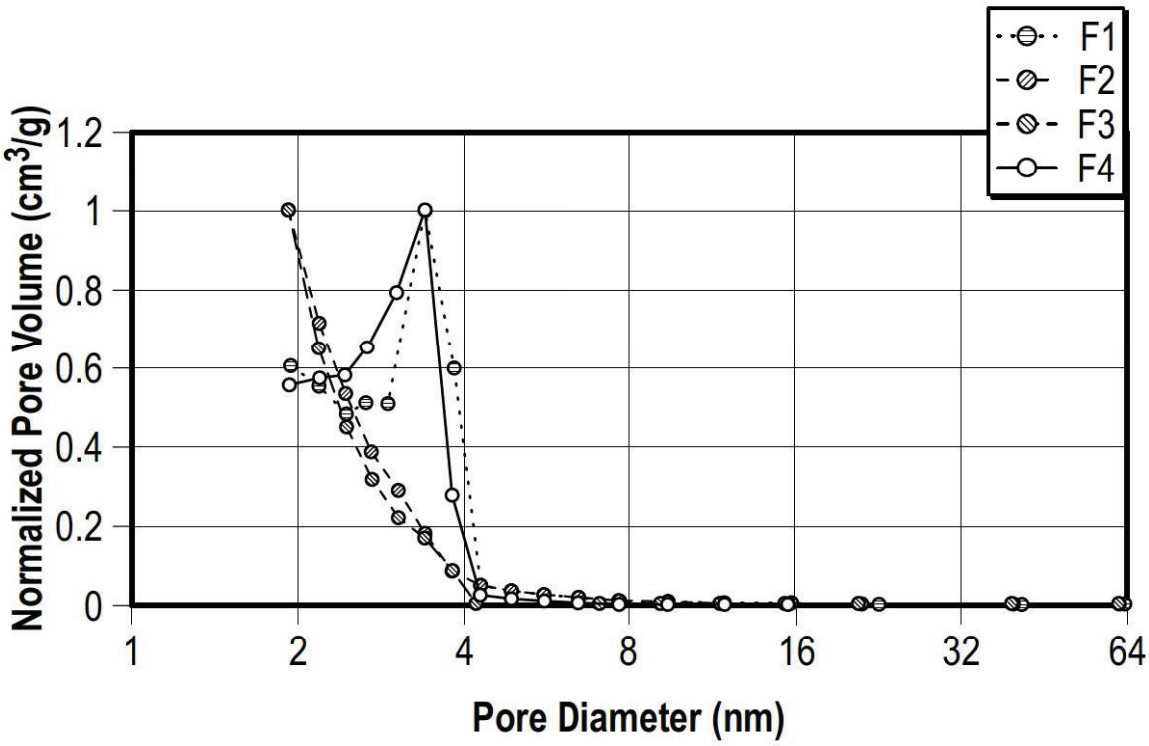

F1
F2
F3
F4
Normalized Pore Volume (cm3/g)
1.2
1
0.8
0.6
0.4
0.2
0
1
2
4
8
16
32
64
Pore Diameter (nm)

FIG. 81

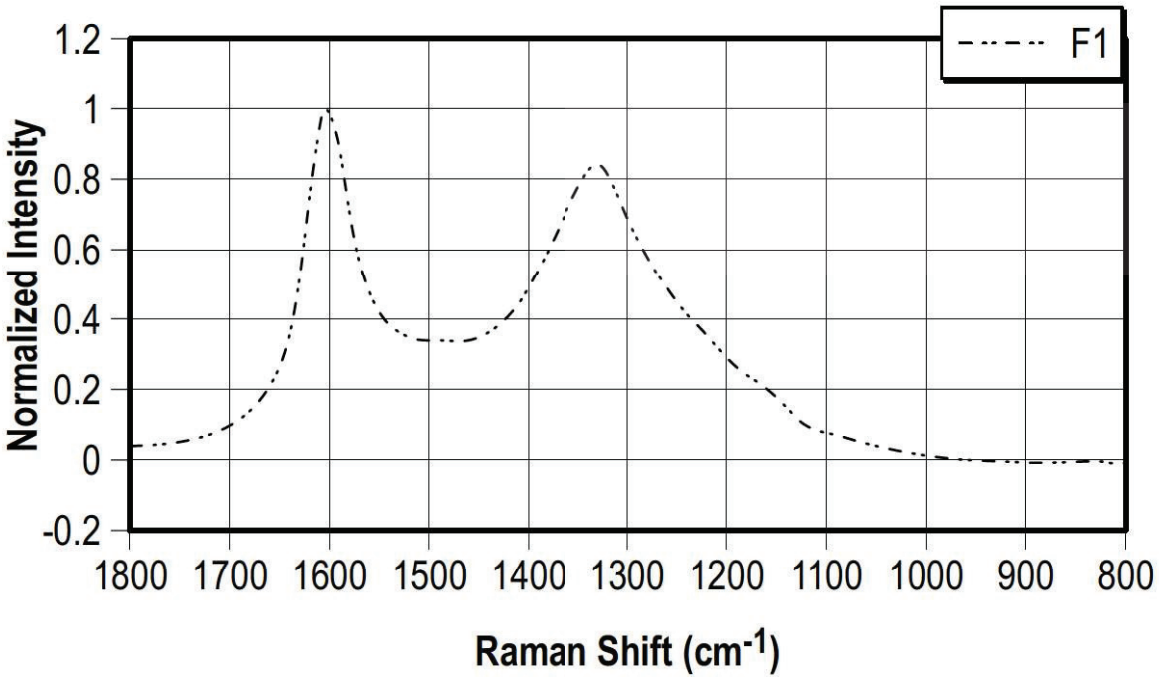

F1
1.2
1
0.8
0.6
0.4
0.2
0
-0.2
Normalized Intensity
1800 1700 1600 1500 1400 1300 1200 1100 1000 900 800
Raman Shift (cm-1)

FIG. 82A

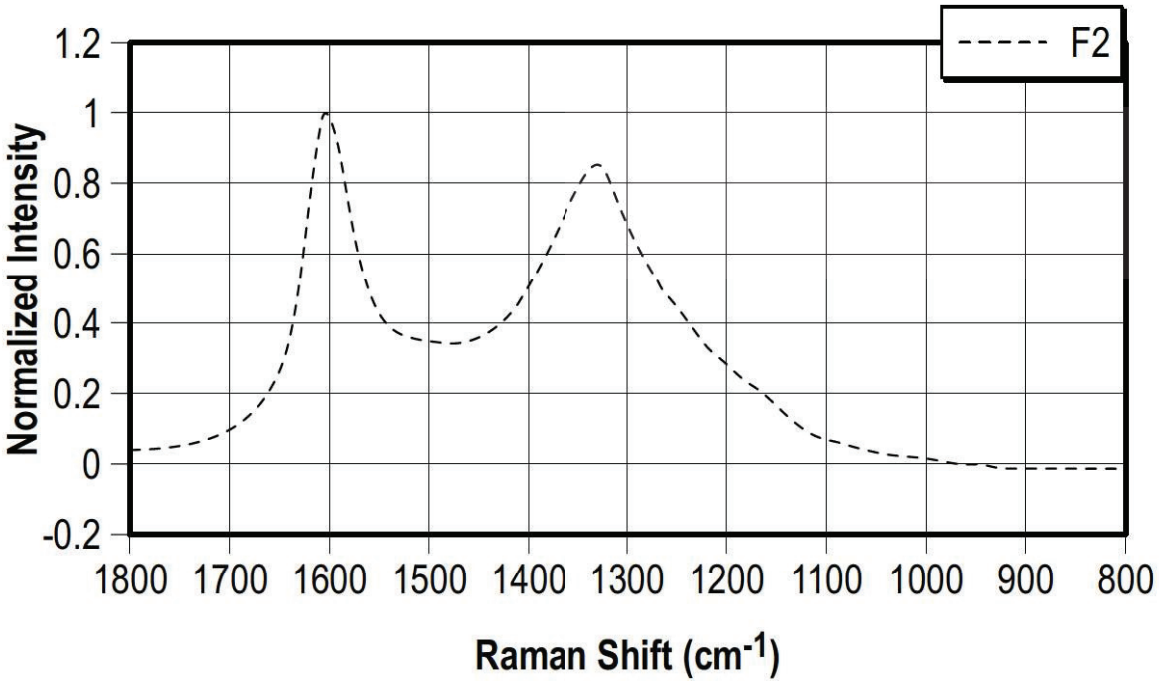

F2
1.2
1
0.8
0.6
0.4
0.2
0
-0.2
Normalized Intensity
1800 1700 1600 1500 1400 1300 1200 1100 1000 900 800
Raman Shift (cm-1)

FIG. 82B

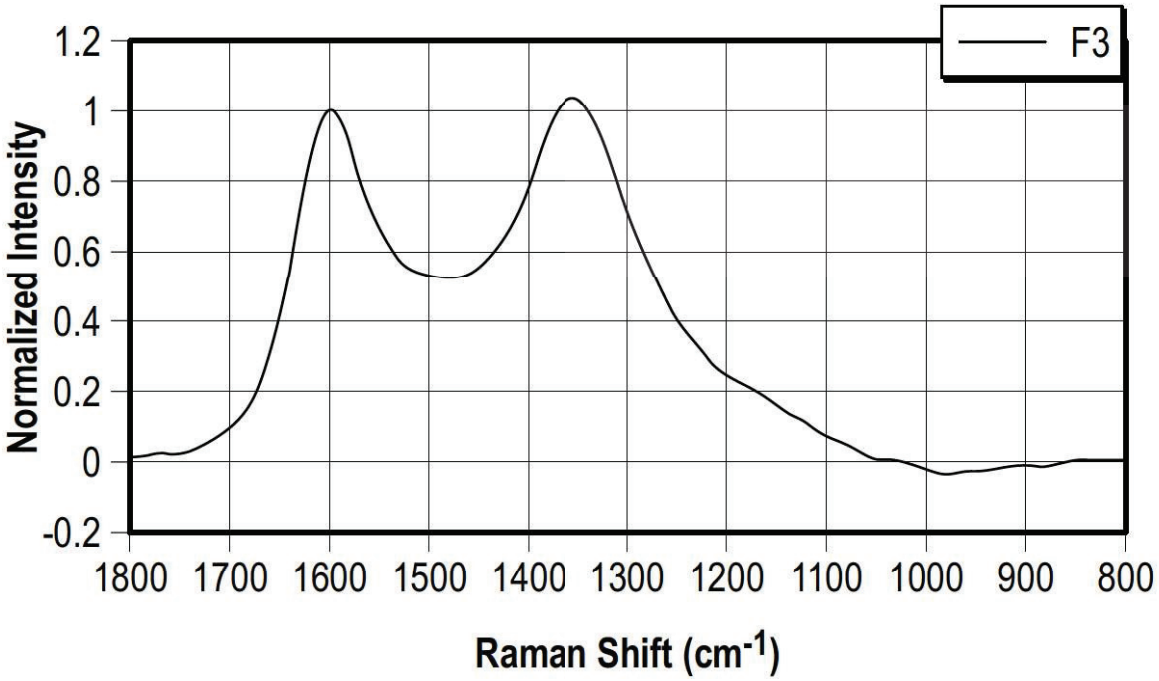

F3
1.2
1
0.8
0.6
0.4
0.2
0
-0.2
Normalized Intensity
1800 1700 1600 1500 1400 1300 1200 1100 1000 900 800
Raman Shift (cm-1)

FIG. 82C

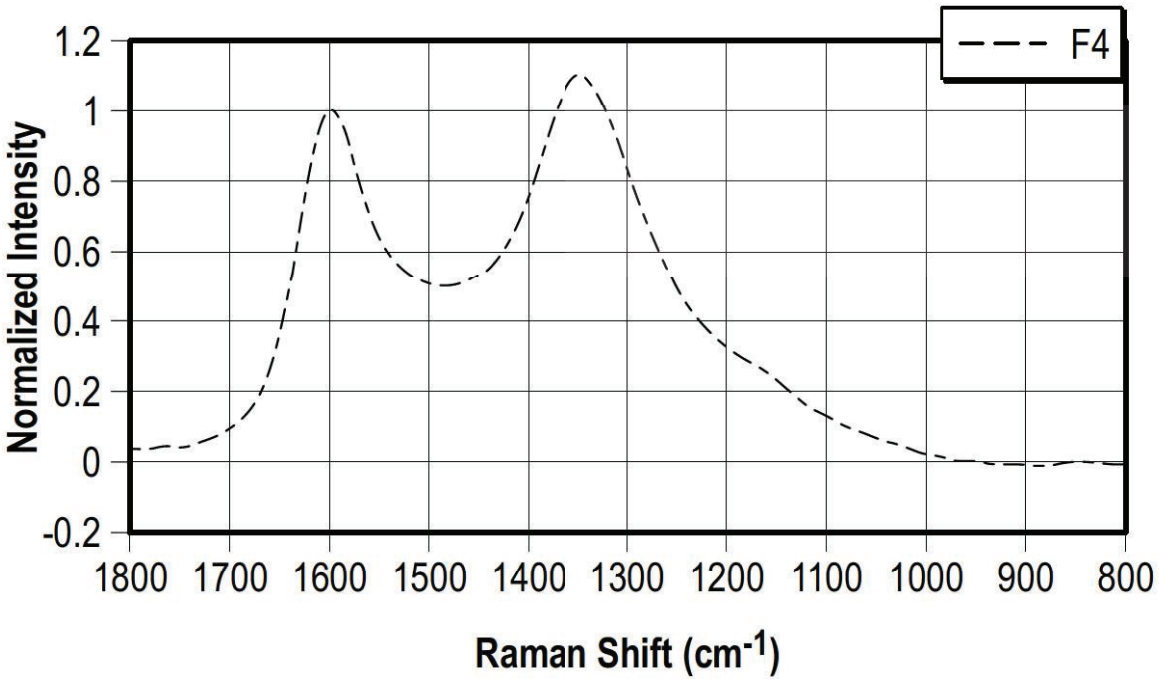

F4
1.2
1
0.8
0.6
0.4
0.2
0
-0.2
Normalized Intensity
1800 1700 1600 1500 1400 1300 1200 1100 1000 900 800
Raman Shift (cm-1)

FIG. 82D

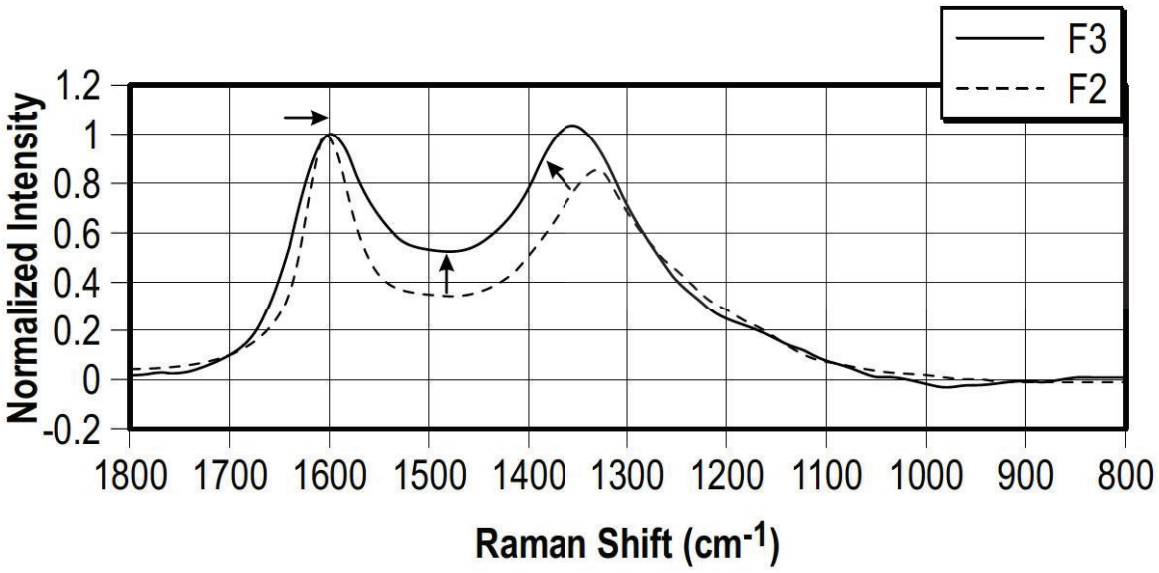

F3
F2
Normalized Intensity
1.2
1
0.8
0.6
0.4
0.2
0
-0.2
1800 1700 1600 1500 1400 1300 1200 1100 1000 900 800
Raman Shift (cm-1)

FIG. 83

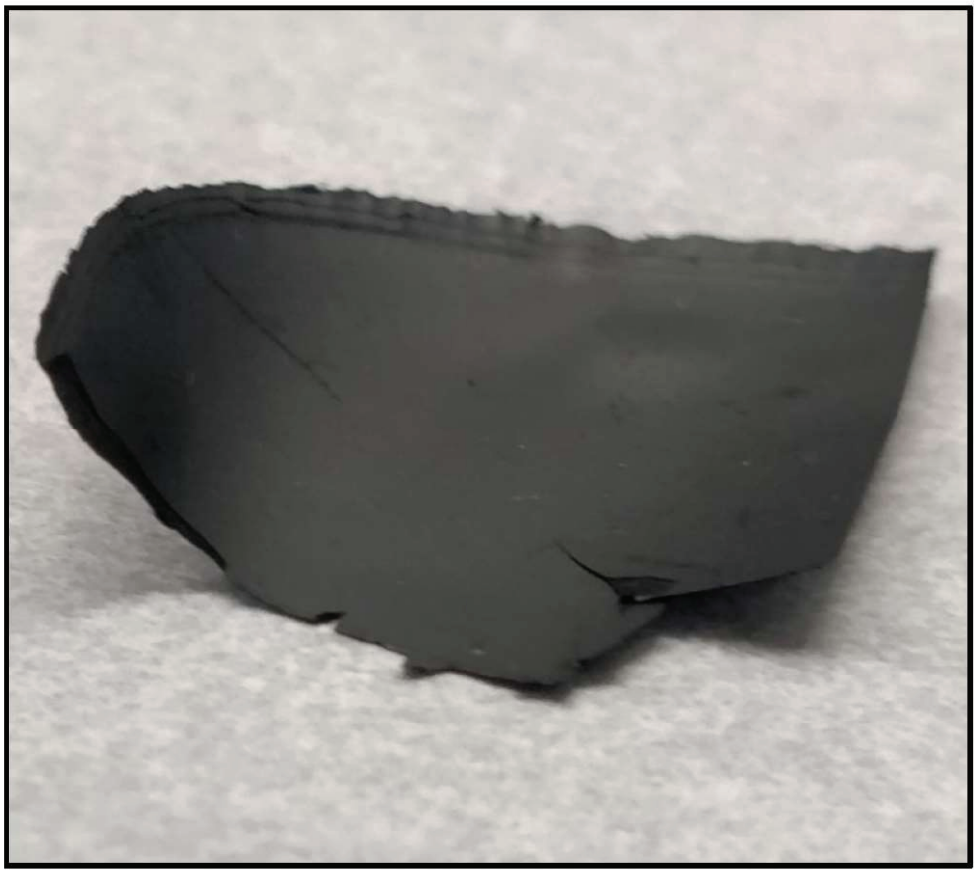


FIG. 84A

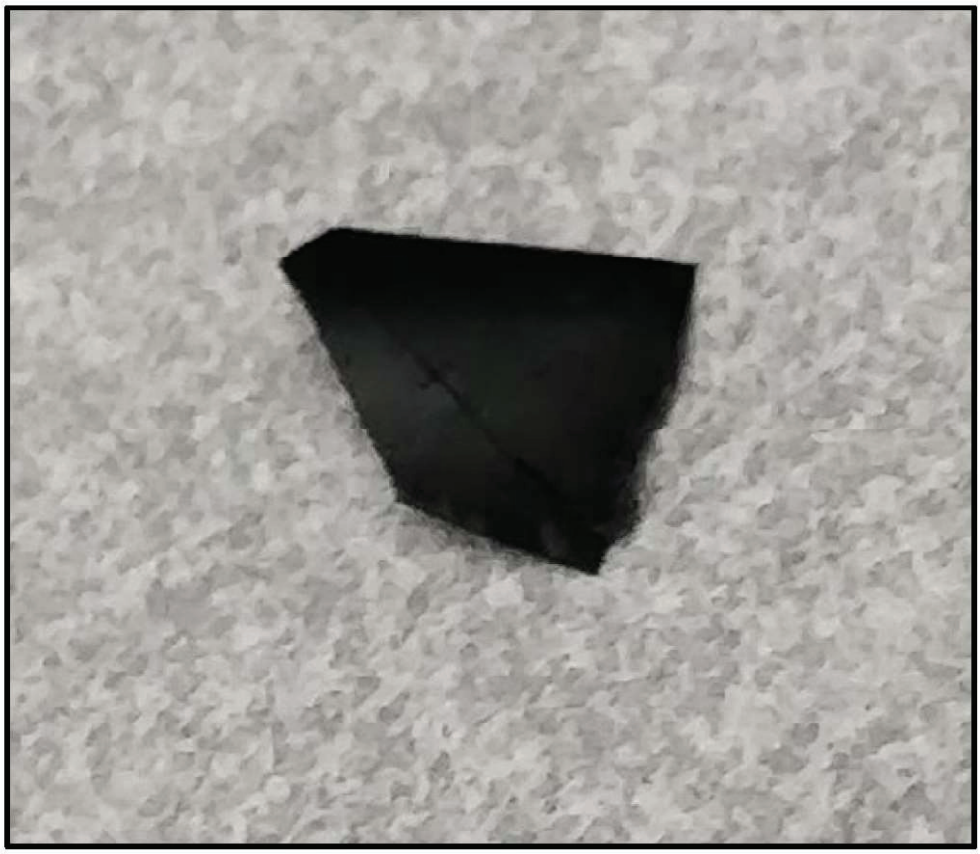


FIG. 84B

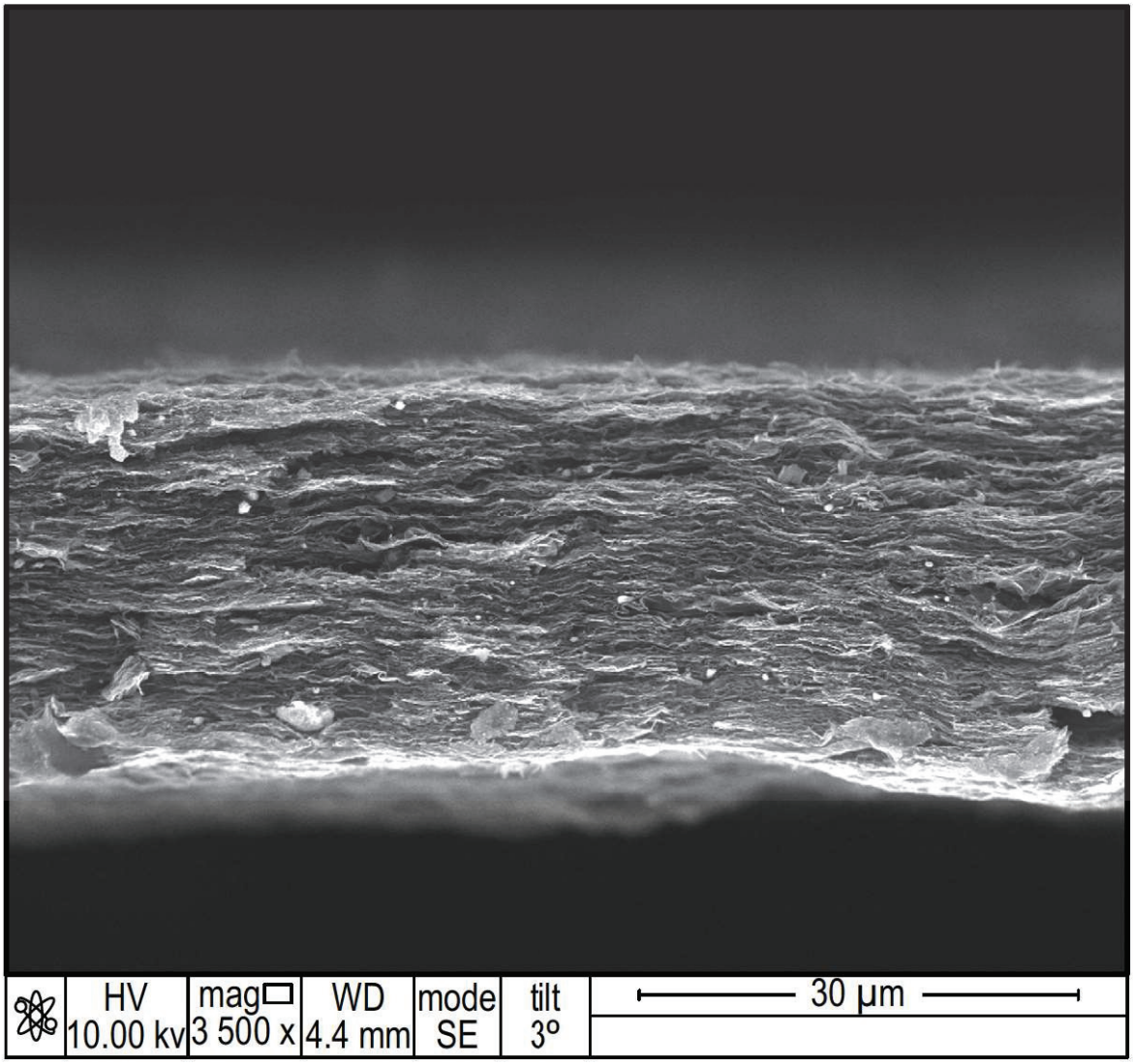



FIG. 85A

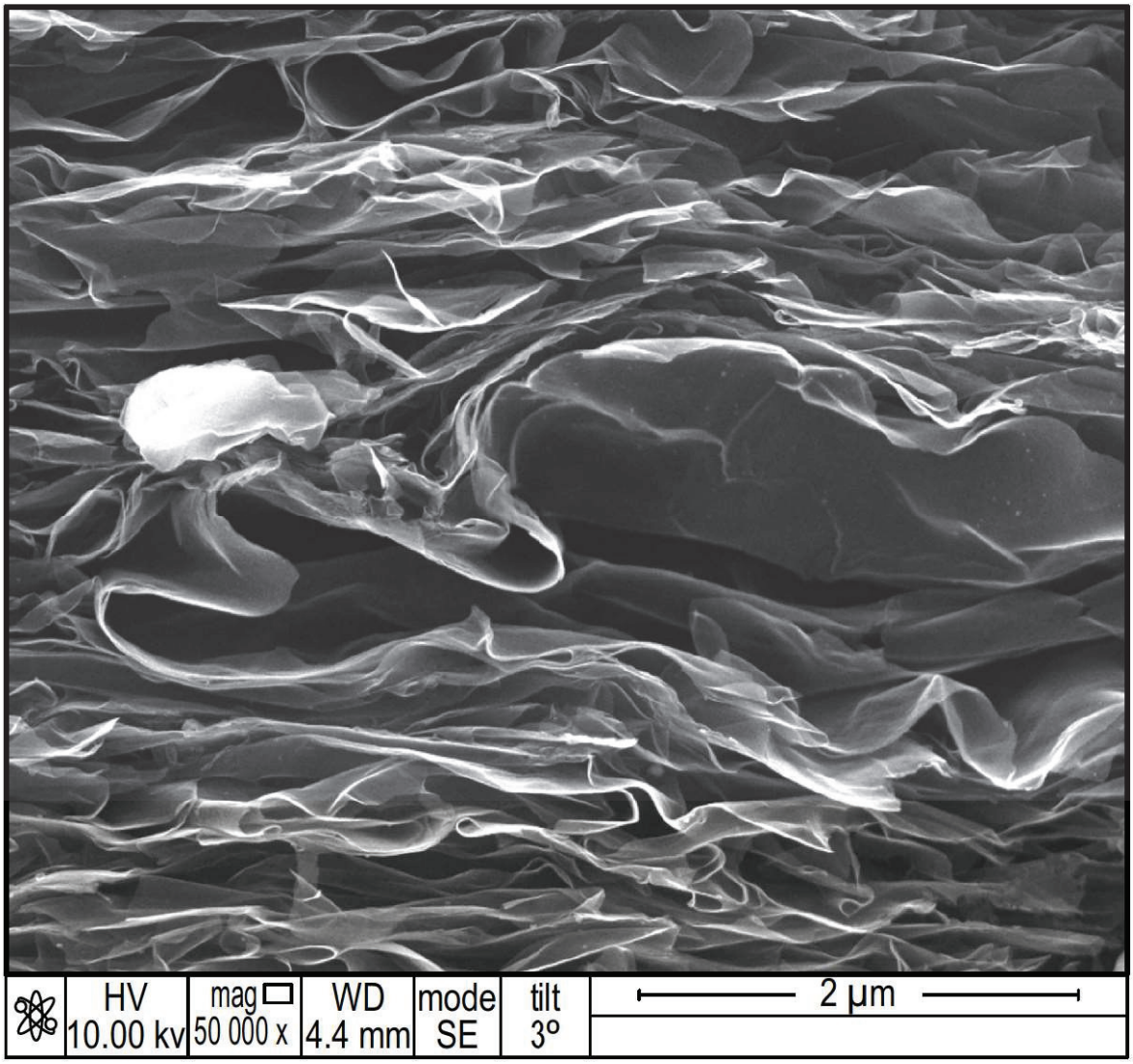



FIG. 85B

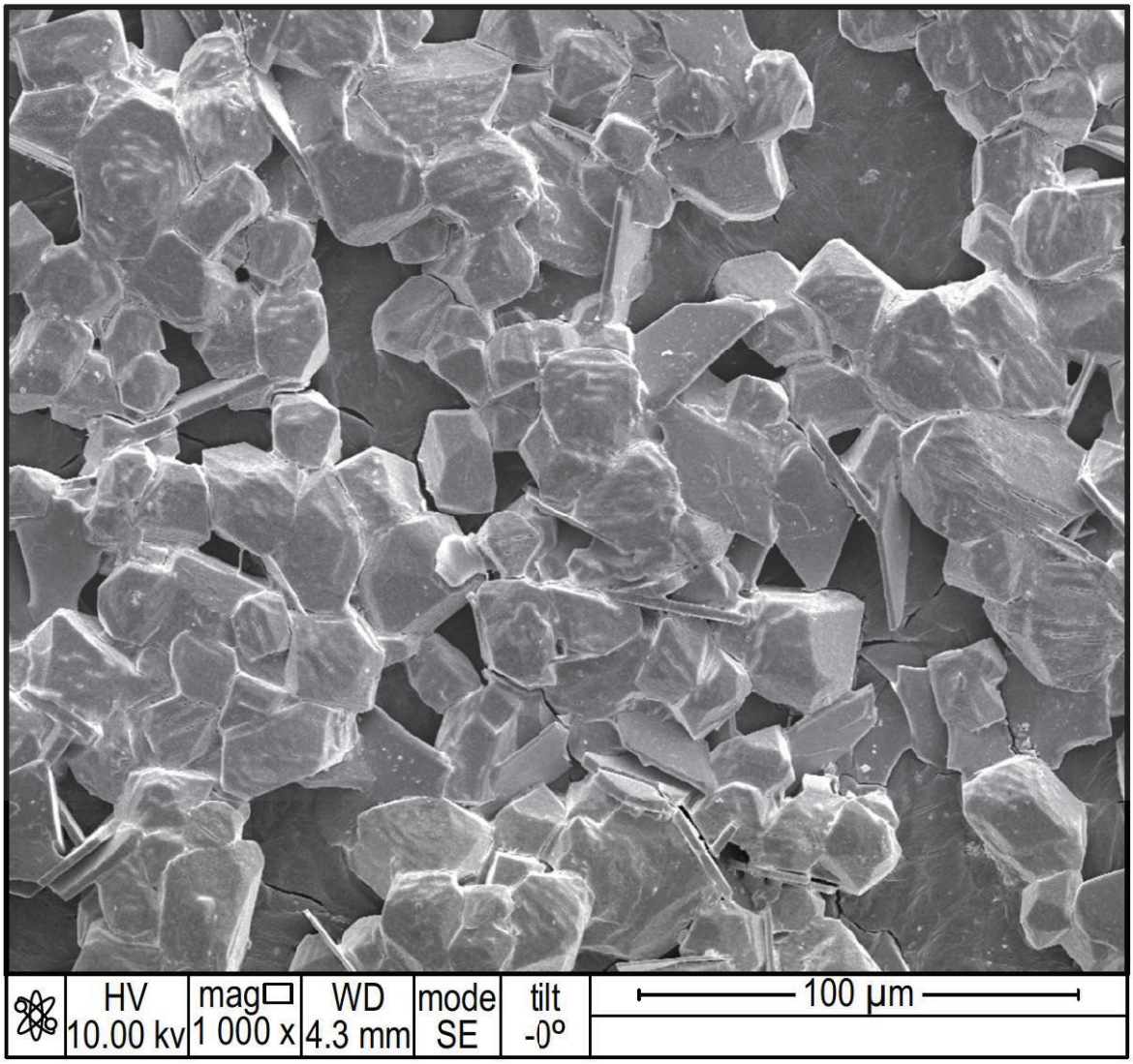



FIG. 85C

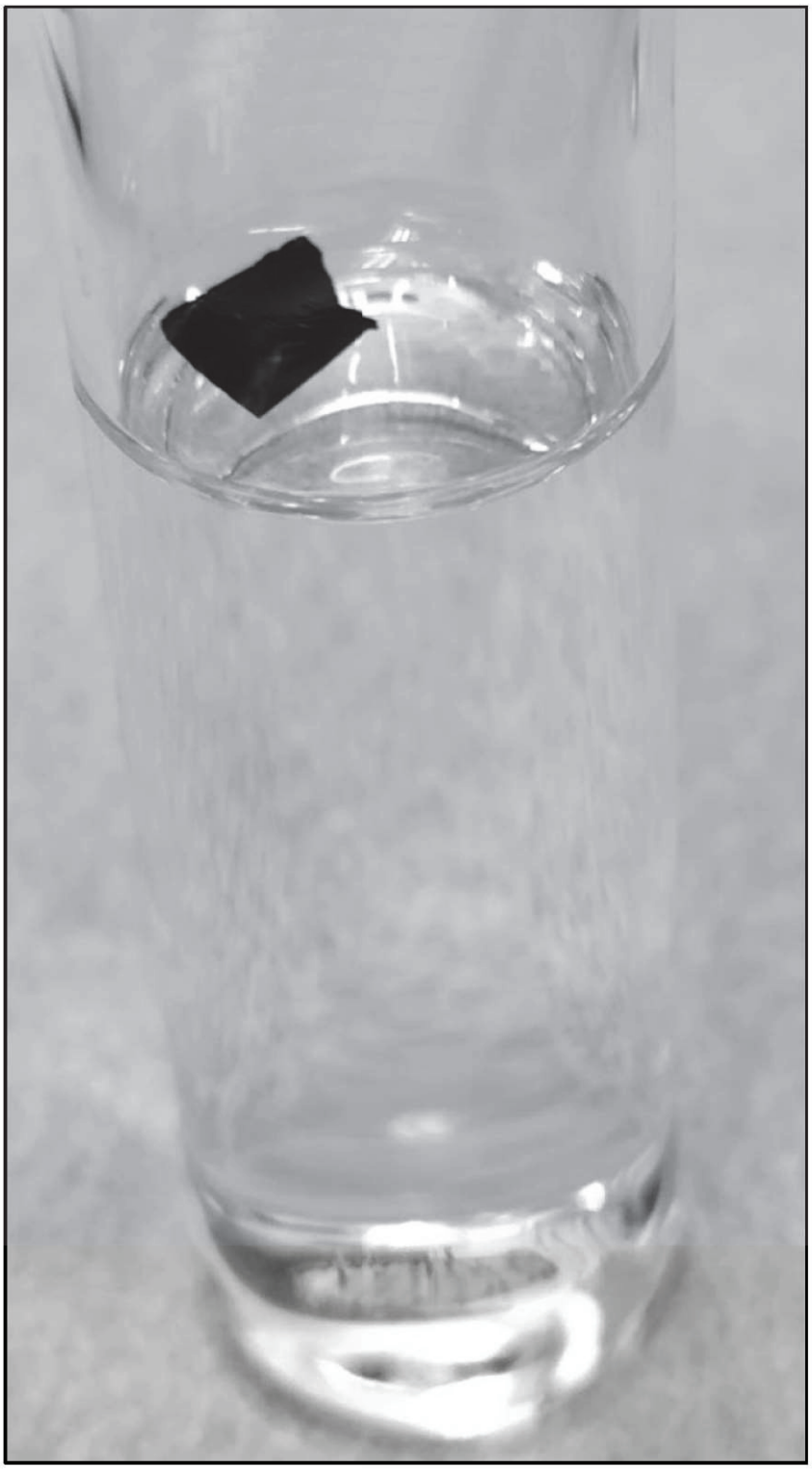


FIG. 86A

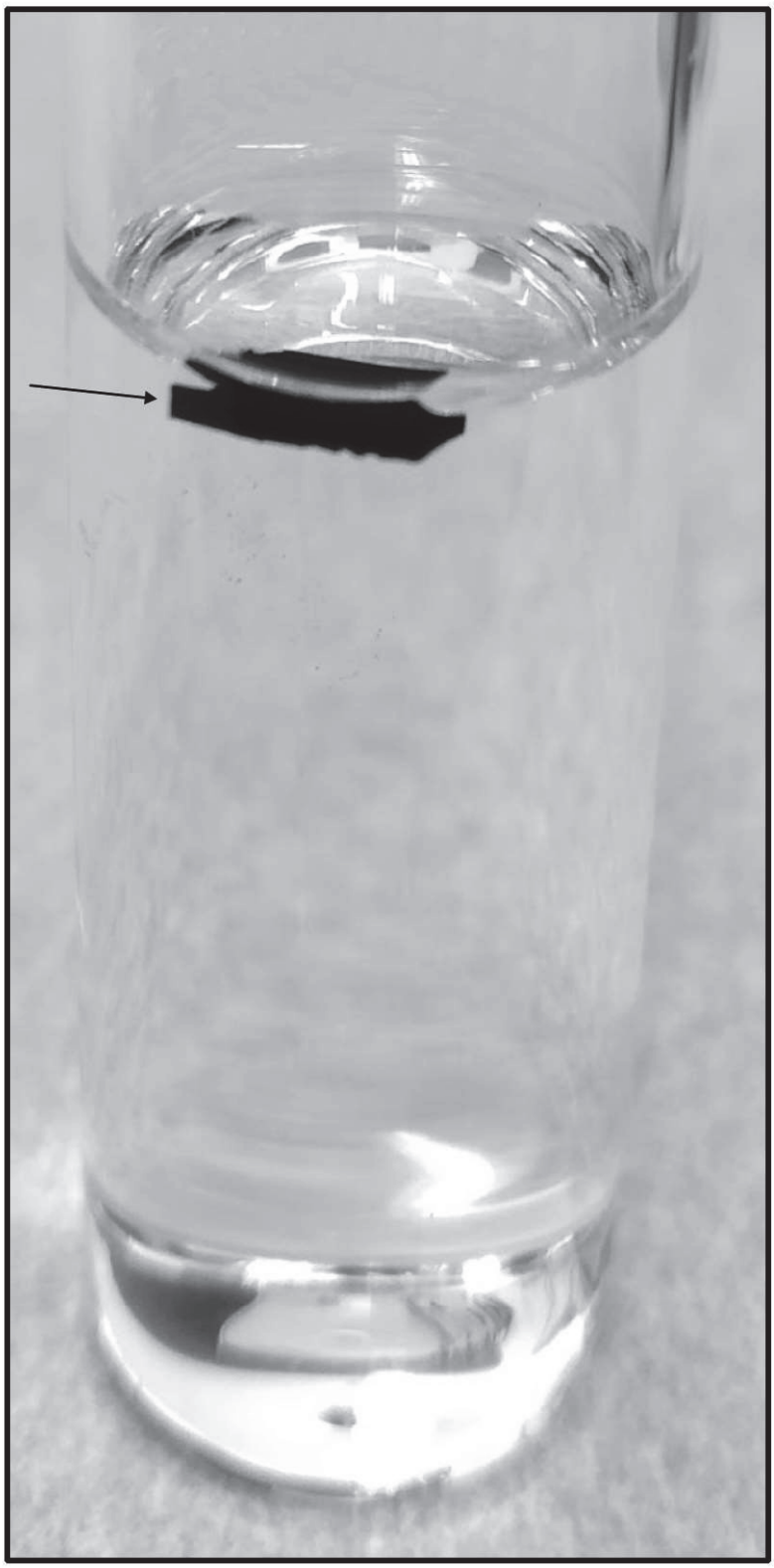


FIG. 86B

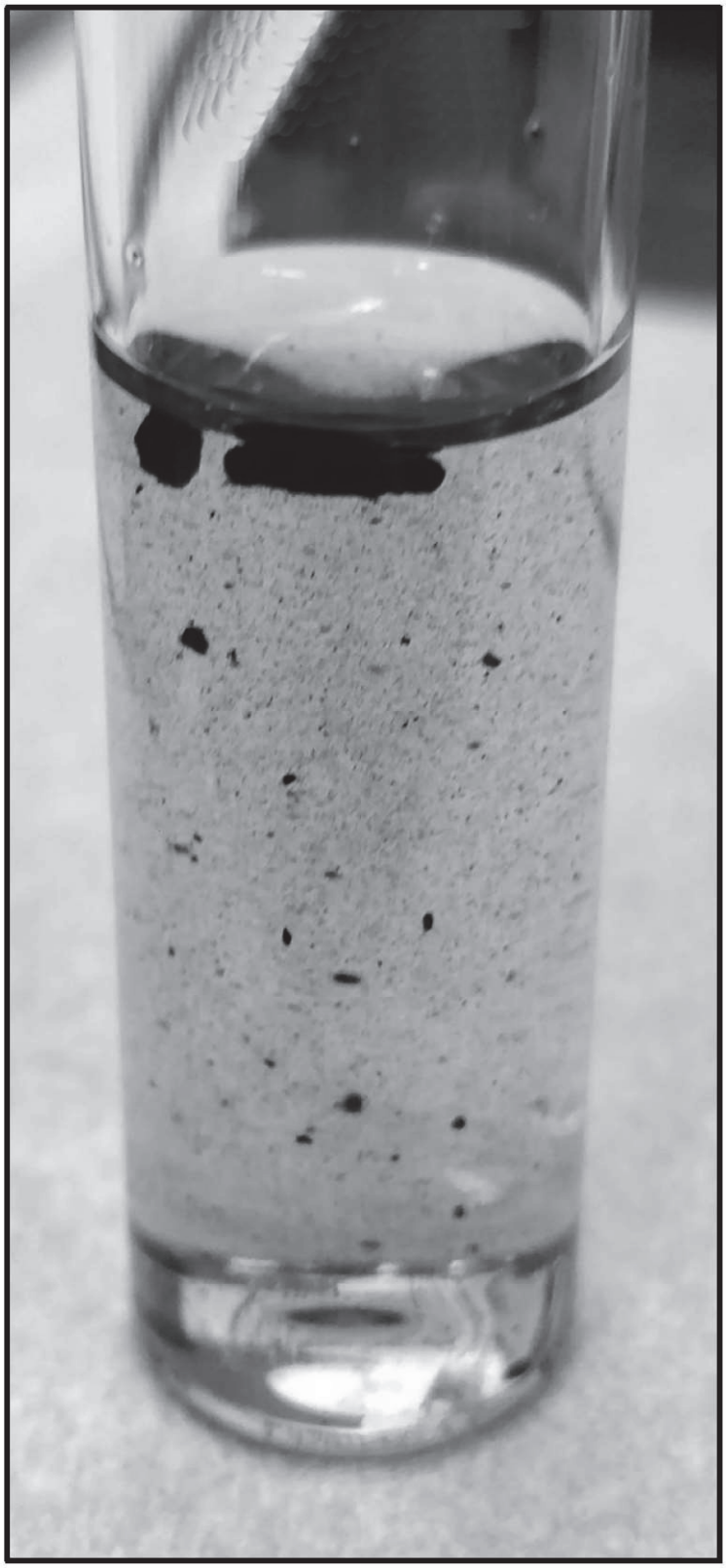


FIG. 86C

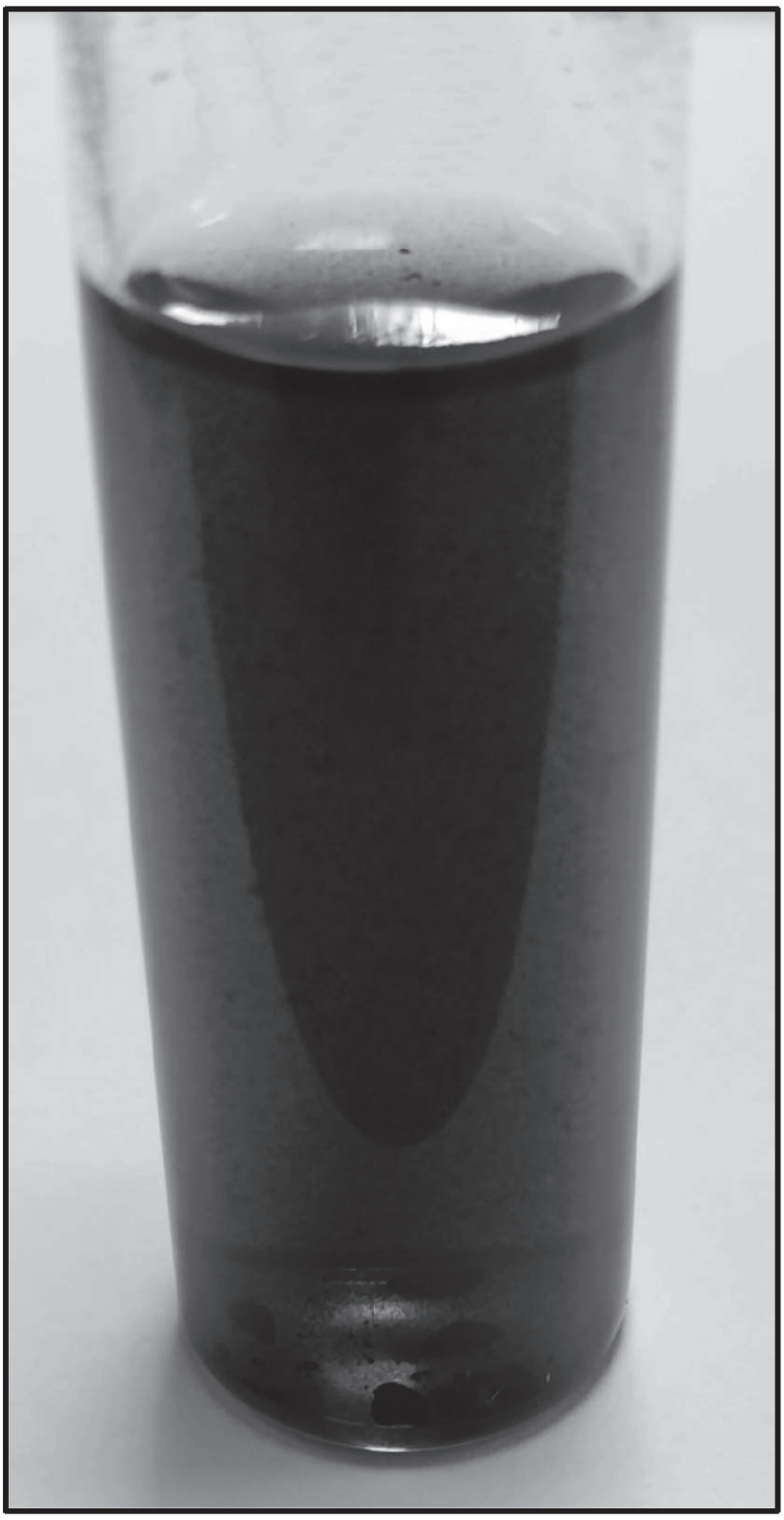


FIG. 86D



FIG. 87A



FIG. 87B



FIG. 87C

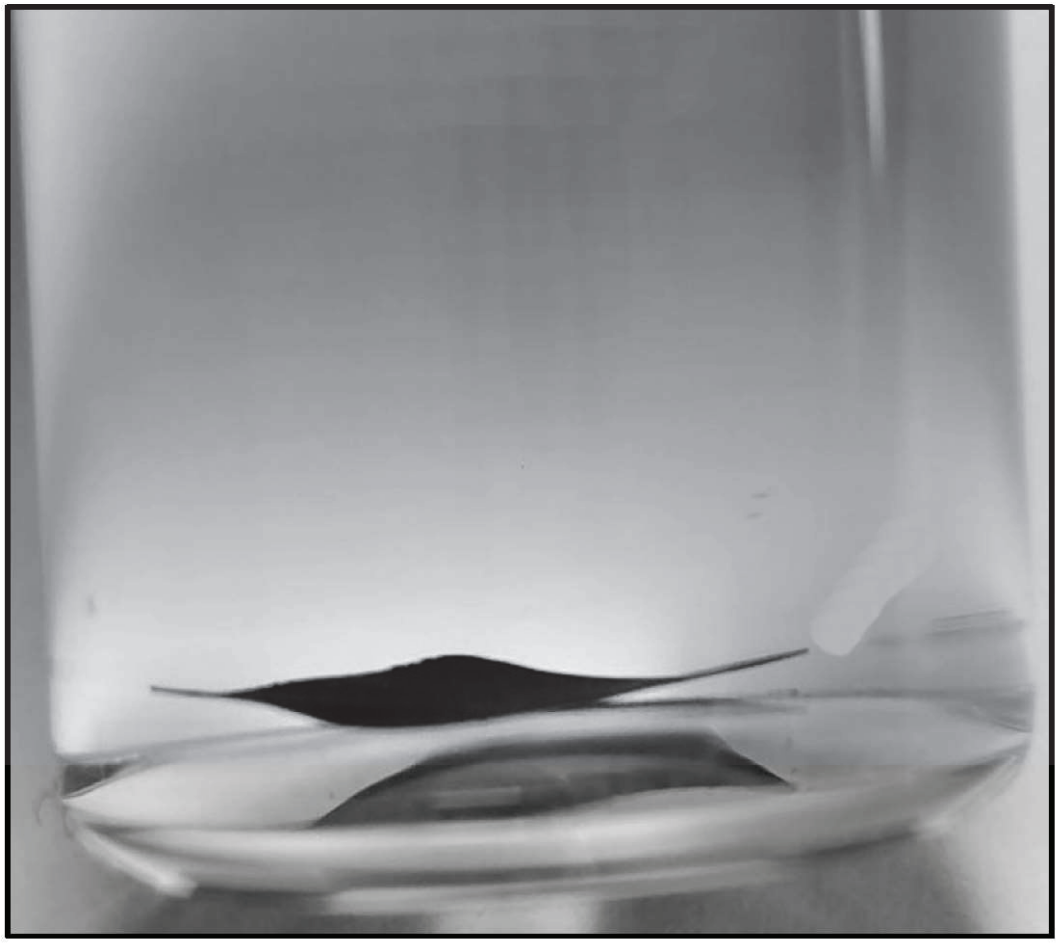


FIG. 87D

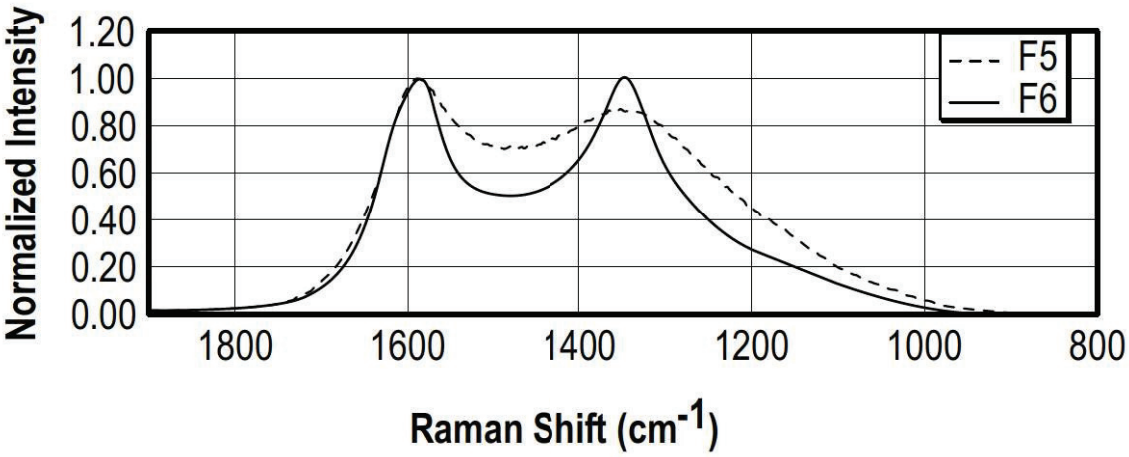

Normalized Intensity
1.20
1.00
0.80
0.60
0.40
0.20
0.00
1800
1600
1400
1200
1000
800
Raman Shift (cm-1)
F5
F6

FIG. 88A

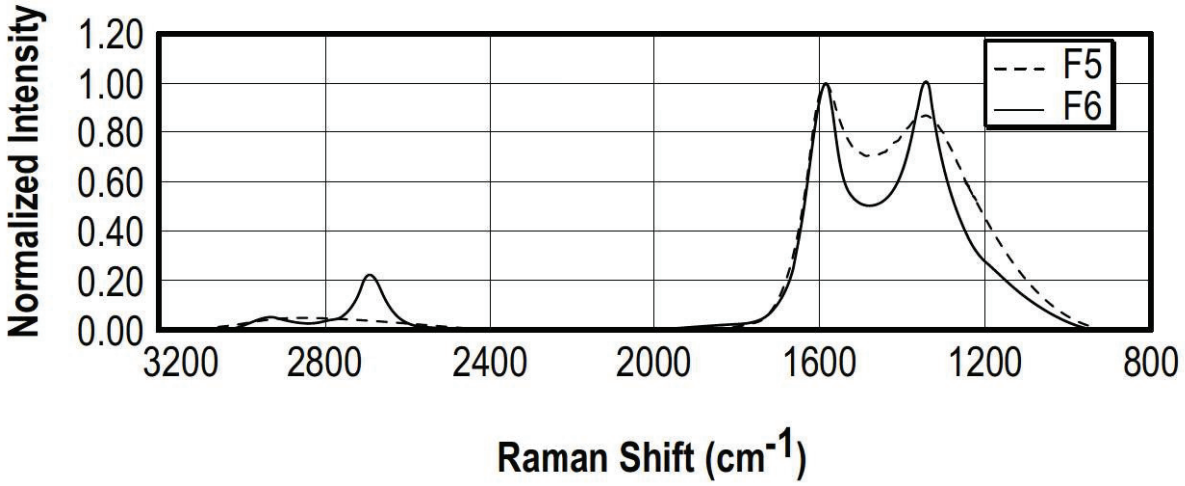

Normalized Intensity
1.20
1.00
0.80
0.60
0.40
0.20
0.00
3200
2800
2400
2000
1600
1200
800
F5
F6
Raman Shift (cm-1)

FIG. 88B

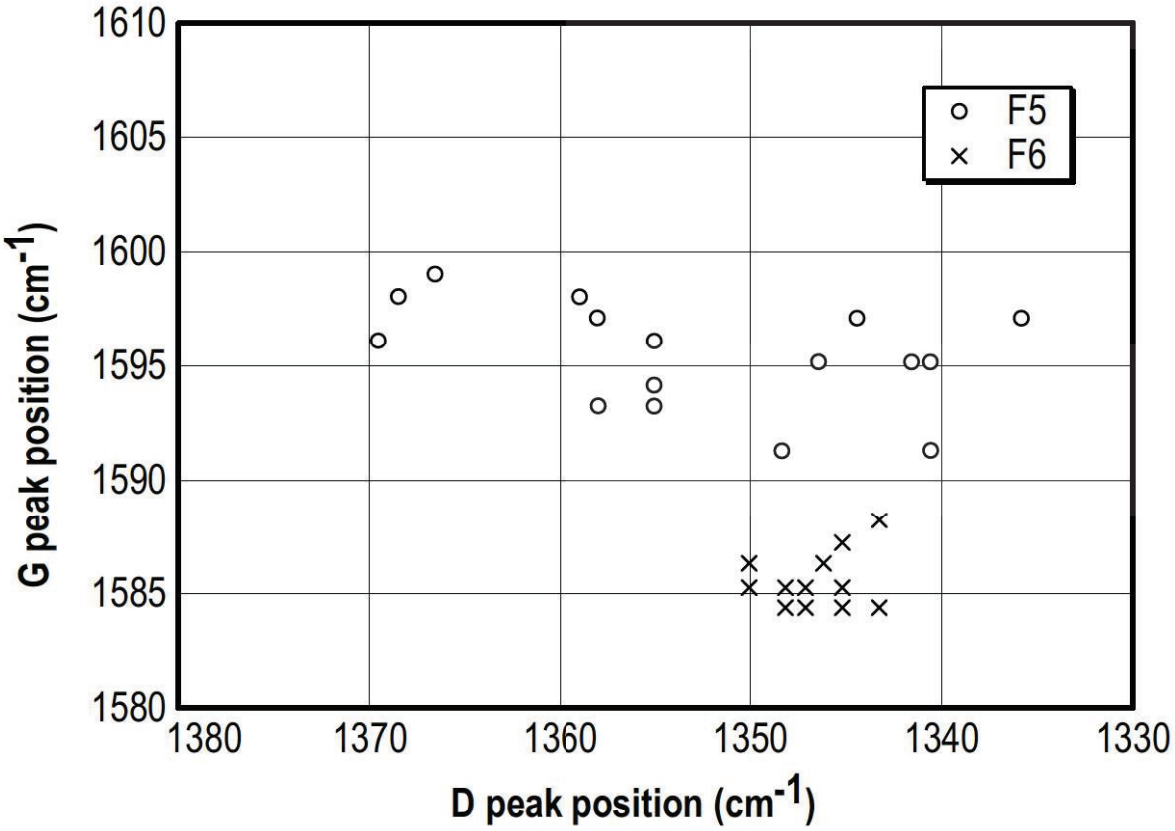

1610
1605
1600
1595
1590
1585
1580
1380
1370
1360
1350
1340
1330
G peak position (cm-1)
D peak position (cm-1)
F5
F6

FIG. 88C

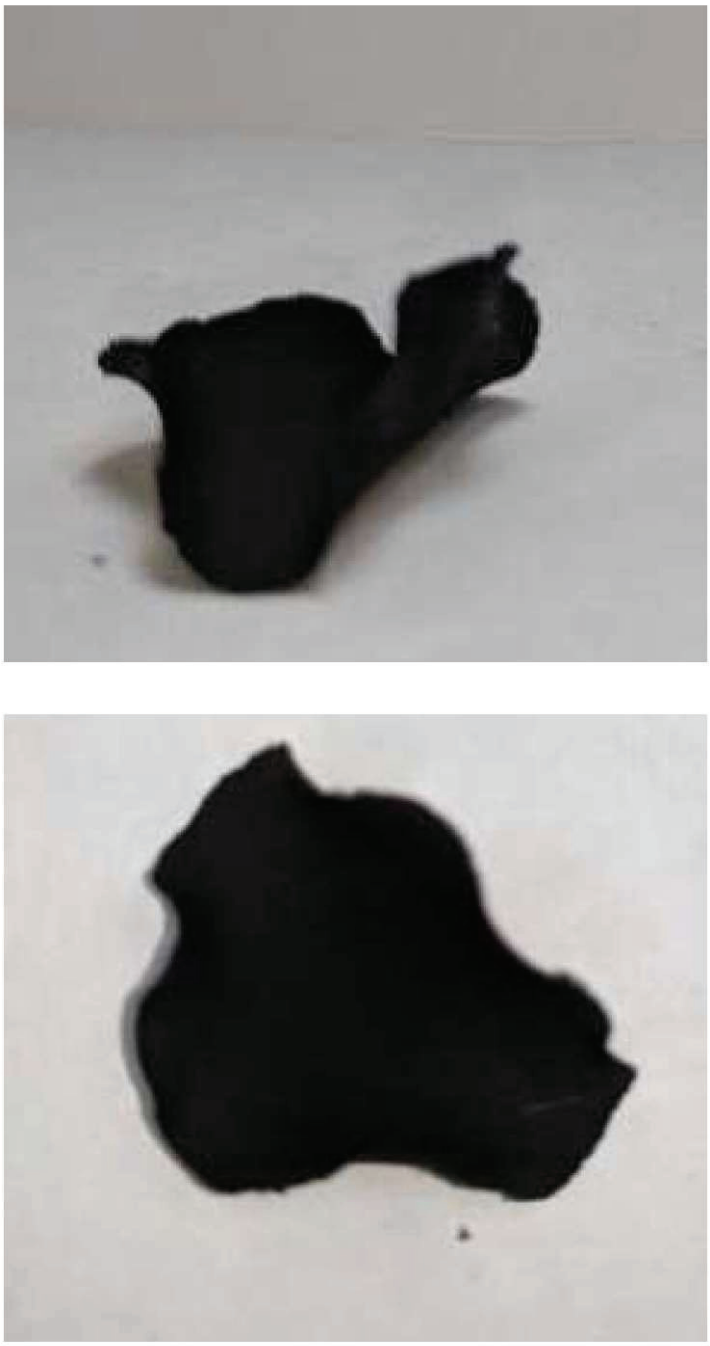


Fig. 89

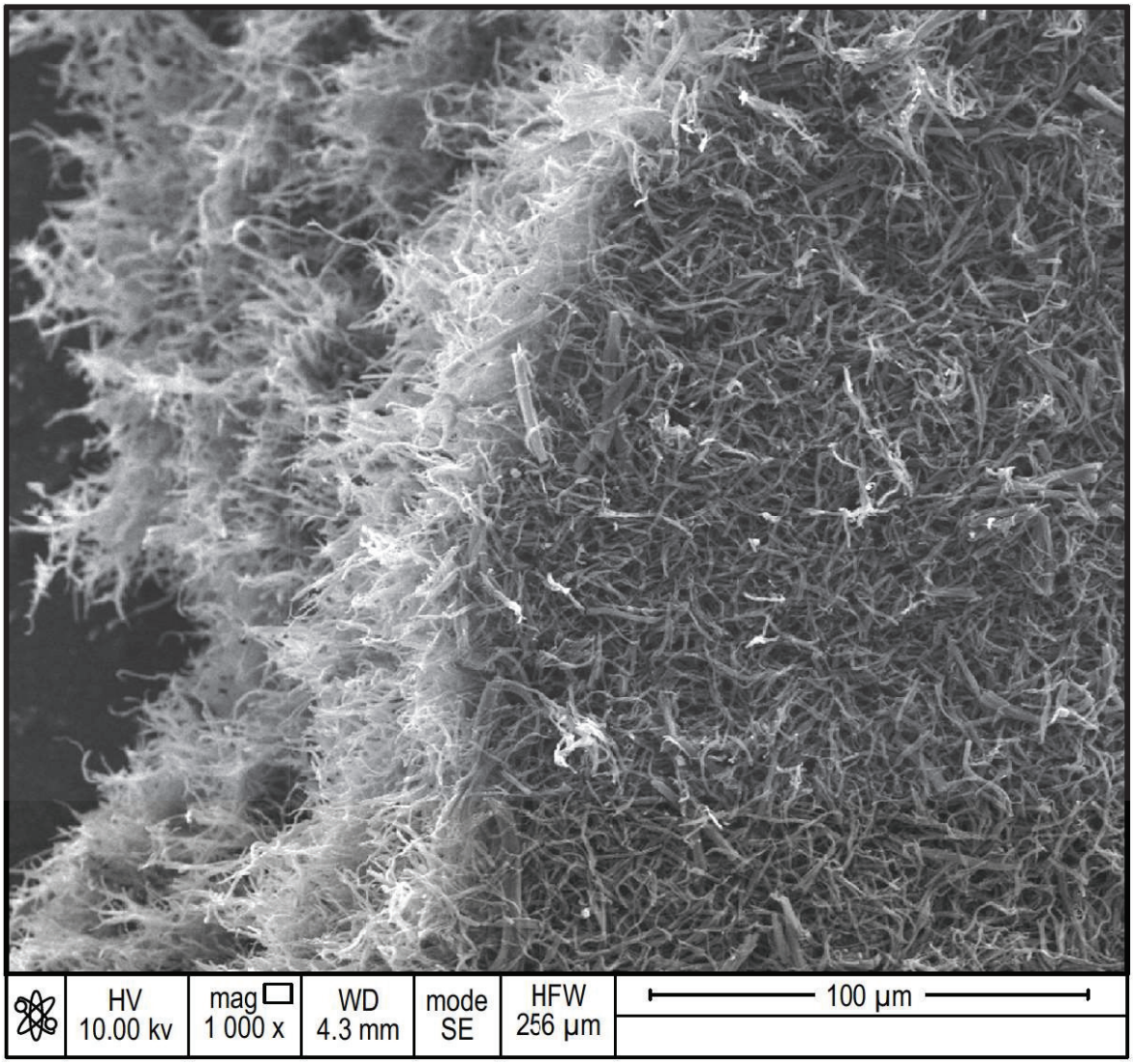



FIG. 90A

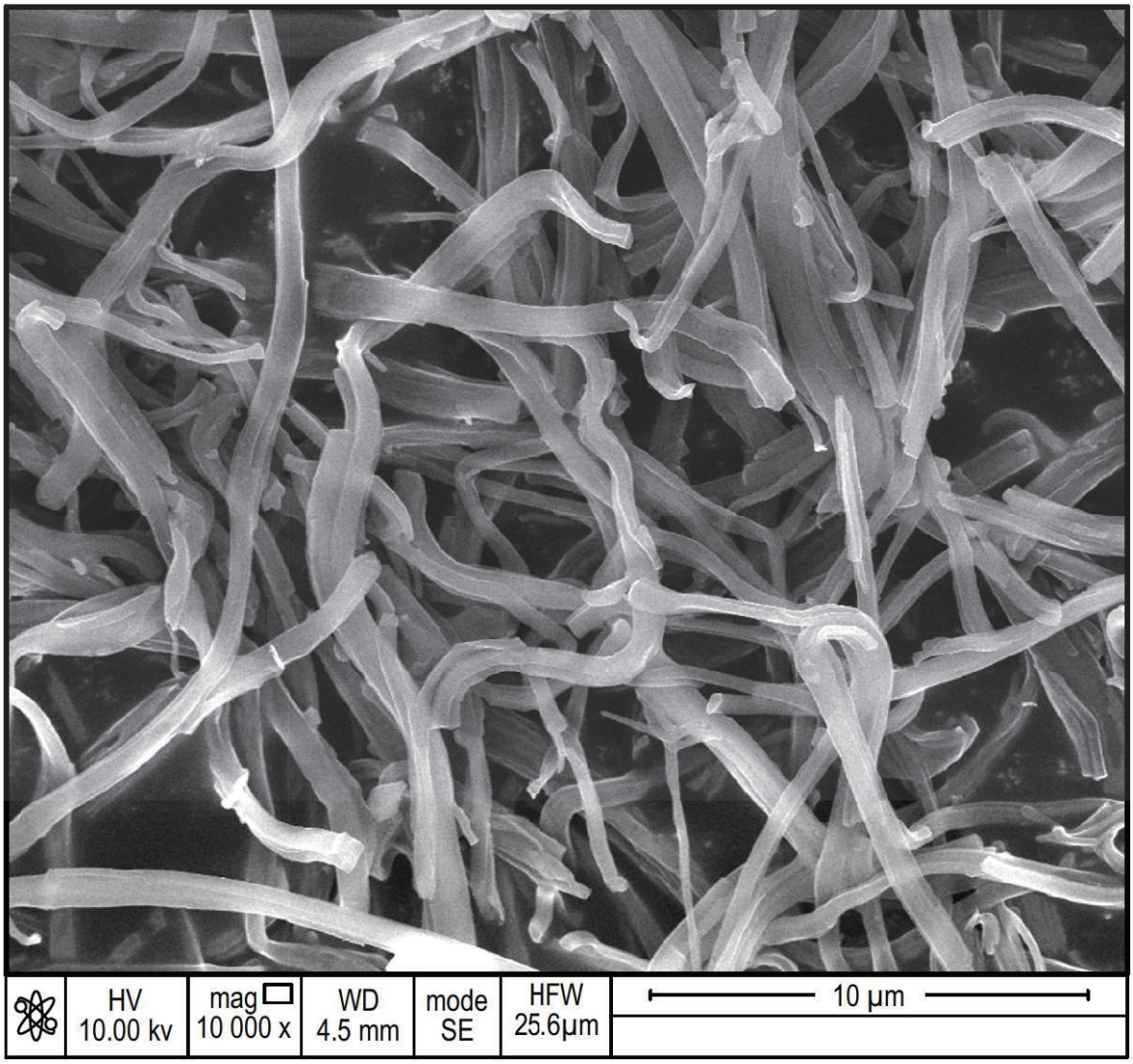



FIG. 90B

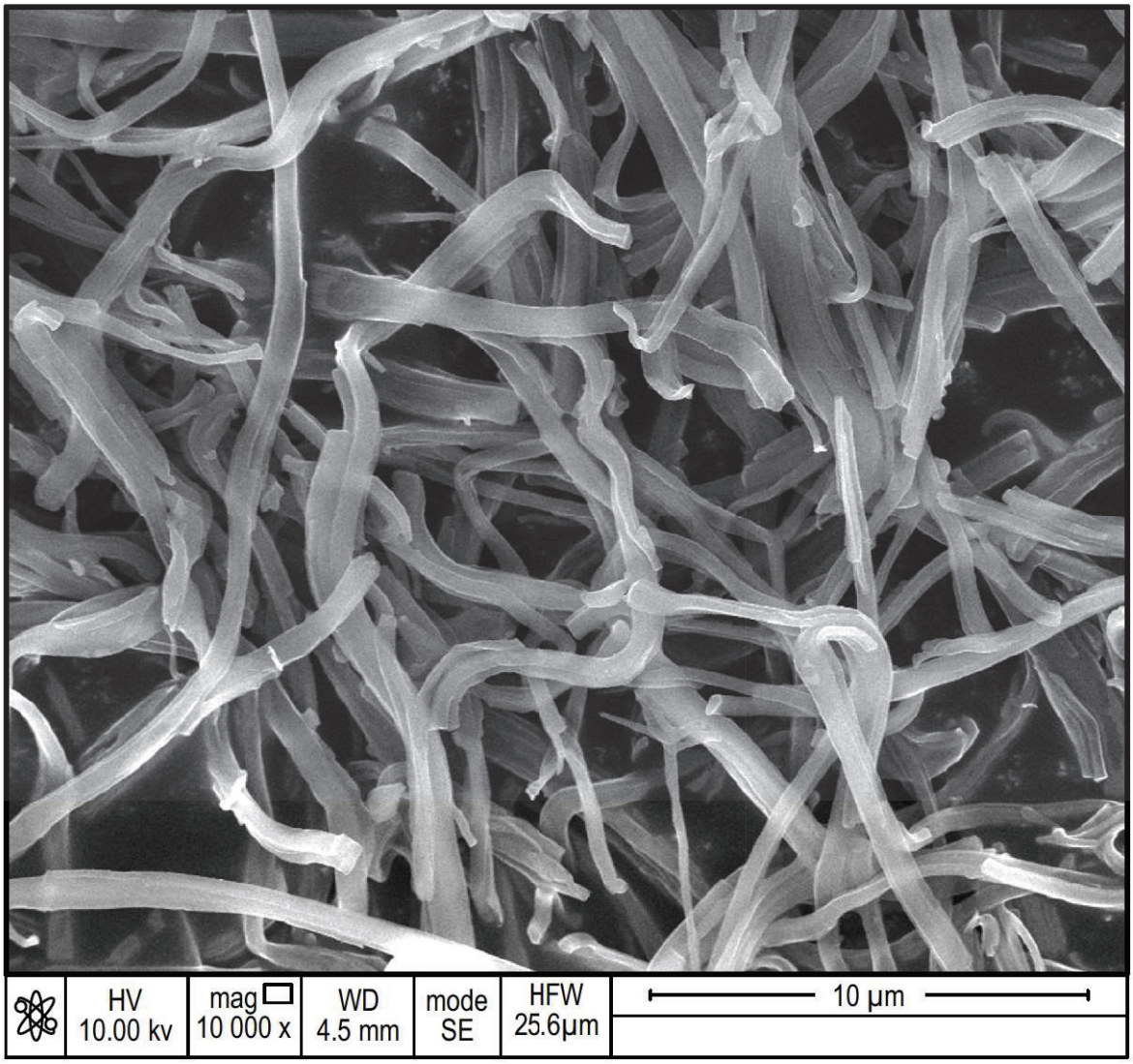



FIG. 91A

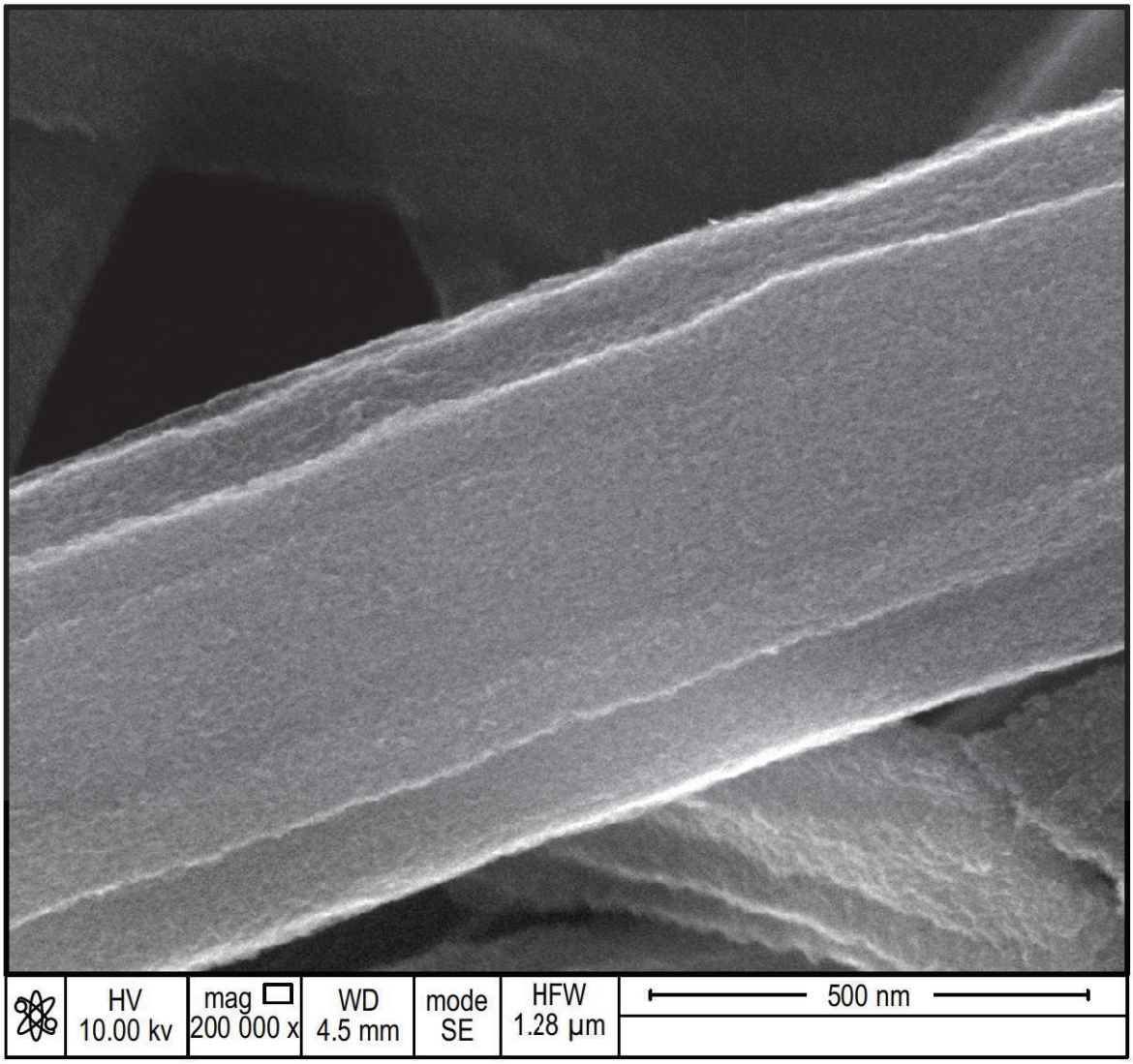



FIG. 91B

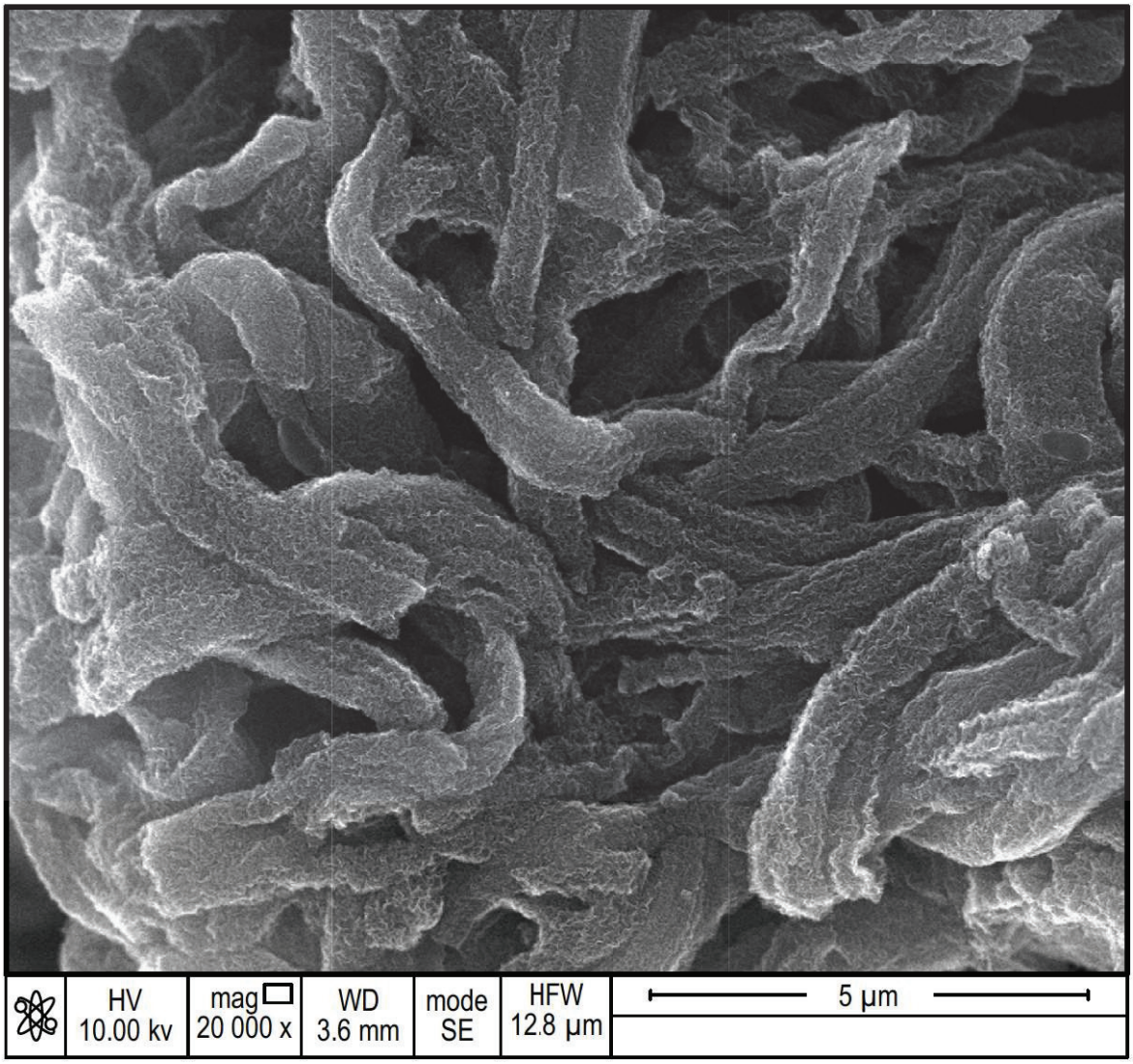



FIG. 92A

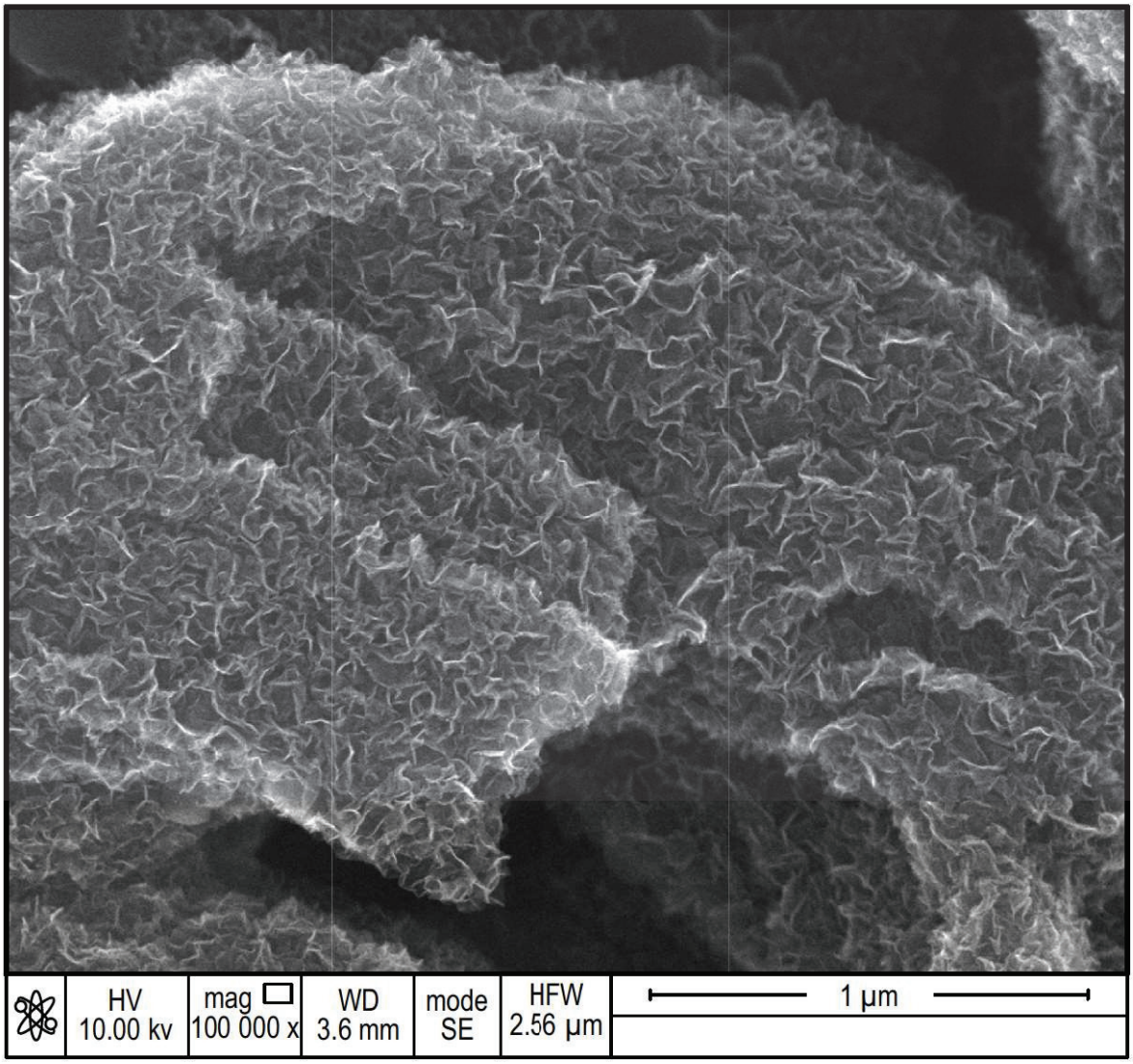



FIG. 92B

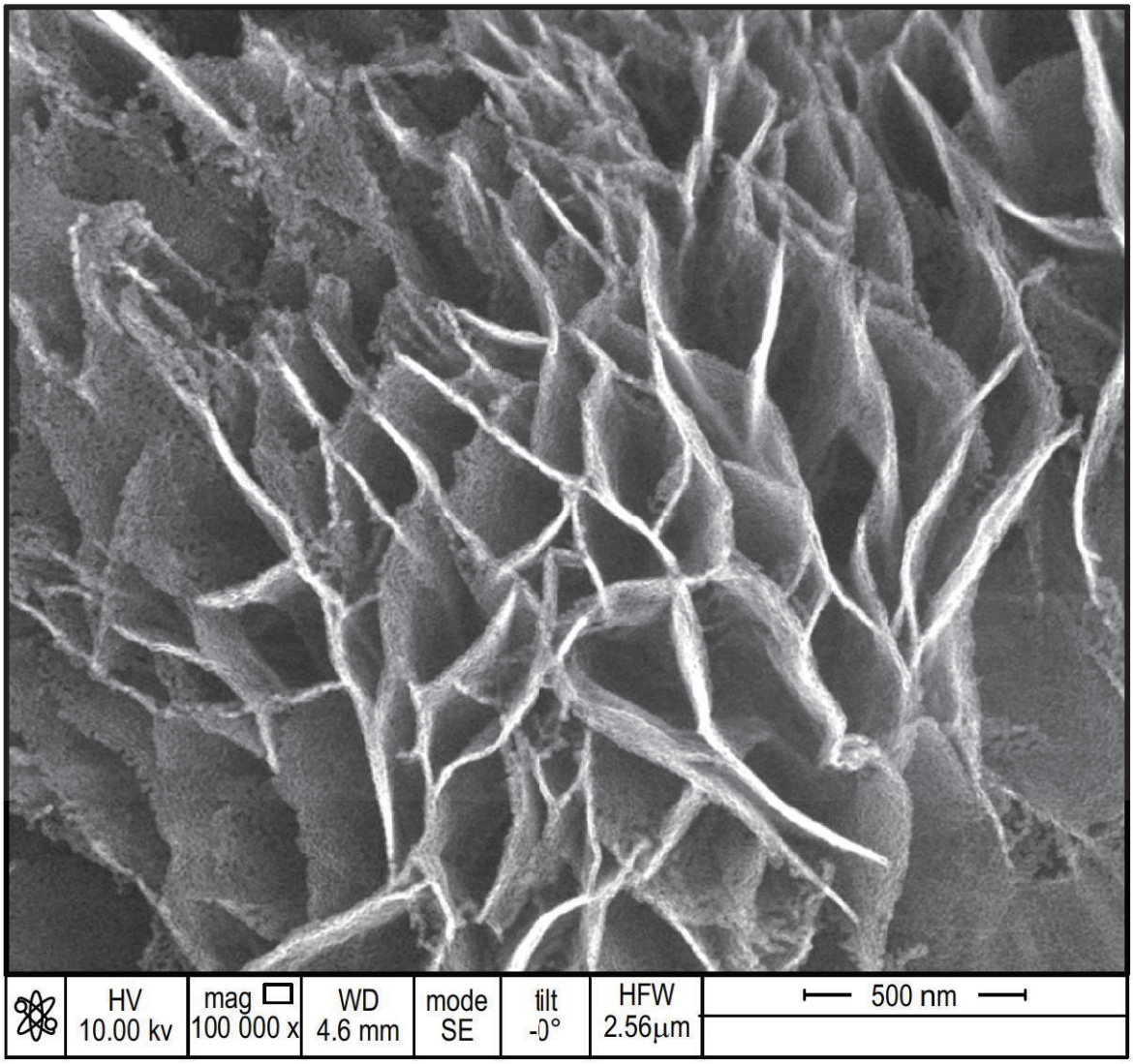



FIG. 93

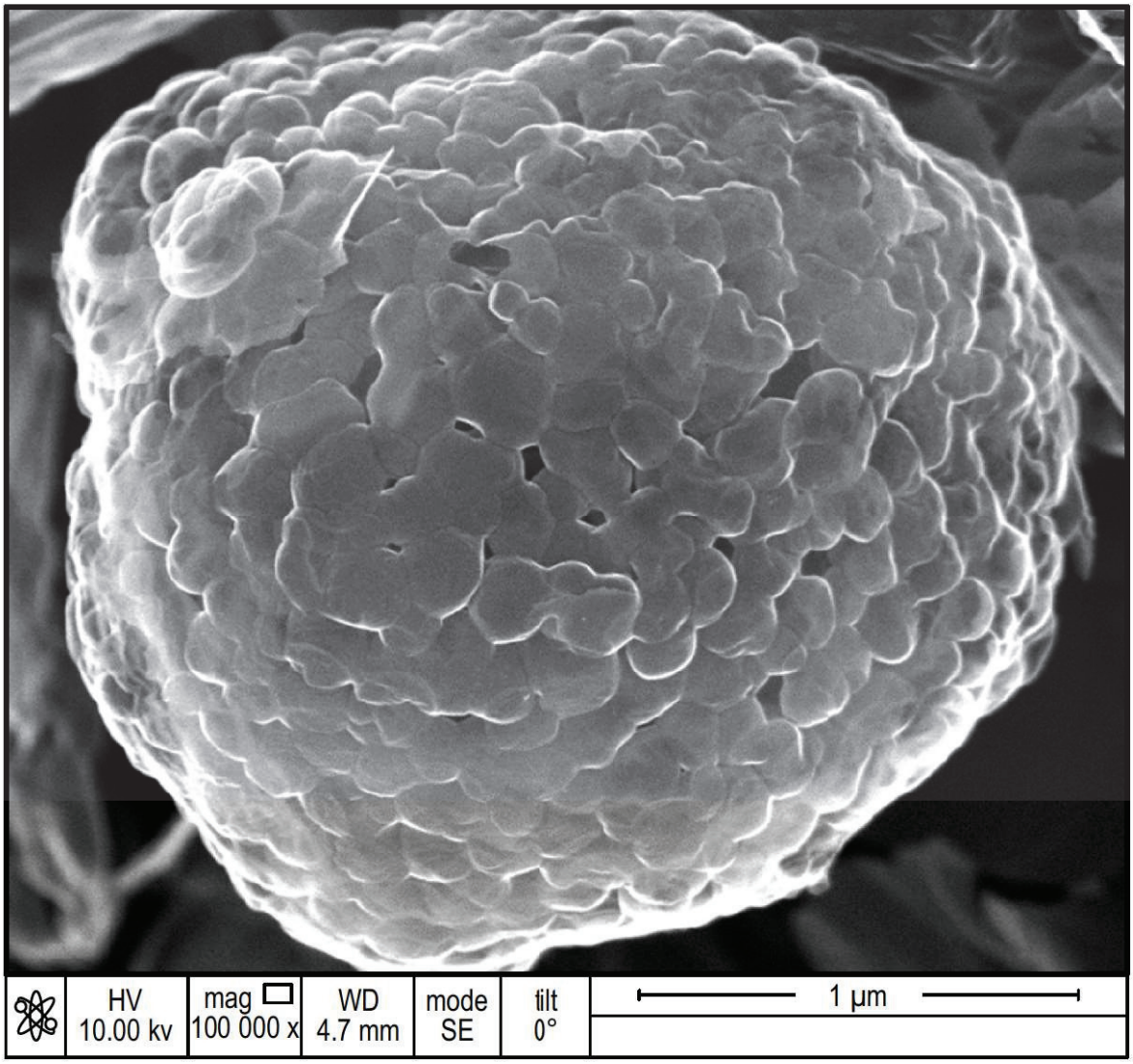



FIG. 94A

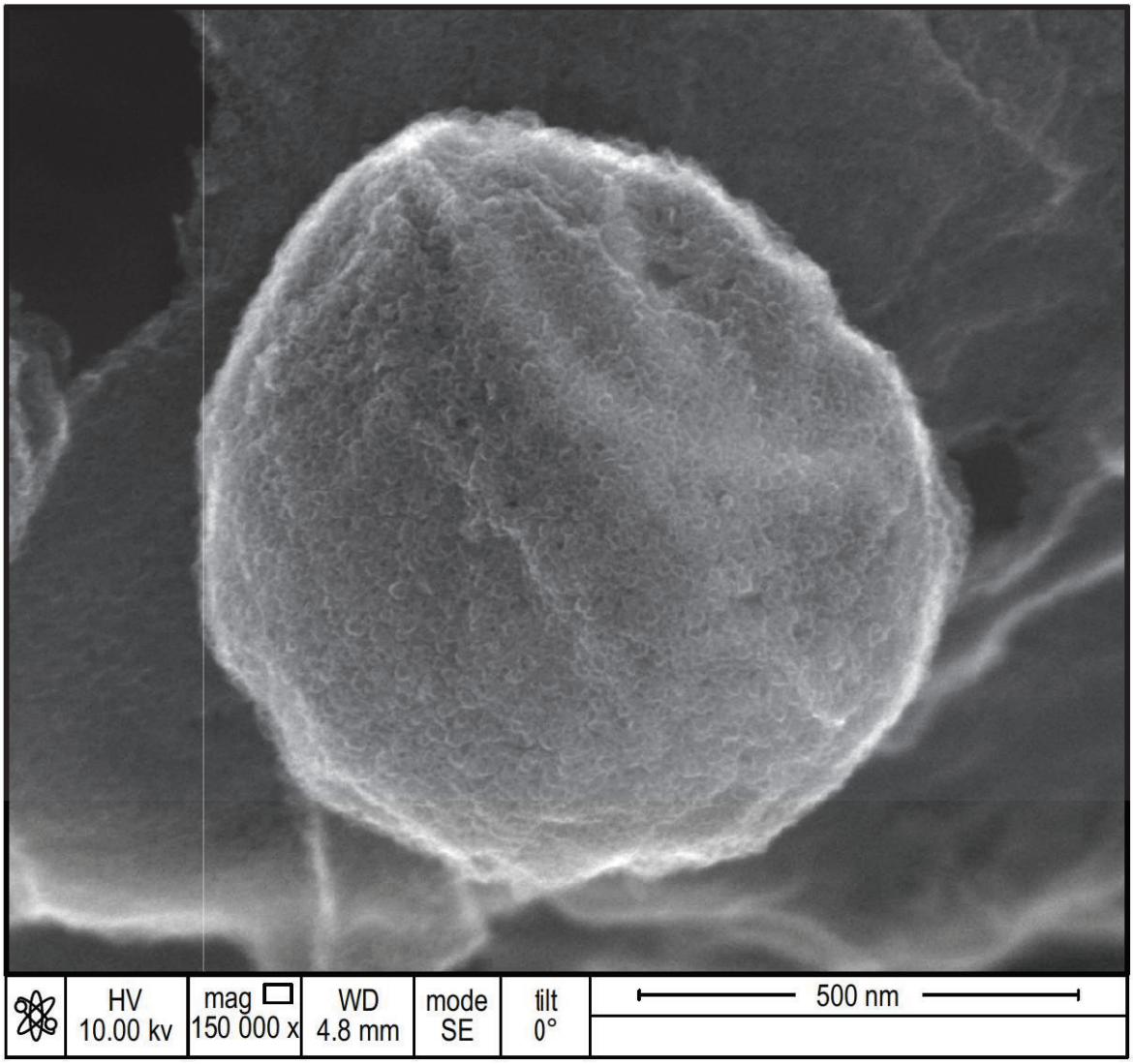



FIG. 94B

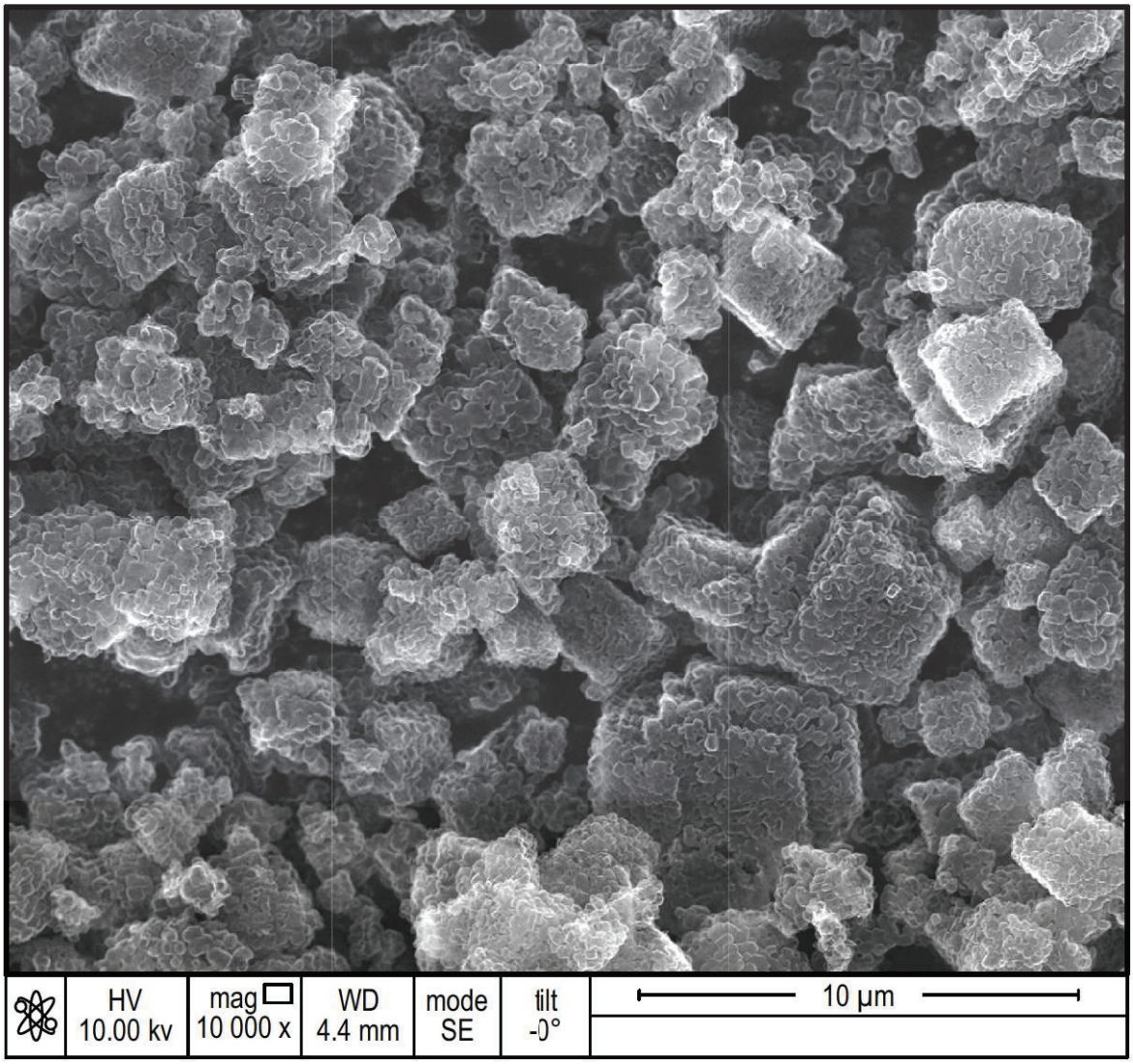



FIG. 95A

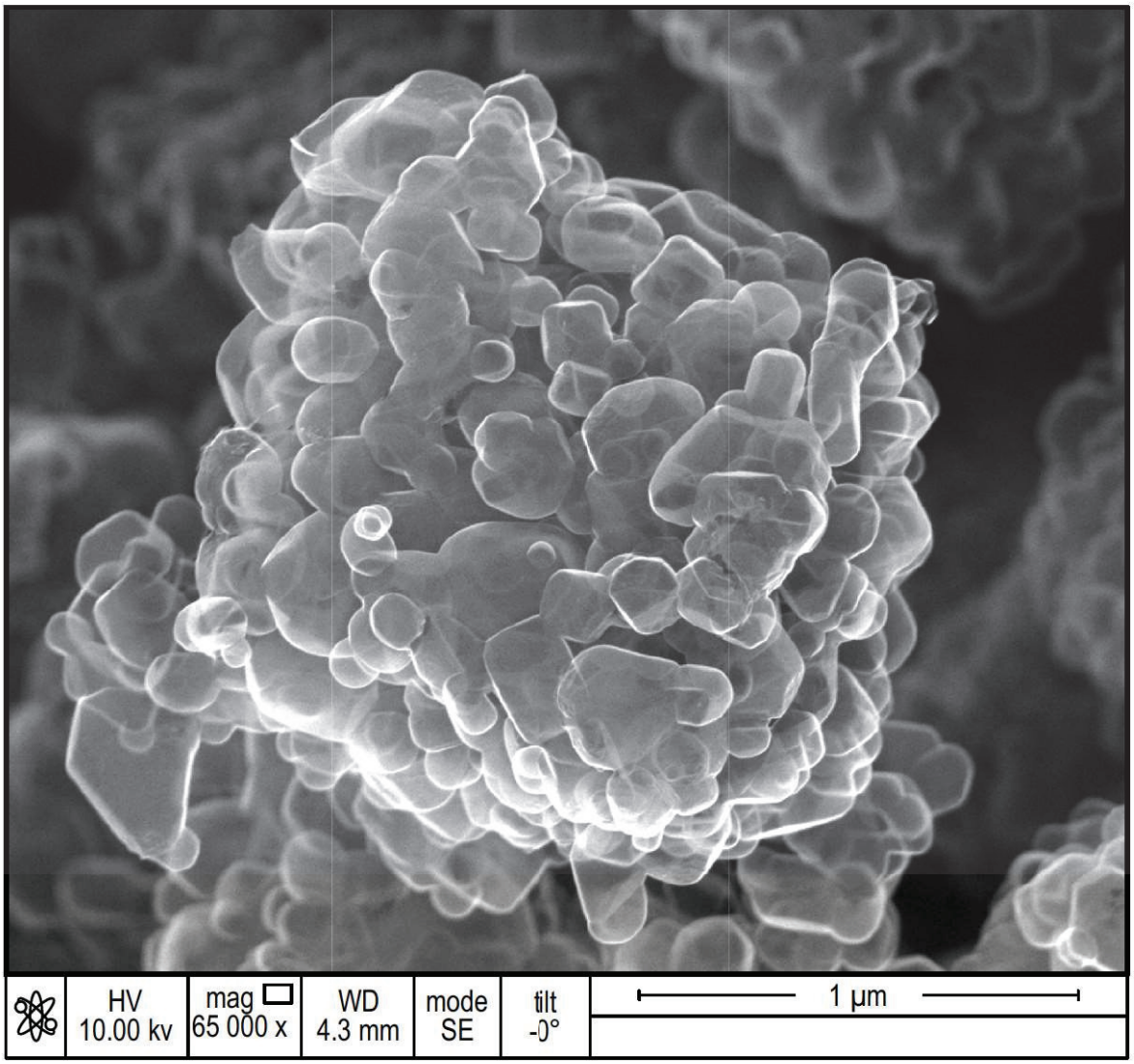
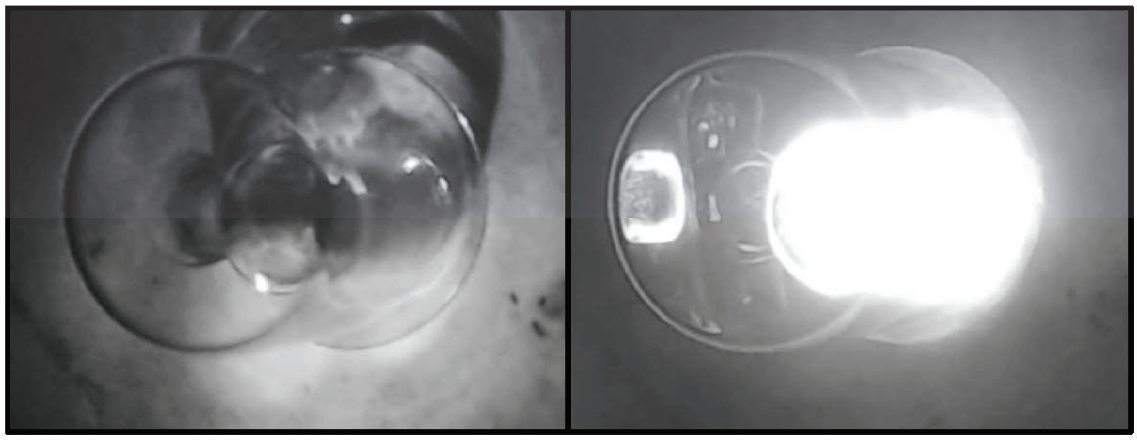



FIG. 95B



Before microwave irradiation During microwave irradiation

FIG. 96

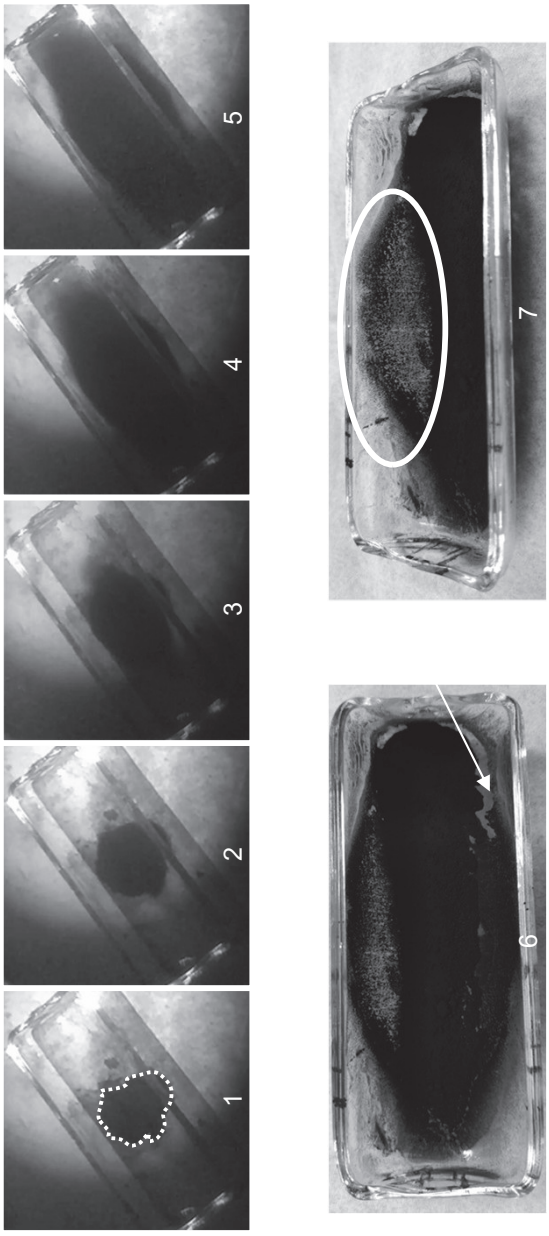



FIG. 97

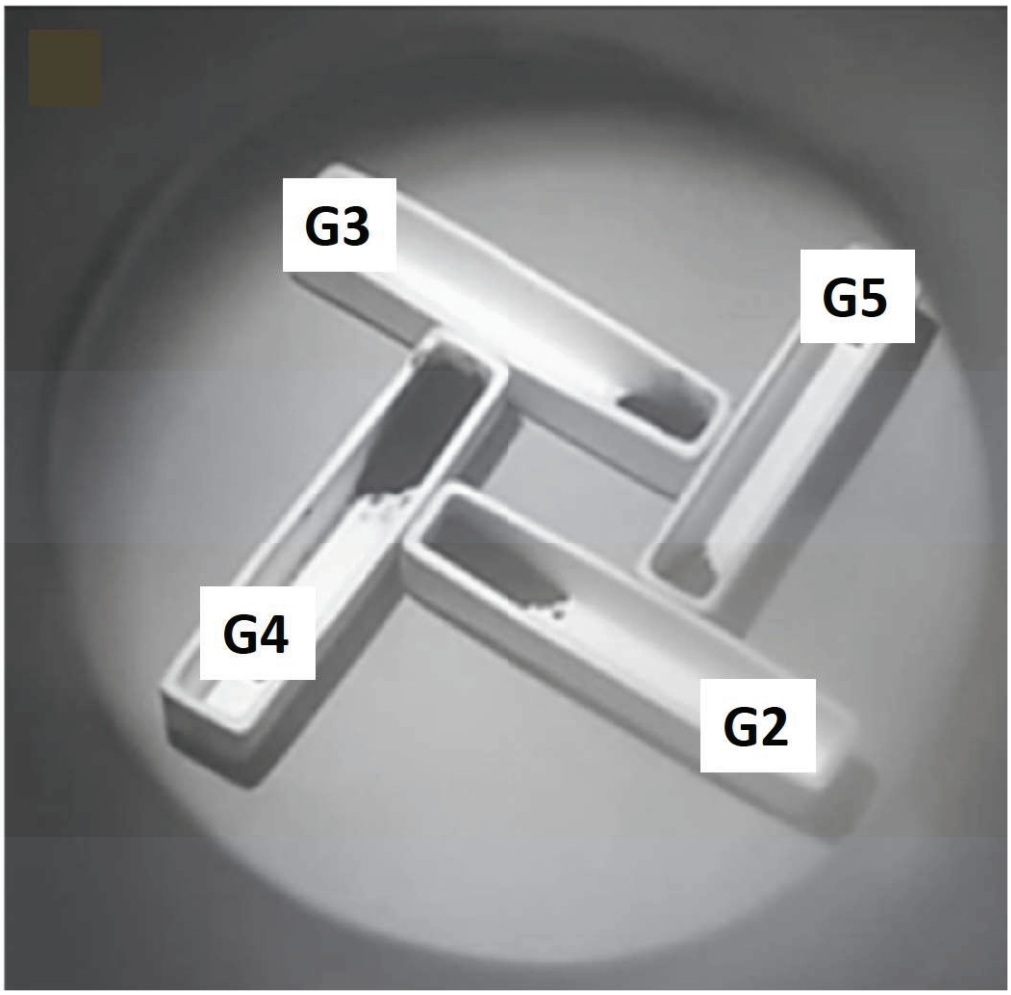



Fig. 98A

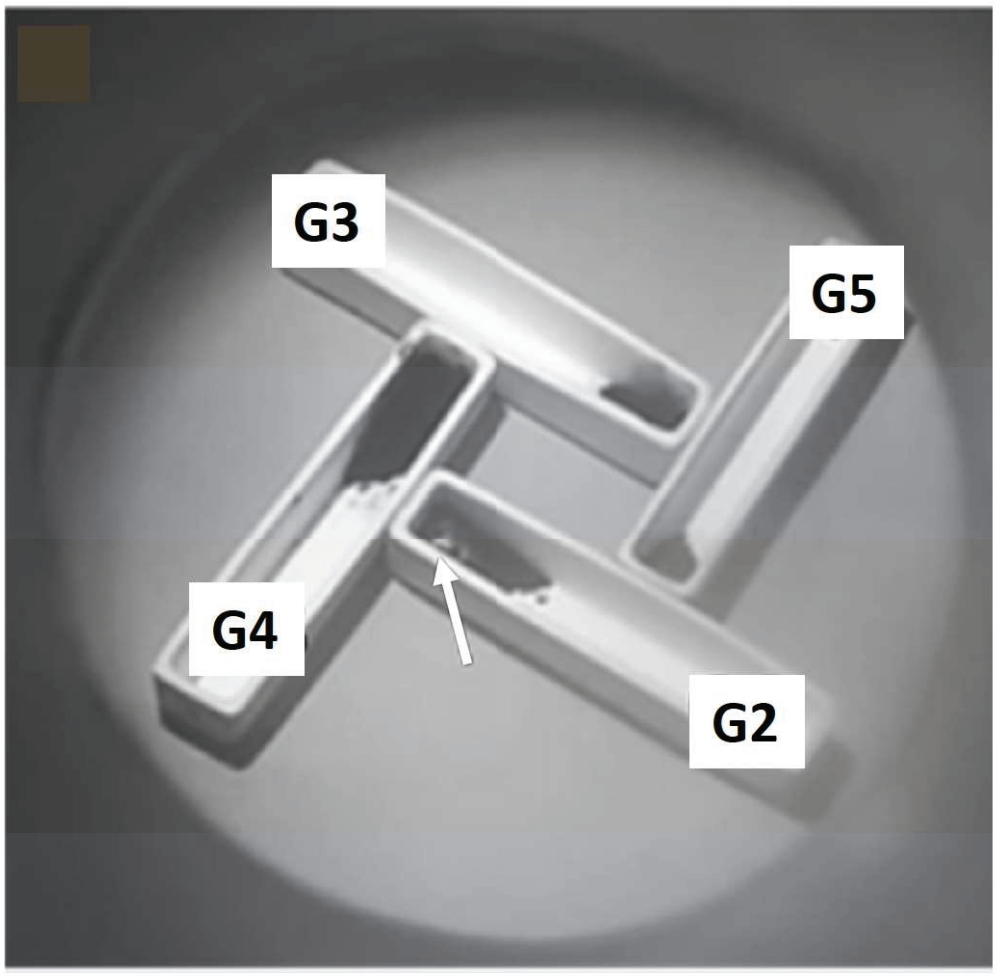



Fig. 98B

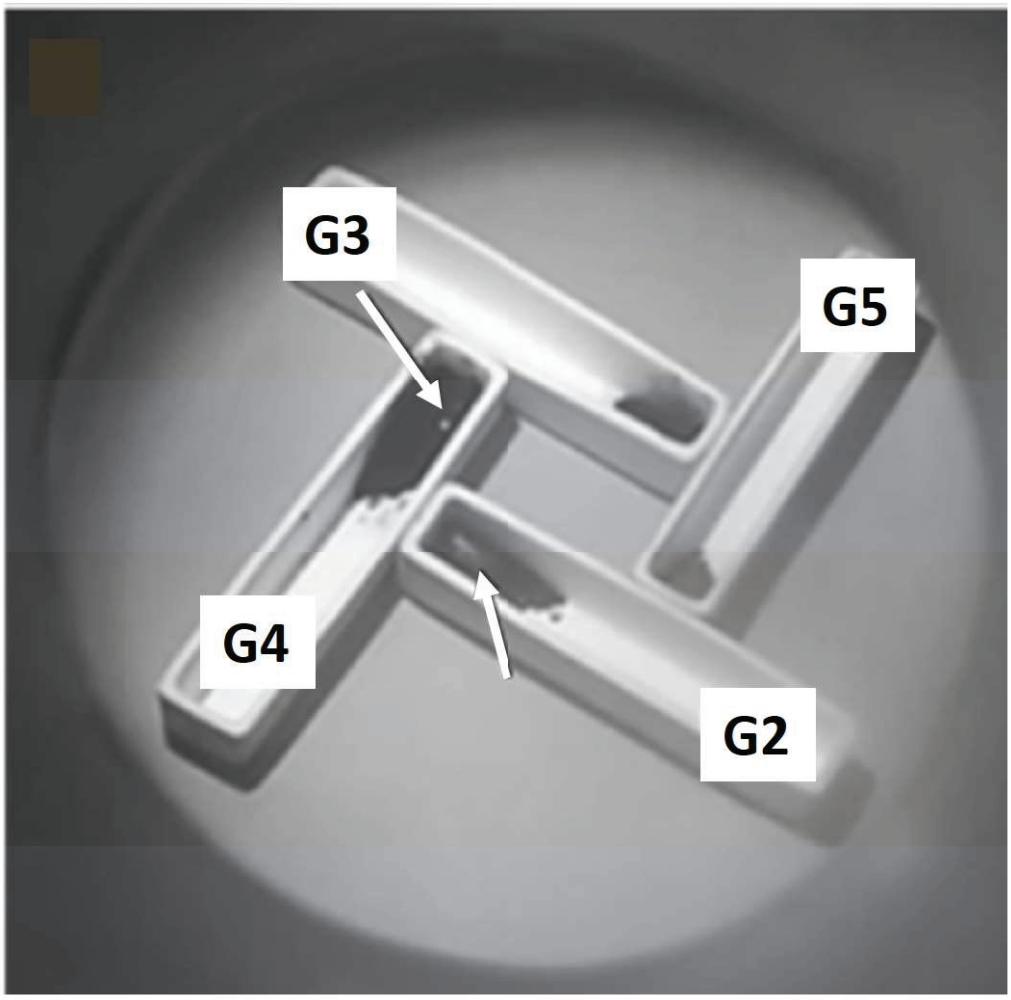



Fig. 98C

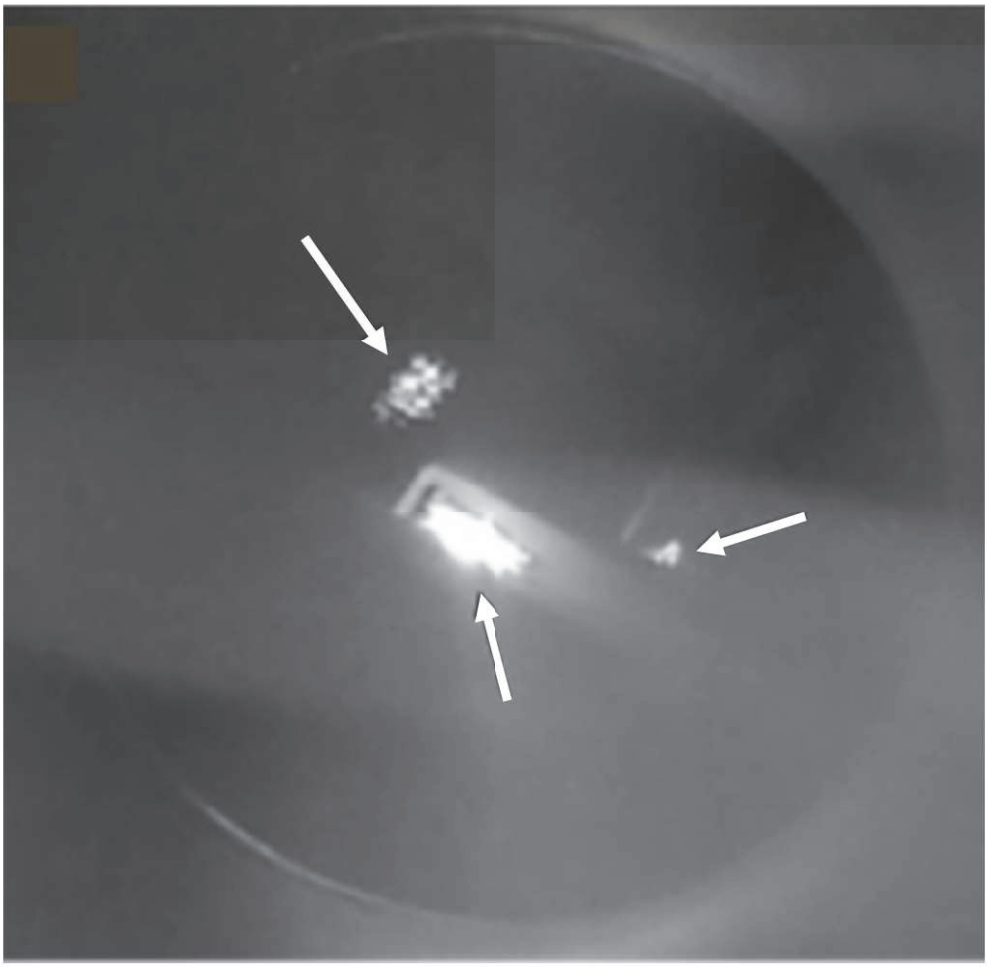


Fig. 98D

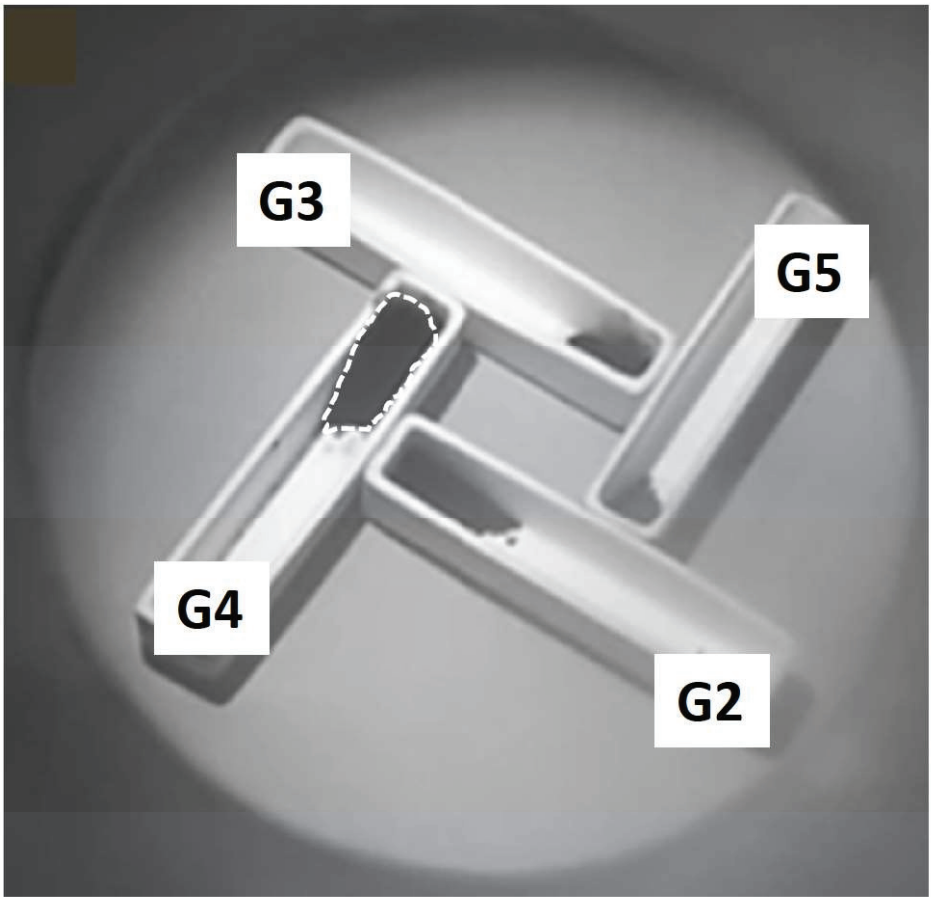



Fig. 99A

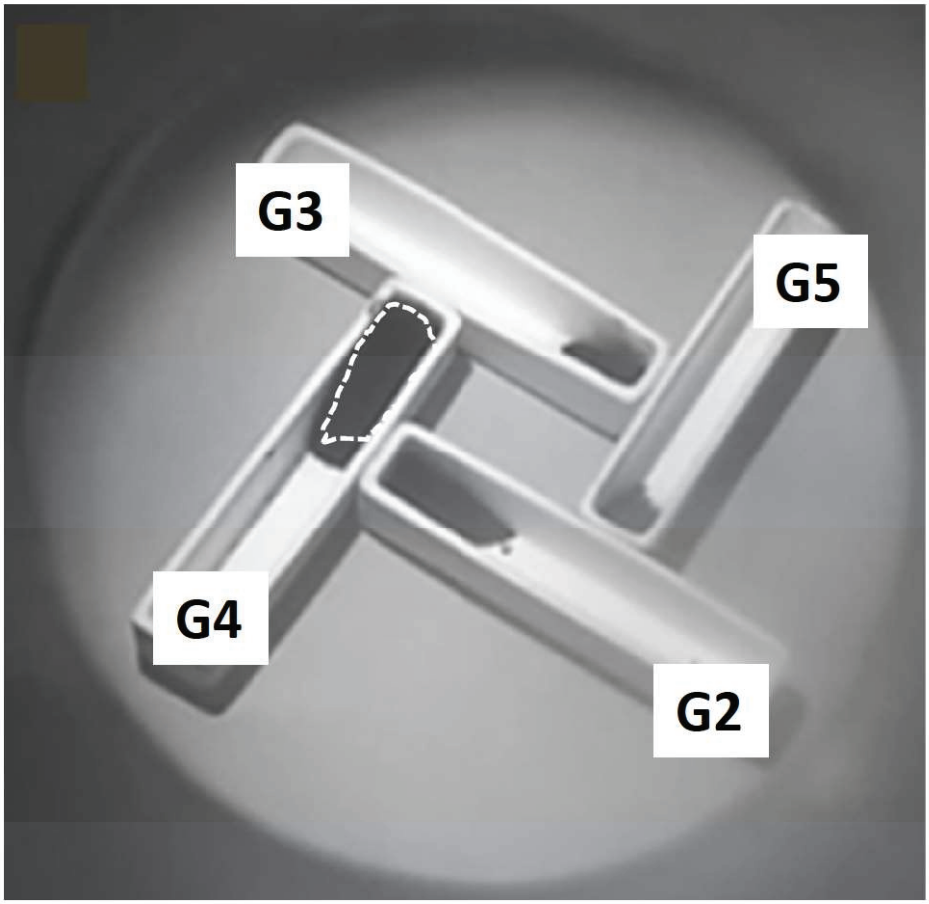



Fig. 99B

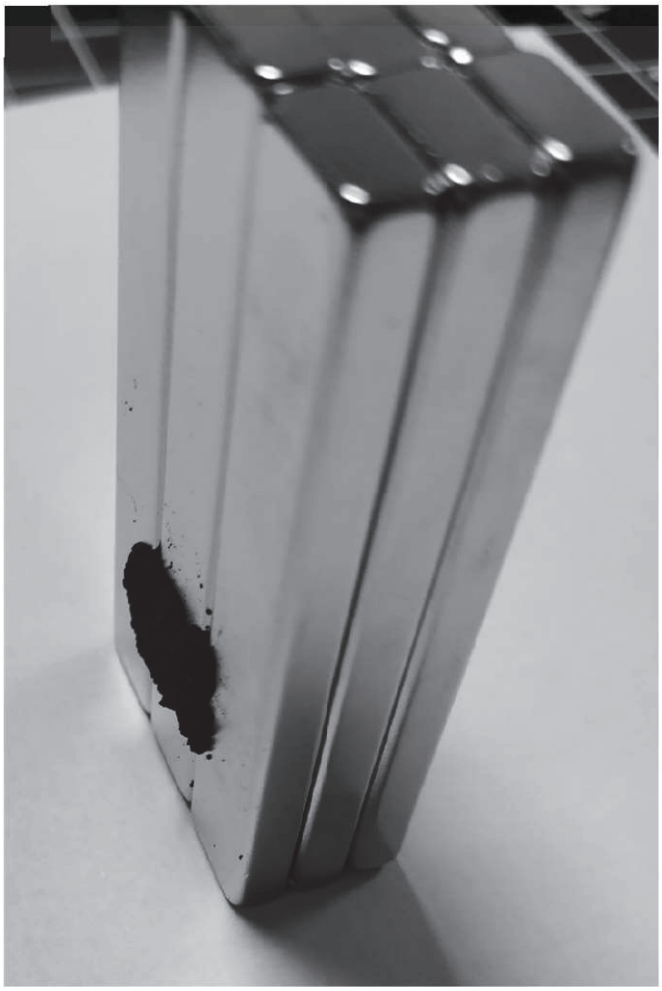


Fig. 100A

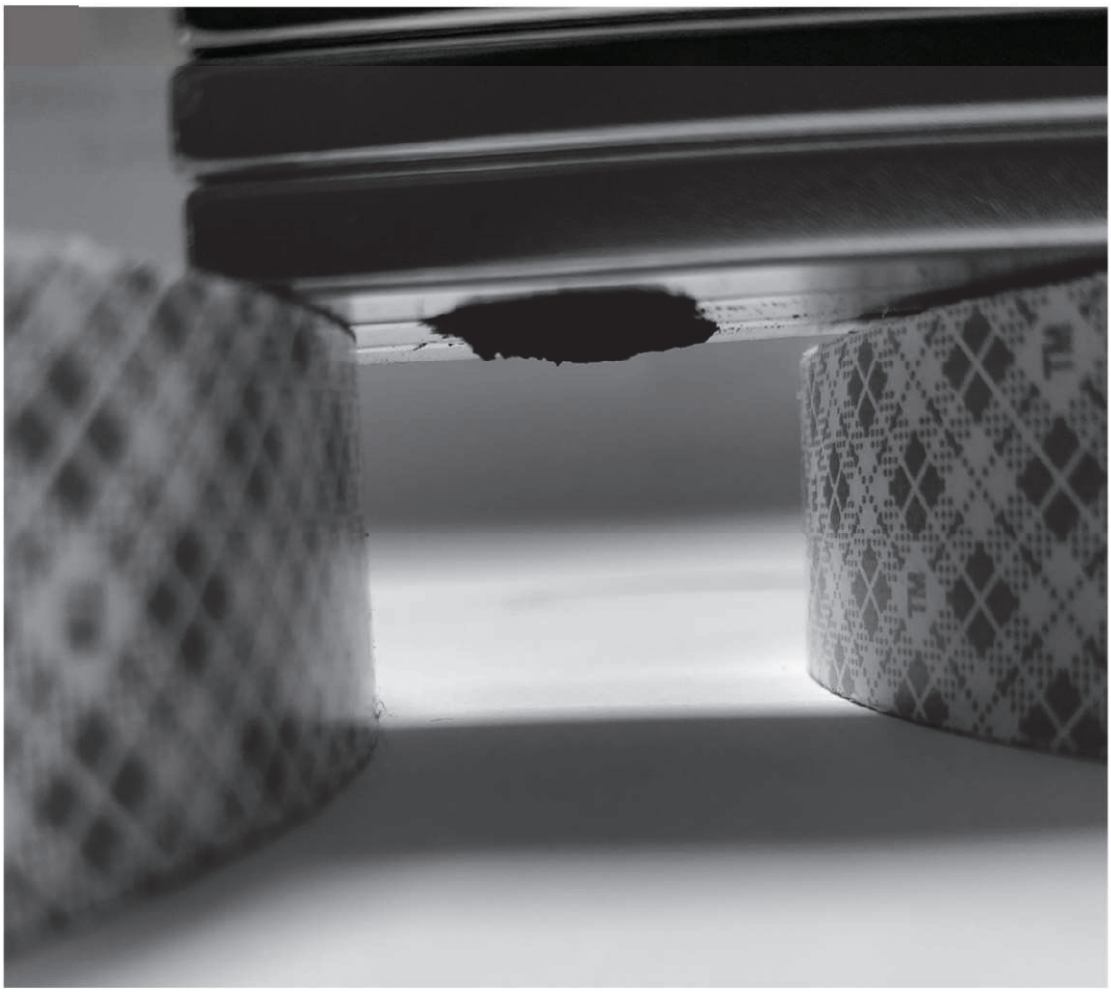


Fig. 100B

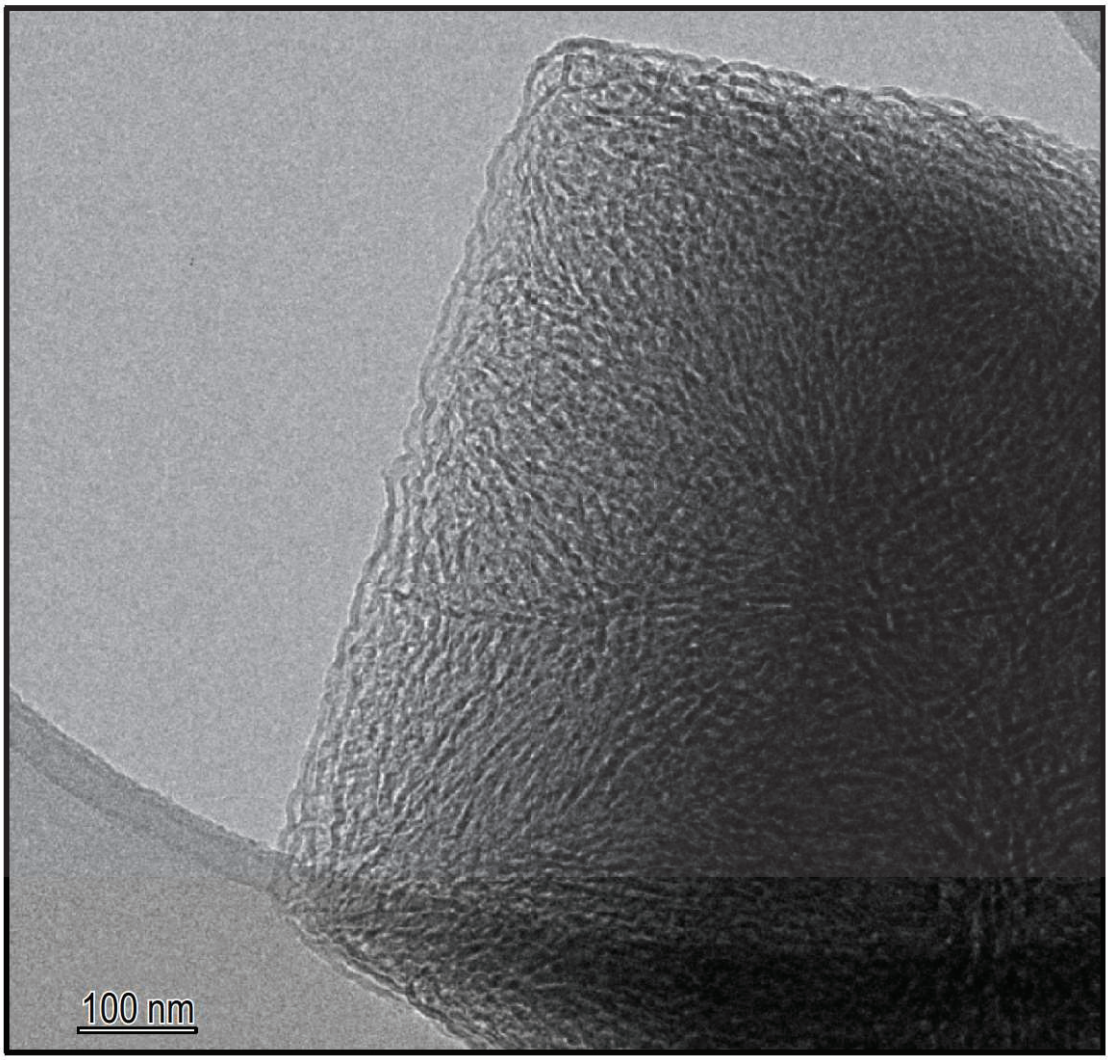



FIG. 101A

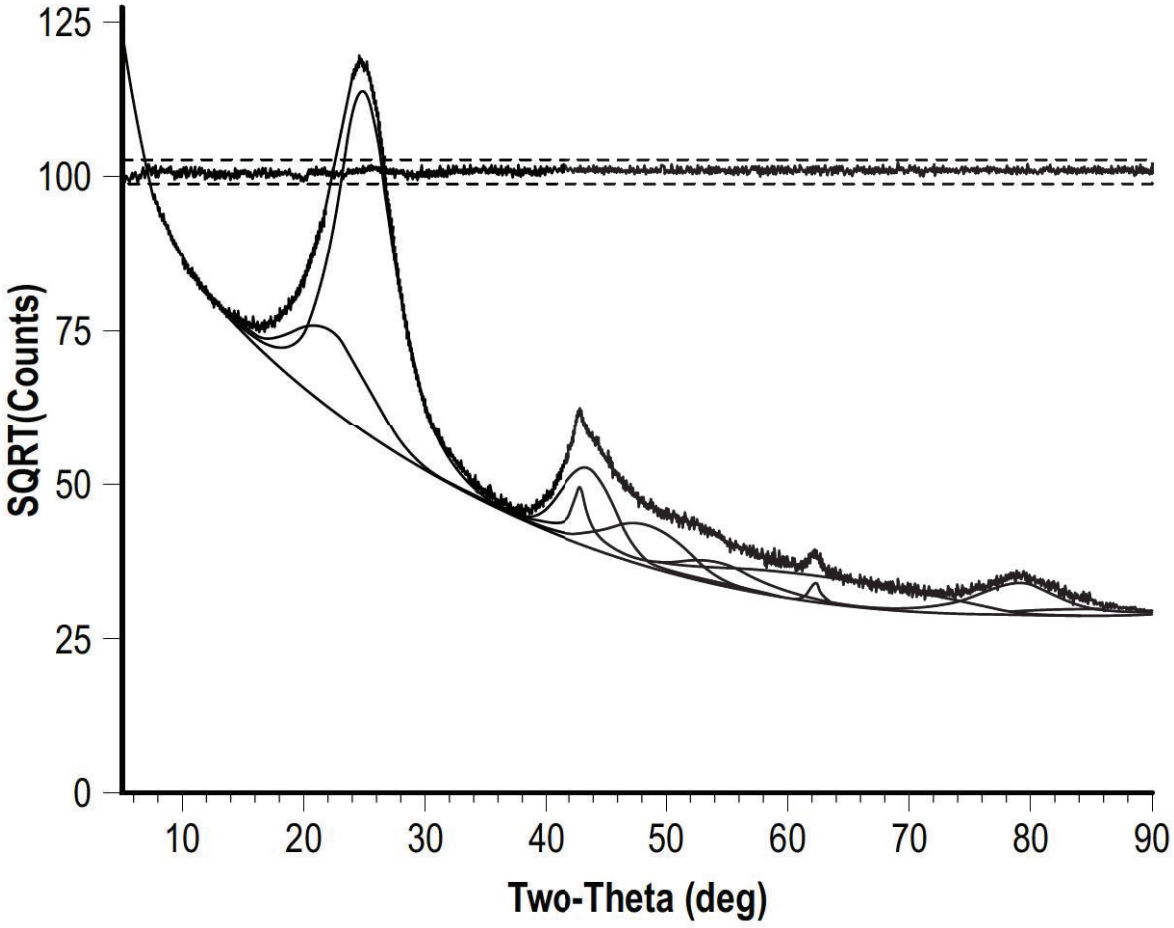

125
100
75
50
25
0
SQRT(Counts)
10
20
30
40
50
60
70
80
90
Two-Theta (deg)

FIG. 101B

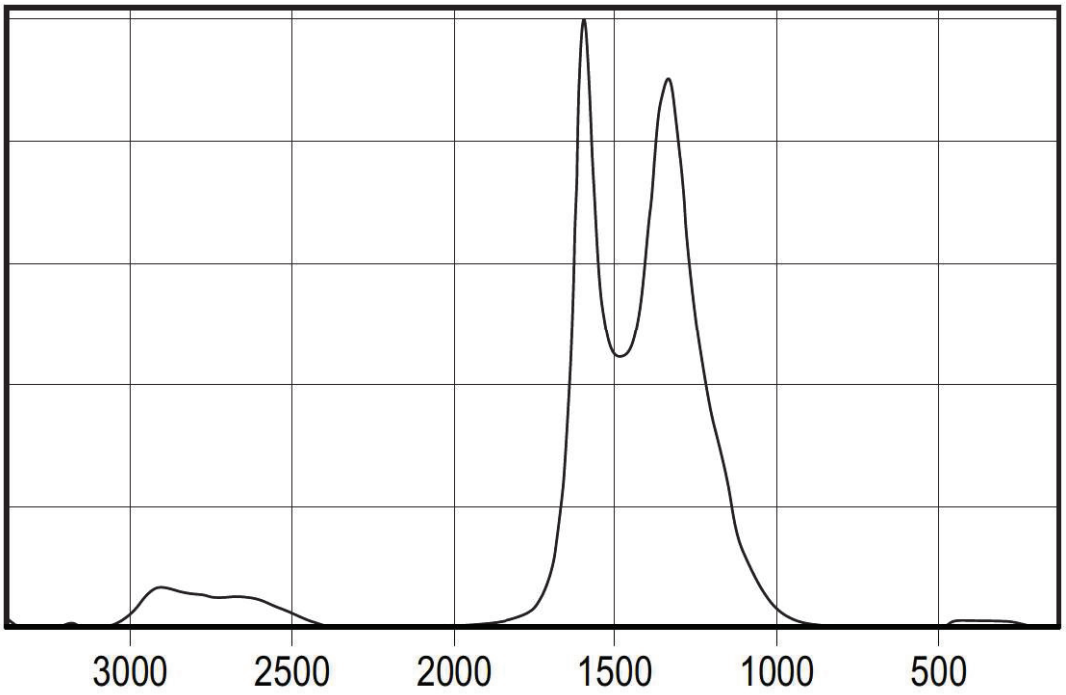



FIG. 101C

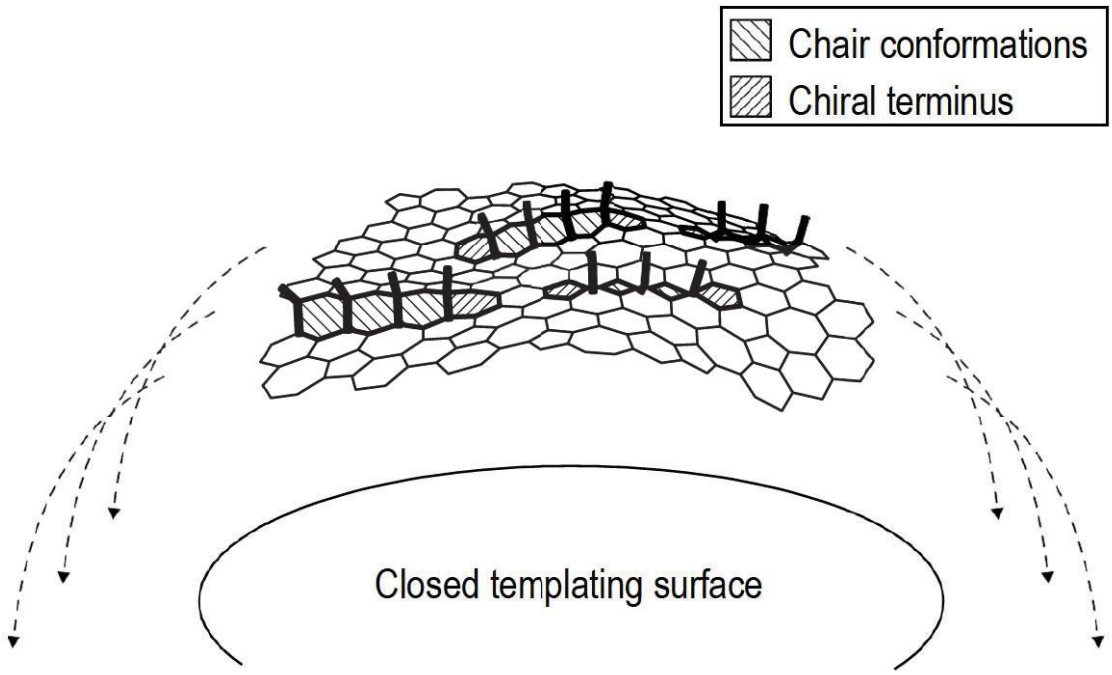

Chair conformations
Chiral terminus
Closed templating surface

FIG. 102



FIG. 103A



FIG. 103B

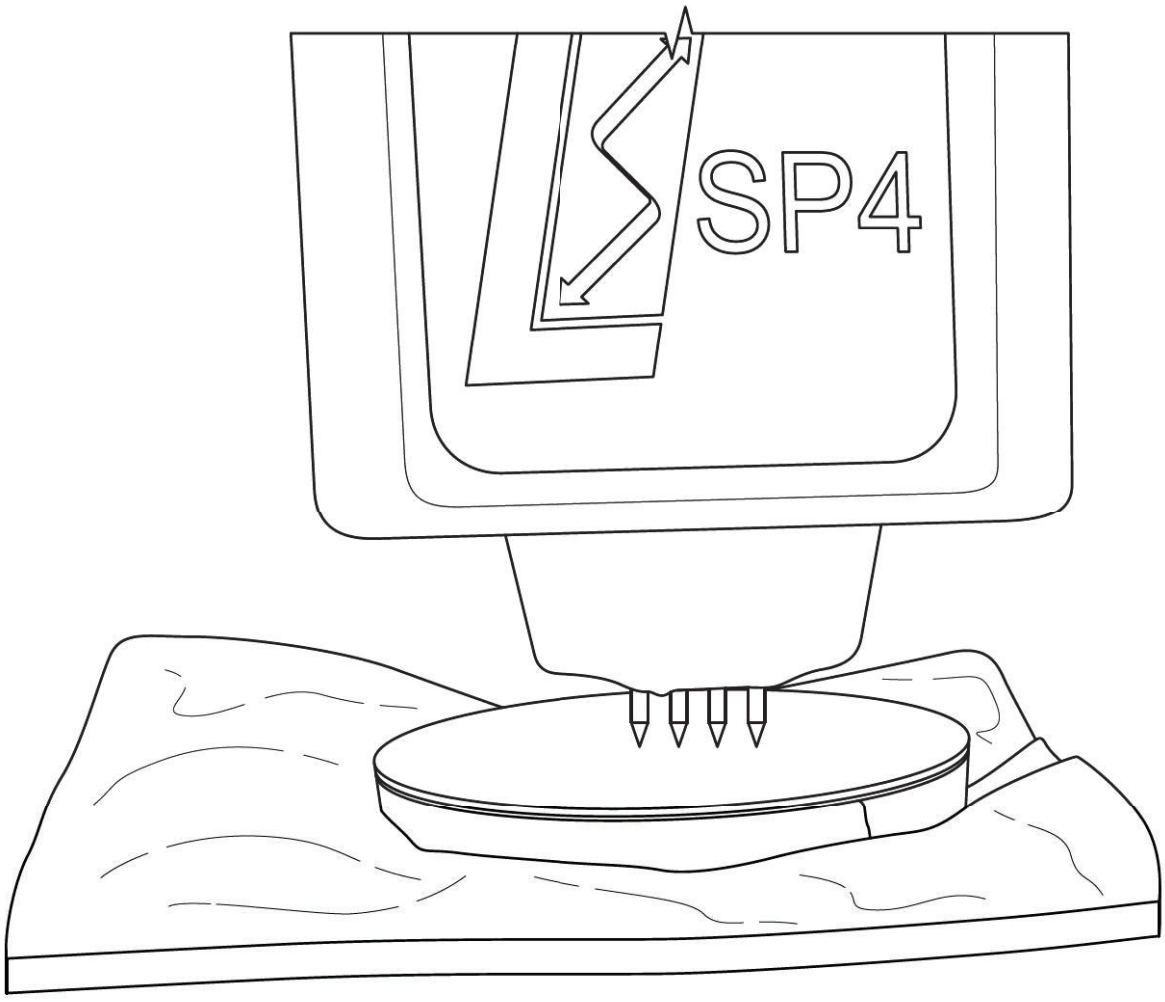



FIG. 104

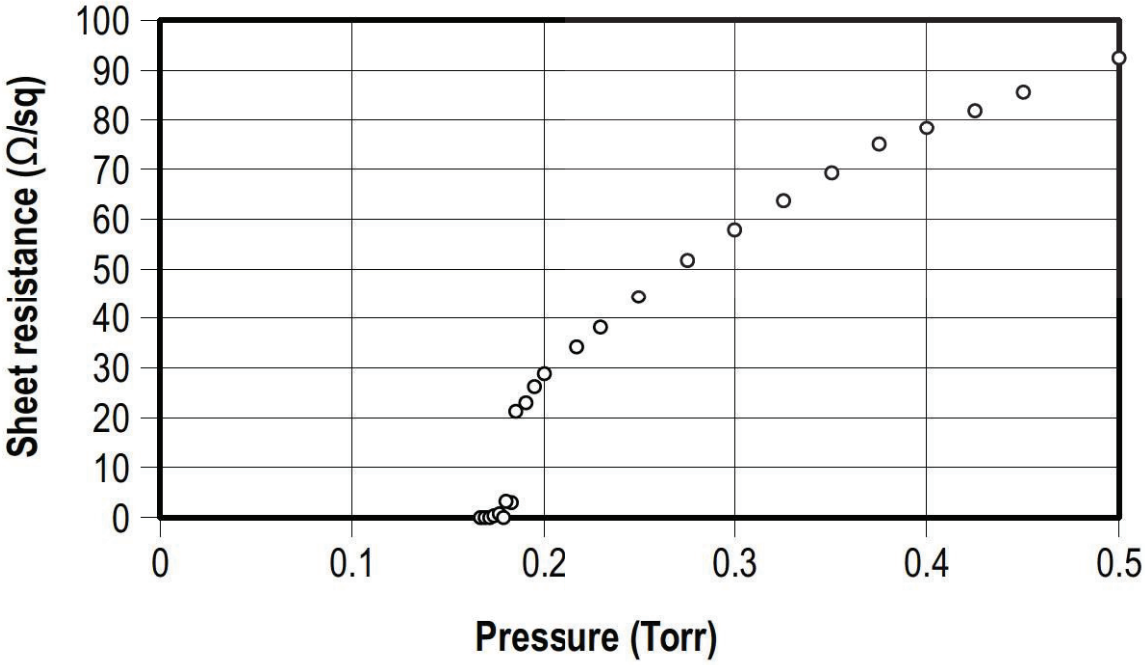

Sheet resistance (Ω/sq)
100
90
80
70
60
50
40
30
20
10
0
0
0.1
0.2
0.3
0.4
0.5
Pressure (Torr)

FIG. 105

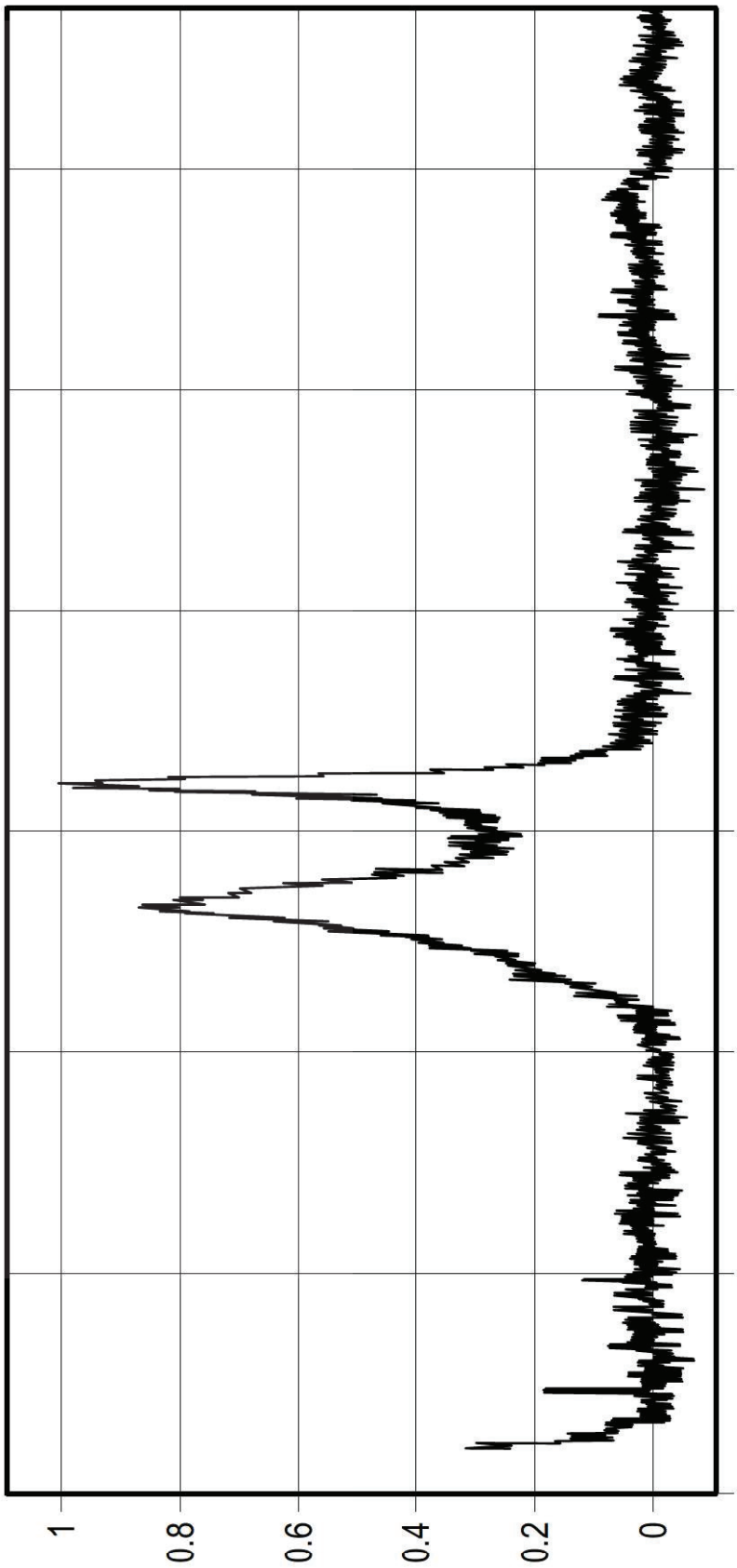



FIG. 106

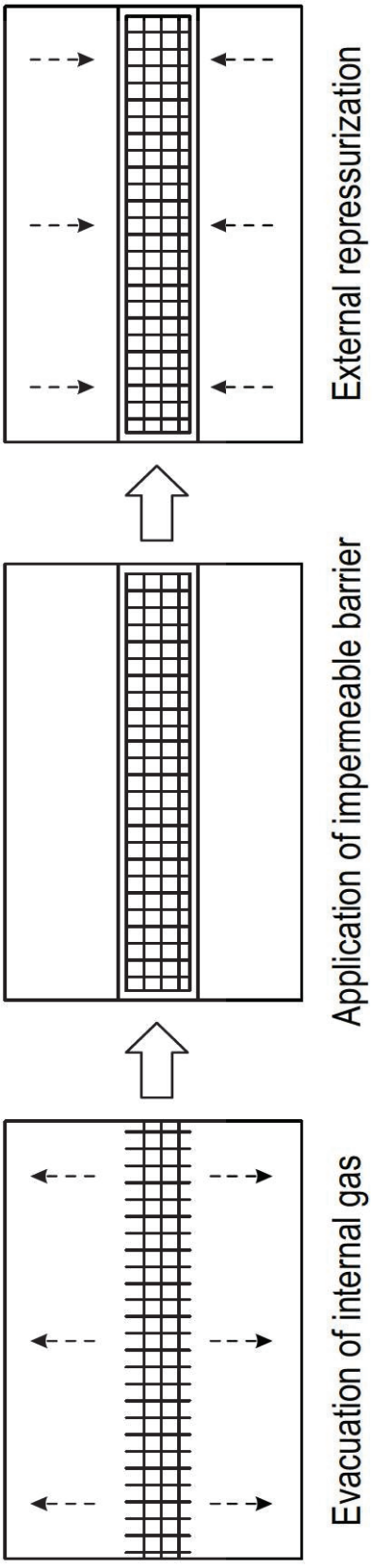

Evacuation of internal gas
Application of impermeable barrier
External repressurization

FIG. 107

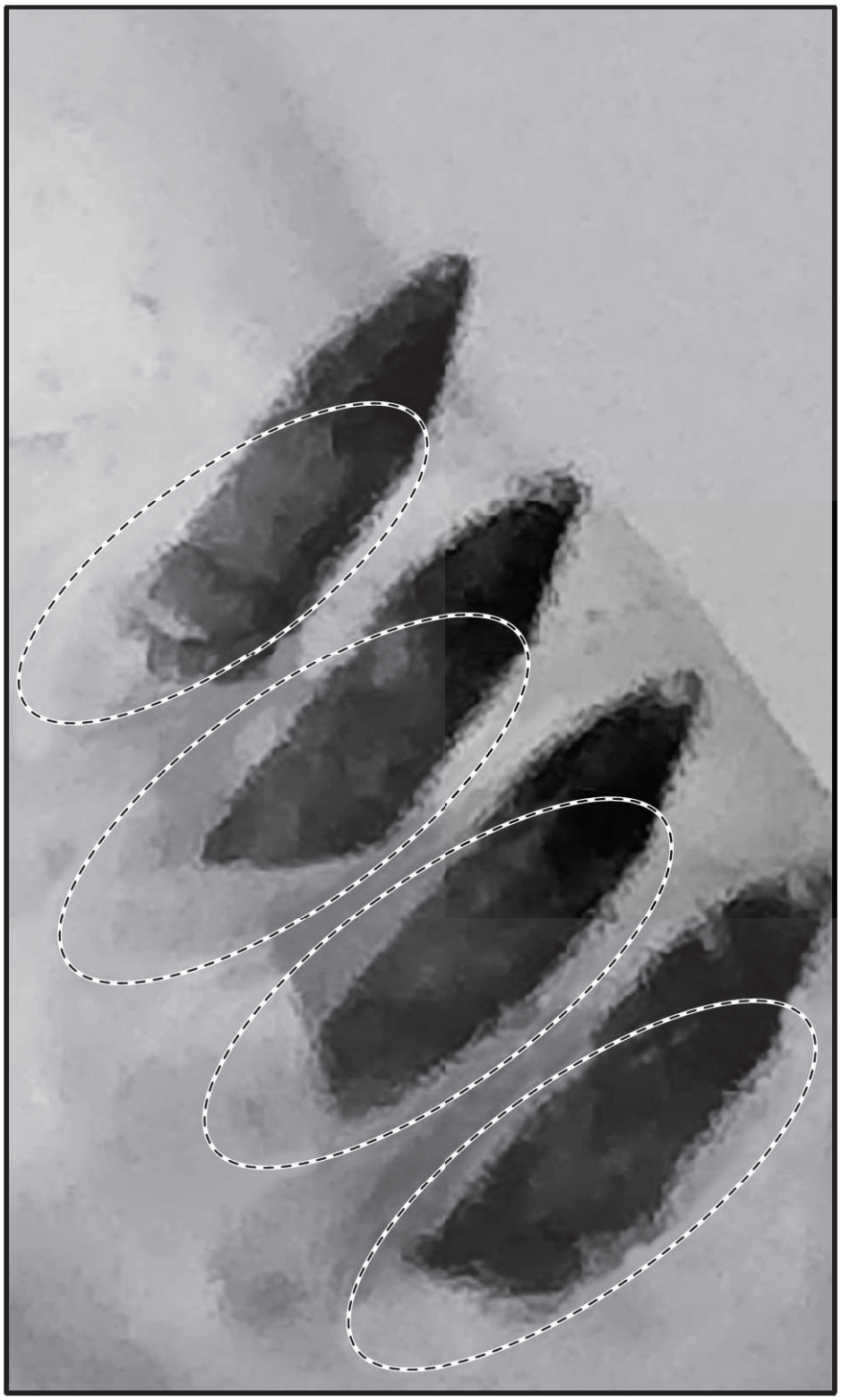


FIG. 108

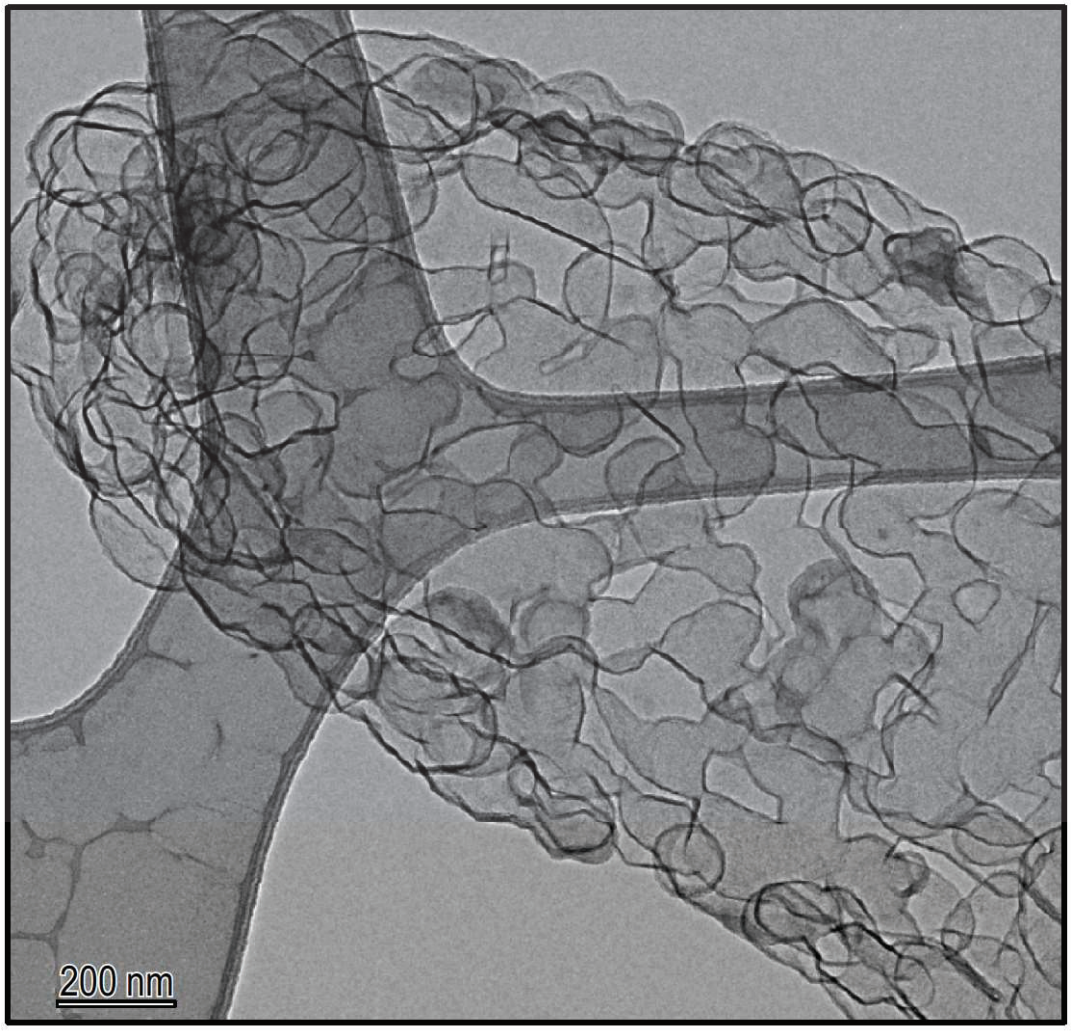



FIG. 109A

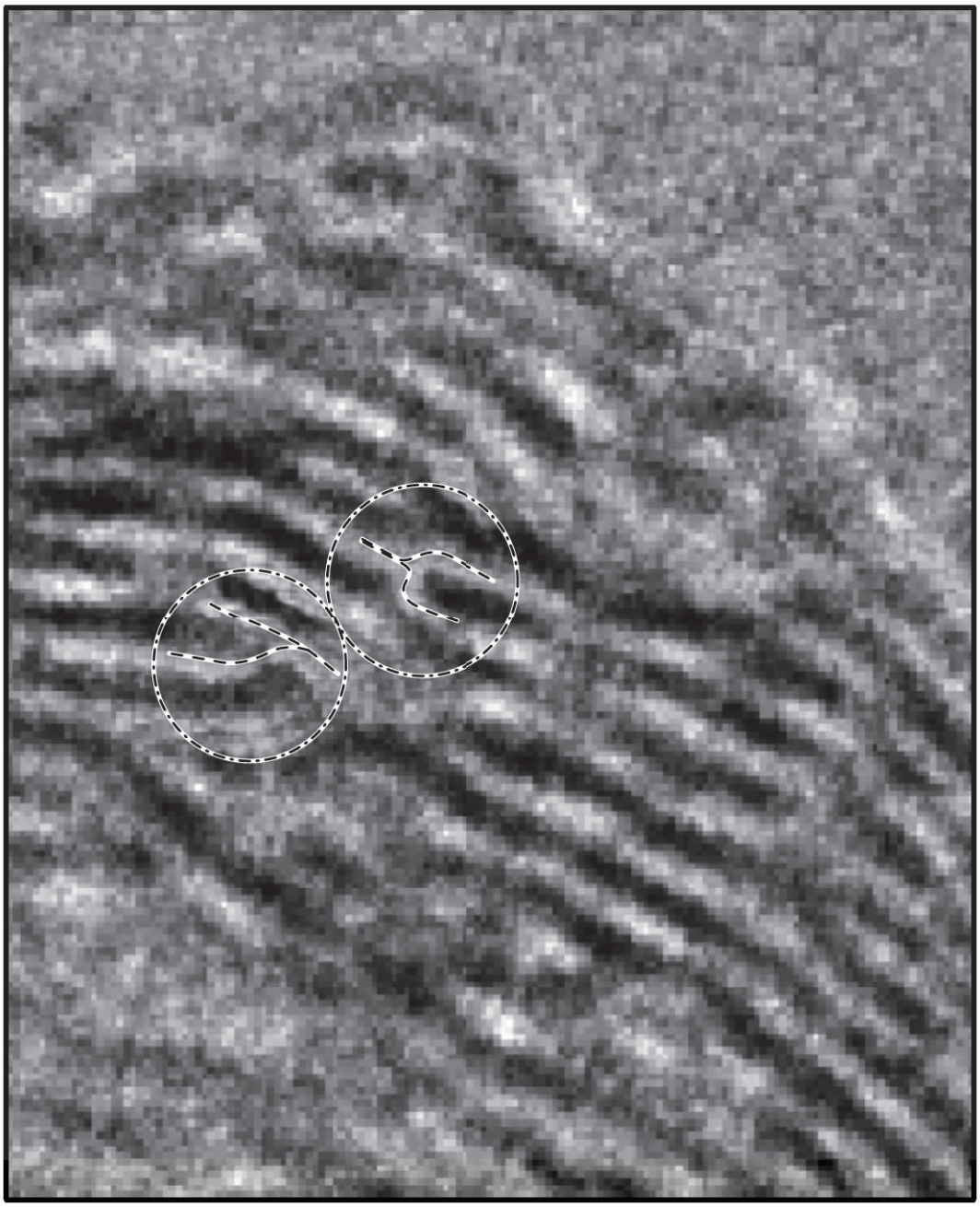


FIG. 109B

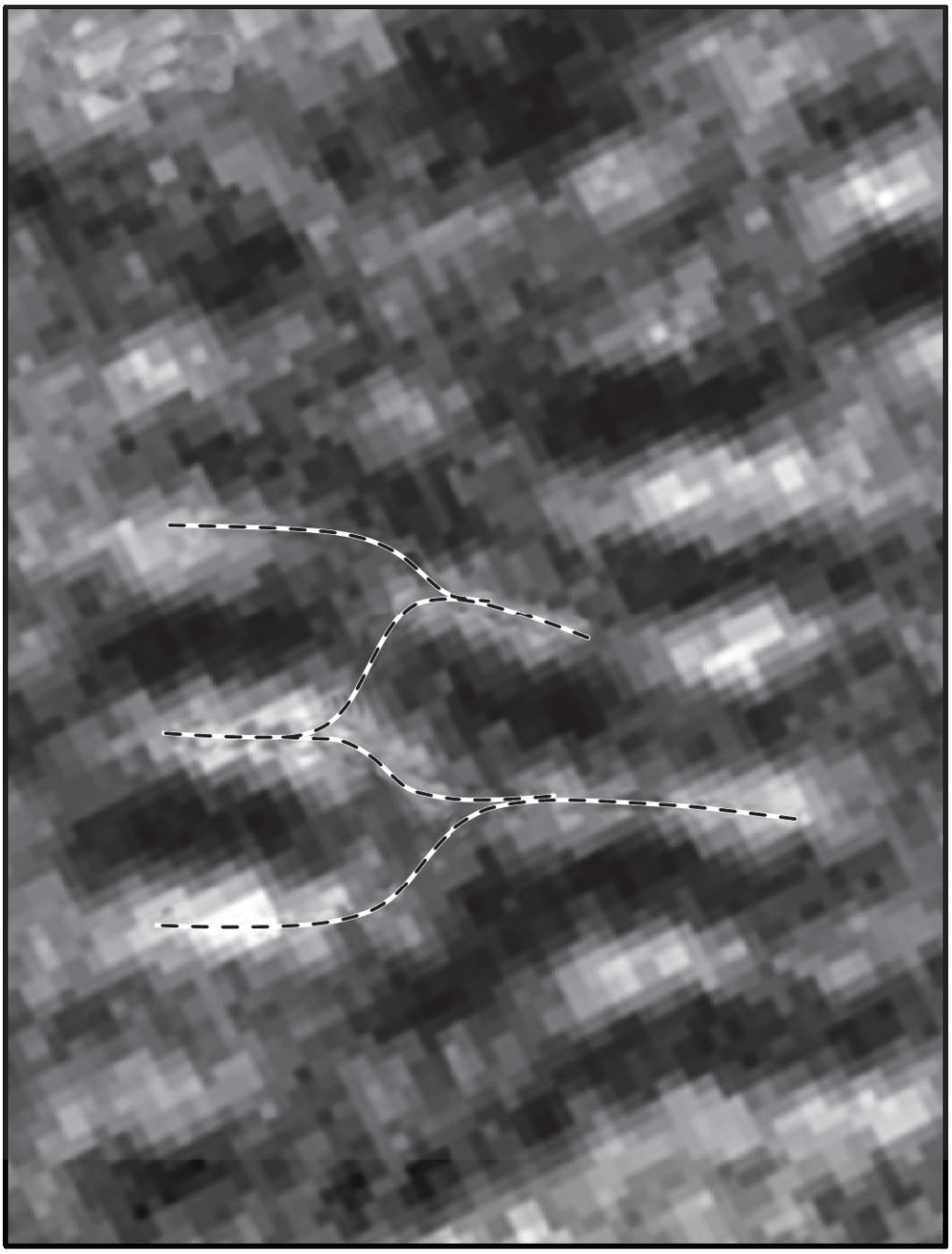


FIG. 109C